The EUMETSAT Network of Satellite Application Facilities

NWP SAF
Numerical Weather Prediction

Report of Associate Scientist mission

Document NWPSAF-MO-VS-020

Version 1.0

24 May 2007

Comparison of radiative transfer models for AMSU-B in presence of ice clouds

N. Courcoux, A. Doherty, and T.R. Sreerekha

Met Office

ECMWF

Royal Netherlands Meteorological Institute
Ministry of Transport, Public Works and Water Management

METEO FRANCE
Toujours un temps d'avance

Comparison of radiative transfer models for AMSU-B in presence of ice clouds

N. Courcoux, A. Doherty, and T.R. Sreerekha

This documentation was developed within the context of the EUMETSAT Satellite Application Facility on Numerical Weather Prediction (NWP SAF), under the Cooperation Agreement dated 1 December, 2006, between EUMETSAT and the Met Office, UK, by one or more partners within the NWP SAF. The partners in the NWP SAF are the Met Office, ECMWF, KNMI and Météo France.

1 Aim of the study

The aim of this study is to compare the Radiative Transfer for TOVS SCATTering (RTTOVSCATT) [*Bauer et al.*, 2006] and the Atmospheric Radiative Transfer Simulator (ARTS) (*Eriksson et al.* [2004], *Davis et al.* [2005],*Emde et al.* [2004]) models in presence of ice clouds using identical ice microphysics so that only the radiative transfer model (RTM) differences are compared.

2 Methodology

Simulations of brightness temperature (BT) are carried out for two emissivities (0.45 and 0.95), 3 viewing angles (nadir, 25°, and 50°), and 2 effective radii of the ice scatterers (50 and 100 μm) for the 5 Advanced Microwave Sounding Unit-B (AMSU-B) channels at 89, 150, 183.31±1, 183.31±3, and 183.31±7 GHz. AMSU-B [*Saunders et al.*, 1995] is a cross-track scanning instrument flying onboard the satellites of the National Oceanic and Atmospheric Agency (NOAA) 15, 16, and 17.

2.1 Profiles

The profiles used for the simulations are 4 subsets of the European Centre for Medium-range Weather Forecasts (ECMWF) ERA-40 reanalysis data, representing the atmospheric variability for 4 different cases, namely, ocean summer, ocean winter, land summer, and land winter scenarios.

The ocean summer data set contains 9000 profiles for July that are located in the North Atlantic (the exact location of these profiles is shown by the grey area on the upper left map in Figure 1). The ocean winter data set contains as well 9000 profiles located in the North Atlantic (Figure 1 upper right map) but they are for January. The land summer data set contains 25000 profiles for January, located in Africa and Amazonia (Figure 1 lower left map) and the land winter data set contains 5000 profiles for January located in North America and in Europe (Figure 1 lower right map). All profiles contain, the temperature profile, the specific humidity, the rain profile, the snow profile, the cloud liquid water profile, the cloud ice water profile, the cloud cover, the surface pressure, the 2 meter temperature, the surface wind speed component, the surface temperature, the land sea mask, and the longitude and latitude.

2.2 Determination of the single scattering properties

In order to model cirrus cloud properties the gamma size distribution described by *Evans and Stephens* [1995] is often used:

$$n(r) = a.r^{\alpha}.exp(-br)$$

α describes the width of the distribution (the distribution is getting narrower with decreasing α), a and b can be related to the physical quantities effective radius and Ice Mass Content (IMC). The effective radius R_{eff} for spherical

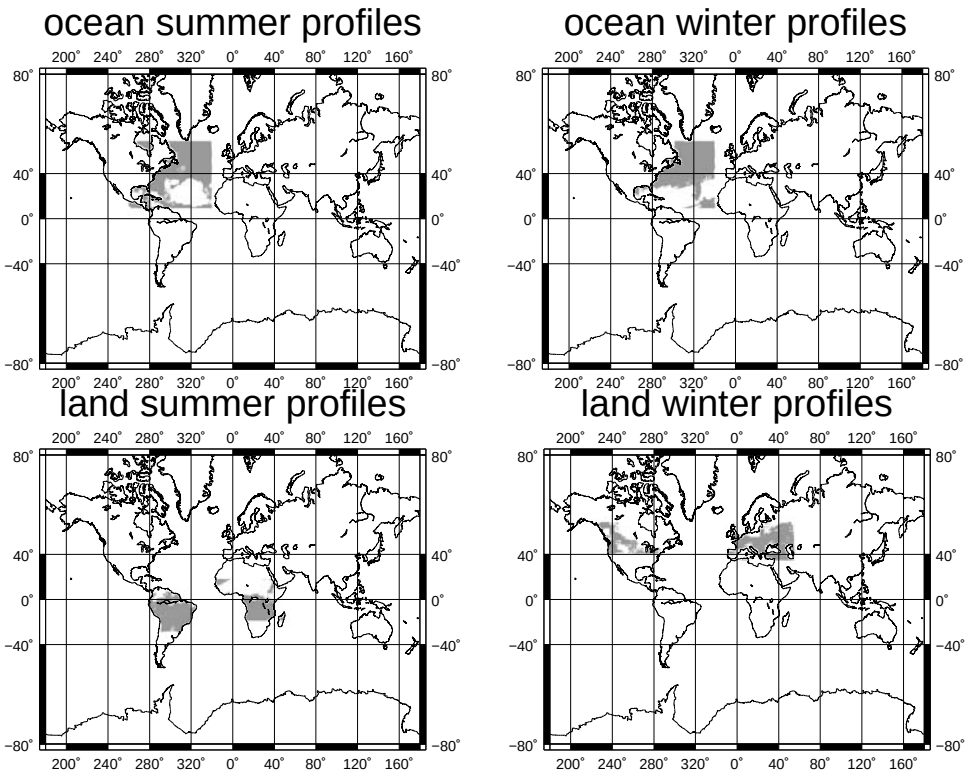

Figure 1: Location of the ECMWF profiles for the 4 data sets.

particles (what we are using for the comparison) is defined as the ratio of the of the third moment of the size distribution to the second moment.

$$R_{eff} = \frac{M_2}{M_3}$$
$$R_{eff} = \frac{\int_0^\infty [n(r).r^3.\mathrm{d}r]}{\int_0^\infty [n(r).r^2.\mathrm{d}r]}$$
$$R_{eff} = \frac{a\int_0^\infty [r^{\alpha+3}exp(-br)]}{a\int_0^\infty [r^{\alpha+2}exp(-br)]}$$

Since $\int_0^\infty [x^n e^{-ax}.\mathrm{d}x] = \frac{\Gamma(n+1)}{a^{n+1}}$ (for $n > -1$ and $a > 0$) $= \frac{n!}{a^{n+1}}$ (for $n > 0$)

$$R_{eff} = \frac{(\alpha+3)!}{b^{\alpha+3+1}} \cdot \frac{b^{\alpha+2+1}}{(\alpha+2)!}$$
$$R_{eff} = \frac{\alpha+3}{b} \Longrightarrow b = \frac{\alpha+3}{R_{eff}}$$

For the relationship between IMC, a and b,

$$Volume = \frac{4}{3}.\pi.M_3$$
$IMC = \frac{4}{3}.\pi.\rho.M_3$ ρ being the density of ice.
$$IMC = \frac{\frac{4}{3}.\pi.\rho.a.(\alpha+3)!}{b^{\alpha+4}}$$
$$a = \frac{IMC}{\frac{4}{3}.\pi.\rho.b^{-(\alpha+4)}.(\alpha+3)!}$$

The Particle Number Density (PND) can also be derived from the particle size distribution:

$$pnd = \int_0^{\infty}[a.r^{\alpha}.exp(-br).\mathrm{d}r], \text{ when } \alpha = 1 \; pnd = a\frac{1}{b^2}$$
$$pnd = \frac{IMC}{\frac{4}{3}.\pi.\rho.(\alpha+4)!}\frac{4^5}{R_{eff}^5}\frac{R_{eff}^2}{4^2}$$
$$pnd = \frac{2.IMC}{\pi.\rho.R_{eff}^3}$$

However the gamma distribution from *Evans and Stephens* [1995] defined above is written slightly differently than the one defined by *Mishchenko and Travis* [1998] (defined below) and used in the T matrix code which is used in this study to derive the single scattering properties.

Gamma distribution defined by *Mishchenko and Travis* [1998]:
$n(r) = \frac{1}{A.B.\Gamma(\frac{1-2.B}{B})}(\frac{r}{A.B})^{\frac{1-3.B}{B}}exp(\frac{-r}{A.B})$

The *Mishchenko and Travis* [1998] distribution $A = R_{eff}$ and $B = V_{reff}$, the effective variance.
if $\alpha = 1$ then $\frac{1-3B}{B} = 1 \Longrightarrow B = \frac{1}{4}$
So for the distributions to coincide the variance should be chosen to be equal to 0.25. So if $B = 0.25$ the *Mishchenko and Travis* [1998] can be written:
$n(r) = \frac{1}{0.25.A}^2 rexp(\frac{-}{r}0.25.A) = n(r) = \frac{1}{0.25.R_{eff}^2}.r.exp(\frac{-}{r}0.25.R_{eff})$ and the *Evans and Stephens* [1995] can be written:
$n(r) = a.r^{\alpha}.exp(-br)$ $b = \frac{\alpha+3}{R_{eff}}$, $\alpha = 1$ $b = \frac{4}{R_{eff}}$ So the exponent term is similar for both distributions.

Furthermore, although the limits of the gamma size distribution are from 0 to infinity, since it is solved numerically, it is necessary to specify an upper and lower limit for the size distribution. The limits have to be chosen so that they correspond to the real range of crystal size, so to be consistent with *Evans and Stephens* [1995], the minimum particle size has been chosen to be 20 μm and the maximum 2000 μm.

The single scattering properties have been produced using:

- a gamma distribution with a variance of 0.25 for the ice particle size distribution,
- a particle radius ranging from 20 to 2000 μm.
- an effective radius of the ice particles of 50 and 100 μm.

The T-matrix code [*Mishchenko and Travis*, 1998] has been used to obtain the extinction coefficient, the single scattering albedo and the asymmetry parameter used in RTTOVSCATT, as well as to obtain the phase matrix used in ARTS.

3 Results

3.1 Presentation of the results

For each combination of emissivity, viewing angle and effective radius, and for each data set the BT were simulated by ARTS and by RTTOVSCATT (RTTOV was used for clear sky simulations instead of RTTOVSCATT).

The results are displayed in 2 ways (scatter plots and histograms) in multiple plots figures. Each figure contains 15 plots arranged in 3 columns and

5 lines and corresponds to a particular combination of emissivity, viewing angle and effective radius. In each figure the first column of plots features the clear sky results, the second column, the cloudy results and the third column the cloud signal, each line of plots corresponds to the results (clear, cloudy, and cloud signal) for a given AMSU-B channel, from channel 16 for the first line of plots to channel 20 for the fifth line of plots. The scatter plots are presented as RTTOV BT against ARTS BT (or RTTOV cloud signal against ARTS cloud signal). With scatter plots it is impossible to evaluate the number of points plotted at the same location on the plot, the histograms are presented to have a quantitative evaluation of the occurrence of BT range for both models. The number of occurrence of the BT are displayed on the histogram with a plain line for RTTOV and a dashed line for ARTS. All the histograms have 15 BT bins, the width of the bins varies for each histogram according to the corresponding range of the BT.

In this study, the cloud signal is defined as clear sky BT minus cloudy BT. Furthermore the cloud signal is calculated using each model own clear sky simulation (ARTS cloud signal corresponds to ARTS clear sky BT-ARTS cloudy BT and RTTOVSCATT cloud signal corresponds to RTTOV clear sky BT-RTTOVSCATT cloud BT).

Firstly, the results for the ocean summer data set are shown and discussed in detail, then the results for the three other data sets are discussed and the plots for these data sets are shown in the appendix.

3.2 Inconsistency between RTTOV and RTTOVSCATT clear sky results

At first, the results from ARTS and RTTOV for the clear sky case were in very good agreement (figure 2, first column). However, for the cloud signal all the cases showed an unexpected behaviour. The cloud signal which is defined as the clear sky minus cloudy sky, was negative for all cases and all channels, for RTTOV simulations, (figure 2 last column). Although it is possible under certain conditions that the cloud signal is negative for the AMSU-B window channels, it is totally unexpected to have such a behaviour for AMSU-B sounding channels. Furthermore, if this behaviour was due to the state of the atmosphere it should have been simulated by ARTS as well, which is not the case. It was found that RTTOV clear sky simulations (which were used for the first results and which are visible on Figure 2) gives different results than RTTOVSCATT simulations when ice scatterers are not included in the calculation. Theoretically in that case both RTTOV and RTTOVSCATT should give identical outputs. The origin of this difference is not clear, however, it might arise from different definition of the layer emission between RTTOV and RTTOVSCATT(communication from Peter Bauer).

It was then decided, to be consistent with the cloudy case, to use RTTOVSCATT without including ice scatterers as clear sky case. So all the further described results are produced using RTTOVSCATT without including ice scatterers in the calculation.

Since the clear sky simulations produced by RTTOV were in very good

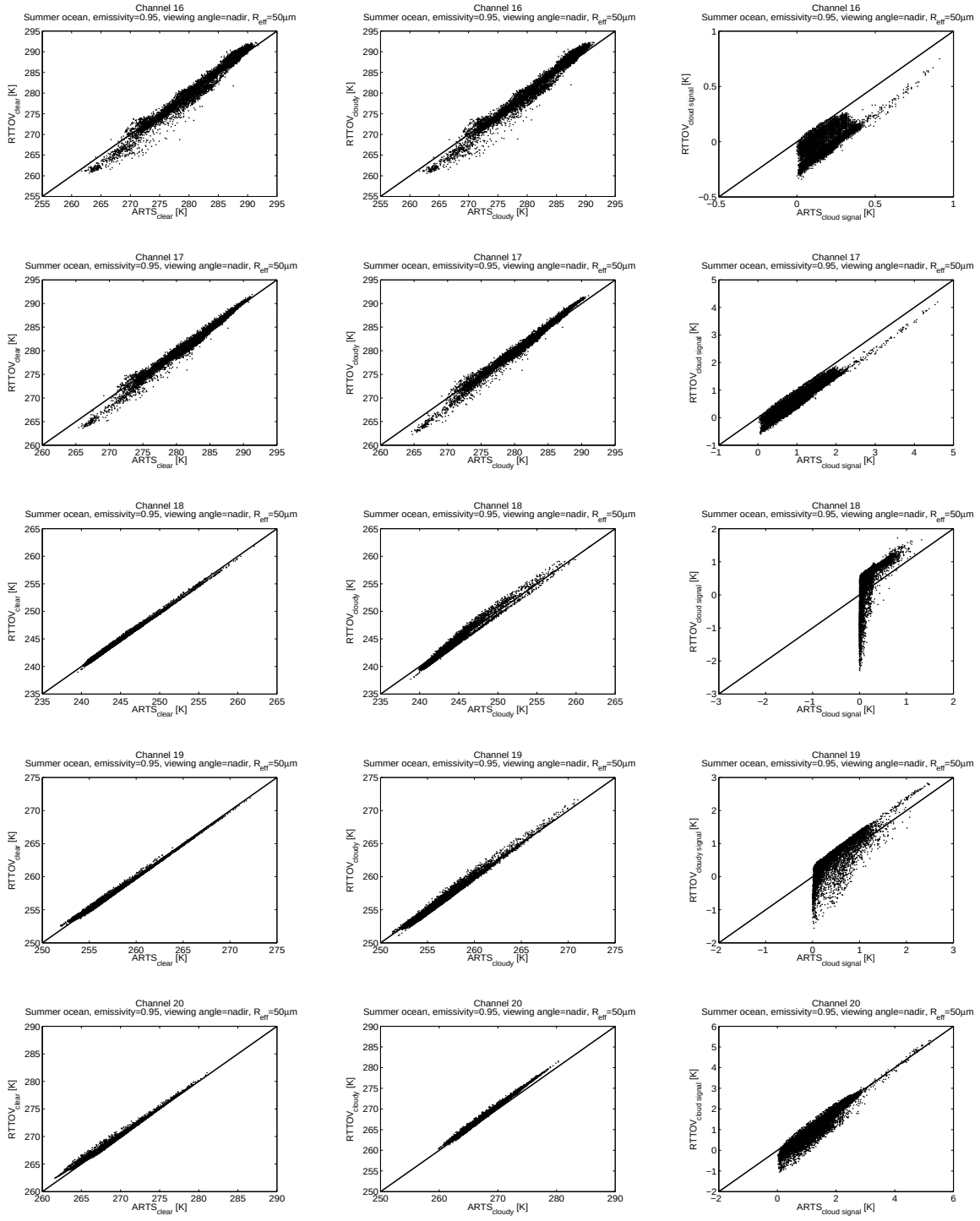

Figure 2: BT simulated for the ocean summer data set by RTTOV (for clear sky simulations) and by RTTOVSCATT (for the cloudy simulations) against BT simulated by ARTS for a particular set of parameters (emissivity=0.95, viewing angle=nadir, and effective radius of the ice particles=50μm). Each line correspond to one AMSU-B channel from top to bottom channel 16 (89 GHz), 17 (150 GHz), 18 (183.31$\pm$1 GHz), 19 (183.31$\pm$3 GHz), and 20 (183.31$\pm$7 GHz). The left column correspond to clear sky simulations, the middle column corresponds to cloudy simulations and the right column corresponds to the cloud signal (clear sky BT minus cloudy BT).

agreement with the ARTS outputs, and that RTTOVSCATT without ice scatterers and RTTOV give different results, the agreement between RTTOVSCATT 'clear sky' and ARTS is not optimal. However, in general the agreement is good for clear sky and cloudy cases. For the cloud signal the agreement depends very much on the channels and the different parameters (emissivity, viewing angle, and effective radius) that are used in the study. The results corresponding to the different combination of parameters will be analysed hereafter.

The results (for clear sky, cloudy sky and cloud signal) are presented with two different types of plots: scatter plots where the RTTOVSCATT simulated BT are plotted against the ARTS simulated BT and histograms where the distribution of the BT simulated by each model are plotted.

3.3 High emissivity case (0.95) with an effective radius of 50 μm for the ocean summer data set

See figures 3 to 8 for the plots corresponding to this case.

For the clear sky simulations (which are independent of the ice scatterers effective radius), the results are similar for each channel independently of the viewing angles.

For Channel 16 and 17 there is no offset between the models, but these channels show more scatter than the other channels. For the sounding channels (18 to 20) the scatter is much less than for the window channels (16 and 17) but there is an offset between the models, RTTOVSCATT shows a higher BT than ARTS (2 or 3 K). Although agreement is good for the results corresponding to nadir and 25° viewing angles, the results show more scatter for the 50° viewing angle. This offset between ARTS and RTTOVSCATT is mostly due to the fact that RTTOVSCATT without including the ice scatterers is used for the clear sky simulation as explained above. It can be compared to figure 2 first column which shows scatter plots in the case when RTTOV, not RTTOVSCATT, is used to simulate the clear sky BT, the results in that case are better.

Concerning the cloudy case, the results also agree well for all channels, although the window channels shows more scatter in that case. The simulation for the largest viewing angle (50 °) shows an offset of about 1 K that is not apparent for the 2 other viewing angles.

For the clear and the cloudy cases, the histograms (figures 4, 6, and 8) show that for all channels the distributions of the BT are similar. Only in the case of the largest viewing angle (50 °) the distribution of the TB simulated by RTTOVSCATT are higher (by about 2 K) than the distribution of the BT simulated by ARTS.

Concerning the cloud signal (clear TB-cloudy TB), differences between the models are larger than the cloud signal in ARTS, this for all channels .

For the cloud signal, like the clear and cloudy case, there is not much difference between the ARTS and RTTOVSCATT simulations produced with the nadir and 25° viewing angle but the simulation produced for the 50° viewing angle shows some better agreement for channels 16 and 20. The scatter plots for channel 16 and 20 show closer agreement between the mod-

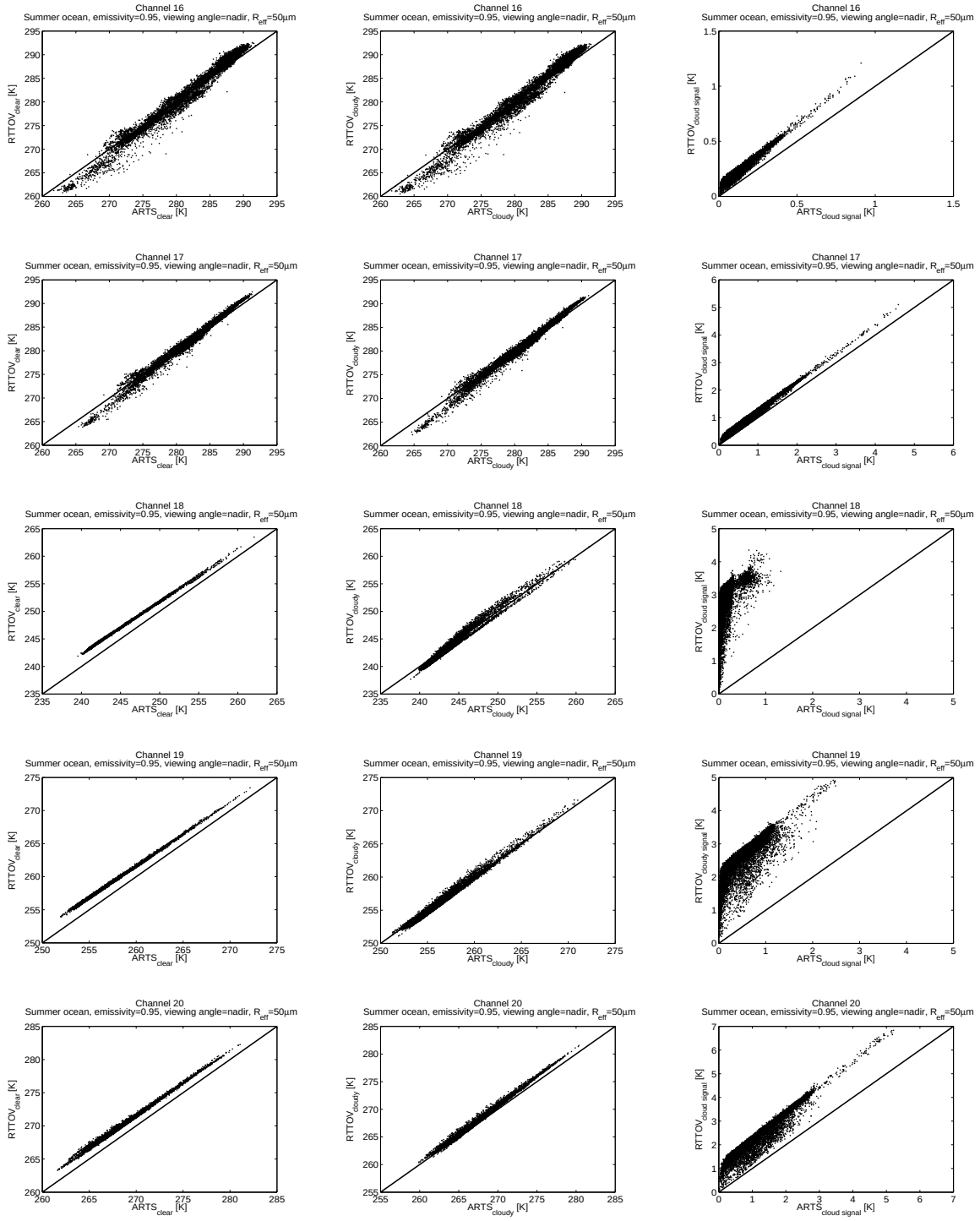

Figure 3: BT simulated for the ocean summer data set by RTTOVSCATT (for both clear sky simulations and cloudy simulations) against BT simulated by ARTS for a particular set of parameters (emissivity=0.95, viewing angle=nadir, and effective radius of the ice particles= 50μm). Each line correspond to one AMSU-B channel from top to bottom channel 16 (89 GHz), 17 (150 GHz), 18 (183.31±1 GHz), 19 (183.31±3 GHz), and 20 (183.31±7 GHz). The left column correspond to clear sky simulations, the middle column corresponds to cloudy simulations and the right column corresponds to the cloud signal (clear sky BT minus cloudy BT).

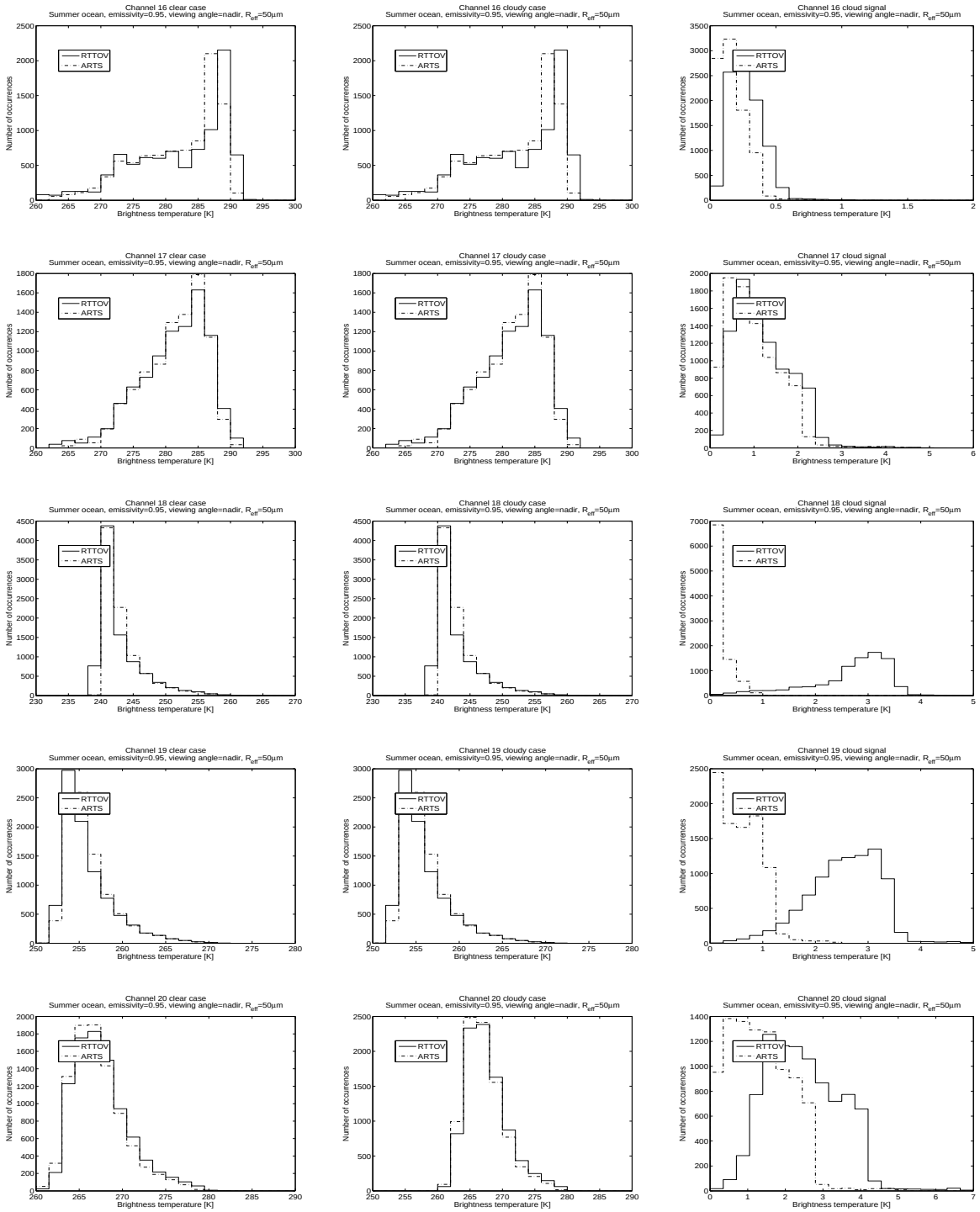

Figure 4: Histograms of BT simulated for the ocean summer data set by RTTOVSCATT (for both clear sky simulations and cloudy simulations), (plain line), and of BT simulated by ARTS (dashed line) for a particular set of parameters (emissivity=0.95, viewing angle=nadir, and effective radius of the ice particles= 50μm). Each line correspond to one AMSU-B channel from top to bottom channel 16 (89 GHz), 17 (150 GHz), 18 (183.31$\pm$1 GHz), 19 (183.31$\pm$3 GHz), and 20 (183.31$\pm$7 GHz). The left column correspond to clear sky simulations, the middle column corresponds to cloudy simulations and the right column corresponds to the cloud signal (clear sky BT minus cloudy BT).

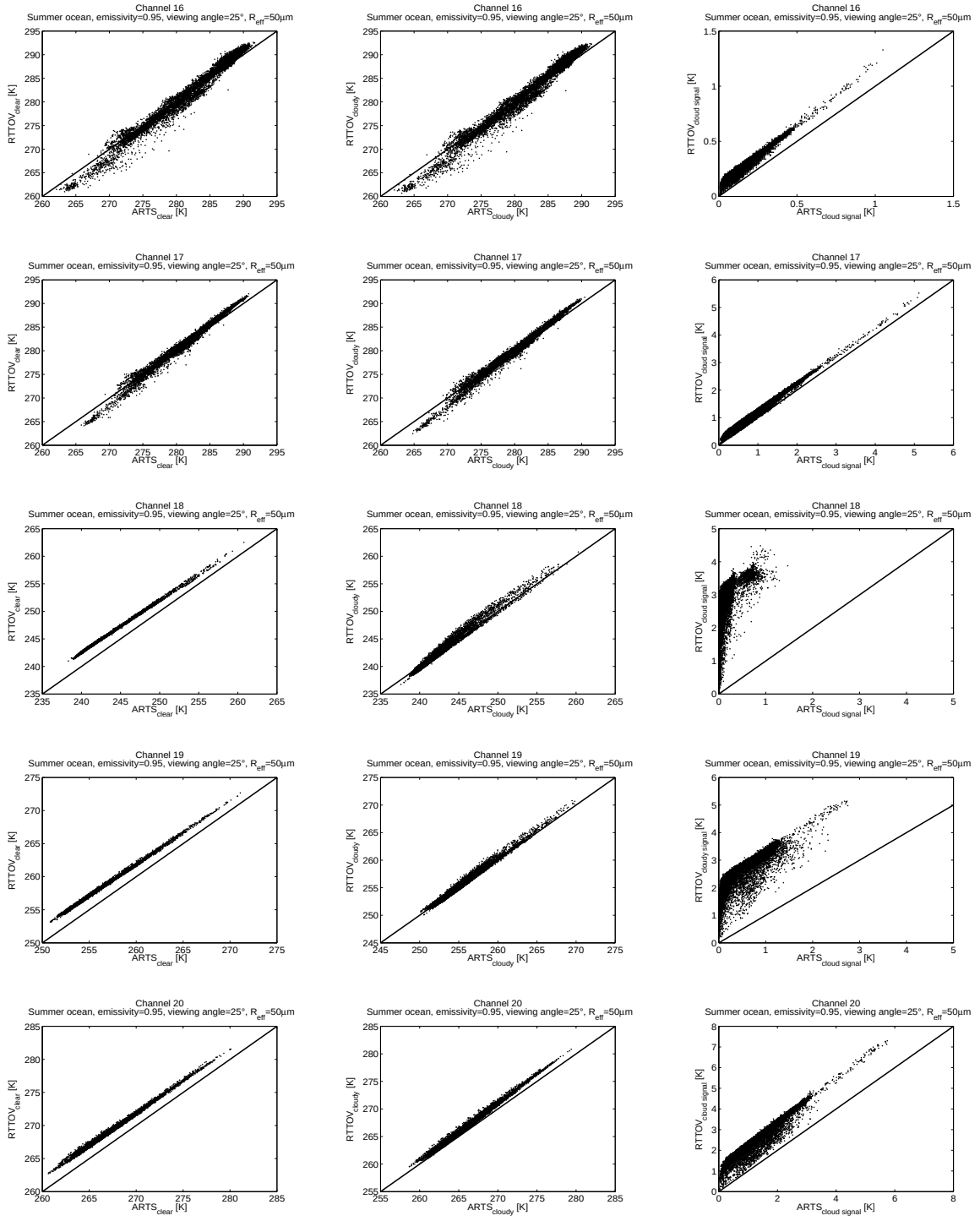

Figure 5: BT simulated for the ocean summer data set by RTTOVSCATT (for both clear sky simulations and cloudy simulations) against BT simulated by ARTS for a particular set of parameters (emissivity=0.95, viewing angle=25°, and effective radius of the ice particles= 50μm). Each line correspond to one AMSU-B channel from top to bottom channel 16 (89 GHz), 17 (150 GHz), 18 (183.31±1 GHz), 19 (183.31±3 GHz), and 20 (183.31±7 GHz). The left column correspond to clear sky simulations, the middle column corresponds to cloudy simulations and the right column corresponds to the cloud signal (clear sky BT minus cloudy BT).

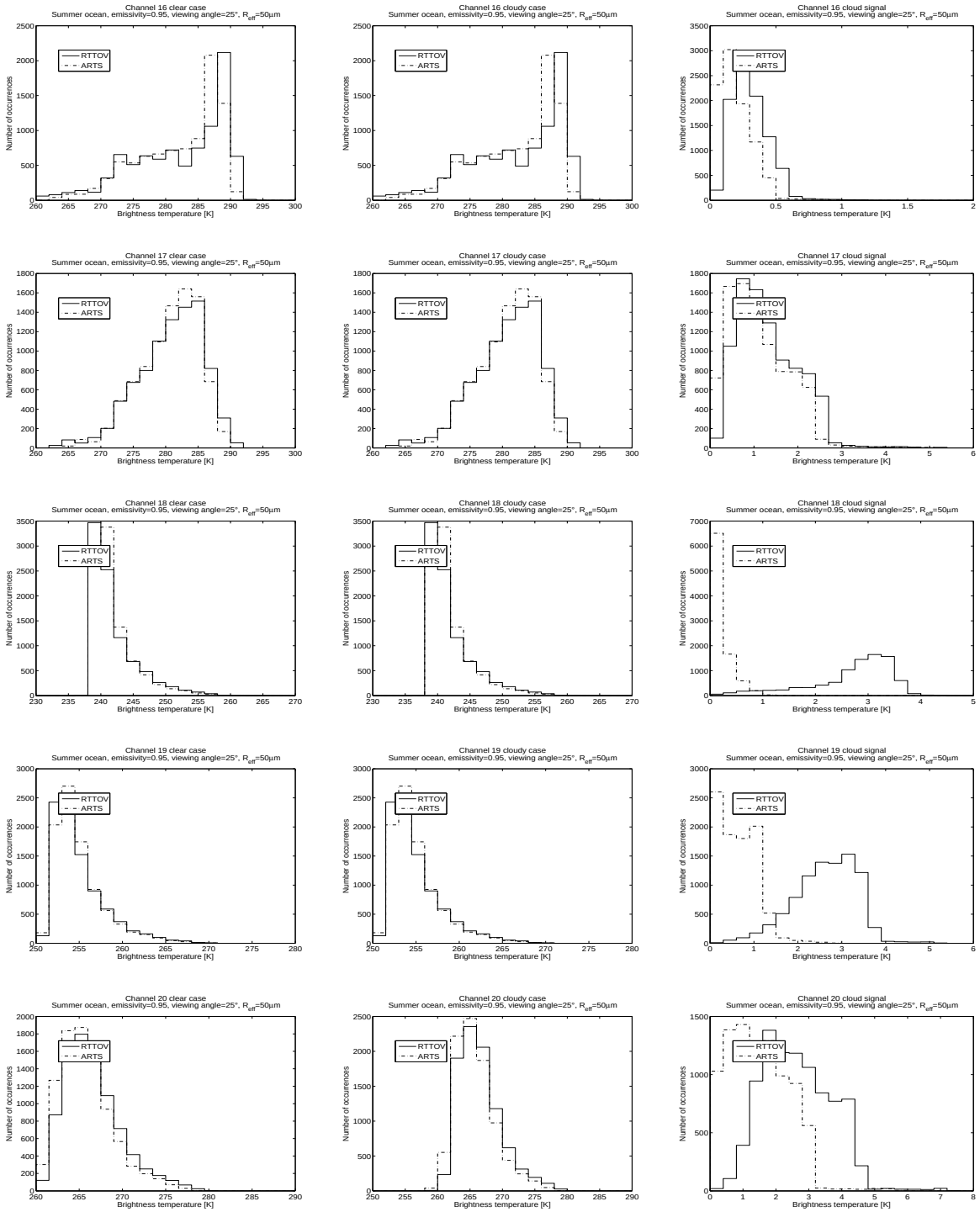

Figure 6: Histograms of BT simulated for the ocean summer data set by RTTOVSCATT (for both clear sky simulations and cloudy simulations), (plain line), and of BT simulated by ARTS (dashed line) for a particular set of parameters (emissivity=0.95, viewing angle=25°, and effective radius of the ice particles= 50μm). Each line correspond to one AMSU-B channel from top to bottom channel 16 (89 GHz), 17 (150 GHz), 18 (183.31±1 GHz), 19 (183.31±3 GHz), and 20 (183.31±7 GHz). The left column correspond to clear sky simulations, the middle column corresponds to cloudy simulations and the right column corresponds to the cloud signal (clear sky BT minus cloudy BT).

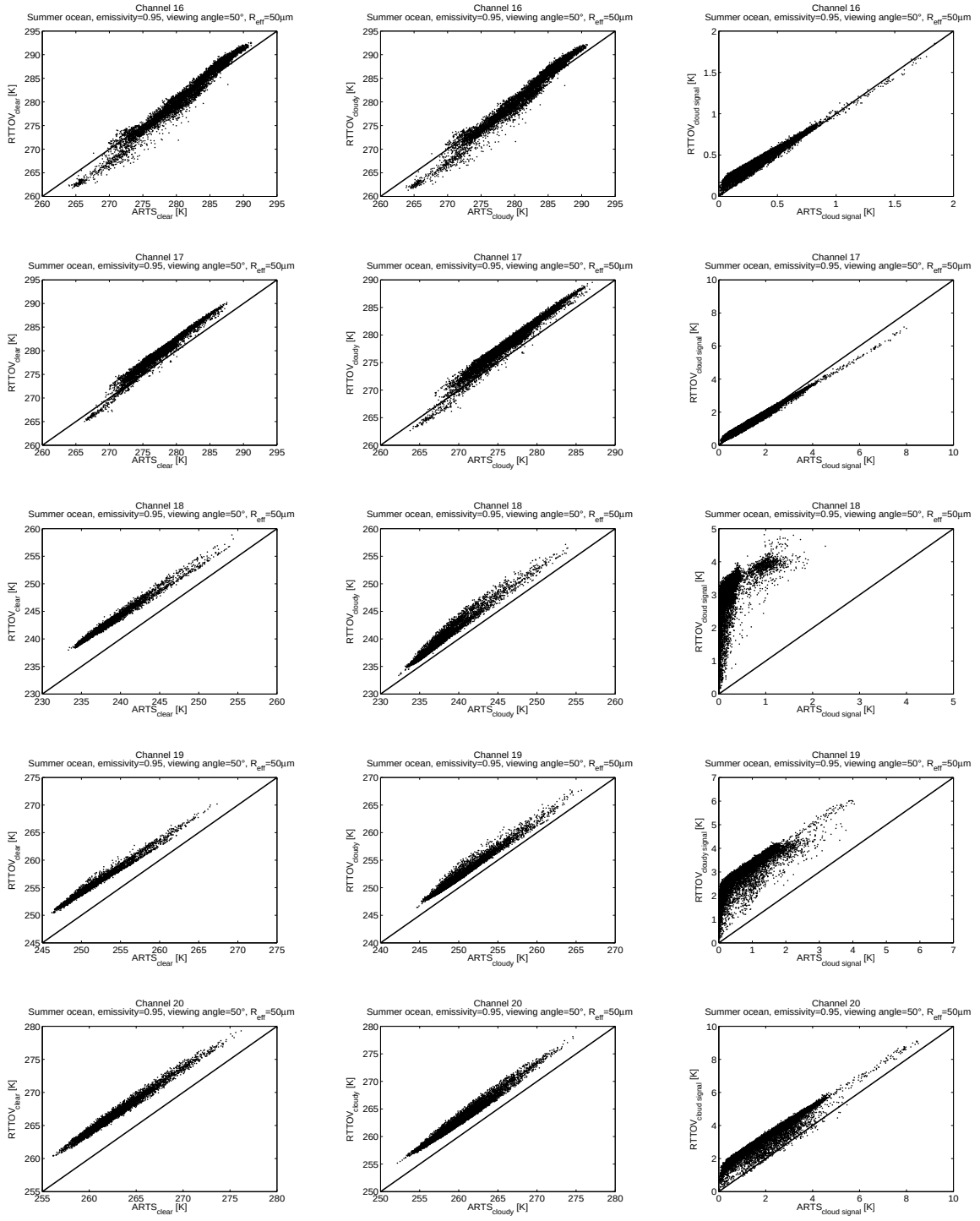

Figure 7: BT simulated for the ocean summer data set by RTTOVSCATT (for both clear sky simulations and cloudy simulations) against BT simulated by ARTS for a particular set of parameters (emissivity=0.95, viewing angle=50°, and effective radius of the ice particles= 50μm). Each line correspond to one AMSU-B channel from top to bottom channel 16 (89 GHz), 17 (150 GHz), 18 (183.31±1 GHz), 19 (183.31±3 GHz), and 20 (183.31±7 GHz). The left column correspond to clear sky simulations, the middle column corresponds to cloudy simulations and the right column corresponds to the cloud signal (clear sky BT minus cloudy BT).

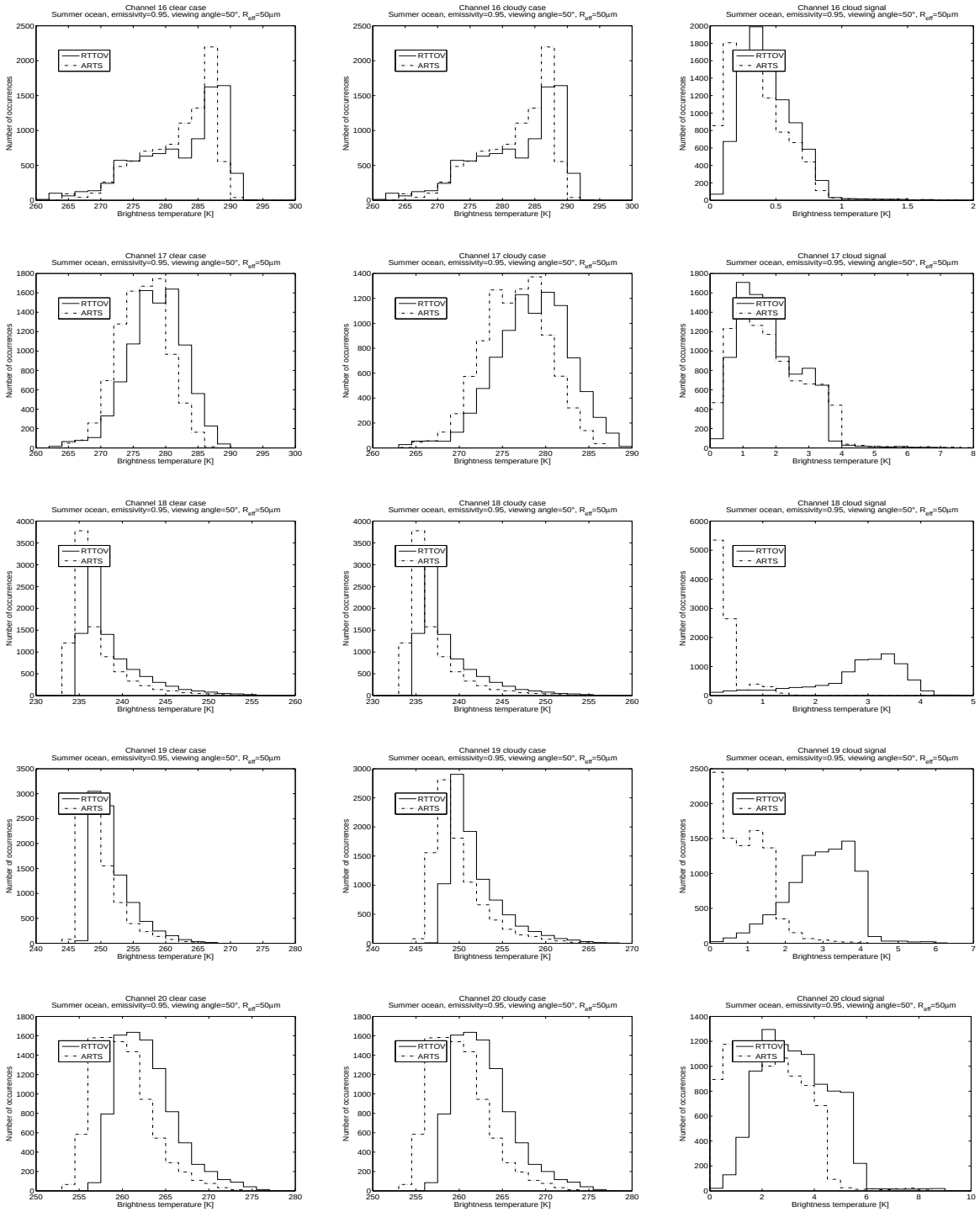

Figure 8: Histograms of BT simulated for the ocean summer data set by RTTOVSCATT (for both clear sky simulations and cloudy simulations), (plain line), and of BT simulated by ARTS (dashed line) for a particular set of parameters (emissivity=0.95, viewing angle=50°, and effective radius of the ice particles= 50μm). Each line correspond to one AMSU-B channel from top to bottom channel 16 (89 GHz), 17 (150 GHz), 18 (183.31±1 GHz), 19 (183.31±3 GHz), and 20 (183.31±7 GHz). The left column correspond to clear sky simulations, the middle column corresponds to cloudy simulations and the right column corresponds to the cloud signal (clear sky BT minus cloudy BT).

els for the cloud signal than for either the clear or cloudy alone.

The cloud signal for the window channels agrees well, however, TB produced by RTTOVSCATT are a bit warmer than those produced by ARTS (this is also visible on the histograms, see figures 4,6, and 8). Furthermore, there is more scatter in the results for weak cloud signal than for strong cloud signal. This behaviour is unexpected since we expect both models to show no cloud signal in the absence of ice and the cloud signal should increase with increasing ice amount. This behaviour is even more pronounced for the sounding channels, for which the agreement between models is not good, most of the scatter is shown for weak cloud signal.

To investigate this behaviour, the upper left panel of figure 9 shows the ARTS cloud signal for channel 20 against Ice Water Path (IWP) and the upper right panel of figure 9 shows the same for RTTOVSCATT. One sees that in the case of ARTS the cloud signal increases with increasing IWP, in the case of RTTOVSCATT the scatter for the lowest IWP is about 1.5 K. Similar figures are plotted for channel 18 on figure 9 lower left panel for ARTS and on figure 9 lower right panel for RTTOVSCATT. These figures show that for channel 18 ARTS doesn't always detect a signal from high IWP points. However, ARTS doesn't show strong cloud signal for very low IWP. In contrast, on the lower right panel of figure 9 it is clearly visible that RTTOVSCATT shows strong cloud signal and much scatter for the lowermost IWP values, the reason for this high sensitivity of RTTOVSCATT at very low IWP has still to be established. This behaviour is unexpected because if some scatter for high IWP values is expected the model should not see strong clouds where there is no ice or a very low amount of ice. Furthermore, if this behaviour is due to the state of the atmosphere, like the variation of the cloud height with respect to the weighting function peak it should be seen by both models. Two more points should be added, for channel 18, ARTS (the lower left panel of figure 9) also shows an odd behaviour, there are 2 main clouds of points, one covering almost the whole range of IWP (up to 0.6 kg/m^2) but having an maximum cloud signal of about 0.4 K, the second one having a high variability for low IWP (between 0.1 and 0.2 K), in between for few points the cloud signal increases with an increasing IWP. It is noticeable that the shape of the ARTS scatter plot for channel 18 and the shape of the RTTOVSCATT scatter plot for channel 18 show some similarities although the amplitudes are different. The first group of points described above (large range of IWP and between 0 and 0.4 K for the cloud signal for ARTS) is also visible on the the RTTOVSCATT scatter plot but it is extended in the cloud signal direction (between 0 and 3.5 K). The second group of points is visible but compressed in the RTTOVSCATT scatter plot compared to the ARTS scatter plot, this group of points occupy one fourth of the total cloud signal amplitude while it is about one third for the ARTS scatter plot. However, the models behave differently, which is also noticeable when looking at the amplitude of the cloud signal, for ARTS, up to 2 K and for RTTOVSCATT, up to 5 K.

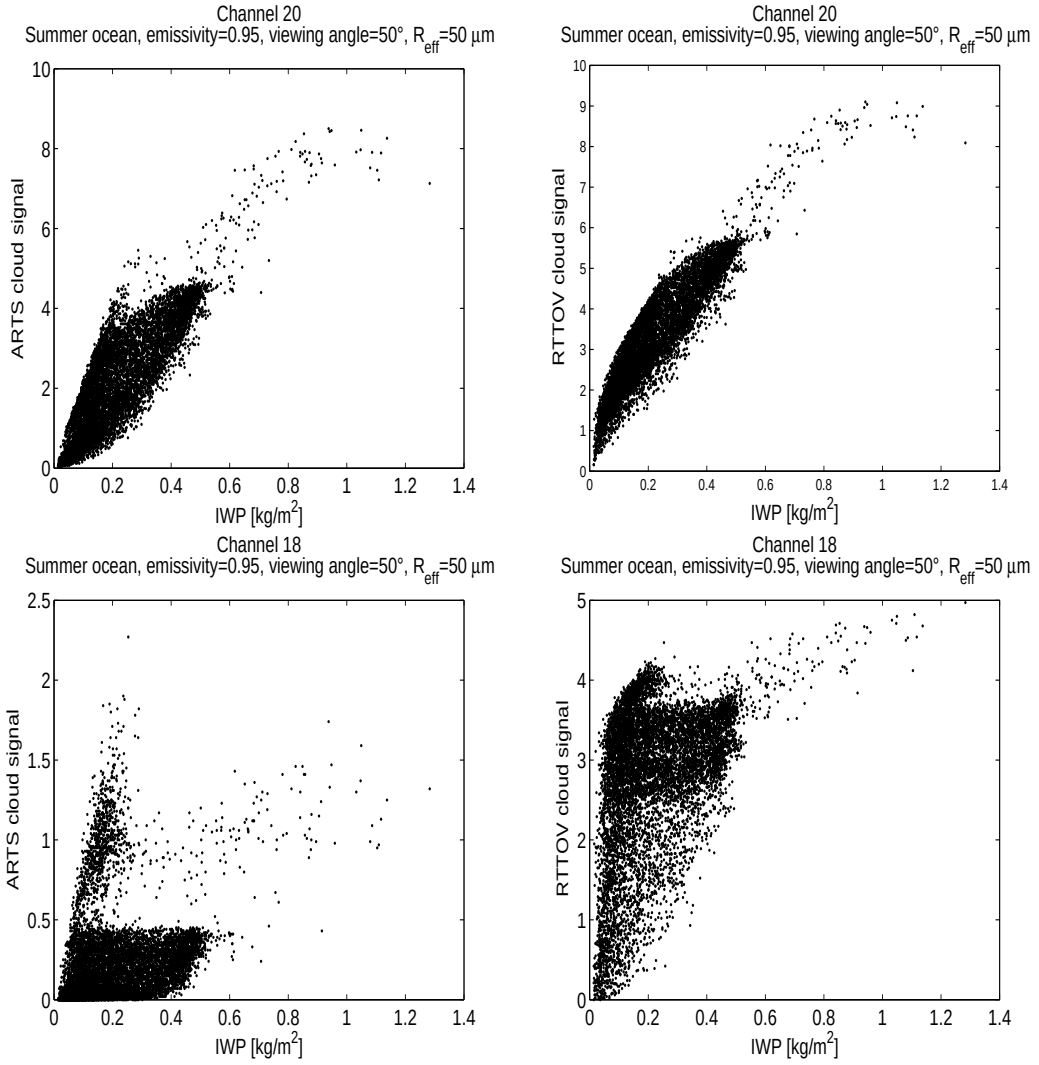

Figure 9: Upper left panel: BT simulated for the ocean summer data set by ARTS for AMSU channel 20 against corresponding IWP (emissivity=0.95, viewing angle=nadir and effective radius=50μm). Upper right panel: BT simulated for the ocean summer data set by RTTOVSCATT for AMSU channel 20 against corresponding IWP (emissivity=0.95, viewing angle=nadir and effective radius=50μm). Lower right panel: similar to he upper right panel but for AMSU channel 18. Lower left panel: similar to the upper left panel but for AMSU channel 18.

3.4 High emissivity case (0.95) combined with an effective radius of the ice scatterers of 100 μm for the ocean summer data set

See figures 10 to 15 for the plots corresponding to this case.

The clear sky results are identical to those produced with 50 μm, since the effective radius of the ice scatterers has no impact on the clear sky results. For the cloudy case, the BT produced with the 100 μm effective radius particles are colder than those produced with the 50 μm effective radius particles however, the model agreement is comparable in both cases. The only difference between the simulations produced with the 2 different effective radii is visible on the cloud signal plots. First of all, for all channels the magnitude of the cloud signal is higher in these simulations with a 100 μm effective radius than for the simulation with the 50 μm effective radius. For channel 16, the agreement is good for the nadir viewing angle and really good for the 25° viewing angle. For the 50° viewing angle, ARTS simulations are warmer than the RTTOVSCATT simulations. The behaviour is the same for channel 17 as for channel 16 except that the agreement is the best for the nadir viewing angle not the 25° viewing angle. For the sounding channels, although the absolute offset between both models is comparable to the previous simulation with an effective radius of 50 μm, the relative offset is less since the cloud signal for this simulation is greater. The agreement between the simulations produced with ARTS and RTTOVSCATT is good for channel 20, RTTOVSCATT showing a greater cloud signal for the nadir and 25° viewing angle, but ARTS showing a greater cloud signal for the 50° viewing angle. For channel 18 and 19, the results are close to the one described for the previous simulation but the agreement between both models improves with increasing viewing angle, however RTTOVSCATT is almost always showing a greater cloud signal (up to 3 K), even a greater cloud signal than ARTS. This is also visible on the histograms.

3.5 Low emissivity case (0.45) combined with an effective radius of the ice scatterers of 50 μm for the ocean summer data set

See figures 16 to 21 for the plots corresponding to this case.

For the simulations produced using the low emissivity (0.45), and an effective radius of 50 μm, the emissivity value has only a very small influence on the results for the sounding channels (18, 19, and 20). This influence is only visible for channel 20 for the clear sky case with a nadir or a 25° the viewing angle, the scatter plot shows a slightly wider spread of the results for the low emissivity case (0.45) than for the high emissivity case (0.95). The emissivity is not expected to have an impact on the sounding channels because in the data set we have used (ocean summer) the profiles are moist and having a surface elevation at sea level. Under these conditions, it is expected that the sounding channels have a low sensitivity to the surface and consequently to the surface emissivity. However there is a similar conclusion in *Buehler et al.* [2006] which described a clear sky comparison of RTTOV and ARTS for the AMSU-B sounding channels. This comparison

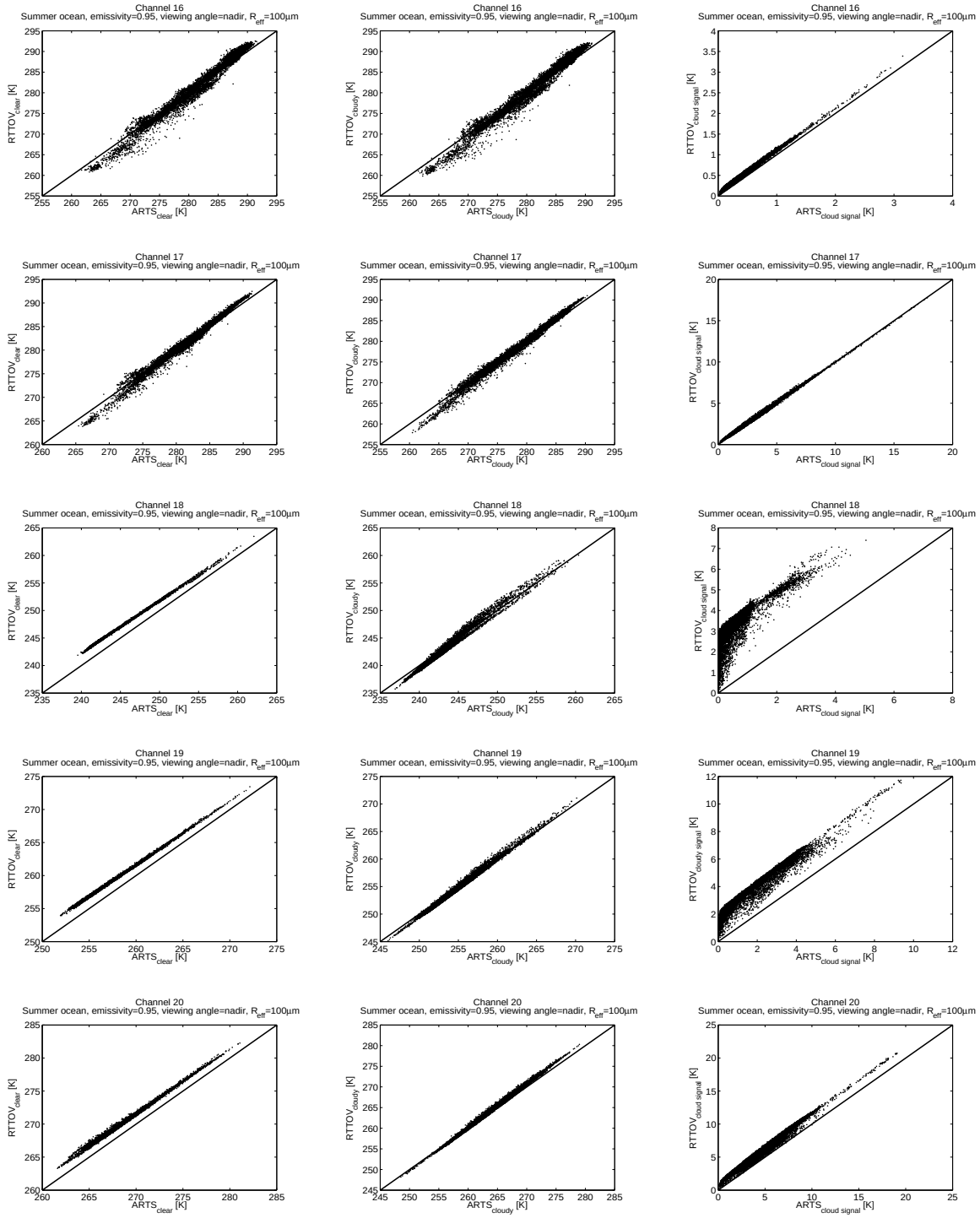

Figure 10: BT simulated for the ocean summer data set by RTTOVSCATT (for both clear sky simulations and cloudy simulations) against BT simulated by ARTS for a particular set of parameters (emissivity=0.95, viewing angle=nadir, and effective radius of the ice particles= 100μm). Each line correspond to one AMSU-B channel from top to bottom channel 16 (89 GHz), 17 (150 GHz), 18 (183.31±1 GHz), 19 (183.31±3 GHz), and 20 (183.31±7 GHz). The left column correspond to clear sky simulations, the middle column corresponds to cloudy simulations and the right column corresponds to the cloud signal (clear sky BT minus cloudy BT).

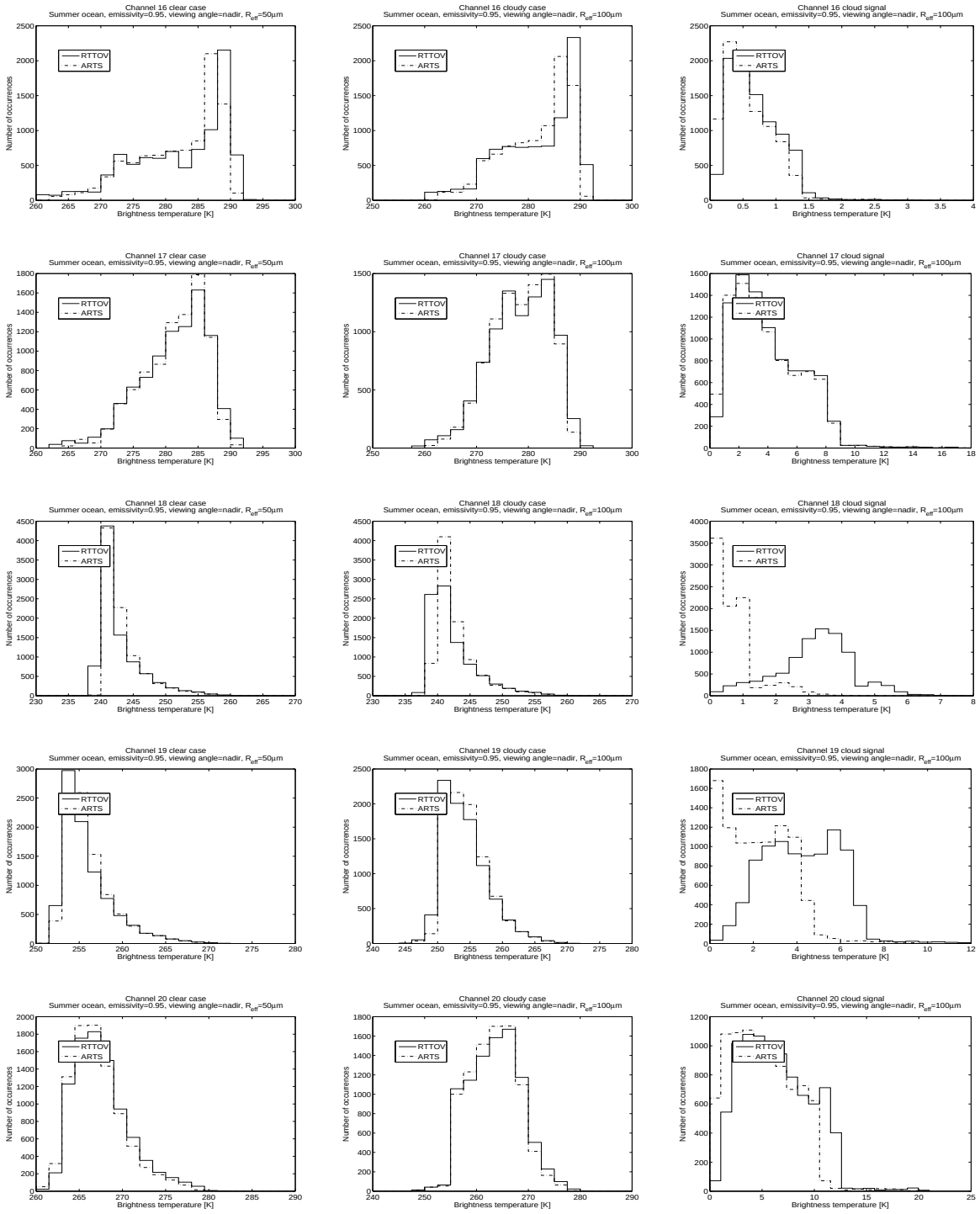

Figure 11: Histograms of BT simulated for the ocean summer data set by RTTOVSCATT (for both clear sky simulations and cloudy simulations), (plain line), and of BT simulated by ARTS (dashed line) for a particular set of parameters (emissivity=0.95, viewing angle=nadir, and effective radius of the ice particles= 100μm). Each line correspond to one AMSU-B channel from top to bottom channel 16 (89 GHz), 17 (150 GHz), 18 (183.31$\pm$1 GHz), 19 (183.31$\pm$3 GHz), and 20 (183.31$\pm$7 GHz). The left column correspond to clear sky simulations, the middle column corresponds to cloudy simulations and the right column corresponds to the cloud signal (clear sky BT minus cloudy BT).

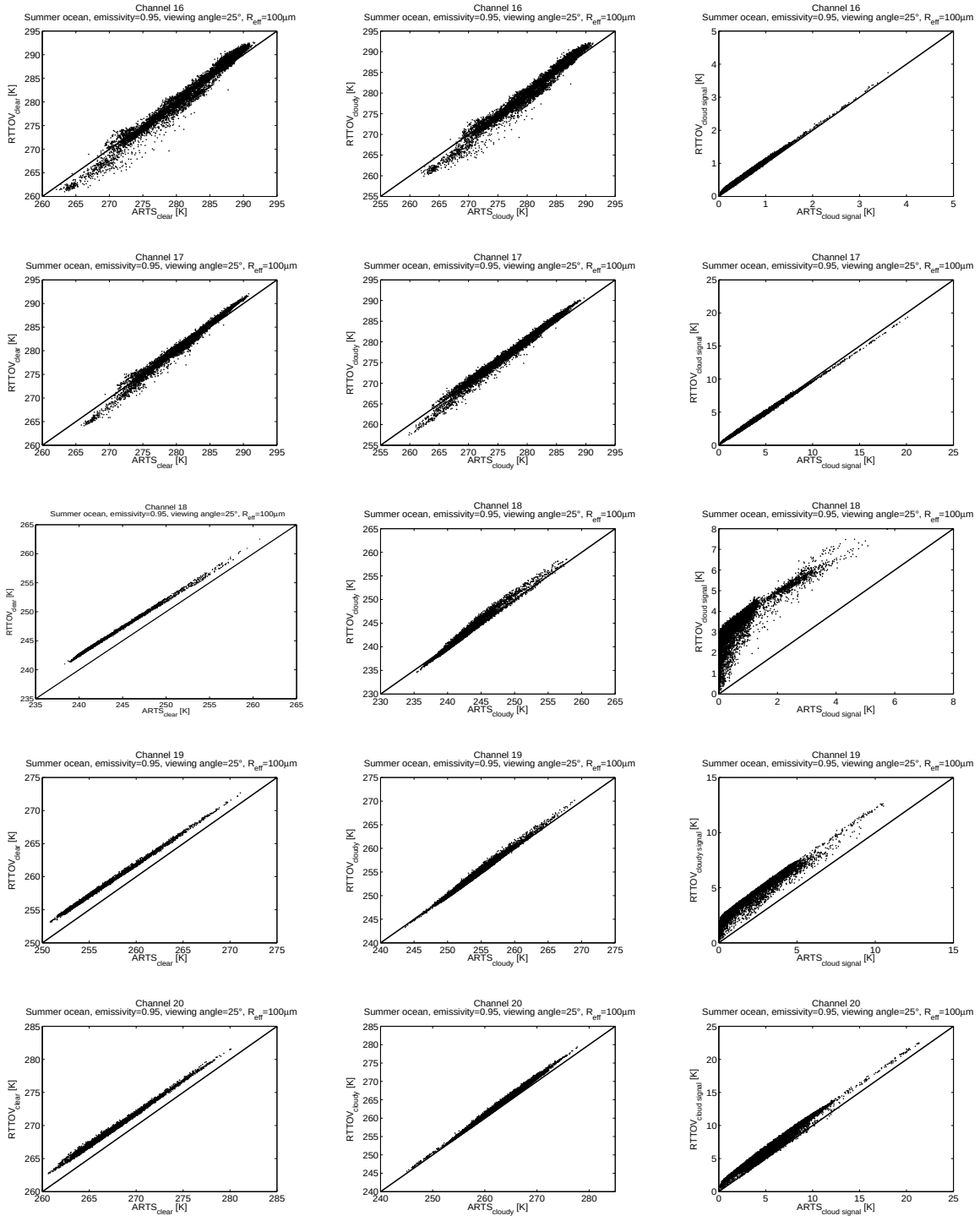

Figure 12: BT simulated for the ocean summer data set by RTTOVSCATT (for both clear sky simulations and cloudy simulations) against BT simulated by ARTS for a particular set of parameters (emissivity=0.95, viewing angle=25°, and effective radius of the ice particles= 100μm). Each line correspond to one AMSU-B channel from top to bottom channel 16 (89 GHz), 17 (150 GHz), 18 (183.31±1 GHz), 19 (183.31±3 GHz), and 20 (183.31±7 GHz). The left column correspond to clear sky simulations, the middle column corresponds to cloudy simulations and the right column corresponds to the cloud signal (clear sky BT minus cloudy BT).

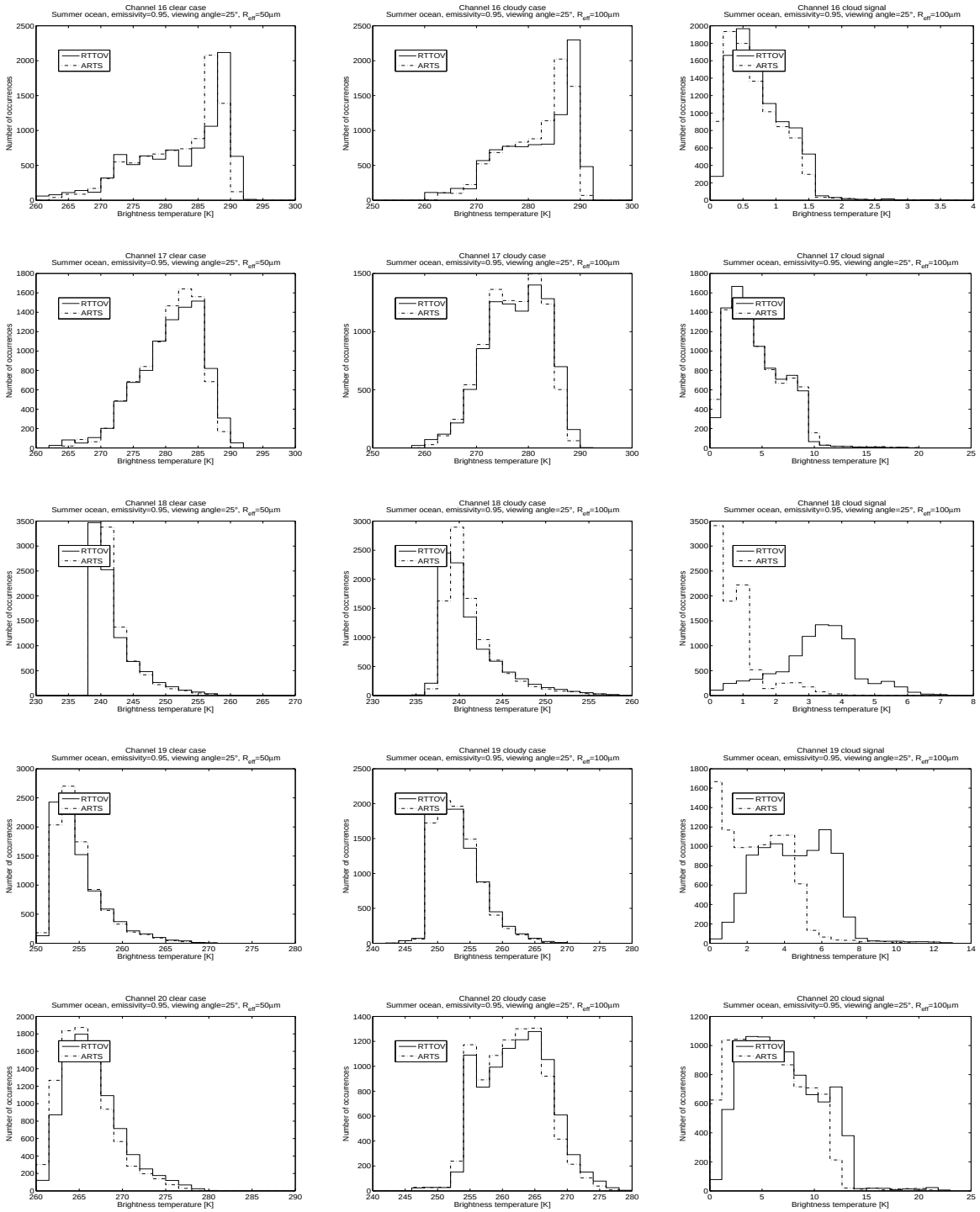

Figure 13: Histograms of BT simulated for the ocean summer data set by RTTOVSCATT (for both clear sky simulations and cloudy simulations), (plain line), and of BT simulated by ARTS (dashed line) for a particular set of parameters (emissivity=0.95, viewing angle=25°, and effective radius of the ice particles= 100μm). Each line correspond to one AMSU-B channel from top to bottom channel 16 (89 GHz), 17 (150 GHz), 18 (183.31±1 GHz), 19 (183.31±3 GHz), and 20 (183.31±7 GHz). The left column correspond to clear sky simulations, the middle column corresponds to cloudy simulations and the right column corresponds to the cloud signal (clear sky BT minus cloudy BT).

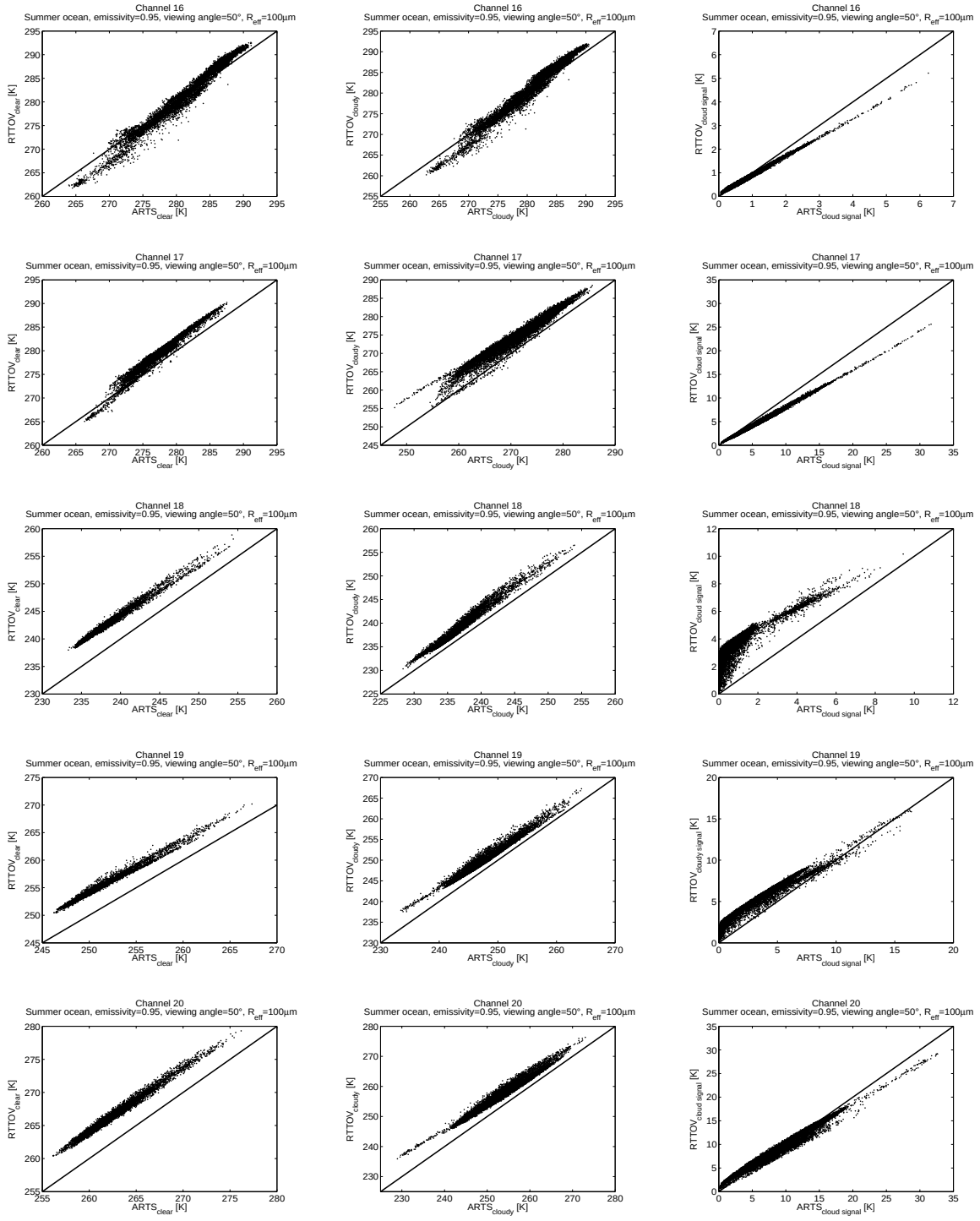

Figure 14: BT simulated for the ocean summer data set by RTTOVSCATT (for both clear sky simulations and cloudy simulations) against BT simulated by ARTS for a particular set of parameters (emissivity=0.95, viewing angle=50°, and effective radius of the ice particles= 100μm). Each line correspond to one AMSU-B channel from top to bottom channel 16 (89 GHz), 17 (150 GHz), 18 (183.31±1 GHz), 19 (183.31±3 GHz), and 20 (183.31±7 GHz). The left column correspond to clear sky simulations, the middle column corresponds to cloudy simulations and the right column corresponds to the cloud signal (clear sky BT minus cloudy BT).

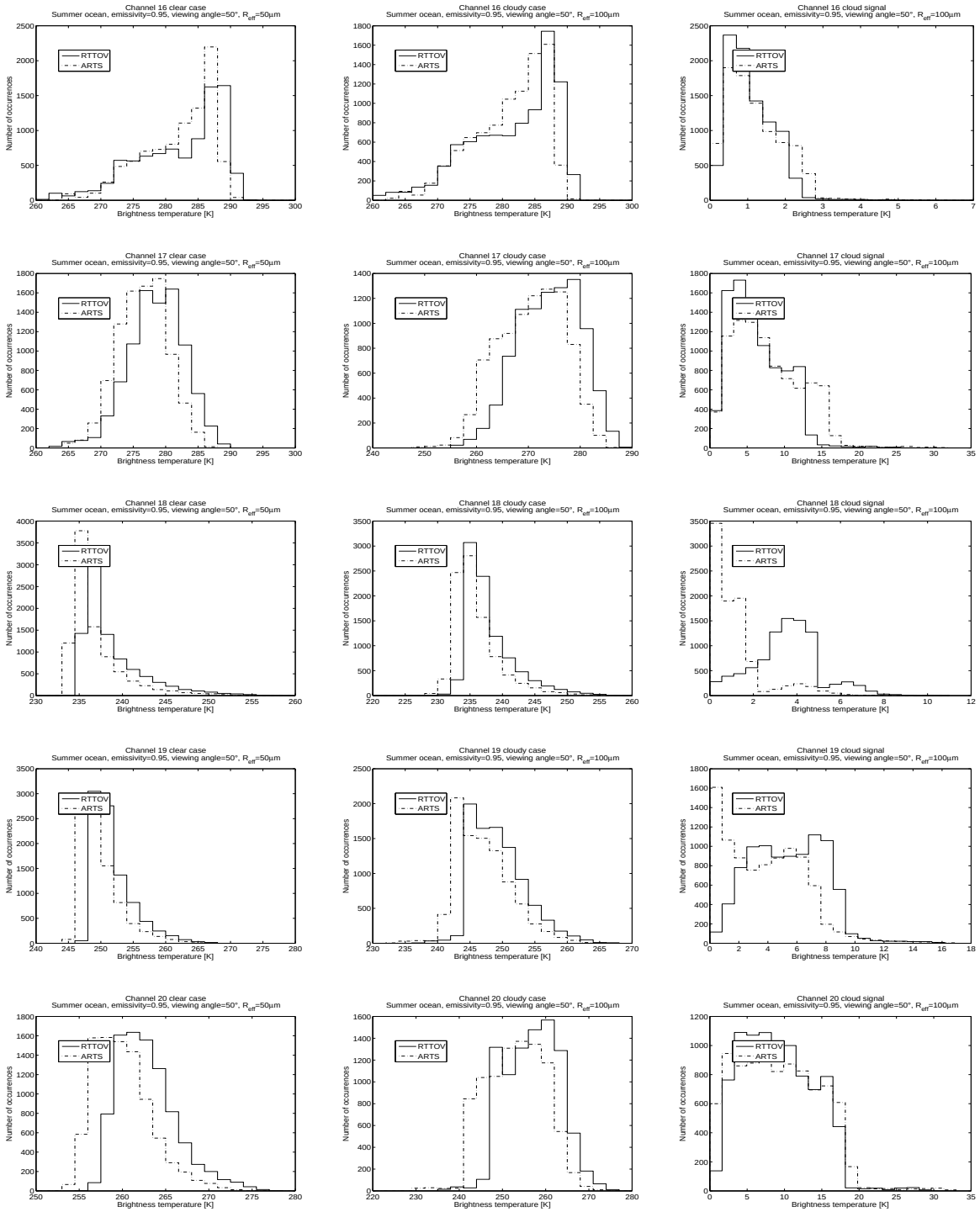

Figure 15: Histograms of BT simulated for the ocean summer data set by RTTOVSCATT (for both clear sky simulations and cloudy simulations), (plain line), and of BT simulated by ARTS (dashed line) for a particular set of parameters (emissivity=0.95, viewing angle=50°, and effective radius of the ice particles= 100μm). Each line correspond to one AMSU-B channel from top to bottom channel 16 (89 GHz), 17 (150 GHz), 18 (183.31±1 GHz), 19 (183.31±3 GHz), and 20 (183.31±7 GHz). The left column correspond to clear sky simulations, the middle column corresponds to cloudy simulations and the right column corresponds to the cloud signal (clear sky BT minus cloudy BT).

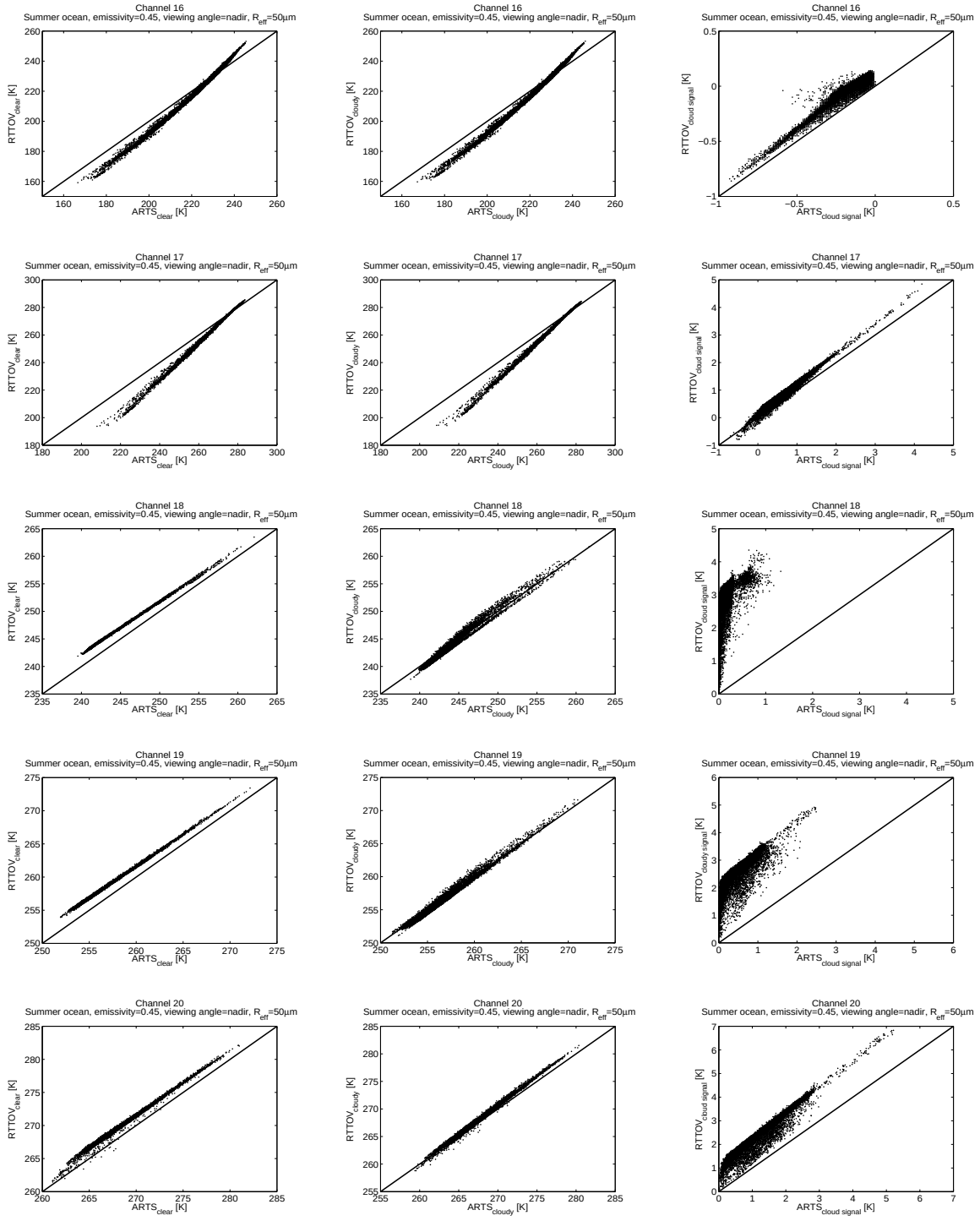

Figure 16: BT simulated for the ocean summer data set by RTTOVSCATT (for both clear sky simulations and cloudy simulations) against BT simulated by ARTS for a particular set of parameters (emissivity=0.45, viewing angle=nadir, and effective radius of the ice particles= 50μm). Each line correspond to one AMSU-B channel from top to bottom channel 16 (89 GHz), 17 (150 GHz), 18 (183.31±1 GHz), 19 (183.31±3 GHz), and 20 (183.31±7 GHz). The left column correspond to clear sky simulations, the middle column corresponds to cloudy simulations and the right column corresponds to the cloud signal (clear sky BT minus cloudy BT).

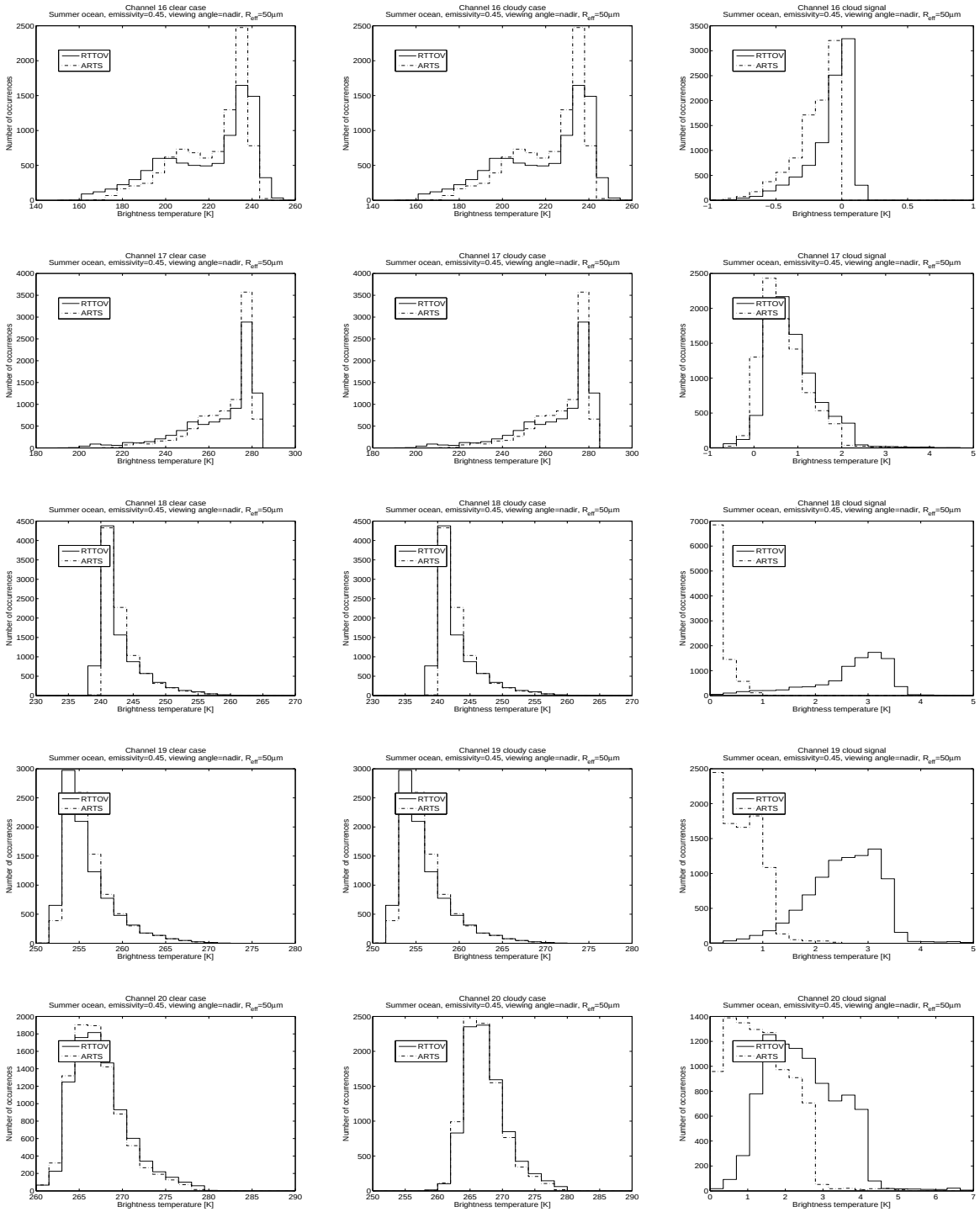

Figure 17: Histograms of BT simulated for the ocean summer data set by RTTOVSCATT (for both clear sky simulations and cloudy simulations), (plain line), and of BT simulated by ARTS (dashed line) for a particular set of parameters (emissivity=0.45, viewing angle=nadir, and effective radius of the ice particles= 50μm). Each line correspond to one AMSU-B channel from top to bottom channel 16 (89 GHz), 17 (150 GHz), 18 (183.31$\pm$1 GHz), 19 (183.31$\pm$3 GHz), and 20 (183.31$\pm$7 GHz). The left column correspond to clear sky simulations, the middle column corresponds to cloudy simulations and the right column corresponds to the cloud signal (clear sky BT minus cloudy BT).

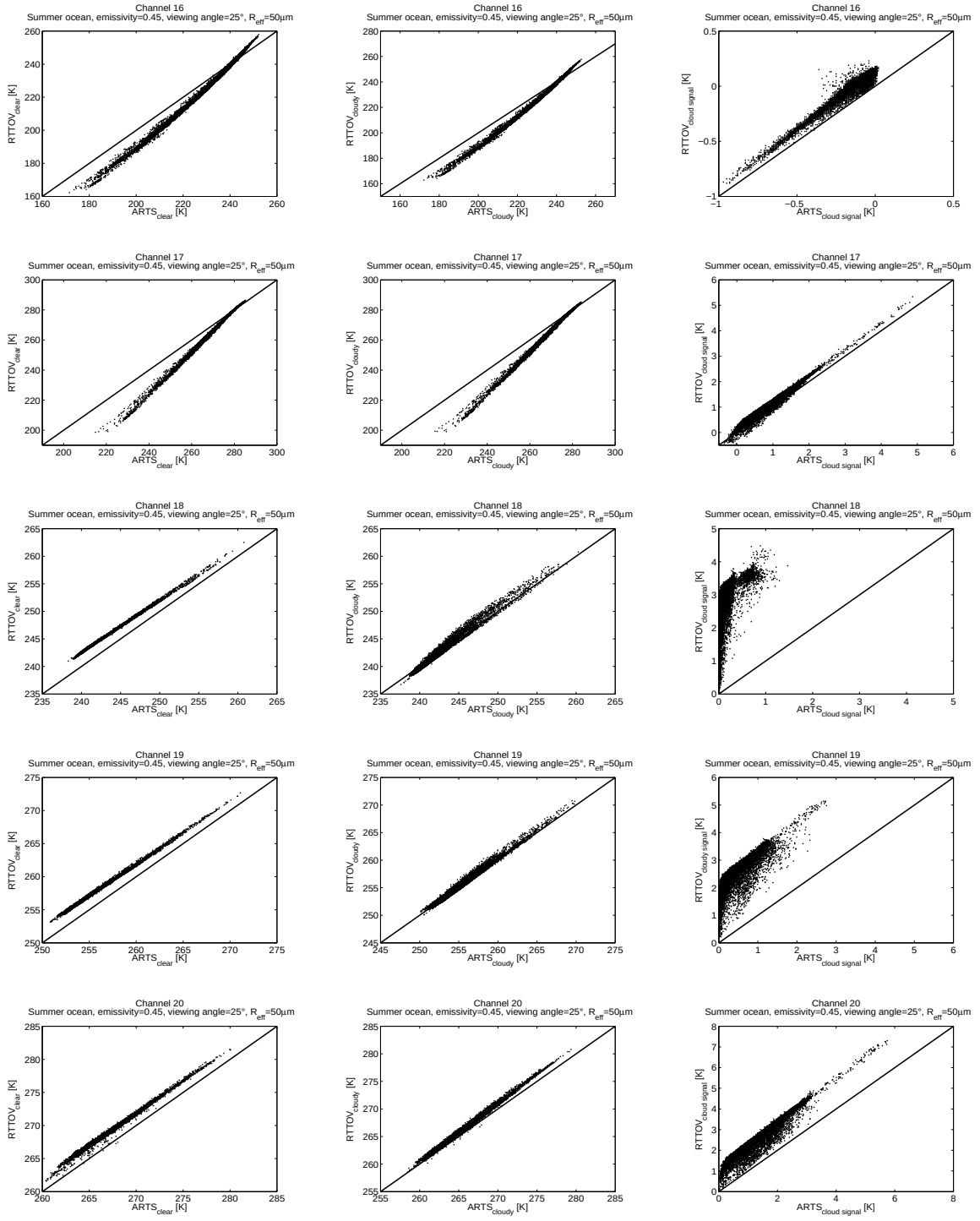

Figure 18: BT simulated for the ocean summer data set by RTTOVSCATT (for both clear sky simulations and cloudy simulations) against BT simulated by ARTS for a particular set of parameters (emissivity=0.45, viewing angle=25°, and effective radius of the ice particles= 50μm). Each line correspond to one AMSU-B channel from top to bottom channel 16 (89 GHz), 17 (150 GHz), 18 (183.31±1 GHz), 19 (183.31±3 GHz), and 20 (183.31±7 GHz). The left column correspond to clear sky simulations, the middle column corresponds to cloudy simulations and the right column corresponds to the cloud signal (clear sky BT minus cloudy BT).

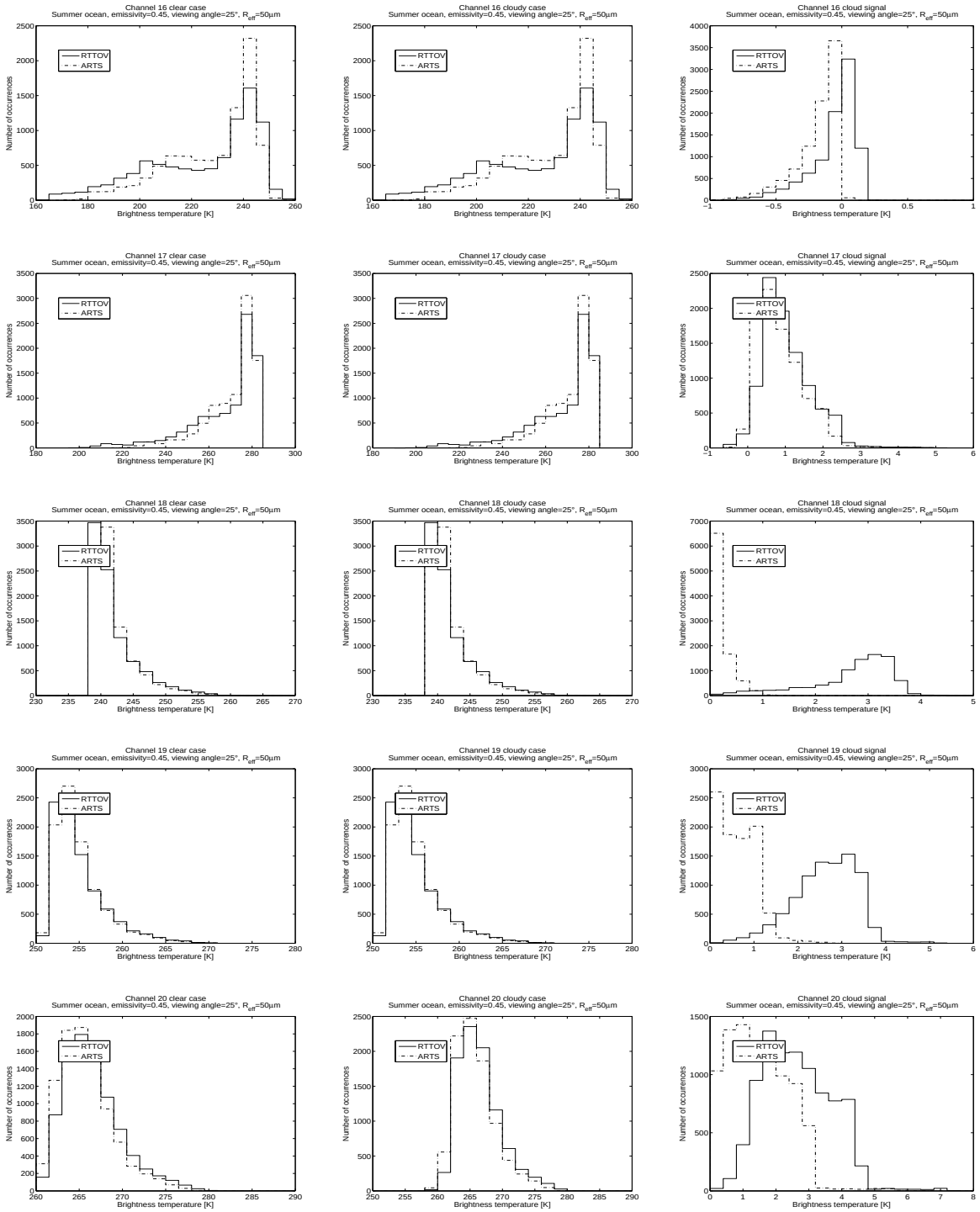

Figure 19: Histograms of BT simulated for the ocean summer data set by RTTOVSCATT (for both clear sky simulations and cloudy simulations), (plain line), and of BT simulated by ARTS (dashed line) for a particular set of parameters (emissivity=0.45, viewing angle=25°, and effective radius of the ice particles= 50μm). Each line correspond to one AMSU-B channel from top to bottom channel 16 (89 GHz), 17 (150 GHz), 18 (183.31±1 GHz), 19 (183.31±3 GHz), and 20 (183.31±7 GHz). The left column correspond to clear sky simulations, the middle column corresponds to cloudy simulations and the right column corresponds to the cloud signal (clear sky BT minus cloudy BT).

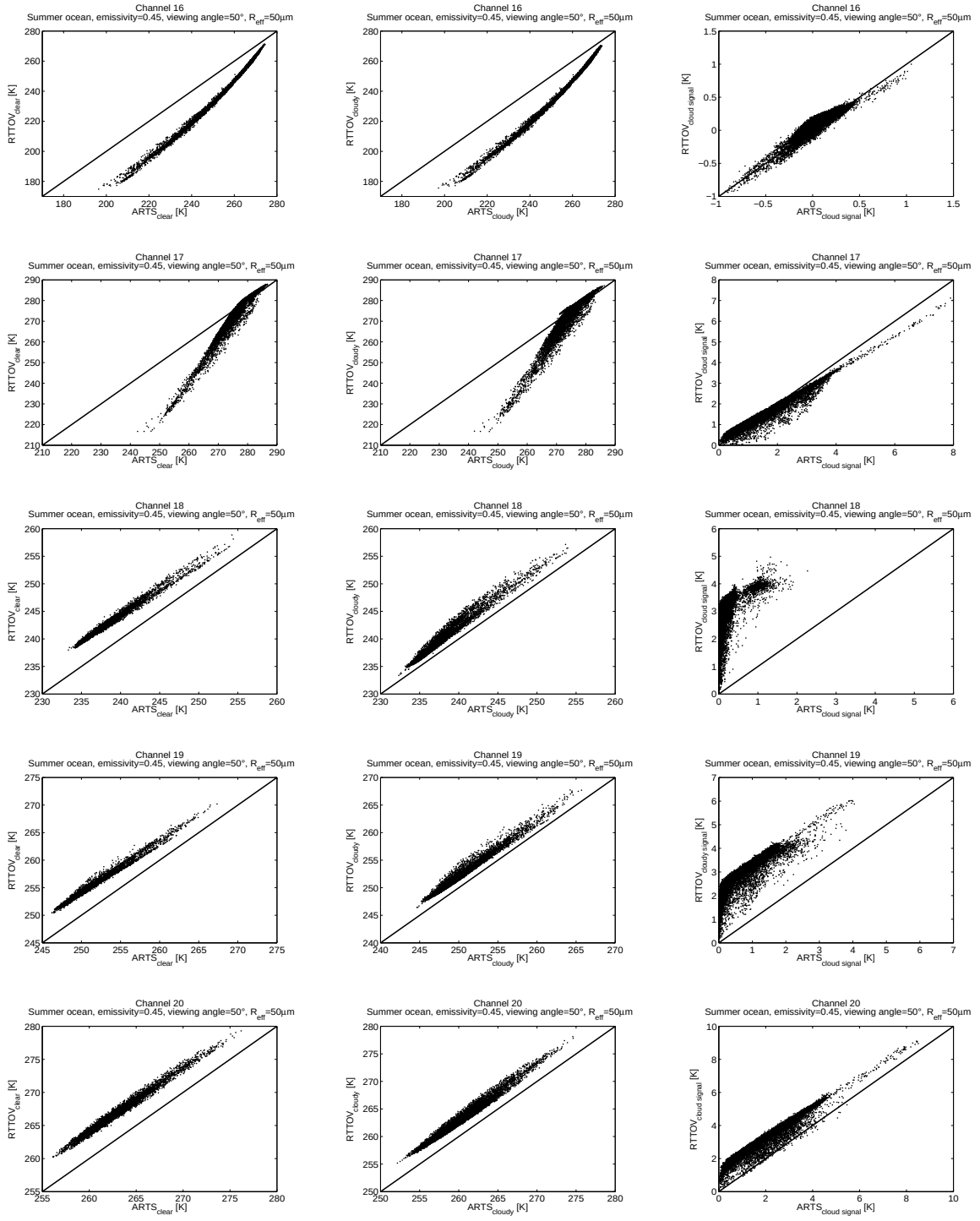

Figure 20: BT simulated for the ocean summer data set by RTTOVSCATT (for both clear sky simulations and cloudy simulations) against BT simulated by ARTS for a particular set of parameters (emissivity=0.45, viewing angle=50°, and effective radius of the ice particles= 50μm). Each line correspond to one AMSU-B channel from top to bottom channel 16 (89 GHz), 17 (150 GHz), 18 (183.31±1 GHz), 19 (183.31±3 GHz), and 20 (183.31±7 GHz). The left column correspond to clear sky simulations, the middle column corresponds to cloudy simulations and the right column corresponds to the cloud signal (clear sky BT minus cloudy BT).

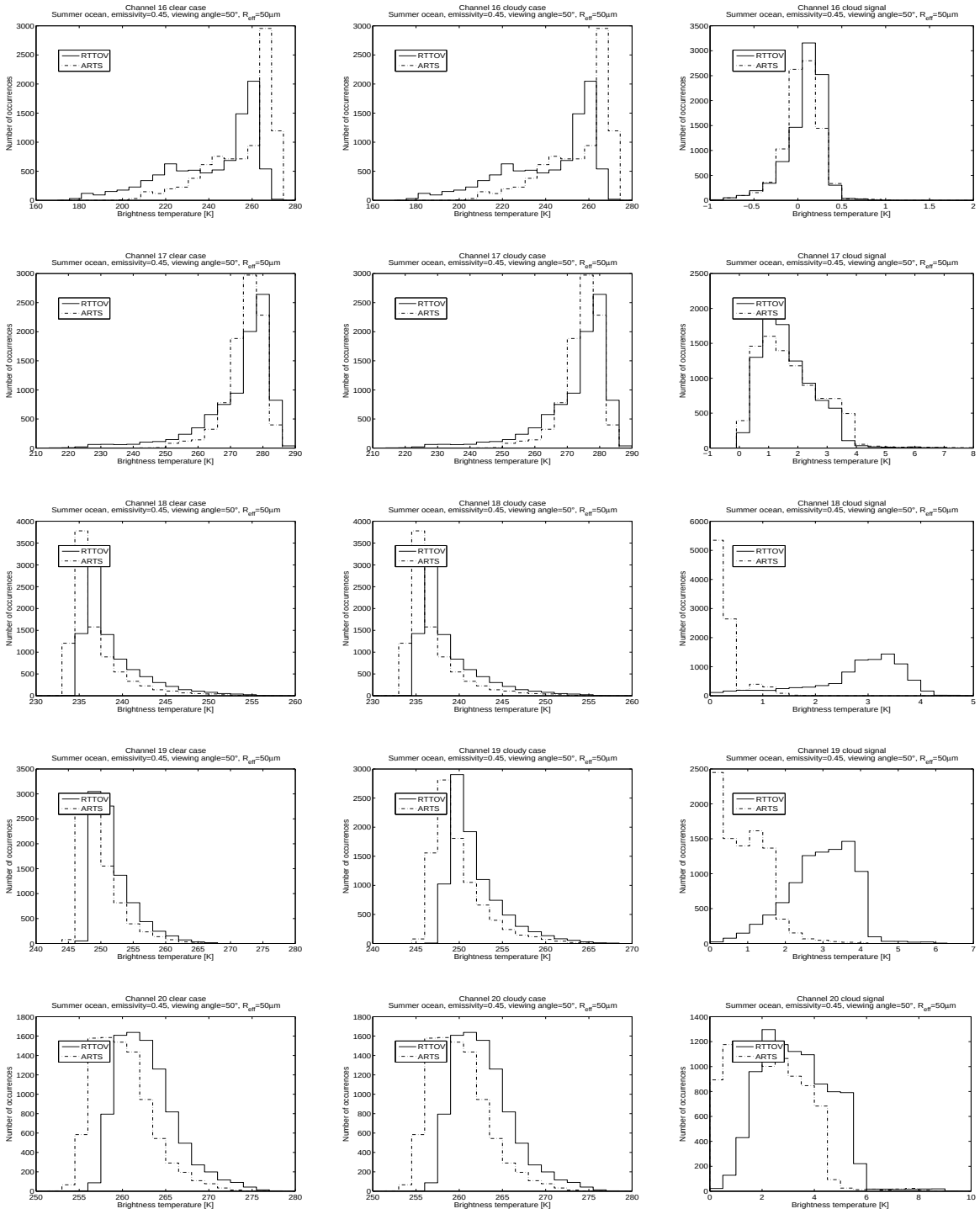

Figure 21: Histograms of BT simulated for the ocean summer data set by RTTOVSCATT (for both clear sky simulations and cloudy simulations), (plain line), and of BT simulated by ARTS (dashed line) for a particular set of parameters (emissivity=0.45, viewing angle=50°, and effective radius of the ice particles= 50μm). Each line correspond to one AMSU-B channel from top to bottom channel 16 (89 GHz), 17 (150 GHz), 18 (183.31±1 GHz), 19 (183.31±3 GHz), and 20 (183.31±7 GHz). The left column correspond to clear sky simulations, the middle column corresponds to cloudy simulations and the right column corresponds to the cloud signal (clear sky BT minus cloudy BT).

has shown that the clear sky results between these two models agreed better for a higher emissivity value (the emissivity values used were 0.6 and 0.95), the agreement being the best for channel 18 (for which the differences are only for extremely dry profiles) and the worse for channel 20 (for which the differences can also appear for moister profiles). For the surface channels (16 and 17), the emissivity value has an influence on the results, the model results agree better with the high emissivity (0.95) than with the low emissivity (0.45). For the other sounding channels the emissivity value has no impact on the clear sky results. The emissivity value has no impact either on the cloudy results nor on the cloud signal results for the sounding channels, the results being similar for the simulation with the effective radius of 50 μm independently of the emissivity value which is used.

For the surface channels the results are different. The agreement is not good between both models for the clear sky and cloudy cases for the lowest BT, ARTS being warmer than RTTOVSCATT. These differences are increasing with increasing viewing angle. For the highest BT the agreement is better. For channel 16, the cloud signal presents an offset (RTTOVSCATT showing a greater cloud signal than ARTS) for the nadir and the 25° viewing angles, the agreement looks better for the 50° viewing angle although there is still a lot of scatter between the model results. For channel 17, the cloud signal agreement is good for the low values of the cloud signal and poorer for higher values, RTTOVSCATT shows greater values for the nadir and 25° viewing angle while ARTS shows greater values for the 50° viewing angle, this case shows also a greater scatter in the results. For the surface channels and with this low emissivity value, the cloud signal goes negative in some cases (particularly for channel 16), this behaviour is expected in the case of a warm cloud over a cold ocean surface.

3.6 Low emissivity case (0.45) combined with an effective distribution radius of the ice scatterers of 100 μm for the ocean summer data set

See figure 22 to 27 for the plots corresponding to this case.

The results for this case are rather similar to the ones for the previous case with the same emissivity but with a smaller effective radius. Because of the greater effective radius the cloud signal has a greater amplitude for all channels (the channels the most affected by this increase of the cloud signal magnitude are channel 17 and 20). The results for the clear sky case and for the cloudy case, for the surface channels are strongly deviating from the diagonal for the lowest BT ARTS being warmer than RTTOVSCATT for low BT, this was also described for the previous case.

4 Results for the land summer, land winter, and ocean winter data sets

The overall results for the land summer, land winter, and ocean winter data sets are similar to the ones for the ocean summer data sets. There are only few slight differences described below.

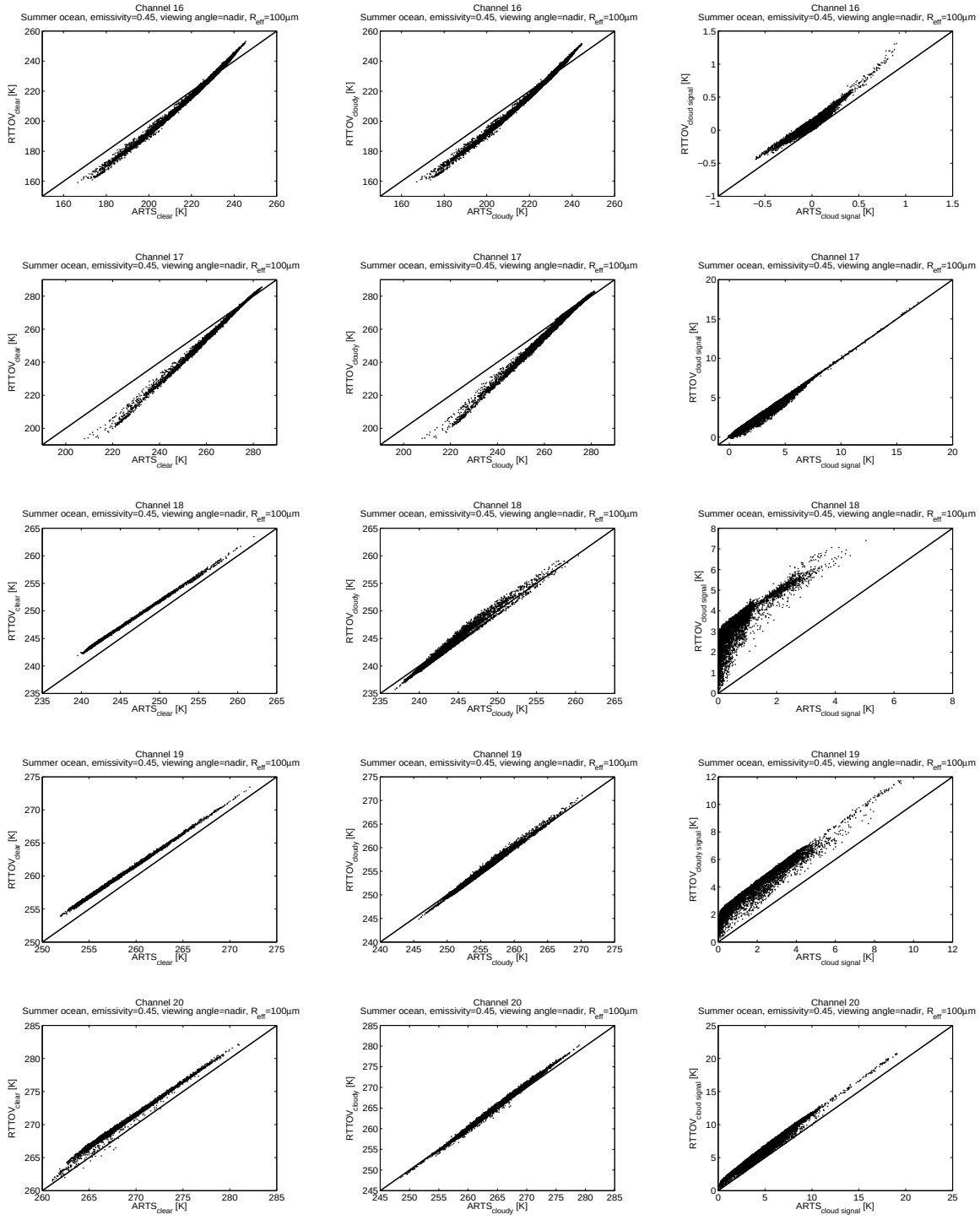

Figure 22: BT simulated for the ocean summer data set by RTTOVSCATT (for both clear sky simulations and cloudy simulations) against BT simulated by ARTS for a particular set of parameters (emissivity=0.45, viewing angle=nadir, and effective radius of the ice particles= 100μm). Each line correspond to one AMSU-B channel from top to bottom channel 16 (89 GHz), 17 (150 GHz), 18 (183.31±1 GHz), 19 (183.31±3 GHz), and 20 (183.31±7 GHz). The left column correspond to clear sky simulations, the middle column corresponds to cloudy simulations and the right column corresponds to the cloud signal (clear sky BT minus cloudy BT).

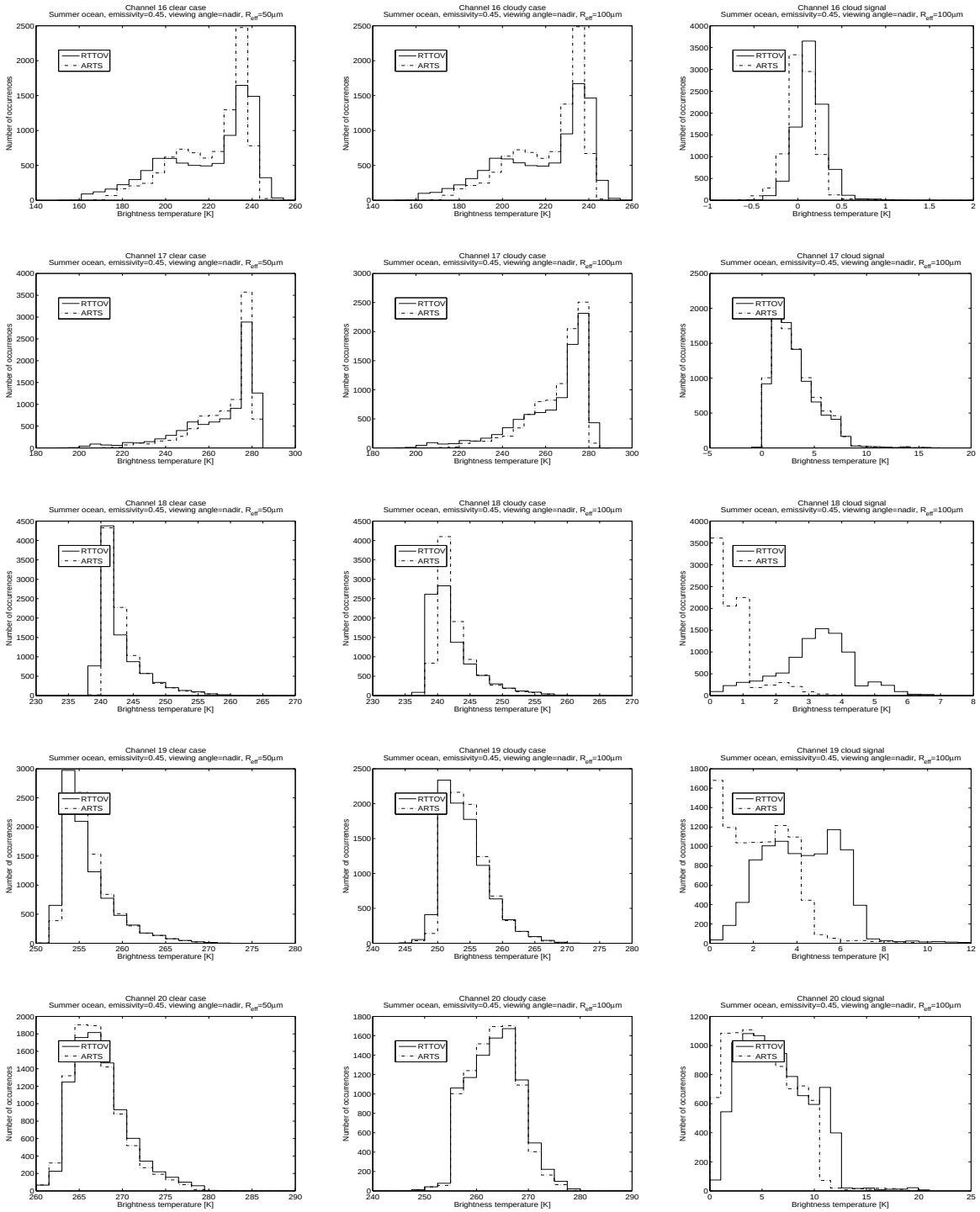

Figure 23: Histograms of BT simulated for the ocean summer data set by RTTOVSCATT (for both clear sky simulations and cloudy simulations), (plain line), and of BT simulated by ARTS (dashed line) for a particular set of parameters (emissivity=0.45, viewing angle=nadir, and effective radius of the ice particles= 100μm). Each line correspond to one AMSU-B channel from top to bottom channel 16 (89 GHz), 17 (150 GHz), 18 (183.31$\pm$1 GHz), 19 (183.31$\pm$3 GHz), and 20 (183.31$\pm$7 GHz). The left column correspond to clear sky simulations, the middle column corresponds to cloudy simulations and the right column corresponds to the cloud signal (clear sky BT minus cloudy BT).

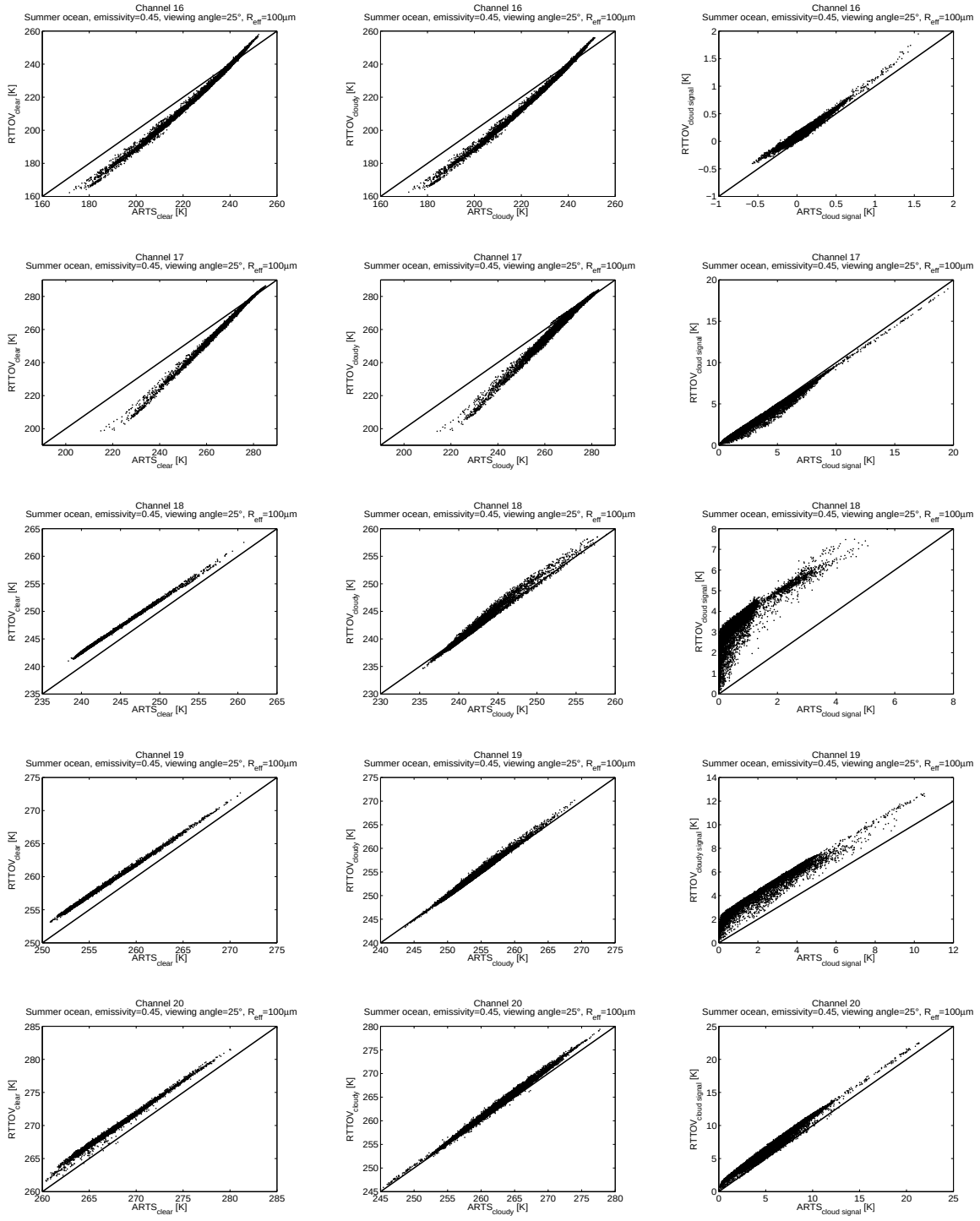

Figure 24: BT simulated for the ocean summer data set by RTTOVSCATT (for both clear sky simulations and cloudy simulations) against BT simulated by ARTS for a particular set of parameters (emissivity=0.45, viewing angle=25°, and effective radius of the ice particles= 100μm). Each line correspond to one AMSU-B channel from top to bottom channel 16 (89 GHz), 17 (150 GHz), 18 (183.31±1 GHz), 19 (183.31±3 GHz), and 20 (183.31±7 GHz). The left column correspond to clear sky simulations, the middle column corresponds to cloudy simulations and the right column corresponds to the cloud signal (clear sky BT minus cloudy BT).

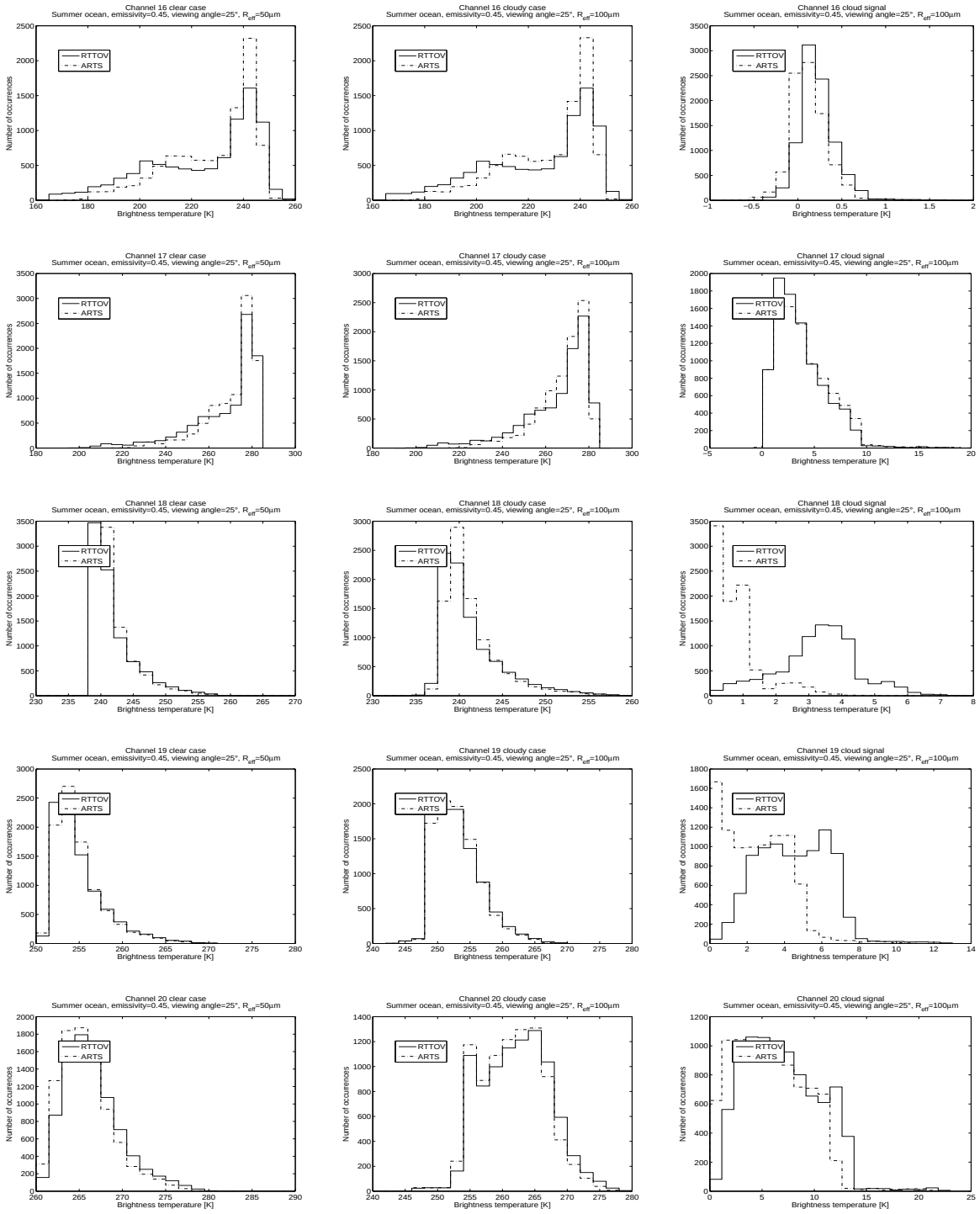

Figure 25: Histograms of BT simulated for the ocean summer data set by RTTOVSCATT (for both clear sky simulations and cloudy simulations), (plain line), and of BT simulated by ARTS (dashed line) for a particular set of parameters (emissivity=0.45, viewing angle=25°, and effective radius of the ice particles= 100μm). Each line correspond to one AMSU-B channel from top to bottom channel 16 (89 GHz), 17 (150 GHz), 18 (183.31±1 GHz), 19 (183.31±3 GHz), and 20 (183.31±7 GHz). The left column correspond to clear sky simulations, the middle column corresponds to cloudy simulations and the right column corresponds to the cloud signal (clear sky BT minus cloudy BT).

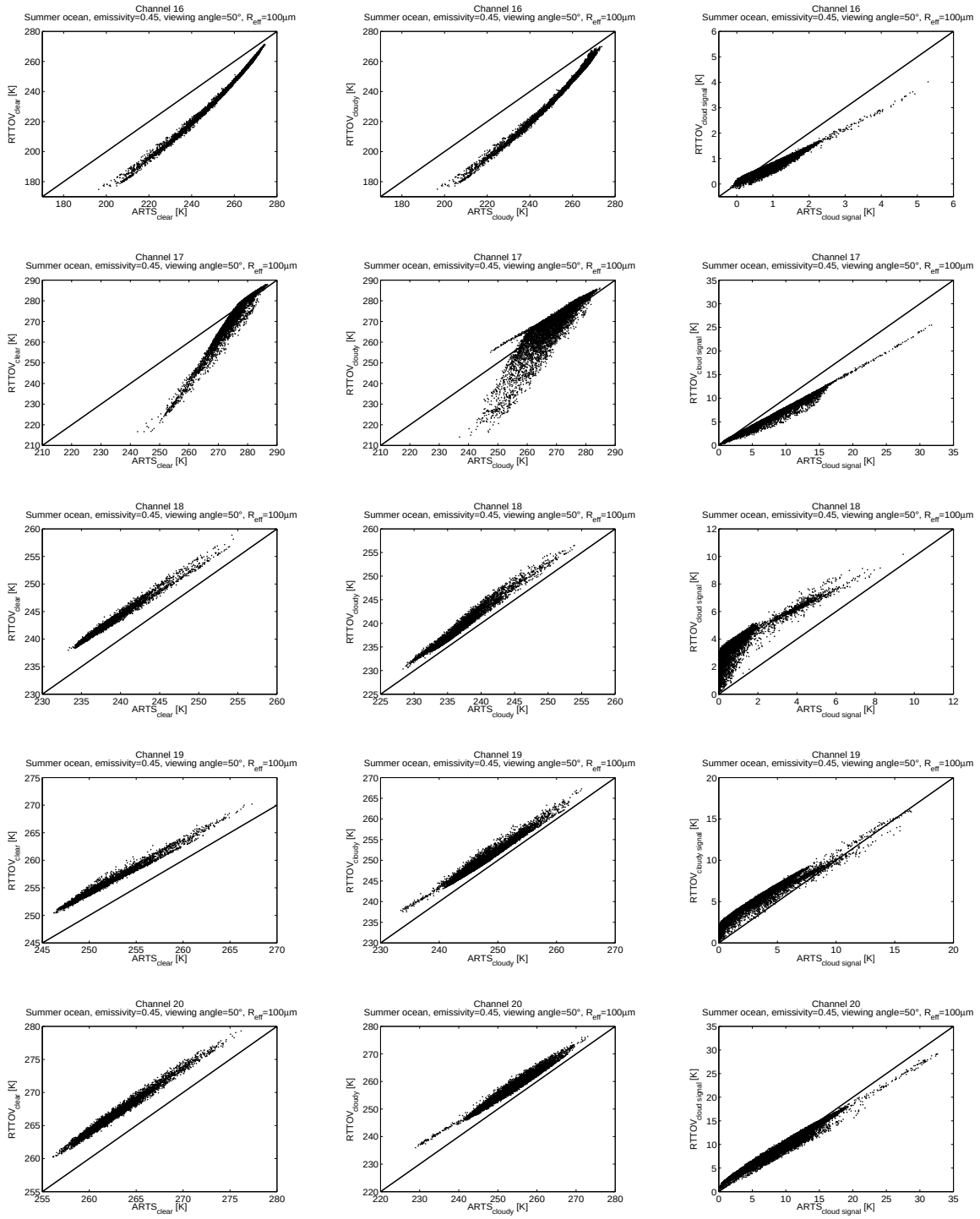

Figure 26: BT simulated for the ocean summer data set for the ocean summer data set by RTTOVSCATT (for both clear sky simulations and cloudy simulations) against BT simulated by ARTS for a particular set of parameters (emissivity=0.45, viewing angle=50°, and effective radius of the ice particles= 100μm). Each line correspond to one AMSU-B channel from top to bottom channel 16 (89 GHz), 17 (150 GHz), 18 (183.31±1 GHz), 19 (183.31±3 GHz), and 20 (183.31±7 GHz). The left column correspond to clear sky simulations, the middle column corresponds to cloudy simulations and the right column corresponds to the cloud signal (clear sky BT minus cloudy BT).

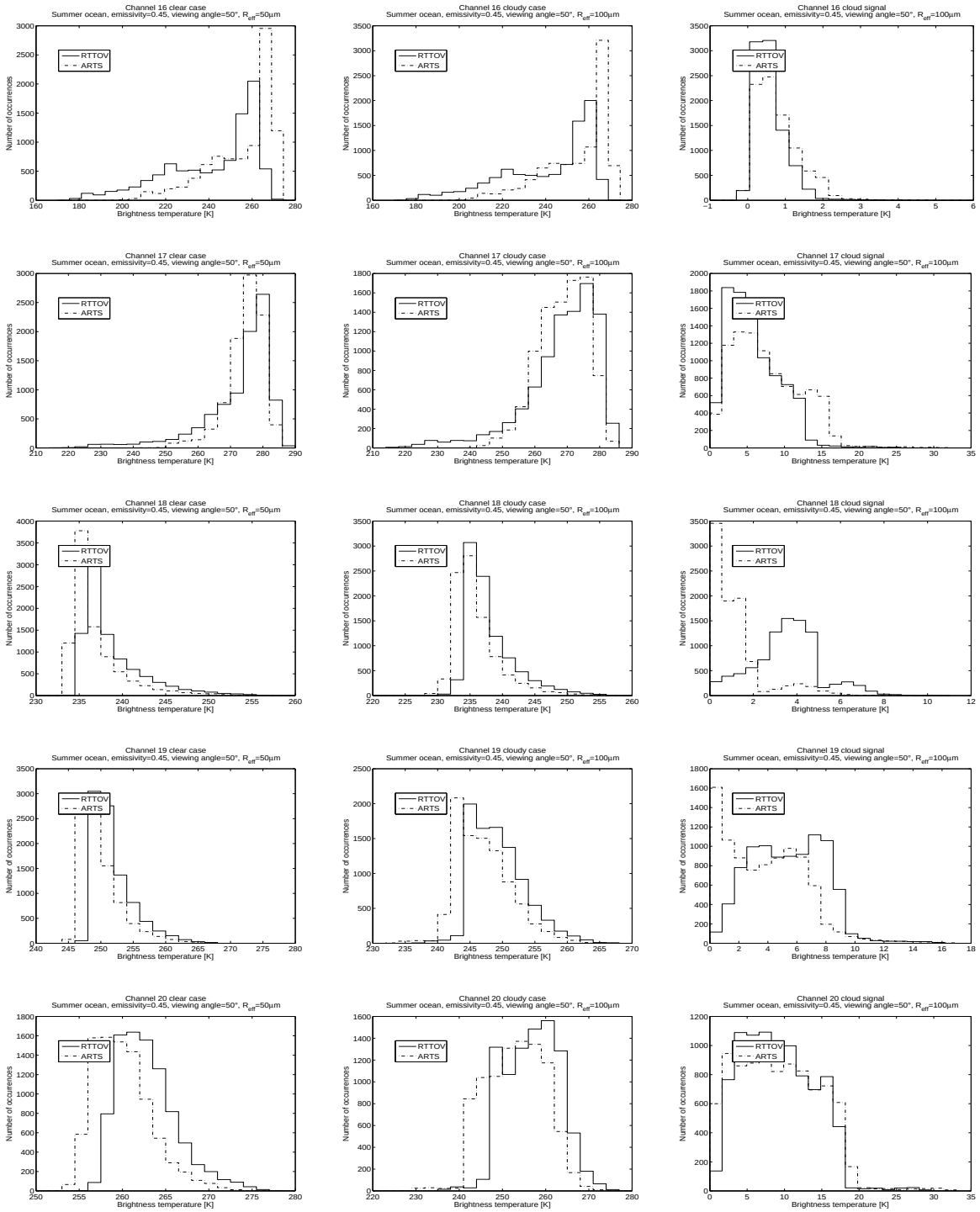

Figure 27: Histograms of BT simulated for the ocean summer data set by RTTOVSCATT (for both clear sky simulations and cloudy simulations), (plain line), and of BT simulated by ARTS (dashed line) for a particular set of parameters (emissivity=0.45, viewing angle=50°, and effective radius of the ice particles= 100μm). Each line correspond to one AMSU-B channel from top to bottom channel 16 (89 GHz), 17 (150 GHz), 18 (183.31±1 GHz), 19 (183.31±3 GHz), and 20 (183.31±7 GHz). The left column correspond to clear sky simulations, the middle column corresponds to cloudy simulations and the right column corresponds to the cloud signal (clear sky BT minus cloudy BT).

4.1 Land summer

For the land summer data set and an emissivity of 0.45, there are some differences for channel 16 and 17 for the clear and cloudy cases the scatter plots follow more the diagonal than for the ocean summer data set. The cloud signal results are similar for both data sets, only for the 50° viewing angle the results are more going off the diagonal for the land summer data set than for the ocean summer data set. Furthermore for the same emissivity (0.45), for channel 20 there are some outliers at low BT that show more than 10 K difference between the models, this was not visible for the ocean summer data set but it concerns only few profiles of the land summer data set.

For the higher emissivity 0.95, the offset for the clear and cloudy cases is less than for the ocean summer data set, for all viewing angles and both effective radius.

4.2 Land winter

Differences are visible in cloud signal results for channel 18 with an emissivity of 0.45 and an effective radius of 100 μm. The highest ARTS cloud signal points which were visible for the ocean summer data set are not visible for the land winter data set, but the highest RTTOV cloud signal points are still there, consequently the scatter plot which followed the diagonal with an offset for the ocean summer data set doesn't follow the diagonal at all for the land winter data set. Similar differences occur for channel 18, 19 and 20 for an emissivity of 0.45 and an effective radius of 50 μm, for the highest emissivity (0.95) and the 50 μm effective radius, this is also visible for channel 18 and to less extend for channel 19.

Like for the land summer data set, for channel 20 for the low surface emissivity (0.45), there are outliers at low BT that show differences of about 10 K.

4.3 Ocean winter

The low BT outliers for channel 20 for the low surface emissivity are also visible for the ocean winter data set results. Furthermore, for channel 20 for the greatest viewing angle (50°) more scatter is visible around the diagonal for the clear and the cloudy case than for the other data sets. As for the land winter data set for channel 18, for the low emissivity value, the values for the ARTS cloud signal are lower than for the the ocean summer data set, the RTTOV cloud signal values not being changed.

For channel 16 and 17, for the higher emissivity value (0.95) for the clear and cloudy cases the scatter plots show a wider scatter around the diagonal, than for the other data sets.

5 Conclusion

The study shows that there are differences related to the clear sky simulations, between the simulation produced with RTTOV and RTTOVSCATT

without including ice scatterers. This is highly unexpected.

Furthermore, RTTOVSCATT shows an unexpected behaviour for low IWP values in all cases which leads to an unexpected cloud signal, this is apparent in all channels but so far it is not clear to us what is the reason for this behaviour.

The results for the ocean summer data set have been described and analysed in detail. In all the cases the viewing angle has little influence on the BT differences between the models when the viewing angles are small. There is, for example, no noticeable difference between a nadir and a 25° viewing angle simulation, but there is a difference when the considered viewing angle is 50°. The differences between both models due to viewing angles appear only for extreme off nadir viewing angles.The emissivity value has only a very small influence on the results for the sounding channels (18, 19, and 20). Although the emissivity is not expected to have an impact on the sounding channel because the profiles in the ocean summer data set are moist and having a surface elevation at sea level, this agrees with the previous study done by *Buehler et al.* [2006], which shows that the differences between ARTS and RTTOV for clear sky simulations are greater for lower emissivity values, even for the AMSU-B sounding channels (these differences depend upon the channel and the profile humidity, for channel 18 these differences are shown only for very dry profiles, but for channel 20 even some normally dry profiles are affected by a difference between both model results). For the surface channels the influence of the emissivity value is greater, the agreement between the results for the lower emissivity value is very bad (about 10 K difference in some cases) for the clear and cloudy cases, however, agreement for the cloud signal is better for the surface channels than for the sounding channels. The only influence that the effective radius has on the results is that the amplitude of the cloud signal increases with increasing effective radius, this makes the scatter plot looking better for the simulations produced with highest effective radius, however, the absolute difference between both models is the same in both cases.

The results for the other data sets, namely, ocean winter, land summer, and land winter data sets are shown in the appendix however, the overall results are similar to the deeply analysed results for the ocean summer data set. Only few differences are visible and were described.

References

Bauer, P., E. Moreau, F. Chevallier, and U. O'Keeffe, Multiple-scattering microwave radiative transfer for data assimilation applications, *Q. J. R. Meteorol. Soc.*, *132*, 1259–1281, 2006.

Buehler, S. A., N. Courcoux, and V. O. John, Radiative transfer calculations for a passive microwave satellite sensor: Comparing a fast model and a line-by-line model, *J. Geophys. Res.*, *111*, D20304, doi: 10.1029/2005JD006552, 2006.

Davis, C., C. Emde, and R. Harwood, A 3D polarized reversed monte carlo

radiative transfer model for mm and sub-mm passive remote sensing in cloudy atmospheres, *IEEE T. Geosci. Remote*, *43*(6), 1096–1101, 2005.

Emde, C., S. A. Buehler, C. Davis, P. Eriksson, T. R. Sreerekha, and C. Teichmann, A polarized discrete ordinate scattering model for simulations of limb and nadir longwave measurements in 1D/3D spherical atmospheres, *J. Geophys. Res.*, *109*(D24), D24207, doi:10.1029/2004JD005140, 2004.

Eriksson, P., S. A. Buehler, C. Emde, T. R. Sreerekha, C. Melsheimer, and O. Lemke, *ARTS-1-1 User Guide*, University of Bremen, 308 pages, regularly updated versions available at www.sat.uni-bremen.de/arts/, 2004.

Evans, K. F., and G. L. Stephens, Microwave radiative transfer through clouds composed of realistically shaped ice crystals. Part I:Single scattering properties, *J. Atmos. Sci.*, *52*(11), 2041–2057, 1995.

Mishchenko, M. I., and L. D. Travis, Capabilities and limitations of a current fortran implementation of the T-matrix method for randomly oriented, rotationally symmetric scatterers, *J. Quant. Spectrosc. Radiat. Transfer*, *60*(3), 309–324, 1998.

Saunders, R. W., T. J. Hewison, S. J. Stringer, and N. C. Atkinson, The radiometric characterization of AMSU-B, *IEEE T. Microw. Theory*, *43*(4), 760–771, 1995.

6 Appendix

These appendix contain the plots (scatter plots and histograms) describing the results of the comparison for the data sets ocean winter (Figure 28 to 51), land summer (Figure 52 to 75), and land winter (Figure 76 to 99).

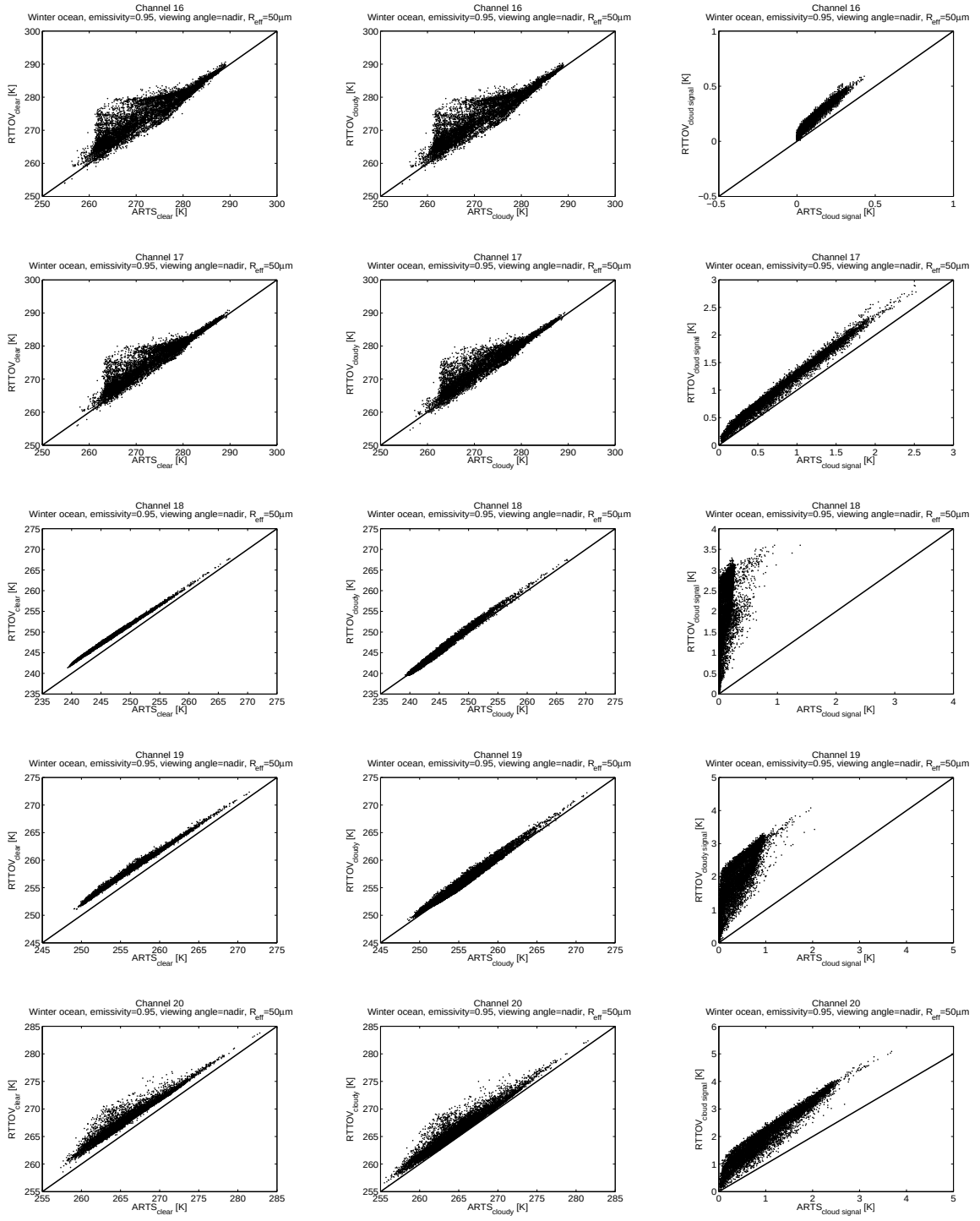

Figure 28: BT simulated for the ocean winter data set by RTTOVSCATT (for both clear sky simulations and cloudy simulations) against BT simulated by ARTS for a particular set of parameters (emissivity=0.95, viewing angle=nadir, and effective radius of the ice particles= 50μm). Each line correspond to one AMSU-B channel from top to bottom channel 16 (89 GHz), 17 (150 GHz), 18 (183.31±1 GHz), 19 (183.31±3 GHz), and 20 (183.31±7 GHz). The left column correspond to clear sky simulations, the middle column corresponds to cloudy simulations and the right column corresponds to the cloud signal (clear sky BT minus cloudy BT).

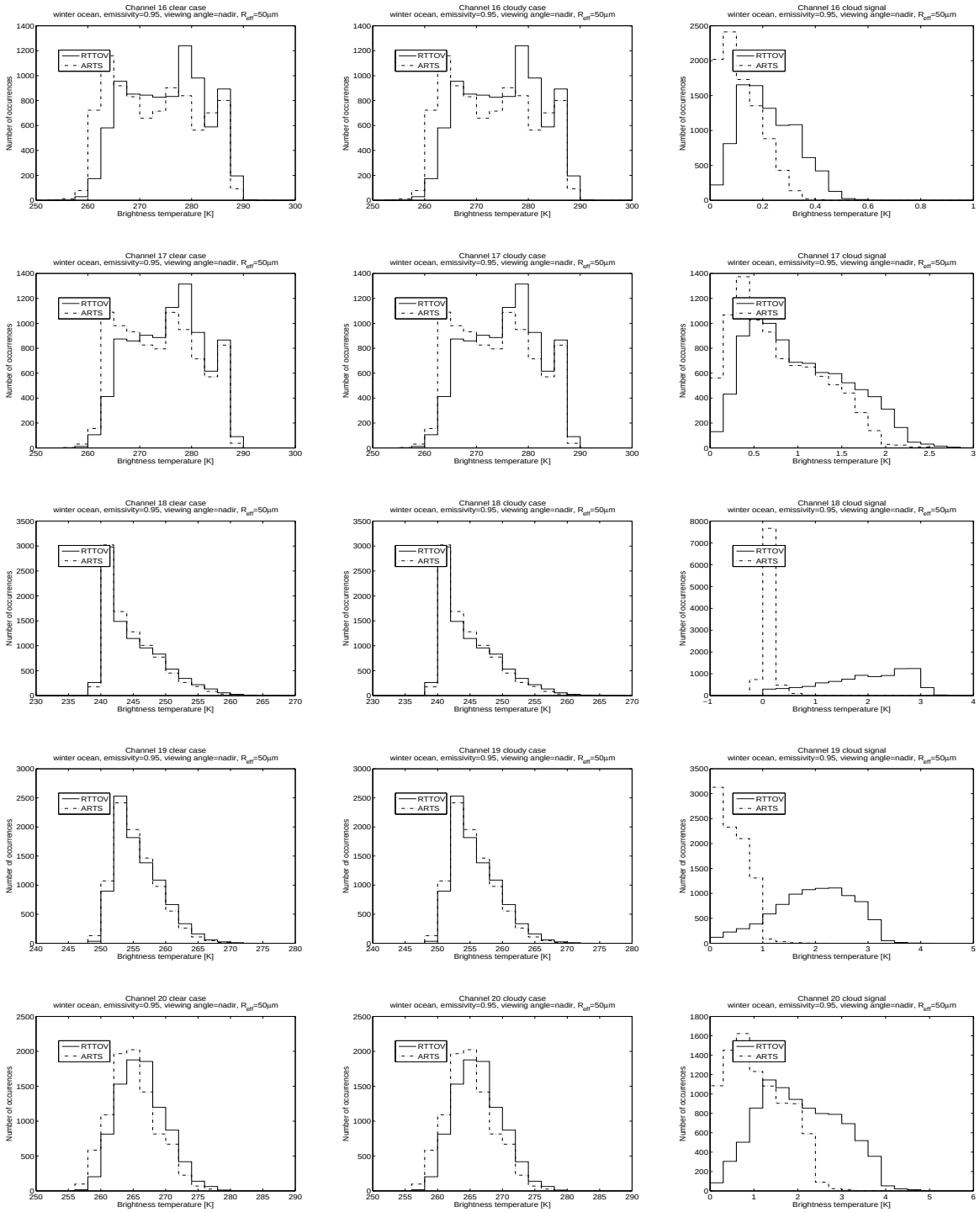

Figure 29: Histograms of BT simulated for the ocean winter data set by RTTOVSCATT (for both clear sky simulations and cloudy simulations), (plain line), and of BT simulated by ARTS (dashed line) for a particular set of parameters (emissivity=0.95, viewing angle=nadir, and effective radius of the ice particles= 50μm). Each line correspond to one AMSU-B channel from top to bottom channel 16 (89 GHz), 17 (150 GHz), 18 (183.31$\pm$1 GHz), 19 (183.31$\pm$3 GHz), and 20 (183.31$\pm$7 GHz). The left column correspond to clear sky simulations, the middle column corresponds to cloudy simulations and the right column corresponds to the cloud signal (clear sky BT minus cloudy BT).

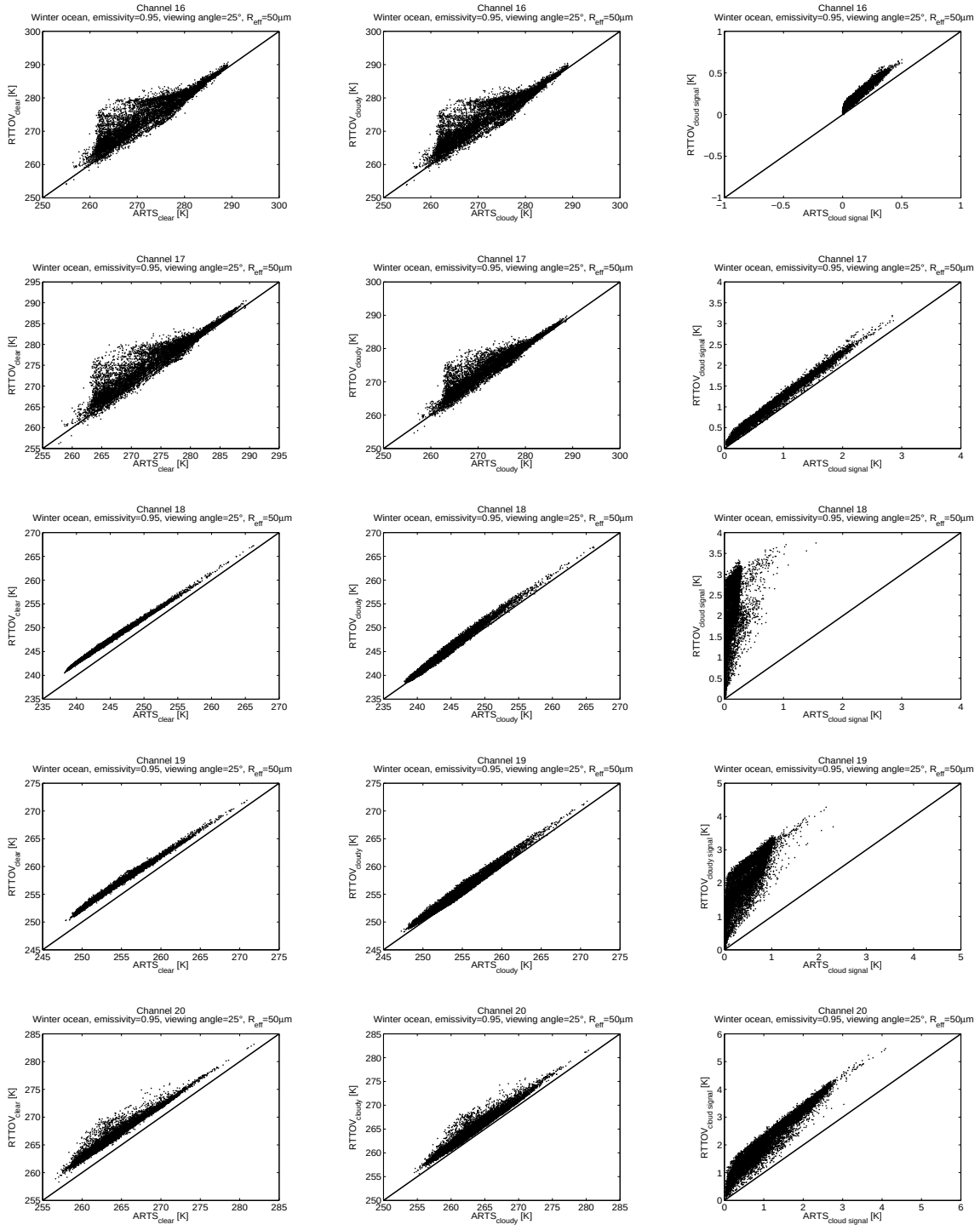

Figure 30: BT simulated for the ocean winter data set by RTTOVSCATT (for both clear sky simulations and cloudy simulations) against BT simulated by ARTS for a particular set of parameters (emissivity=0.95, viewing angle=25°, and effective radius of the ice particles= 50μm). Each line correspond to one AMSU-B channel from top to bottom channel 16 (89 GHz), 17 (150 GHz), 18 (183.31±1 GHz), 19 (183.31±3 GHz), and 20 (183.31±7 GHz). The left column correspond to clear sky simulations, the middle column corresponds to cloudy simulations and the right column corresponds to the cloud signal (clear sky BT minus cloudy BT).

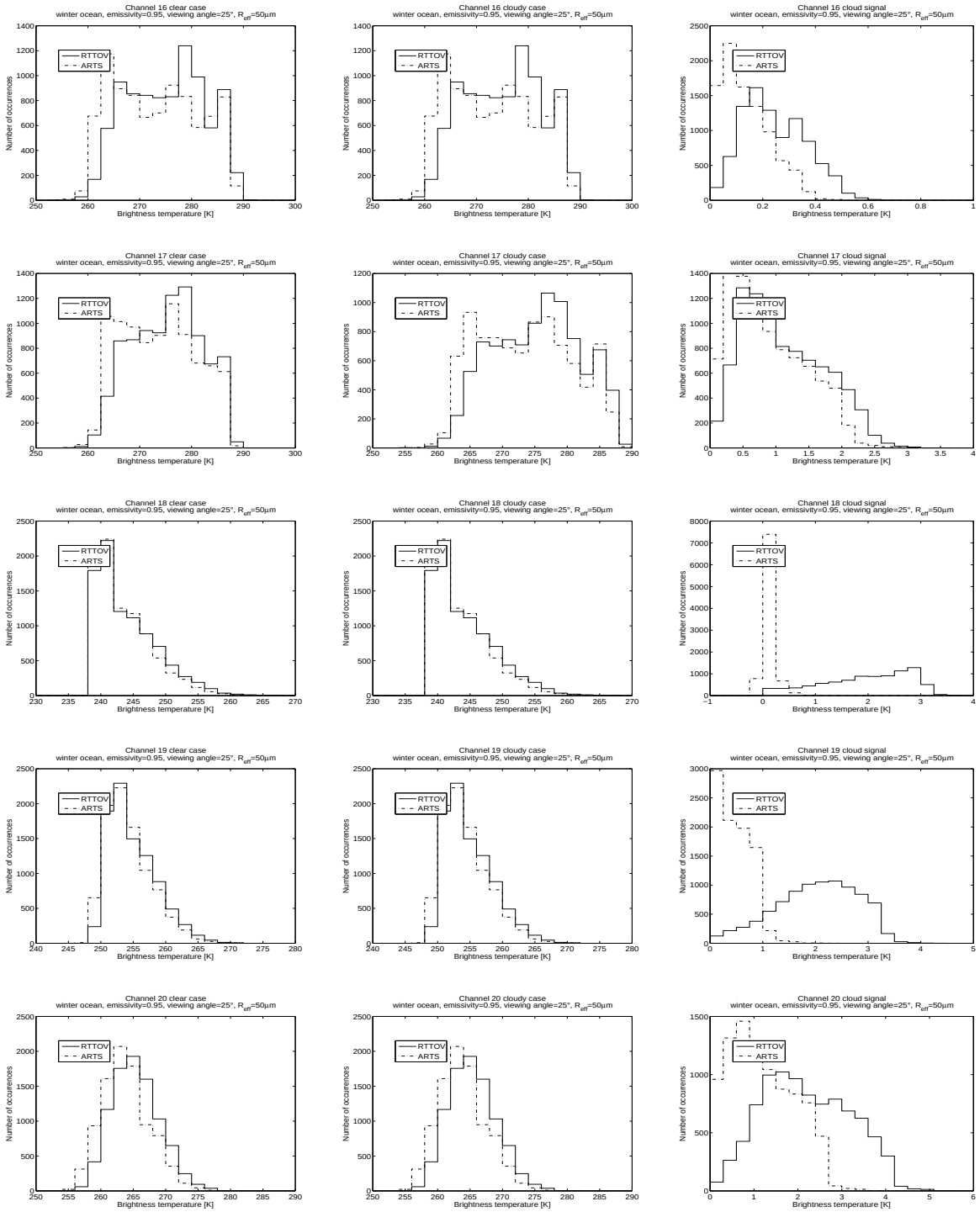

Figure 31: Histograms of BT simulated for the ocean winter data set by RTTOVSCATT (for both clear sky simulations and cloudy simulations), (plain line), and of BT simulated by ARTS (dashed line) for a particular set of parameters (emissivity=0.95, viewing angle=25°, and effective radius of the ice particles= 50μm). Each line correspond to one AMSU-B channel from top to bottom channel 16 (89 GHz), 17 (150 GHz), 18 (183.31±1 GHz), 19 (183.31±3 GHz), and 20 (183.31±7 GHz). The left column correspond to clear sky simulations, the middle column corresponds to cloudy simulations and the right column corresponds to the cloud signal (clear sky BT minus cloudy BT).

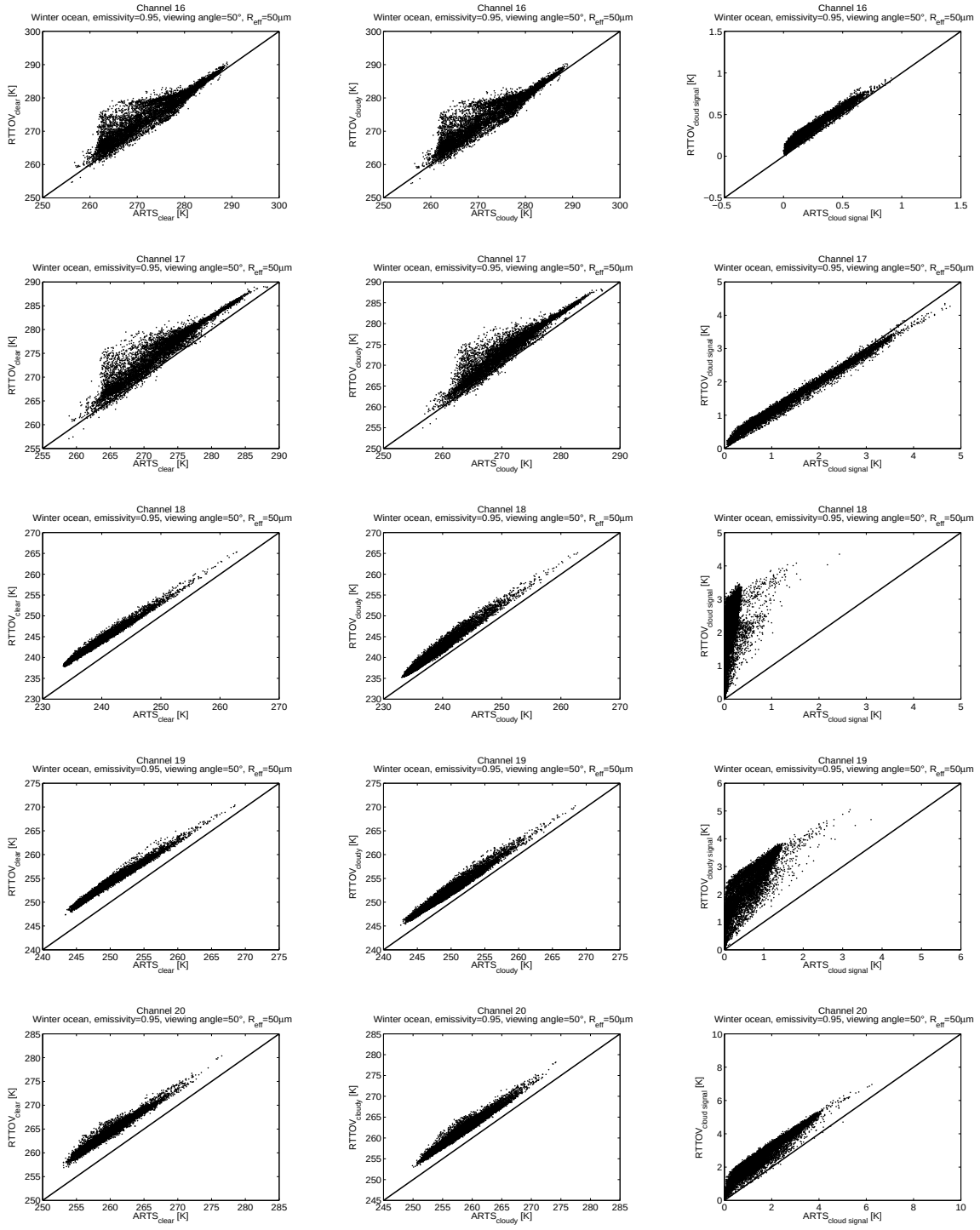

Figure 32: BT simulated for the ocean winter data set by RTTOVSCATT (for both clear sky simulations and cloudy simulations) against BT simulated by ARTS for a particular set of parameters (emissivity=0.95, viewing angle=50°, and effective radius of the ice particles= 50μm). Each line correspond to one AMSU-B channel from top to bottom channel 16 (89 GHz), 17 (150 GHz), 18 (183.31±1 GHz), 19 (183.31±3 GHz), and 20 (183.31±7 GHz). The left column correspond to clear sky simulations, the middle column corresponds to cloudy simulations and the right column corresponds to the cloud signal (clear sky BT minus cloudy BT).

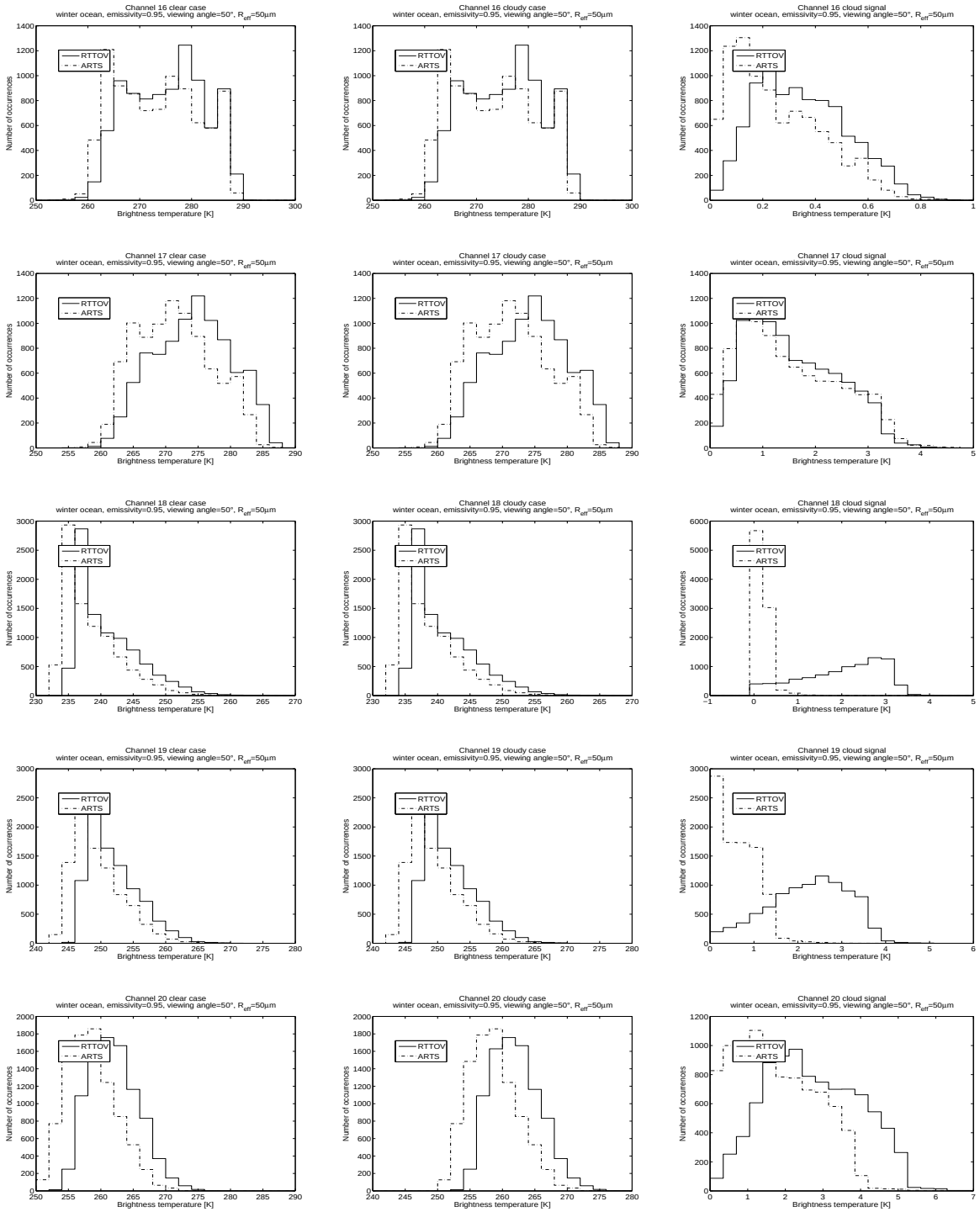

Figure 33: Histograms of BT simulated for the ocean winter data set by RTTOVSCATT (for both clear sky simulations and cloudy simulations), (plain line), and of BT simulated by ARTS (dashed line) for a particular set of parameters (emissivity=0.95, viewing angle=50°, and effective radius of the ice particles= 50μm). Each line correspond to one AMSU-B channel from top to bottom channel 16 (89 GHz), 17 (150 GHz), 18 (183.31±1 GHz), 19 (183.31±3 GHz), and 20 (183.31±7 GHz). The left column correspond to clear sky simulations, the middle column corresponds to cloudy simulations and the right column corresponds to the cloud signal (clear sky BT minus cloudy BT).

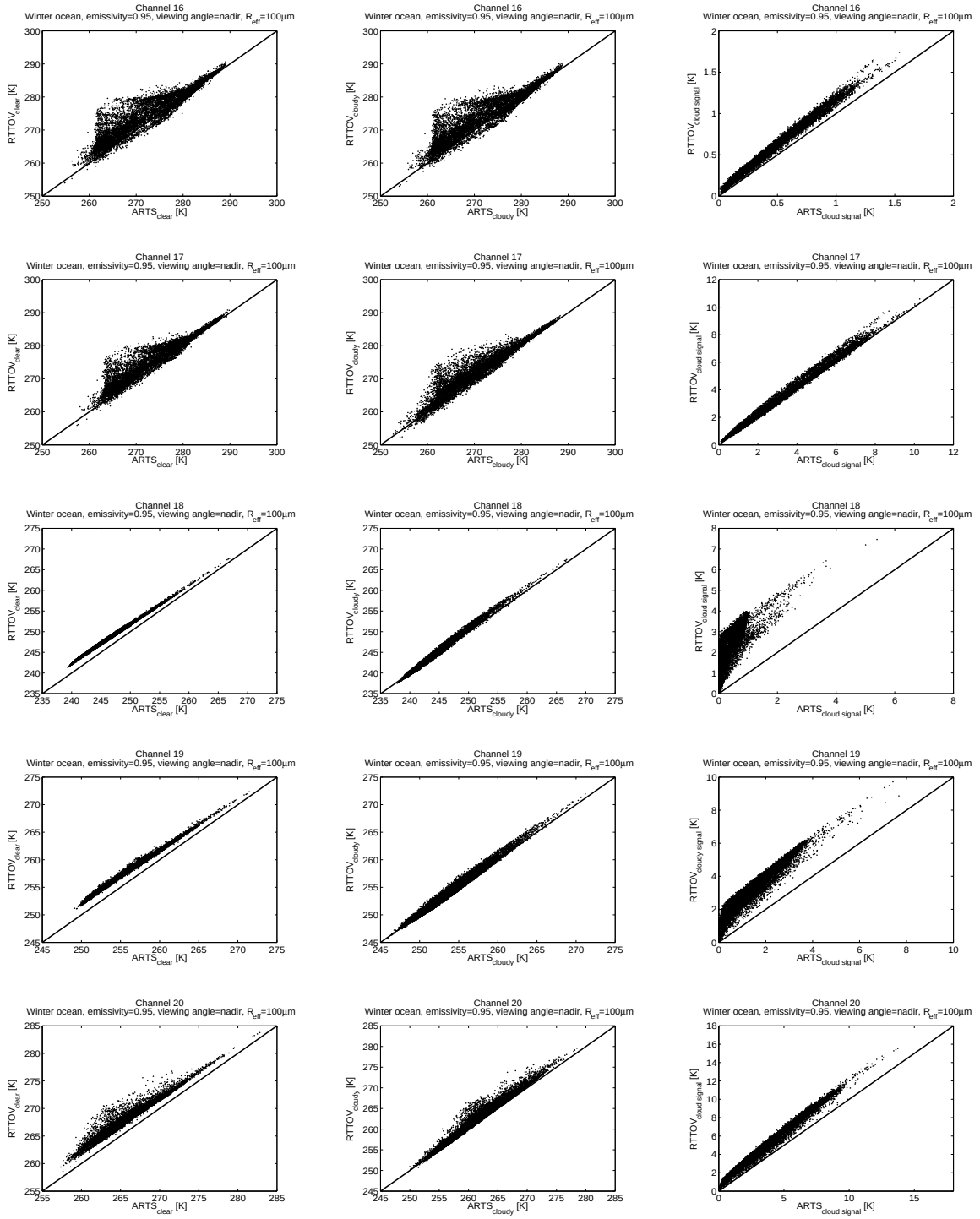

Figure 34: BT simulated for the ocean winter data set by RTTOVSCATT (for both clear sky simulations and cloudy simulations) against BT simulated by ARTS for a particular set of parameters (emissivity=0.95, viewing angle=nadir, and effective radius of the ice particles= 100μm). Each line correspond to one AMSU-B channel from top to bottom channel 16 (89 GHz), 17 (150 GHz), 18 (183.31±1 GHz), 19 (183.31±3 GHz), and 20 (183.31±7 GHz). The left column correspond to clear sky simulations, the middle column corresponds to cloudy simulations and the right column corresponds to the cloud signal (clear sky BT minus cloudy BT).

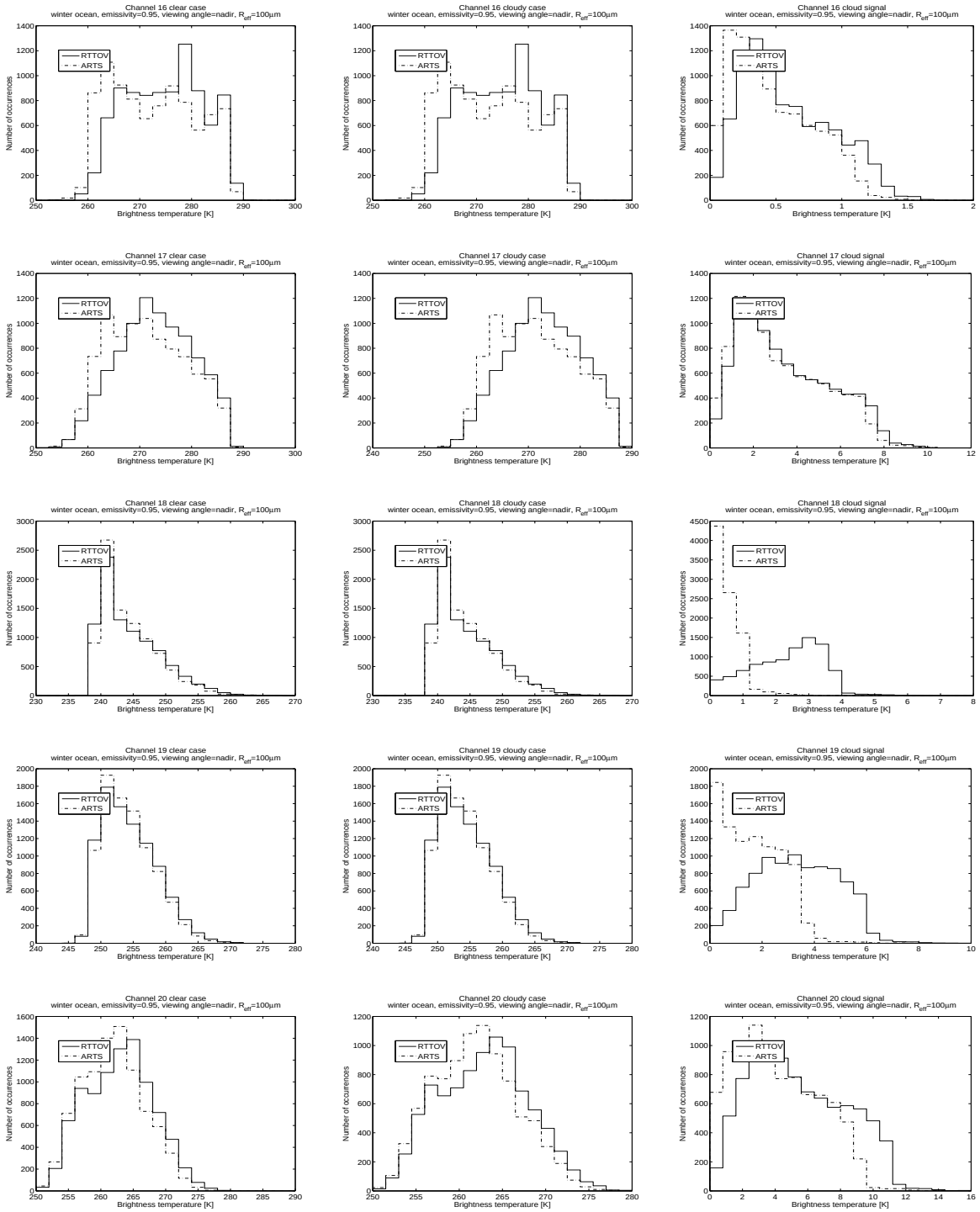

Figure 35: Histograms of BT simulated for the ocean winter data set by RTTOVSCATT (for both clear sky simulations and cloudy simulations), (plain line), and of BT simulated by ARTS (dashed line) for a particular set of parameters (emissivity=0.95, viewing angle=nadir, and effective radius of the ice particles= 100μm). Each line correspond to one AMSU-B channel from top to bottom channel 16 (89 GHz), 17 (150 GHz), 18 (183.31$\pm$1 GHz), 19 (183.31$\pm$3 GHz), and 20 (183.31$\pm$7 GHz). The left column correspond to clear sky simulations, the middle column corresponds to cloudy simulations and the right column corresponds to the cloud signal (clear sky BT minus cloudy BT).

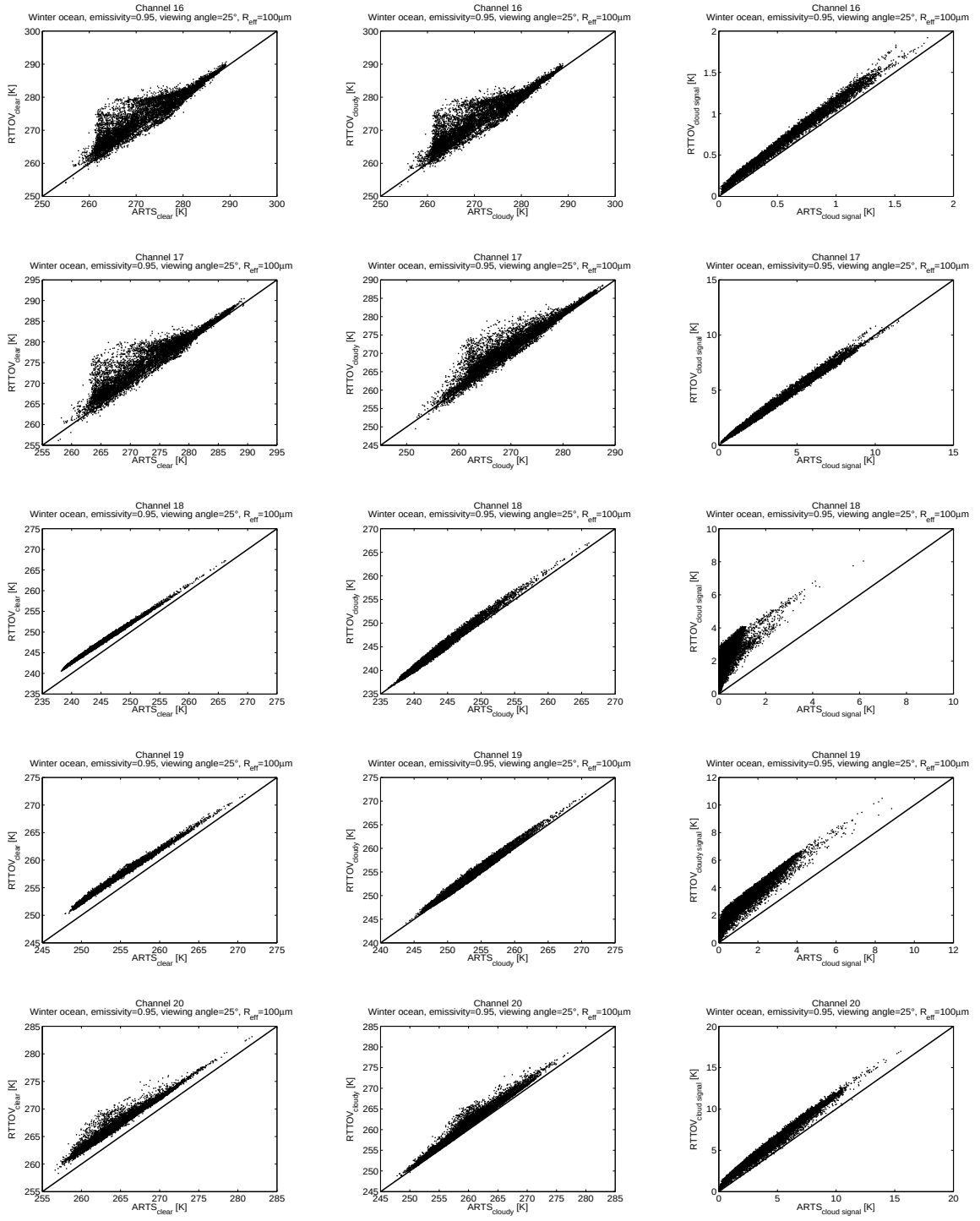

Figure 36: BT simulated for the ocean winter data set by RTTOVSCATT (for both clear sky simulations and cloudy simulations) against BT simulated by ARTS for a particular set of parameters (emissivity=0.95, viewing angle=25°, and effective radius of the ice particles= 100μm). Each line correspond to one AMSU-B channel from top to bottom channel 16 (89 GHz), 17 (150 GHz), 18 (183.31±1 GHz), 19 (183.31±3 GHz), and 20 (183.31±7 GHz). The left column correspond to clear sky simulations, the middle column corresponds to cloudy simulations and the right column corresponds to the cloud signal (clear sky BT minus cloudy BT).

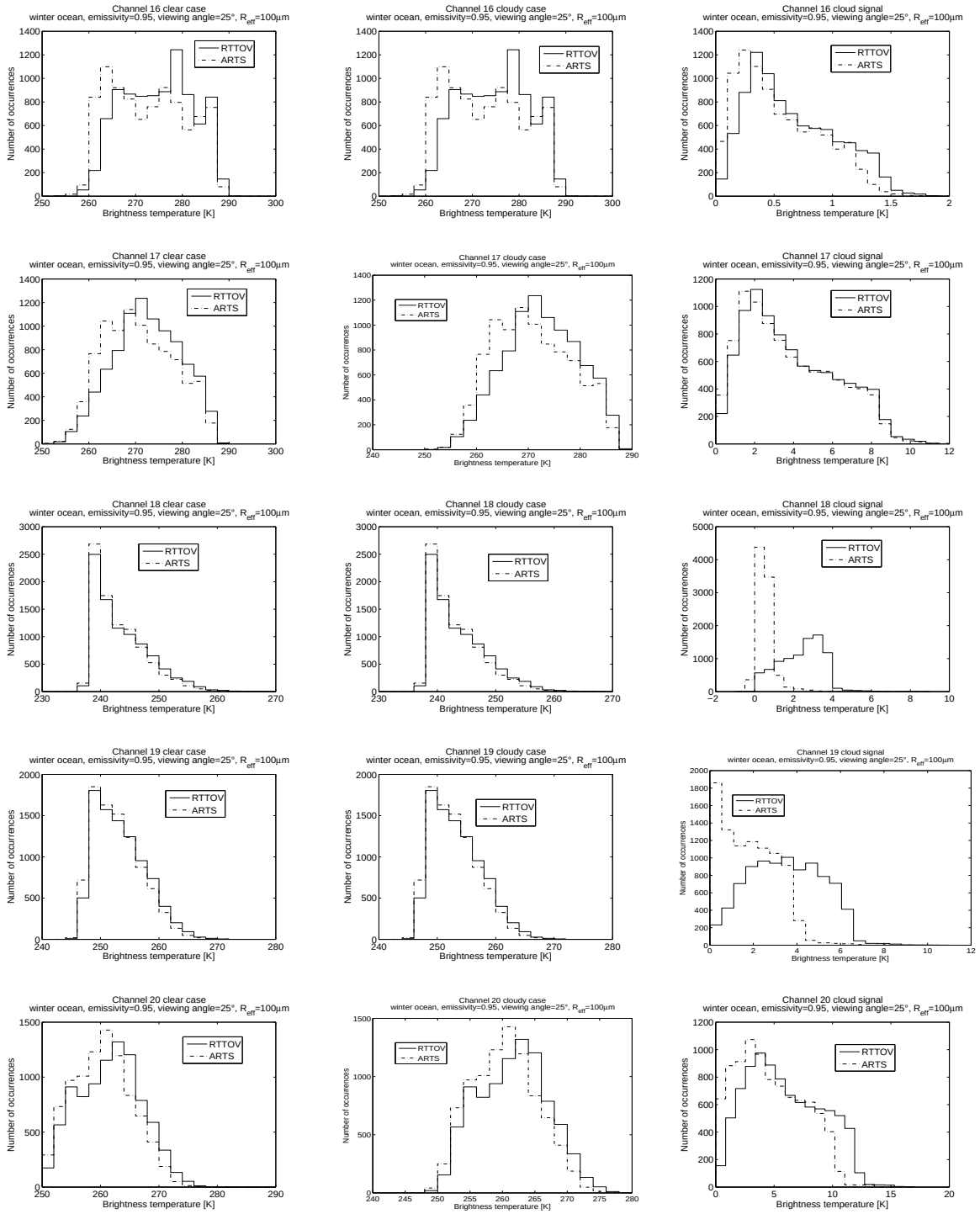

Figure 37: Histograms of BT simulated for the ocean winter data set by RTTOVSCATT (for both clear sky simulations and cloudy simulations), (plain line), and of BT simulated by ARTS (dashed line) for a particular set of parameters (emissivity=0.95, viewing angle=25°, and effective radius of the ice particles= 100μm). Each line correspond to one AMSU-B channel from top to bottom channel 16 (89 GHz), 17 (150 GHz), 18 (183.31±1 GHz), 19 (183.31±3 GHz), and 20 (183.31±7 GHz). The left column correspond to clear sky simulations, the middle column corresponds to cloudy simulations and the right column corresponds to the cloud signal (clear sky BT minus cloudy BT).

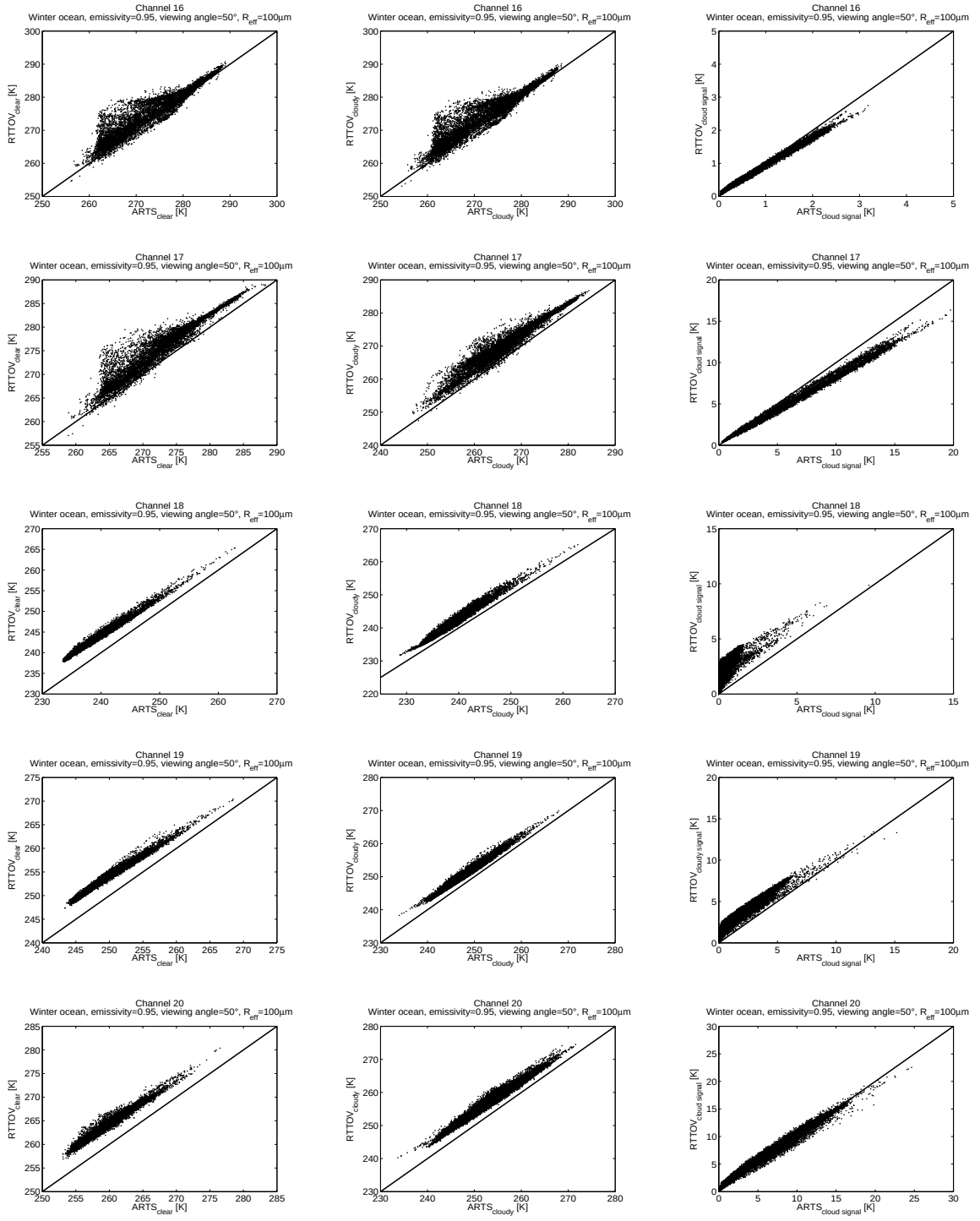

Figure 38: BT simulated for the ocean winter data set by RTTOVSCATT (for both clear sky simulations and cloudy simulations) against BT simulated by ARTS for a particular set of parameters (emissivity=0.95, viewing angle=50°, and effective radius of the ice particles= 100μm). Each line correspond to one AMSU-B channel from top to bottom channel 16 (89 GHz), 17 (150 GHz), 18 (183.31±1 GHz), 19 (183.31±3 GHz), and 20 (183.31±7 GHz). The left column correspond to clear sky simulations, the middle column corresponds to cloudy simulations and the right column corresponds to the cloud signal (clear sky BT minus cloudy BT).

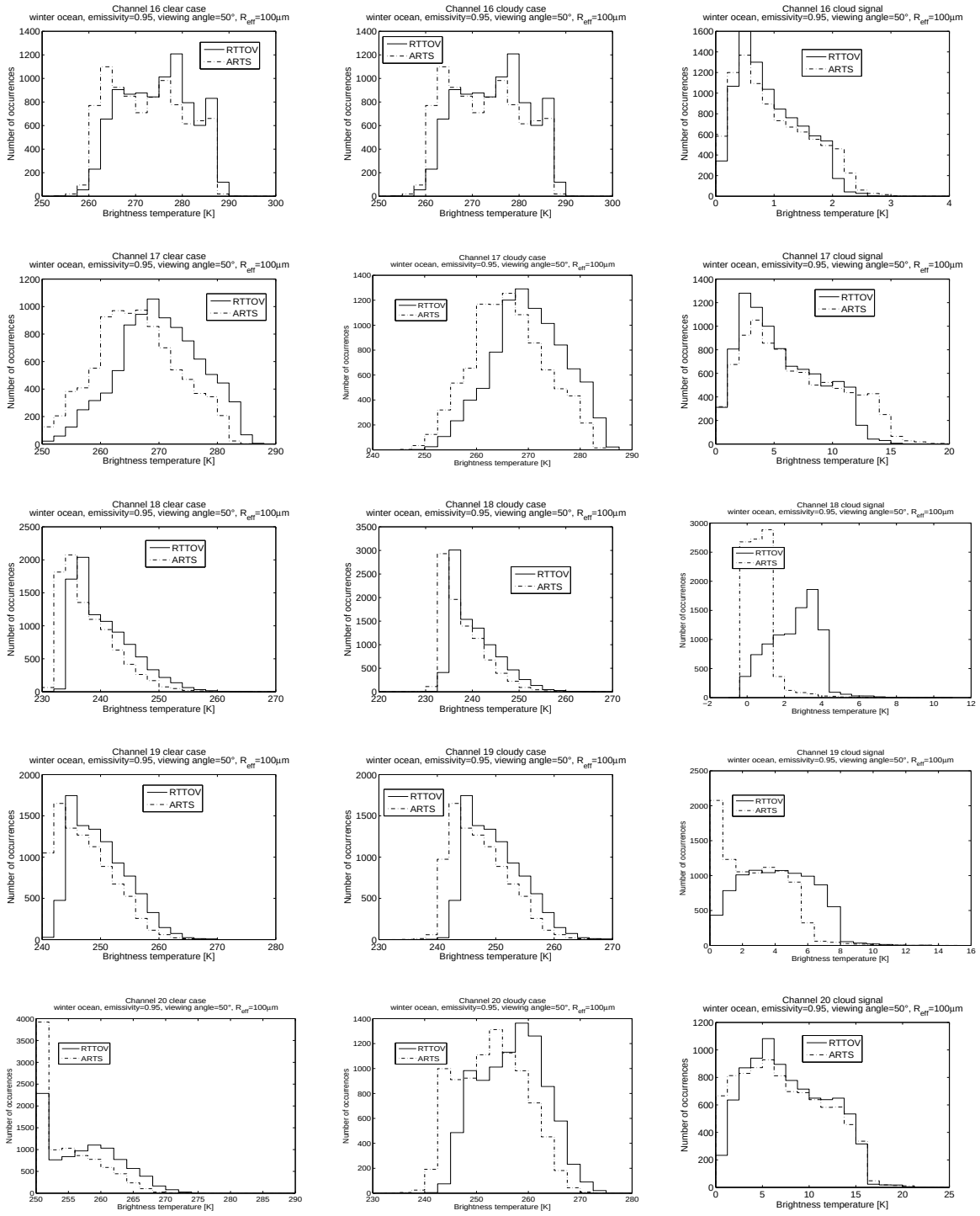

Figure 39: Histograms of BT simulated for the ocean winter data set by RTTOVSCATT (for both clear sky simulations and cloudy simulations), (plain line), and of BT simulated by ARTS (dashed line) for a particular set of parameters (emissivity=0.95, viewing angle=50°, and effective radius of the ice particles= 100μm). Each line correspond to one AMSU-B channel from top to bottom channel 16 (89 GHz), 17 (150 GHz), 18 (183.31±1 GHz), 19 (183.31±3 GHz), and 20 (183.31±7 GHz). The left column correspond to clear sky simulations, the middle column corresponds to cloudy simulations and the right column corresponds to the cloud signal (clear sky BT minus cloudy BT).

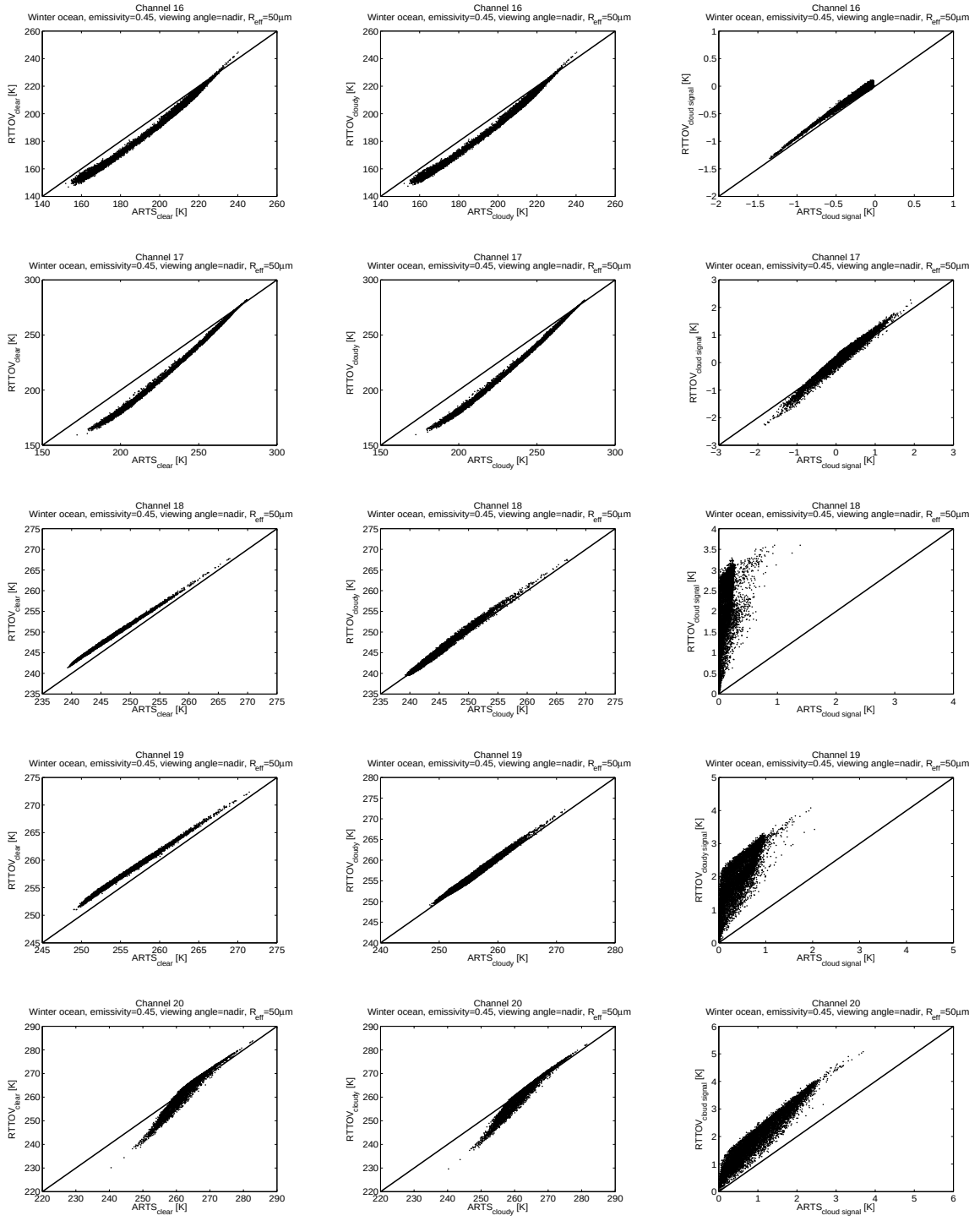

Figure 40: BT simulated for the ocean winter data set by RTTOVSCATT (for both clear sky simulations and cloudy simulations) against BT simulated by ARTS for a particular set of parameters (emissivity=0.45, viewing angle=nadir, and effective radius of the ice particles= 50μm). Each line correspond to one AMSU-B channel from top to bottom channel 16 (89 GHz), 17 (150 GHz), 18 (183.31±1 GHz), 19 (183.31±3 GHz), and 20 (183.31±7 GHz). The left column correspond to clear sky simulations, the middle column corresponds to cloudy simulations and the right column corresponds to the cloud signal (clear sky BT minus cloudy BT).

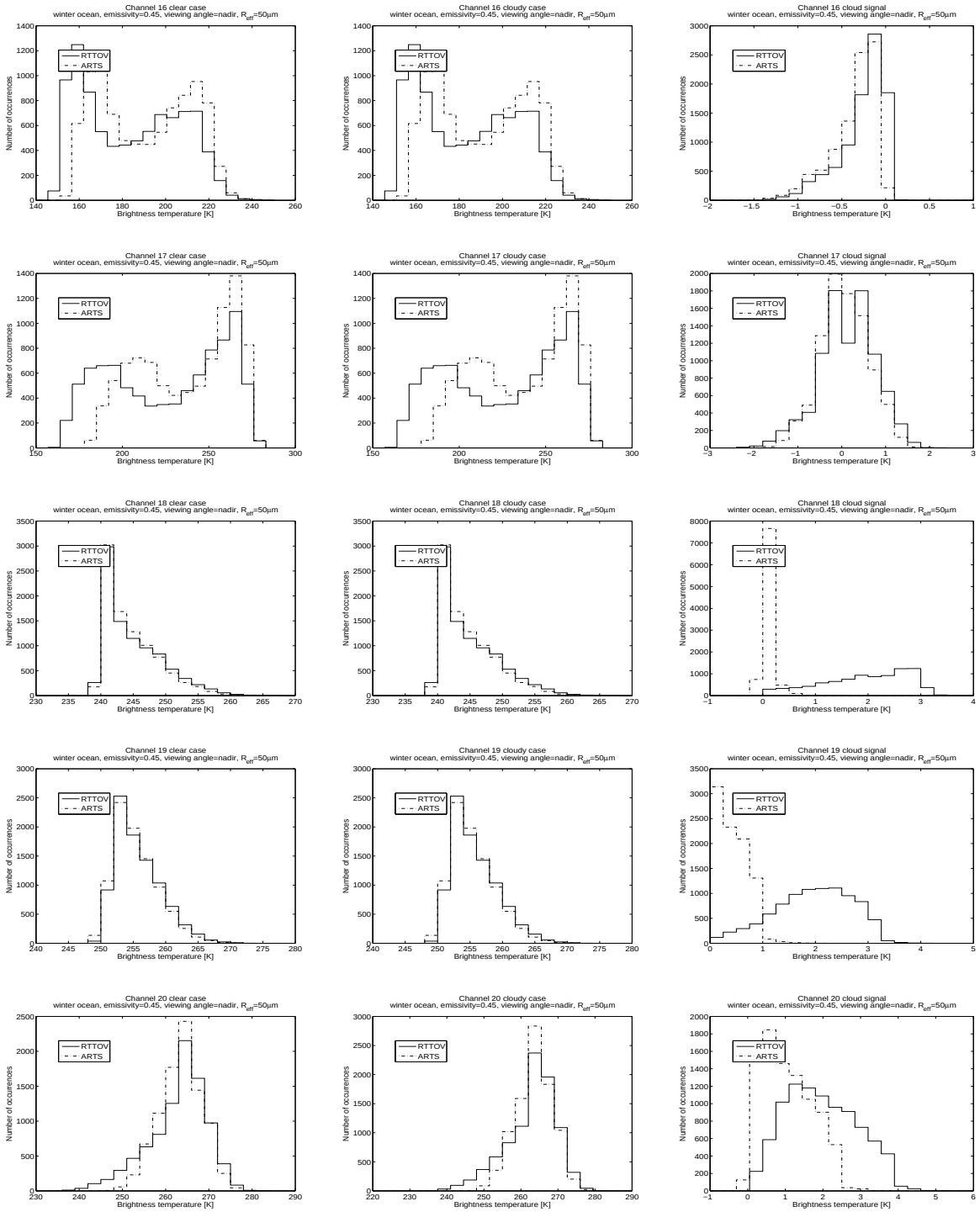

Figure 41: Histograms of BT simulated for the ocean winter data set by RTTOVSCATT (for both clear sky simulations and cloudy simulations), (plain line), and of BT simulated by ARTS (dashed line) for a particular set of parameters (emissivity=0.45, viewing angle=nadir, and effective radius of the ice particles= 50μm). Each line correspond to one AMSU-B channel from top to bottom channel 16 (89 GHz), 17 (150 GHz), 18 (183.31$\pm$1 GHz), 19 (183.31$\pm$3 GHz), and 20 (183.31$\pm$7 GHz). The left column correspond to clear sky simulations, the middle column corresponds to cloudy simulations and the right column corresponds to the cloud signal (clear sky BT minus cloudy BT).

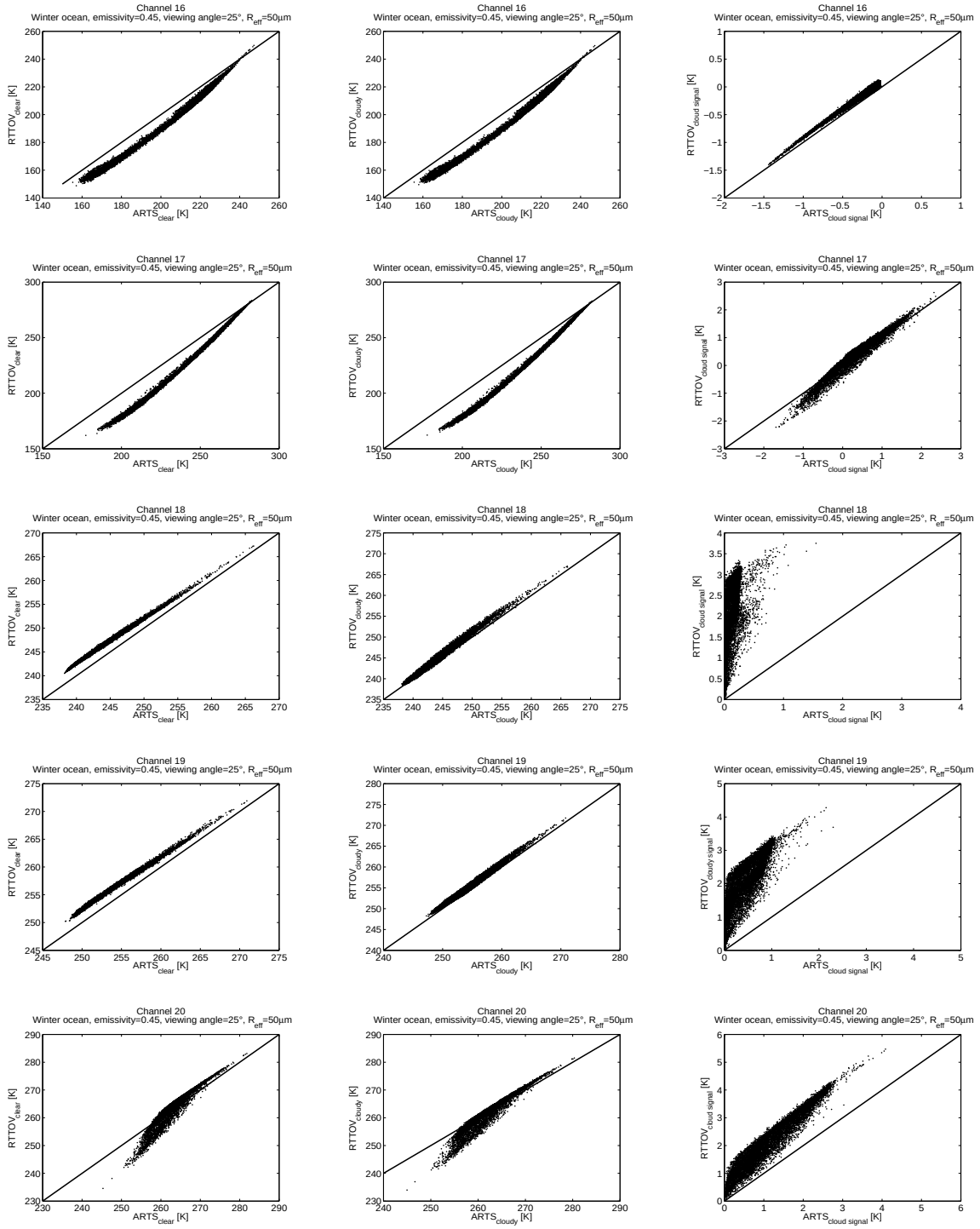

Figure 42: BT simulated for the ocean winter data set by RTTOVSCATT (for both clear sky simulations and cloudy simulations) against BT simulated by ARTS for a particular set of parameters (emissivity=0.45, viewing angle=25°, and effective radius of the ice particles= 50μm). Each line correspond to one AMSU-B channel from top to bottom channel 16 (89 GHz), 17 (150 GHz), 18 (183.31±1 GHz), 19 (183.31±3 GHz), and 20 (183.31±7 GHz). The left column correspond to clear sky simulations, the middle column corresponds to cloudy simulations and the right column corresponds to the cloud signal (clear sky BT minus cloudy BT).

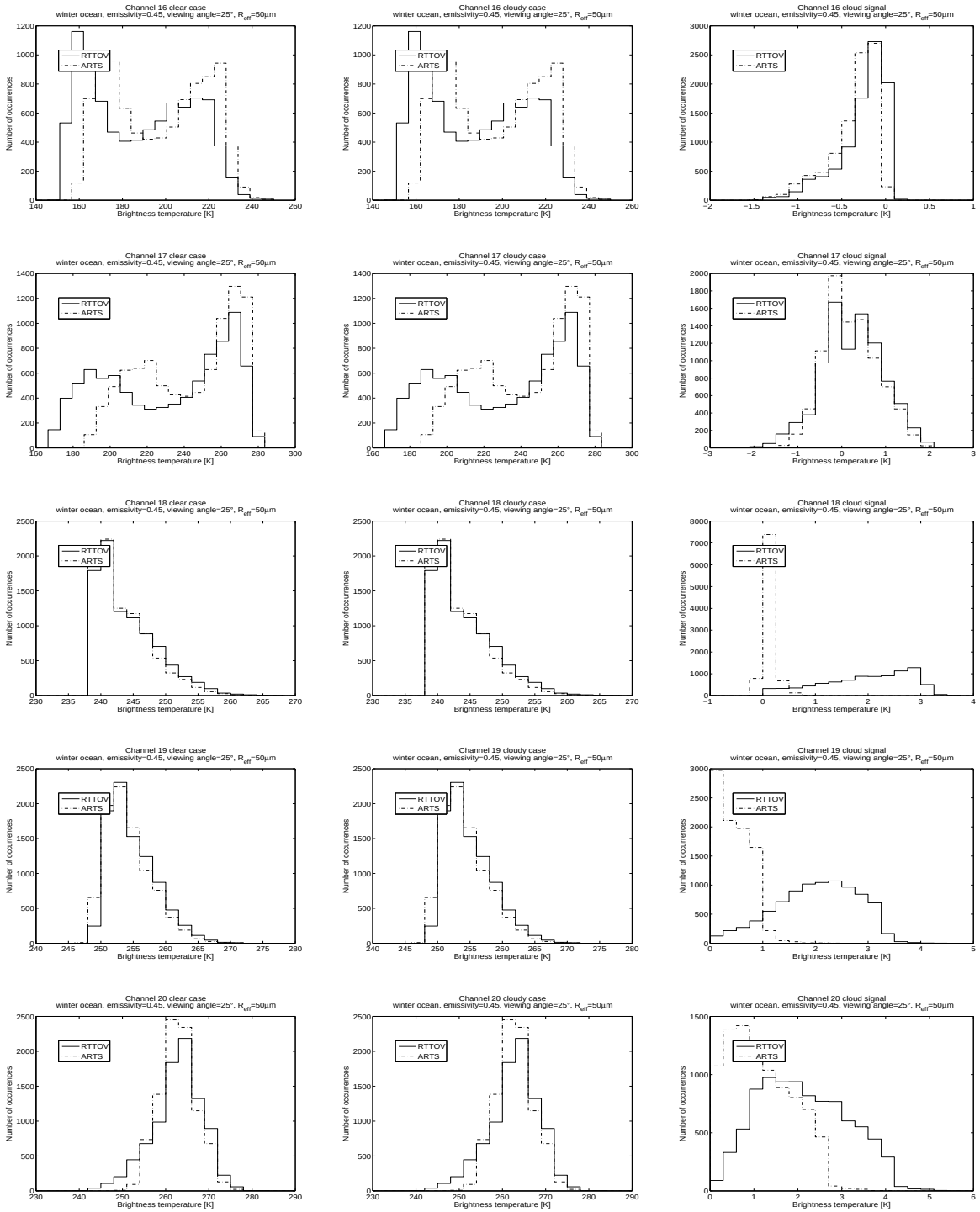

Figure 43: Histograms of BT simulated for the ocean winter data set by RTTOVSCATT (for both clear sky simulations and cloudy simulations), (plain line), and of BT simulated by ARTS (dashed line) for a particular set of parameters (emissivity=0.45, viewing angle=25°, and effective radius of the ice particles= 50μm). Each line correspond to one AMSU-B channel from top to bottom channel 16 (89 GHz), 17 (150 GHz), 18 (183.31±1 GHz), 19 (183.31±3 GHz), and 20 (183.31±7 GHz). The left column correspond to clear sky simulations, the middle column corresponds to cloudy simulations and the right column corresponds to the cloud signal (clear sky BT minus cloudy BT).

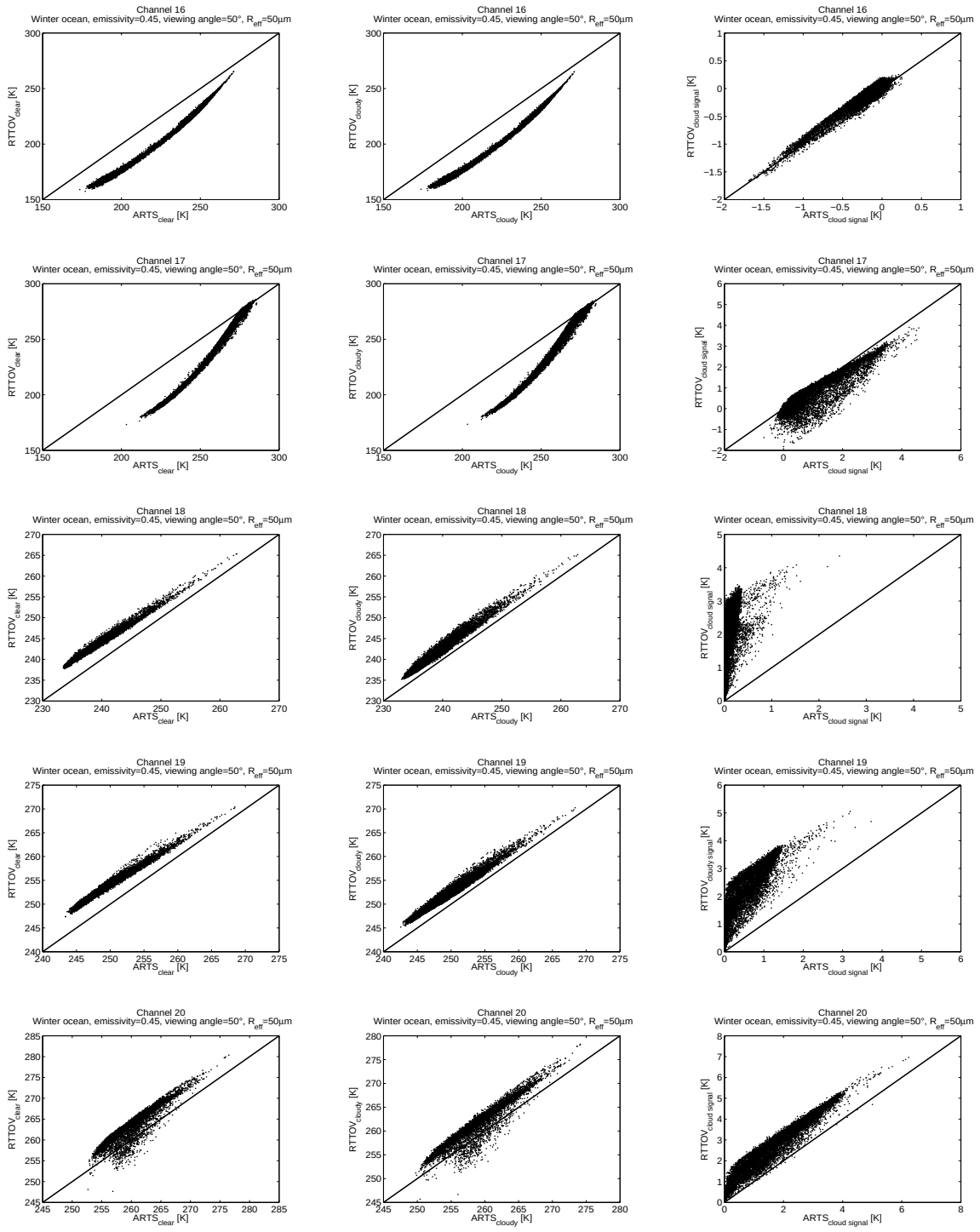

Figure 44: BT simulated for the ocean winter data set by RTTOVSCATT (for both clear sky simulations and cloudy simulations) against BT simulated by ARTS for a particular set of parameters (emissivity=0.45, viewing angle=50°, and effective radius of the ice particles= 50μm). Each line correspond to one AMSU-B channel from top to bottom channel 16 (89 GHz), 17 (150 GHz), 18 (183.31±1 GHz), 19 (183.31±3 GHz), and 20 (183.31±7 GHz). The left column correspond to clear sky simulations, the middle column corresponds to cloudy simulations and the right column corresponds to the cloud signal (clear sky BT minus cloudy BT).

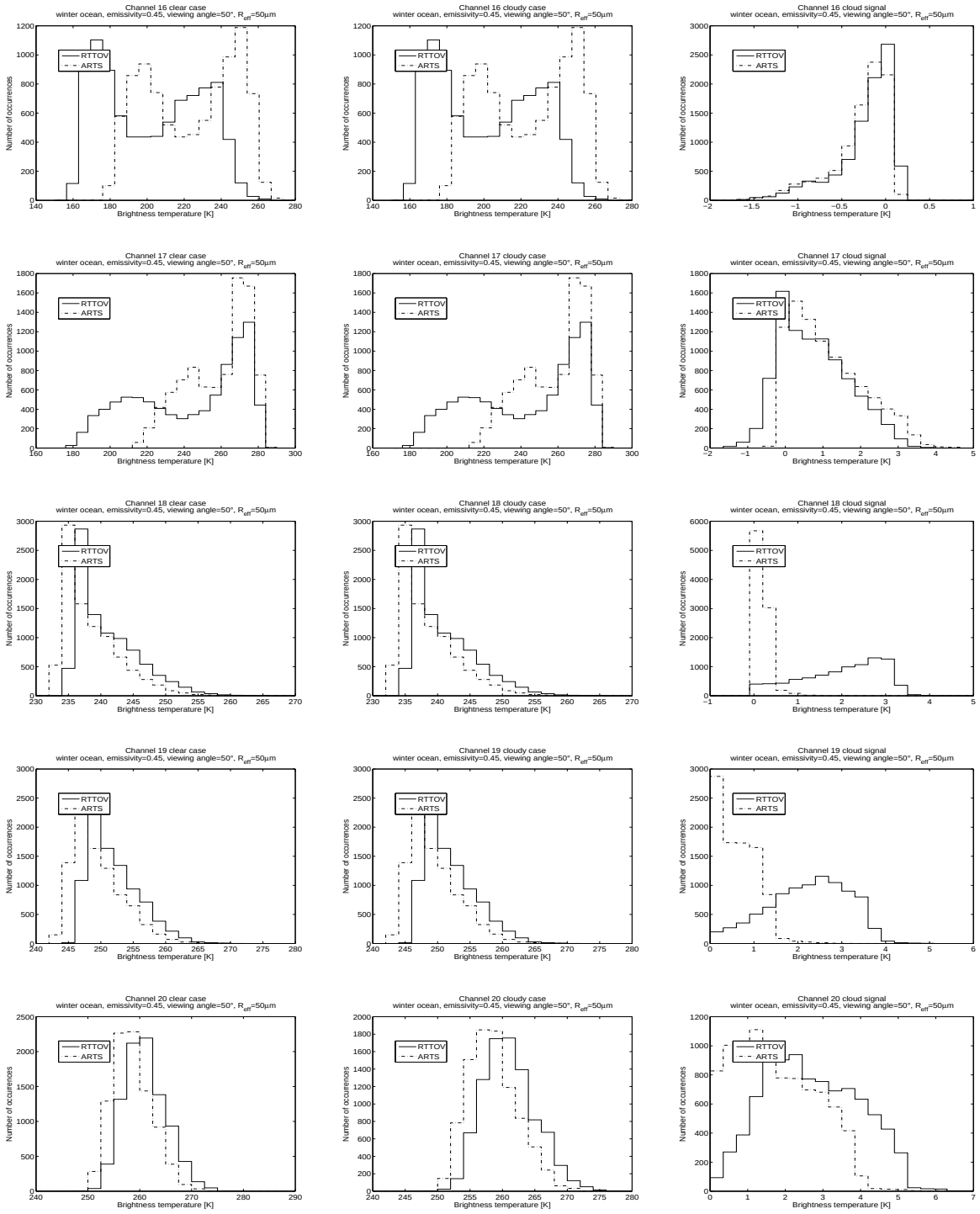

Figure 45: Histograms of BT simulated for the ocean winter data set by RTTOVSCATT (for both clear sky simulations and cloudy simulations), (plain line), and of BT simulated by ARTS (dashed line) for a particular set of parameters (emissivity=0.45, viewing angle=50°, and effective radius of the ice particles= 50μm). Each line correspond to one AMSU-B channel from top to bottom channel 16 (89 GHz), 17 (150 GHz), 18 (183.31±1 GHz), 19 (183.31±3 GHz), and 20 (183.31±7 GHz). The left column correspond to clear sky simulations, the middle column corresponds to cloudy simulations and the right column corresponds to the cloud signal (clear sky BT minus cloudy BT).

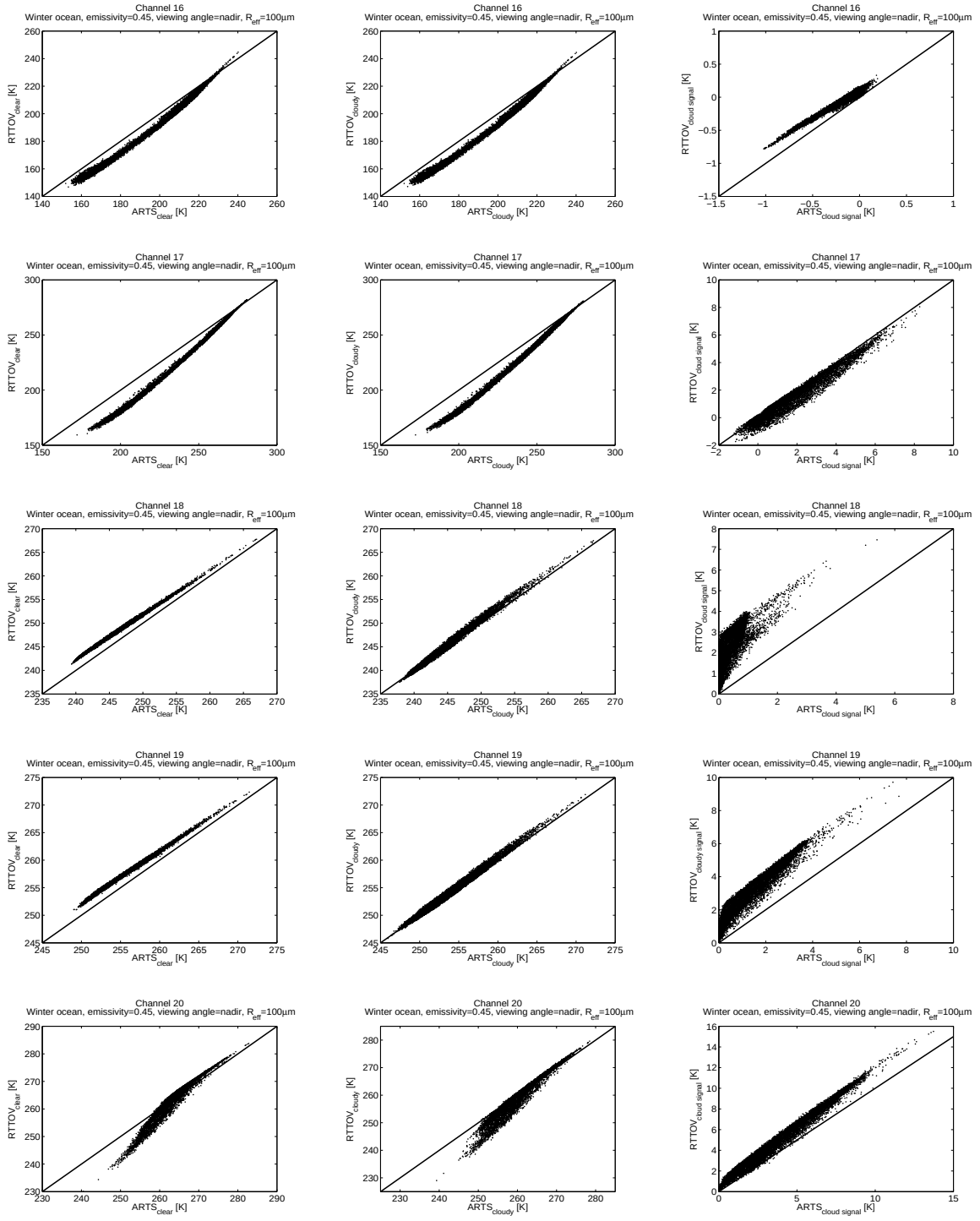

Figure 46: BT simulated for the ocean winter data set by RTTOVSCATT (for both clear sky simulations and cloudy simulations) against BT simulated by ARTS for a particular set of parameters (emissivity=0.45, viewing angle=nadir, and effective radius of the ice particles= 100μm). Each line correspond to one AMSU-B channel from top to bottom channel 16 (89 GHz), 17 (150 GHz), 18 (183.31±1 GHz), 19 (183.31±3 GHz), and 20 (183.31±7 GHz). The left column correspond to clear sky simulations, the middle column corresponds to cloudy simulations and the right column corresponds to the cloud signal (clear sky BT minus cloudy BT).

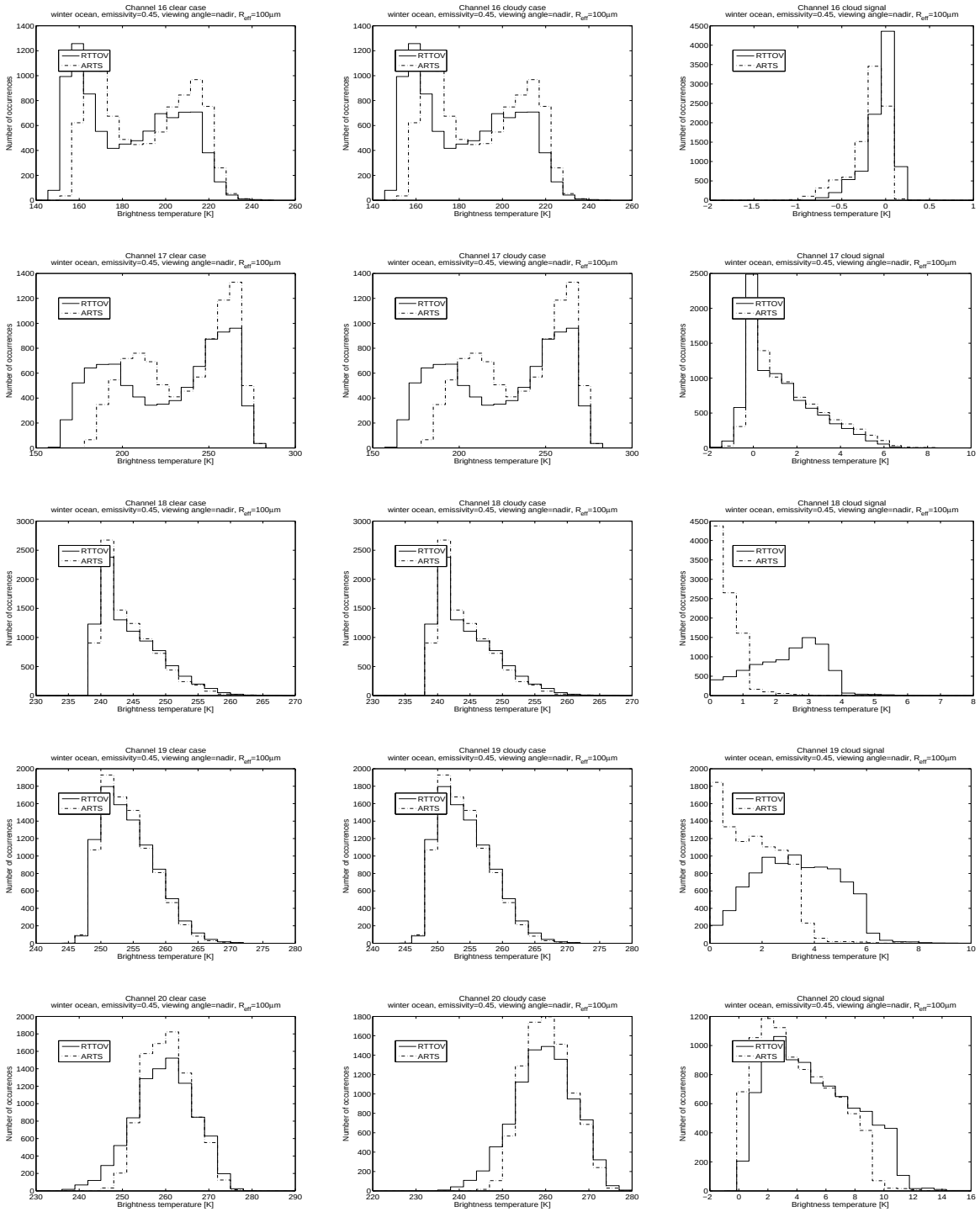

Figure 47: Histograms of BT simulated for the ocean winter data set by RTTOVSCATT (for both clear sky simulations and cloudy simulations), (plain line), and of BT simulated by ARTS (dashed line) for a particular set of parameters (emissivity=0.45, viewing angle=nadir, and effective radius of the ice particles= 100μm). Each line correspond to one AMSU-B channel from top to bottom channel 16 (89 GHz), 17 (150 GHz), 18 (183.31$\pm$1 GHz), 19 (183.31$\pm$3 GHz), and 20 (183.31$\pm$7 GHz). The left column correspond to clear sky simulations, the middle column corresponds to cloudy simulations and the right column corresponds to the cloud signal (clear sky BT minus cloudy BT).

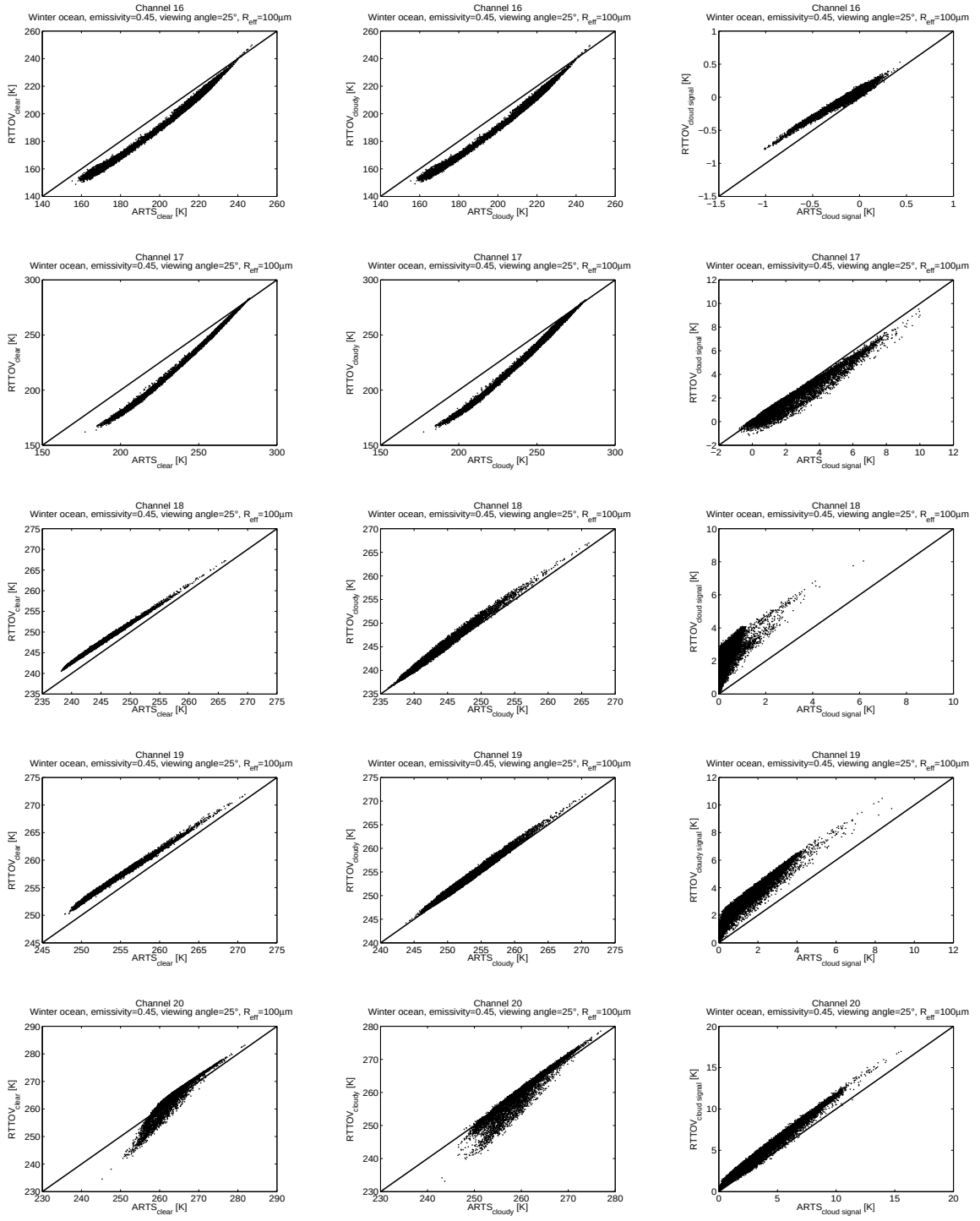

Figure 48: BT simulated for the ocean winter data set by RTTOVSCATT (for both clear sky simulations and cloudy simulations) against BT simulated by ARTS for a particular set of parameters (emissivity=0.45, viewing angle=25°, and effective radius of the ice particles= 100μm). Each line correspond to one AMSU-B channel from top to bottom channel 16 (89 GHz), 17 (150 GHz), 18 (183.31±1 GHz), 19 (183.31±3 GHz), and 20 (183.31±7 GHz). The left column correspond to clear sky simulations, the middle column corresponds to cloudy simulations and the right column corresponds to the cloud signal (clear sky BT minus cloudy BT).

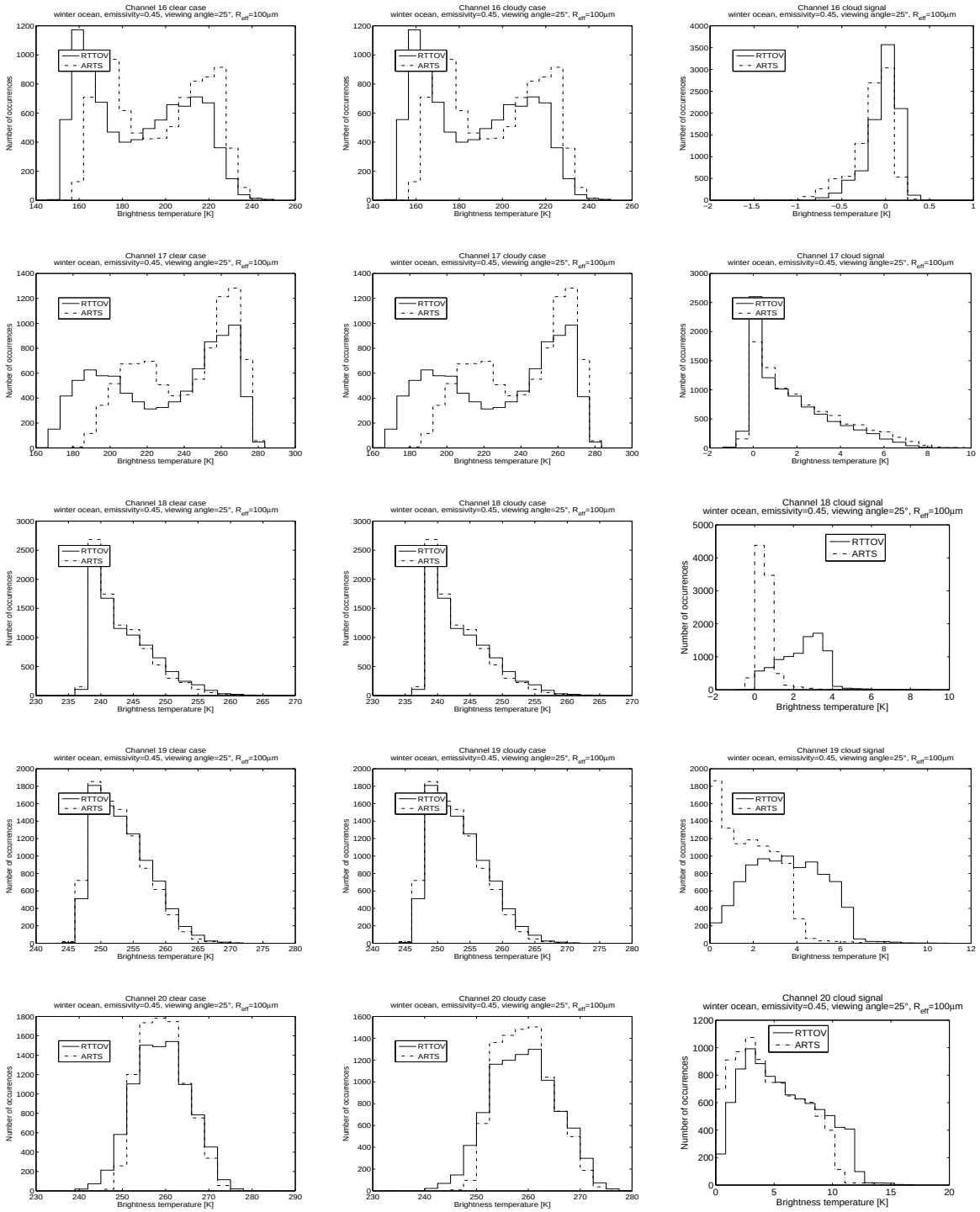

Figure 49: Histograms of BT simulated for the ocean winter data set by RTTOVSCATT (for both clear sky simulations and cloudy simulations), (plain line), and of BT simulated by ARTS (dashed line) for a particular set of parameters (emissivity=0.45, viewing angle=25°, and effective radius of the ice particles= 100μm). Each line correspond to one AMSU-B channel from top to bottom channel 16 (89 GHz), 17 (150 GHz), 18 (183.31±1 GHz), 19 (183.31±3 GHz), and 20 (183.31±7 GHz). The left column correspond to clear sky simulations, the middle column corresponds to cloudy simulations and the right column corresponds to the cloud signal (clear sky BT minus cloudy BT).

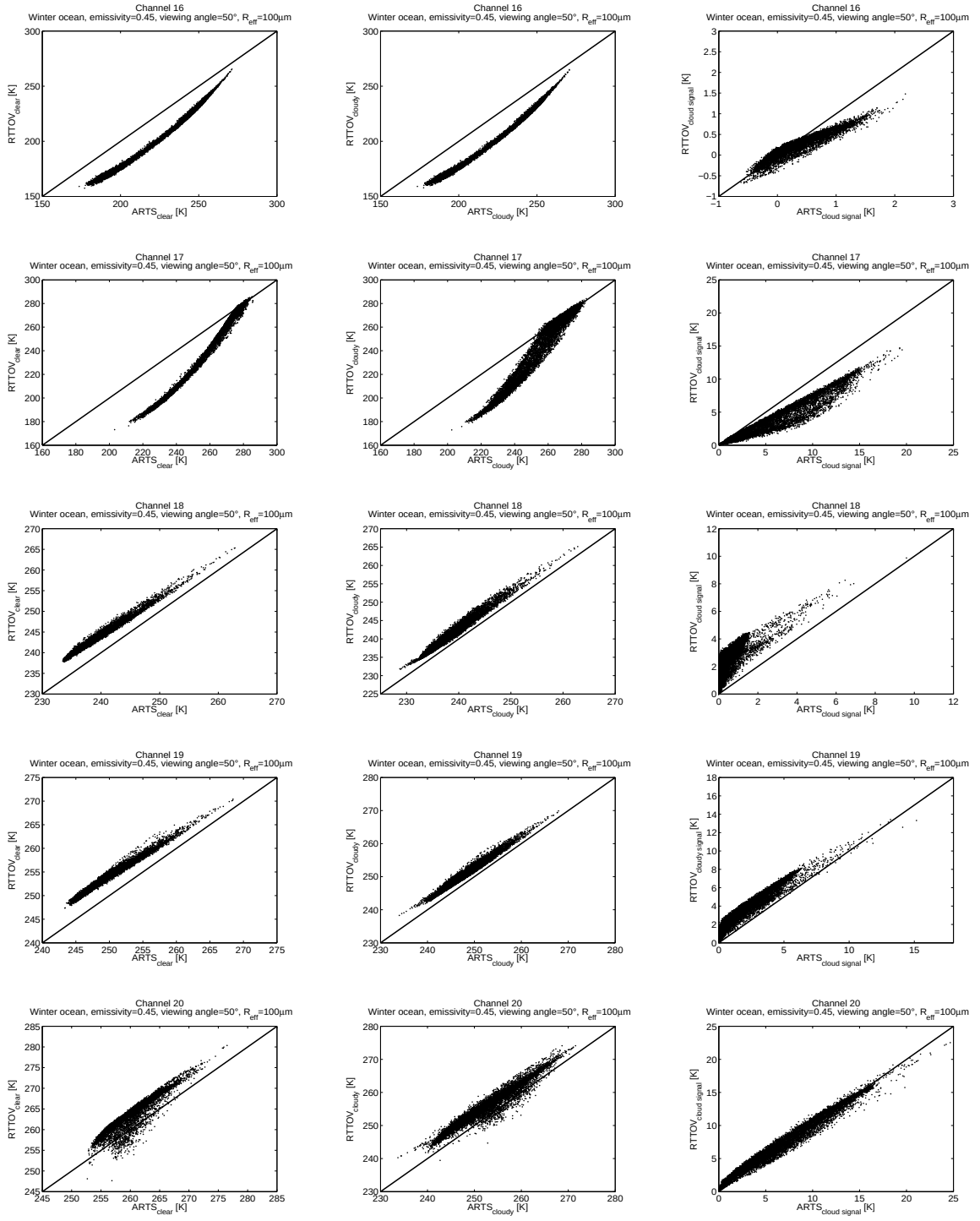

Figure 50: BT simulated for the ocean winter data set by RTTOVSCATT (for both clear sky simulations and cloudy simulations) against BT simulated by ARTS for a particular set of parameters (emissivity=0.45, viewing angle=50°, and effective radius of the ice particles= 100μm). Each line correspond to one AMSU-B channel from top to bottom channel 16 (89 GHz), 17 (150 GHz), 18 (183.31±1 GHz), 19 (183.31±3 GHz), and 20 (183.31±7 GHz). The left column correspond to clear sky simulations, the middle column corresponds to cloudy simulations and the right column corresponds to the cloud signal (clear sky BT minus cloudy BT).

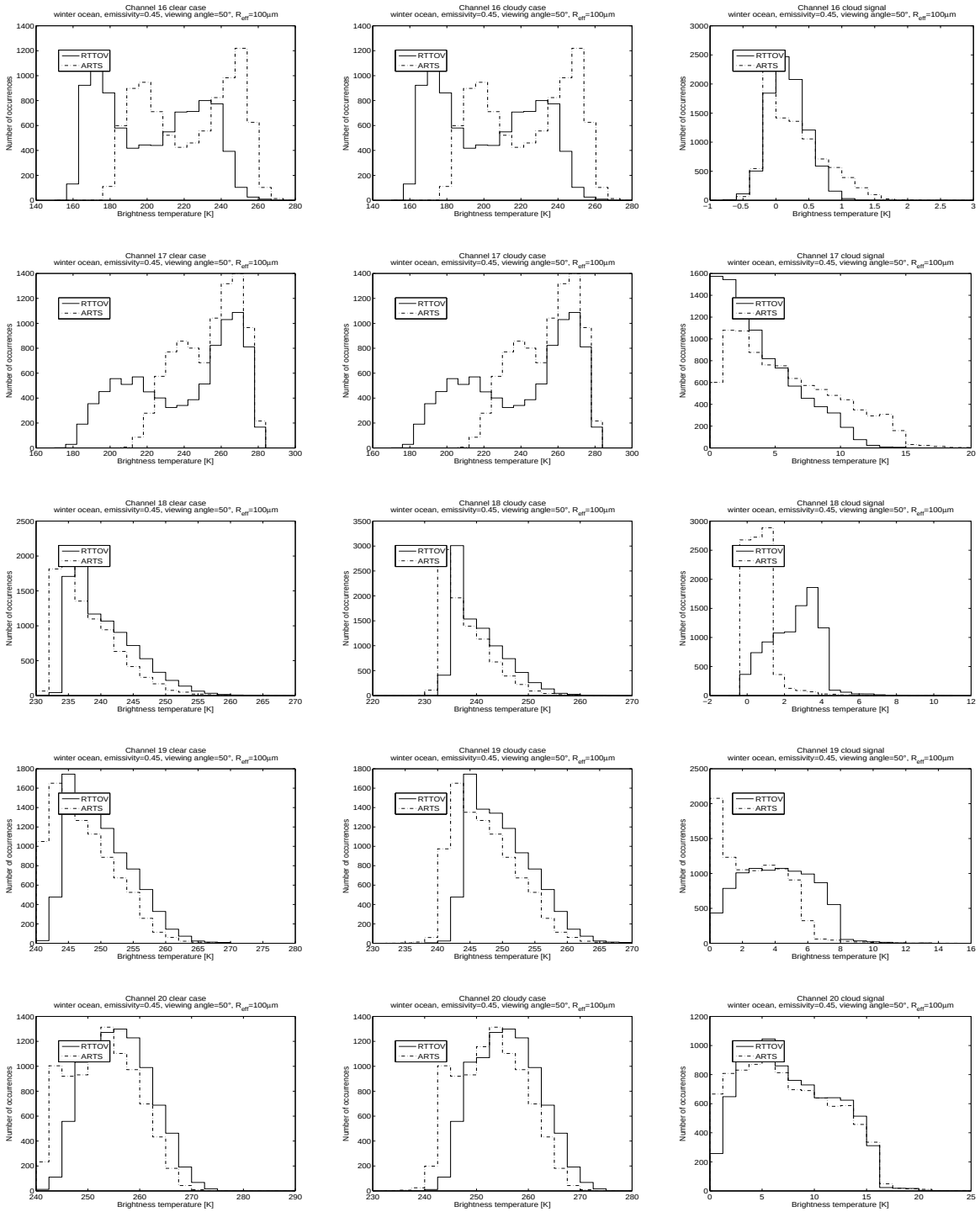

Figure 51: Histograms of BT simulated for the ocean winter data set by RTTOVSCATT (for both clear sky simulations and cloudy simulations), (plain line), and of BT simulated by ARTS (dashed line) for a particular set of parameters (emissivity=0.45, viewing angle=50°, and effective radius of the ice particles= 100μm). Each line correspond to one AMSU-B channel from top to bottom channel 16 (89 GHz), 17 (150 GHz), 18 (183.31±1 GHz), 19 (183.31±3 GHz), and 20 (183.31±7 GHz). The left column correspond to clear sky simulations, the middle column corresponds to cloudy simulations and the right column corresponds to the cloud signal (clear sky BT minus cloudy BT).

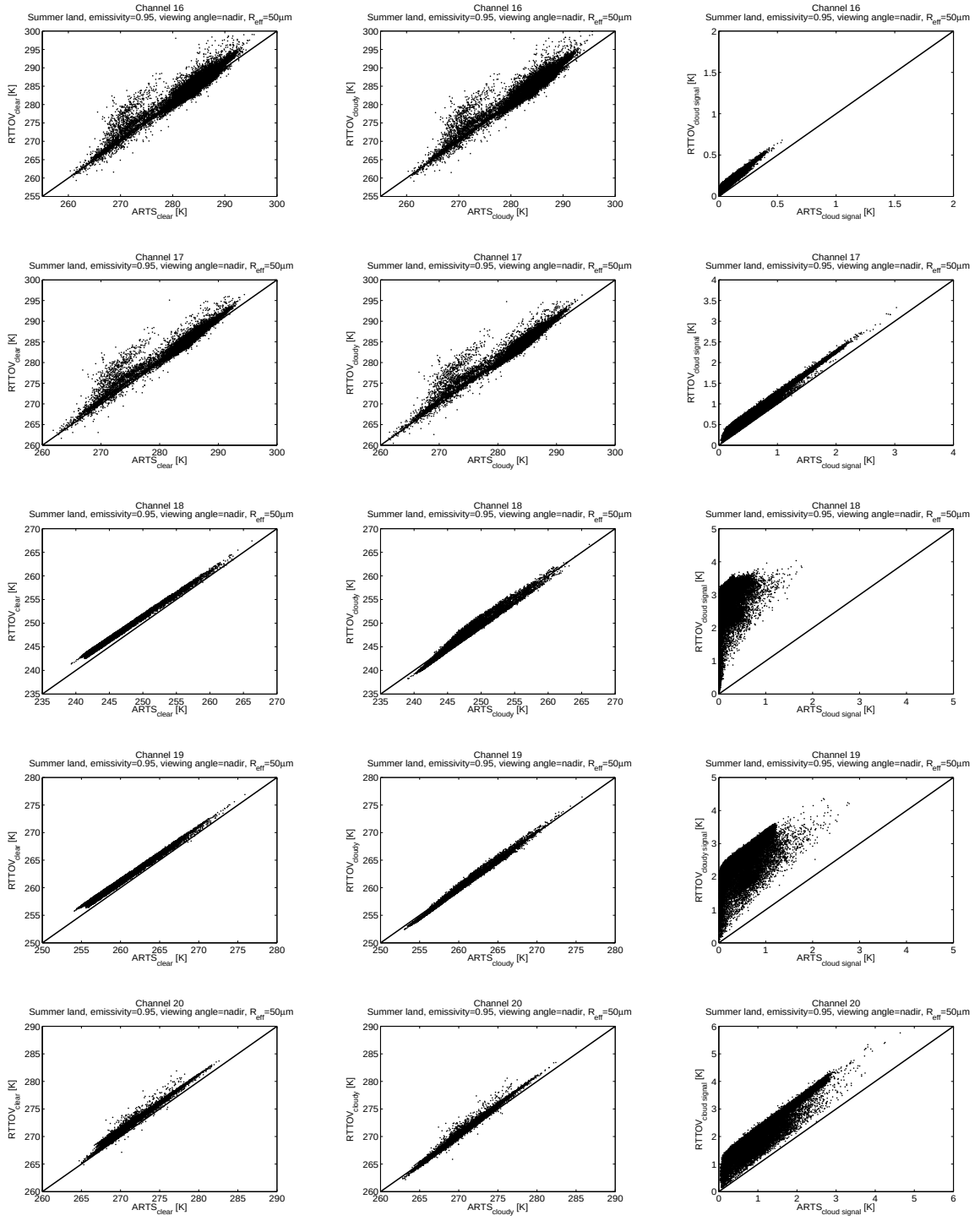

Figure 52: BT simulated for the land summer data set by RTTOVSCATT (for both clear sky simulations and cloudy simulations) against BT simulated by ARTS for a particular set of parameters (emissivity=0.95, viewing angle=nadir, and effective radius of the ice particles= 50μm). Each line correspond to one AMSU-B channel from top to bottom channel 16 (89 GHz), 17 (150 GHz), 18 (183.31±1 GHz), 19 (183.31±3 GHz), and 20 (183.31±7 GHz). The left column correspond to clear sky simulations, the middle column corresponds to cloudy simulations and the right column corresponds to the cloud signal (clear sky BT minus cloudy BT).

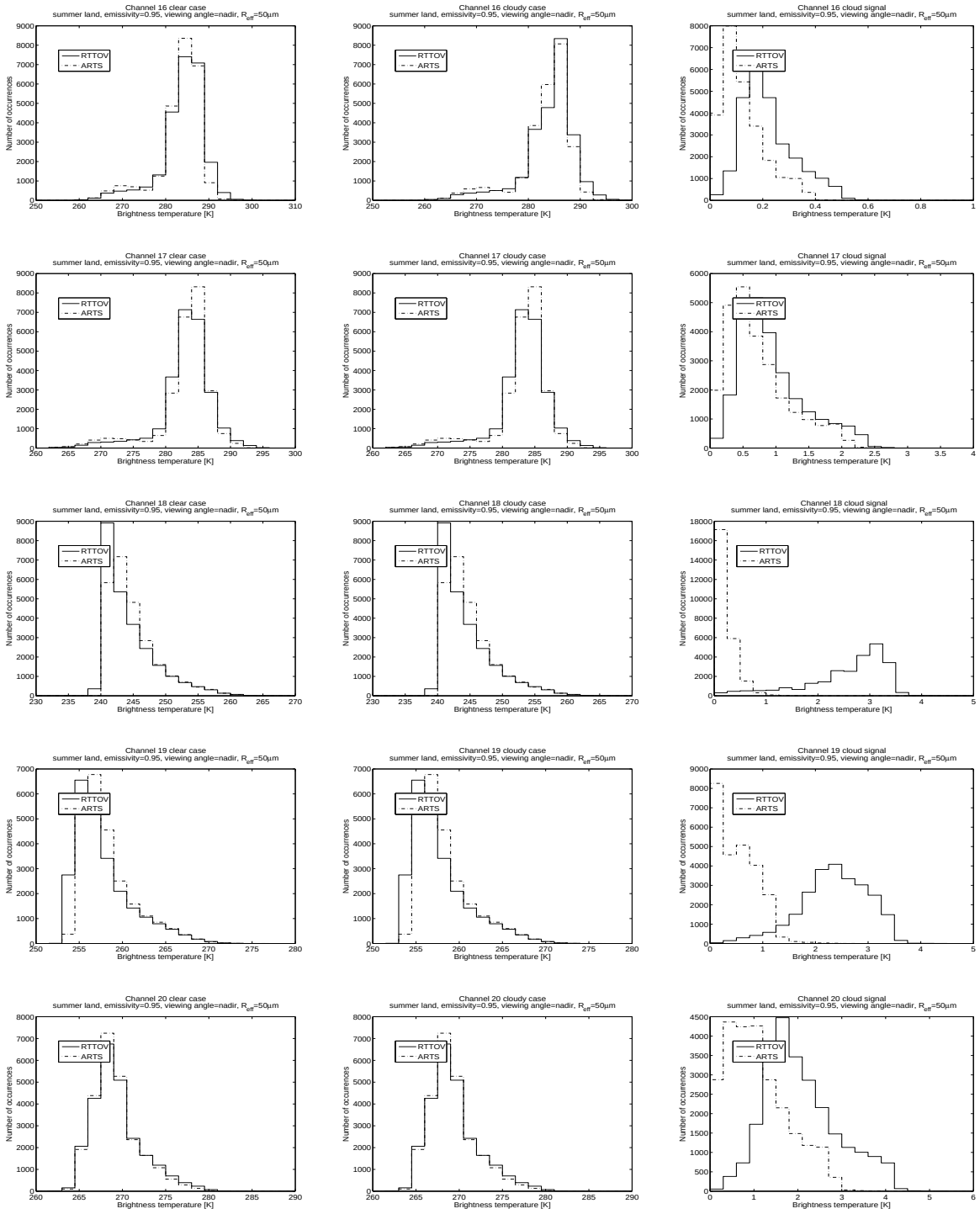

Figure 53: Histograms of BT simulated for the land summer data set by RTTOVSCATT (for both clear sky simulations and cloudy simulations), (plain line), and of BT simulated by ARTS (dashed line) for a particular set of parameters (emissivity=0.95, viewing angle=nadir, and effective radius of the ice particles= 50μm). Each line correspond to one AMSU-B channel from top to bottom channel 16 (89 GHz), 17 (150 GHz), 18 (183.31$\pm$1 GHz), 19 (183.31$\pm$3 GHz), and 20 (183.31$\pm$7 GHz). The left column correspond to clear sky simulations, the middle column corresponds to cloudy simulations and the right column corresponds to the cloud signal (clear sky BT minus cloudy BT).

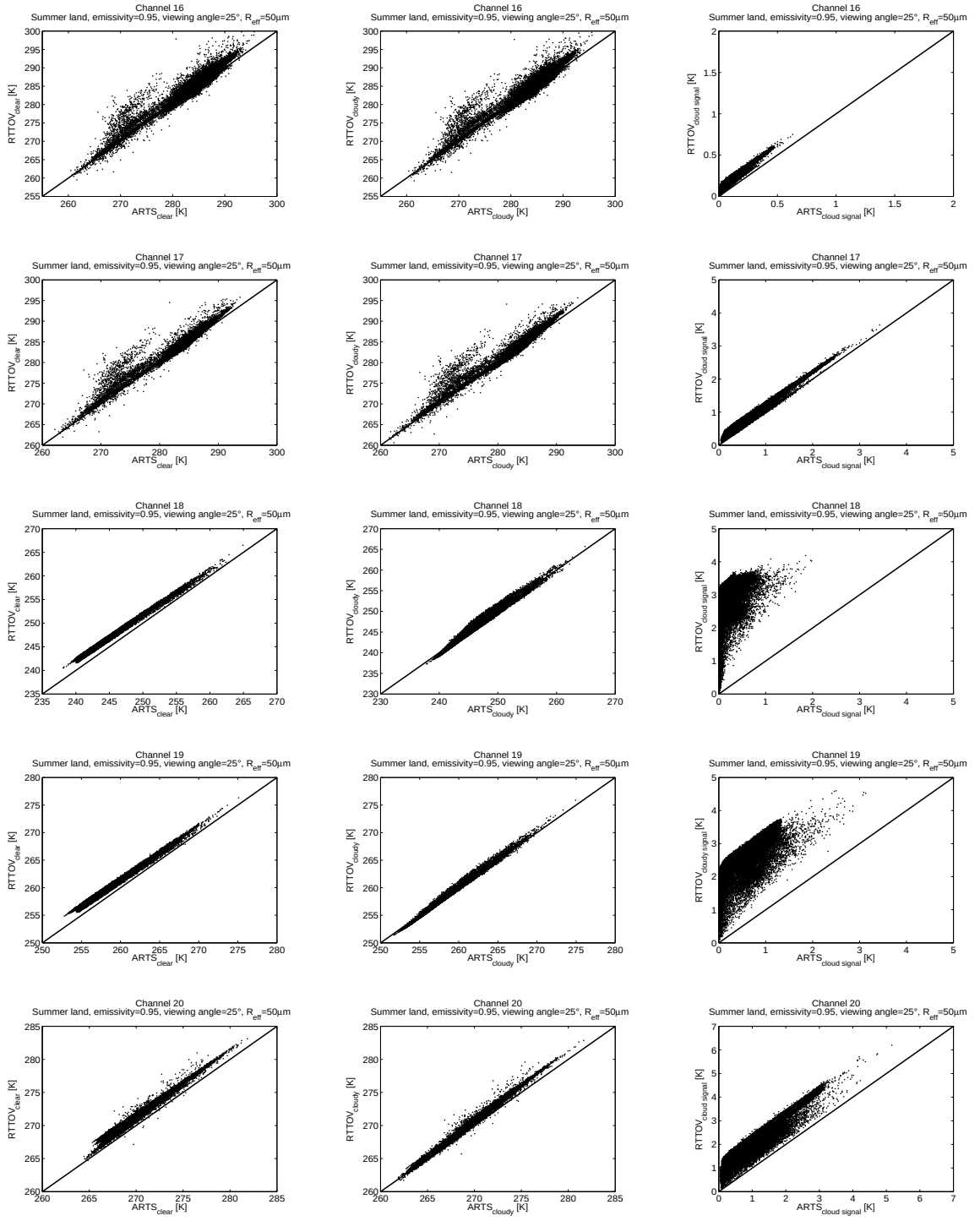

Figure 54: BT simulated for the land summer data set by RTTOVSCATT (for both clear sky simulations and cloudy simulations) against BT simulated by ARTS for a particular set of parameters (emissivity=0.95, viewing angle=25°, and effective radius of the ice particles= 50μm). Each line correspond to one AMSU-B channel from top to bottom channel 16 (89 GHz), 17 (150 GHz), 18 (183.31±1 GHz), 19 (183.31±3 GHz), and 20 (183.31±7 GHz). The left column correspond to clear sky simulations, the middle column corresponds to cloudy simulations and the right column corresponds to the cloud signal (clear sky BT minus cloudy BT).

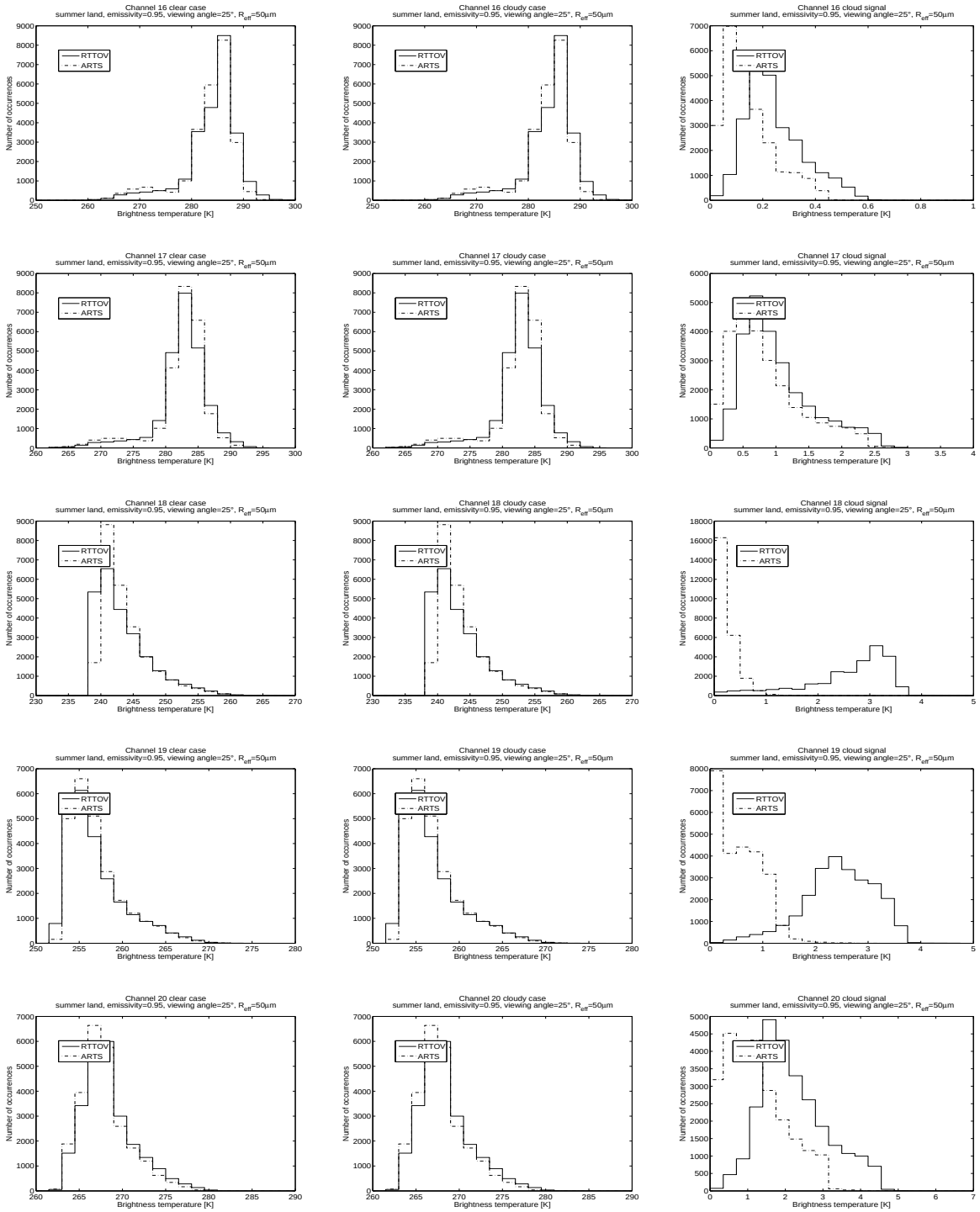

Figure 55: Histograms of BT simulated for the land summer data set by RTTOVSCATT (for both clear sky simulations and cloudy simulations), (plain line), and of BT simulated by ARTS (dashed line) for a particular set of parameters (emissivity=0.95, viewing angle=25°, and effective radius of the ice particles= 50μm). Each line correspond to one AMSU-B channel from top to bottom channel 16 (89 GHz), 17 (150 GHz), 18 (183.31±1 GHz), 19 (183.31±3 GHz), and 20 (183.31±7 GHz). The left column correspond to clear sky simulations, the middle column corresponds to cloudy simulations and the right column corresponds to the cloud signal (clear sky BT minus cloudy BT).

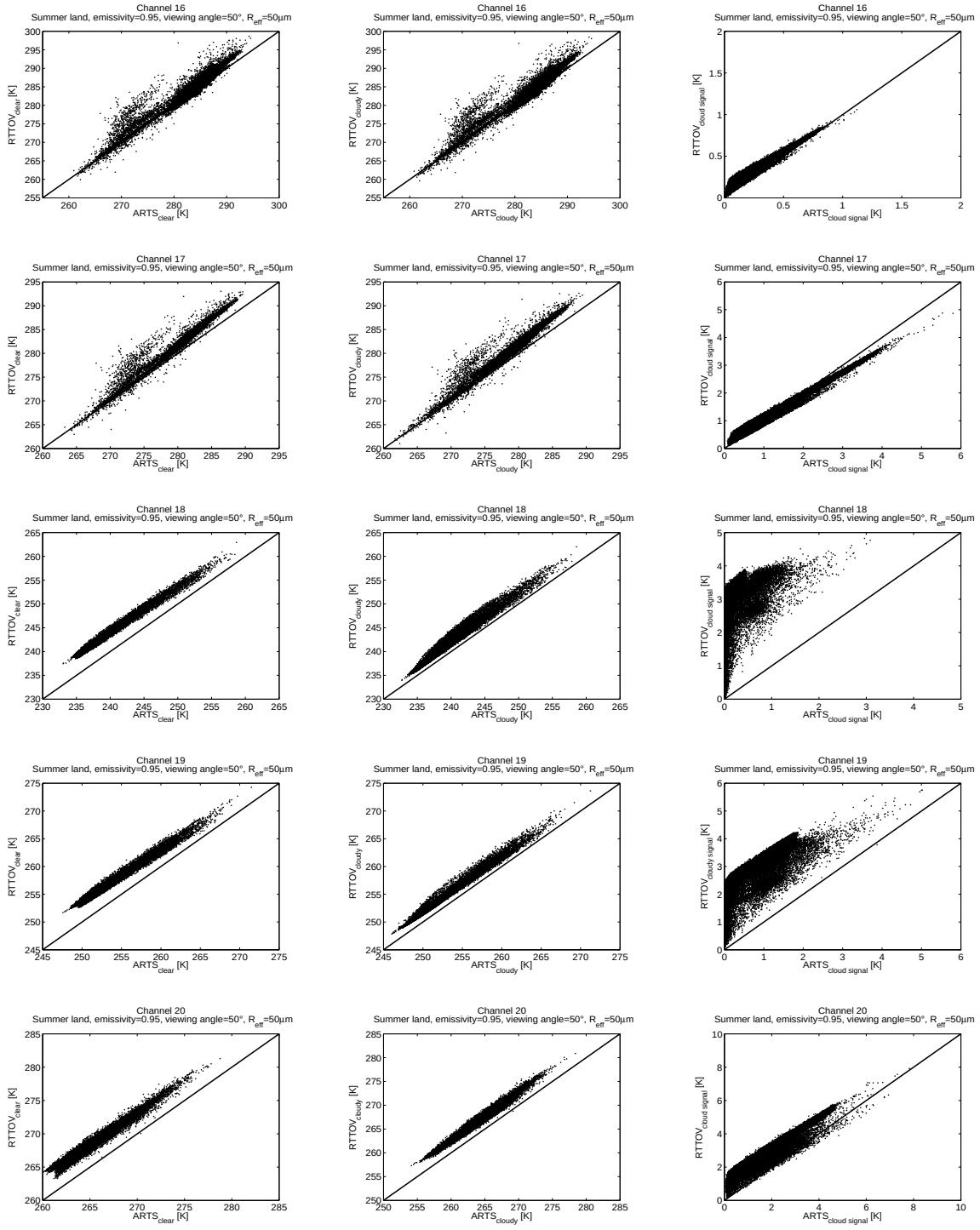

Figure 56: BT simulated for the land summer data set by RTTOVSCATT (for both clear sky simulations and cloudy simulations) against BT simulated by ARTS for a particular set of parameters (emissivity=0.95, viewing angle=50°, and effective radius of the ice particles= 50μm). Each line correspond to one AMSU-B channel from top to bottom channel 16 (89 GHz), 17 (150 GHz), 18 (183.31±1 GHz), 19 (183.31±3 GHz), and 20 (183.31±7 GHz). The left column correspond to clear sky simulations, the middle column corresponds to cloudy simulations and the right column corresponds to the cloud signal (clear sky BT minus cloudy BT).

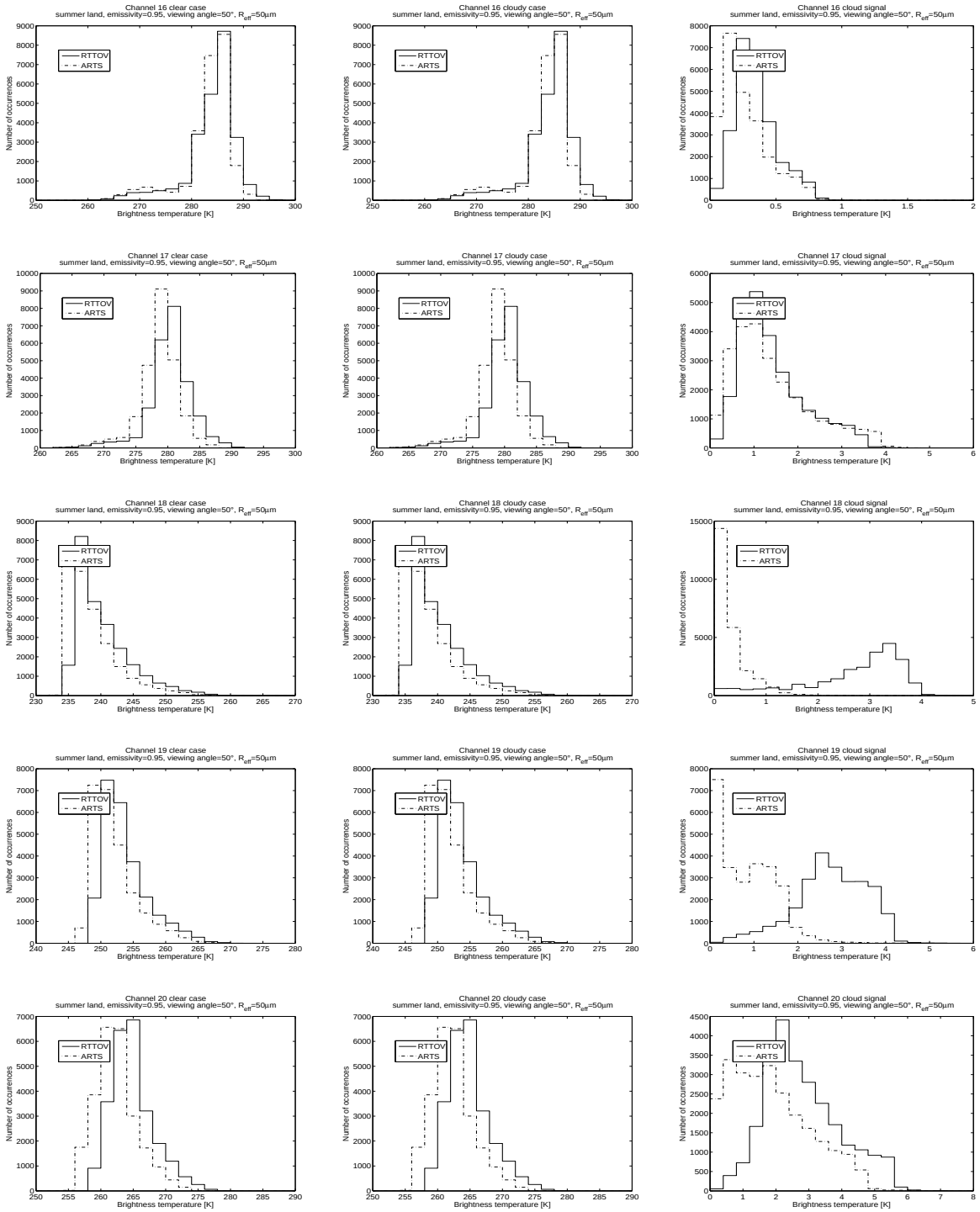

Figure 57: Histograms of BT simulated for the land summer data set by RTTOVSCATT (for both clear sky simulations and cloudy simulations), (plain line), and of BT simulated by ARTS (dashed line) for a particular set of parameters (emissivity=0.95, viewing angle=50°, and effective radius of the ice particles= 50μm). Each line correspond to one AMSU-B channel from top to bottom channel 16 (89 GHz), 17 (150 GHz), 18 (183.31±1 GHz), 19 (183.31±3 GHz), and 20 (183.31±7 GHz). The left column correspond to clear sky simulations, the middle column corresponds to cloudy simulations and the right column corresponds to the cloud signal (clear sky BT minus cloudy BT).

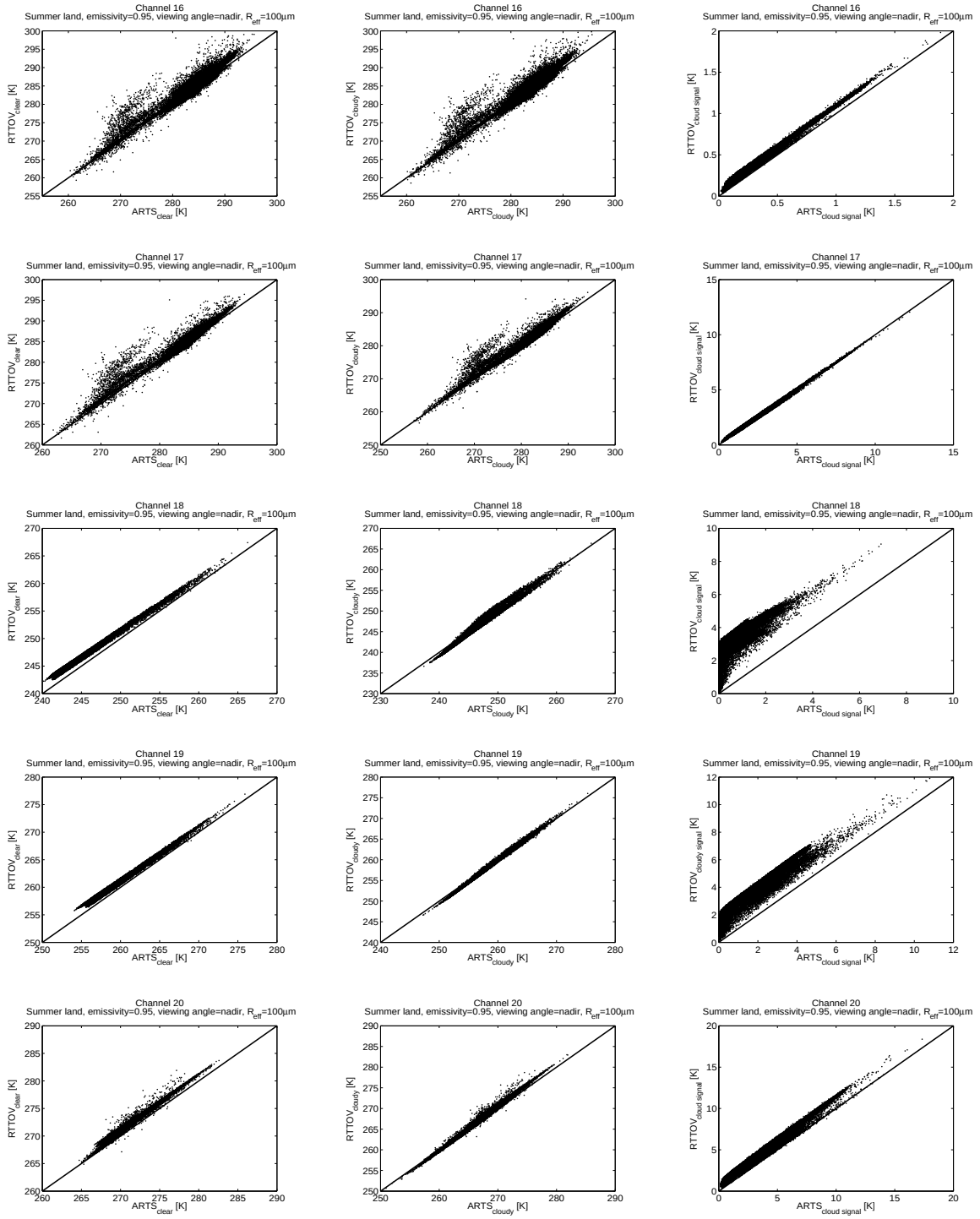

Figure 58: BT simulated for the land summer data set by RTTOVSCATT (for both clear sky simulations and cloudy simulations) against BT simulated by ARTS for a particular set of parameters (emissivity=0.95, viewing angle=nadir, and effective radius of the ice particles= 100μm). Each line correspond to one AMSU-B channel from top to bottom channel 16 (89 GHz), 17 (150 GHz), 18 (183.31±1 GHz), 19 (183.31±3 GHz), and 20 (183.31±7 GHz). The left column correspond to clear sky simulations, the middle column corresponds to cloudy simulations and the right column corresponds to the cloud signal (clear sky BT minus cloudy BT).

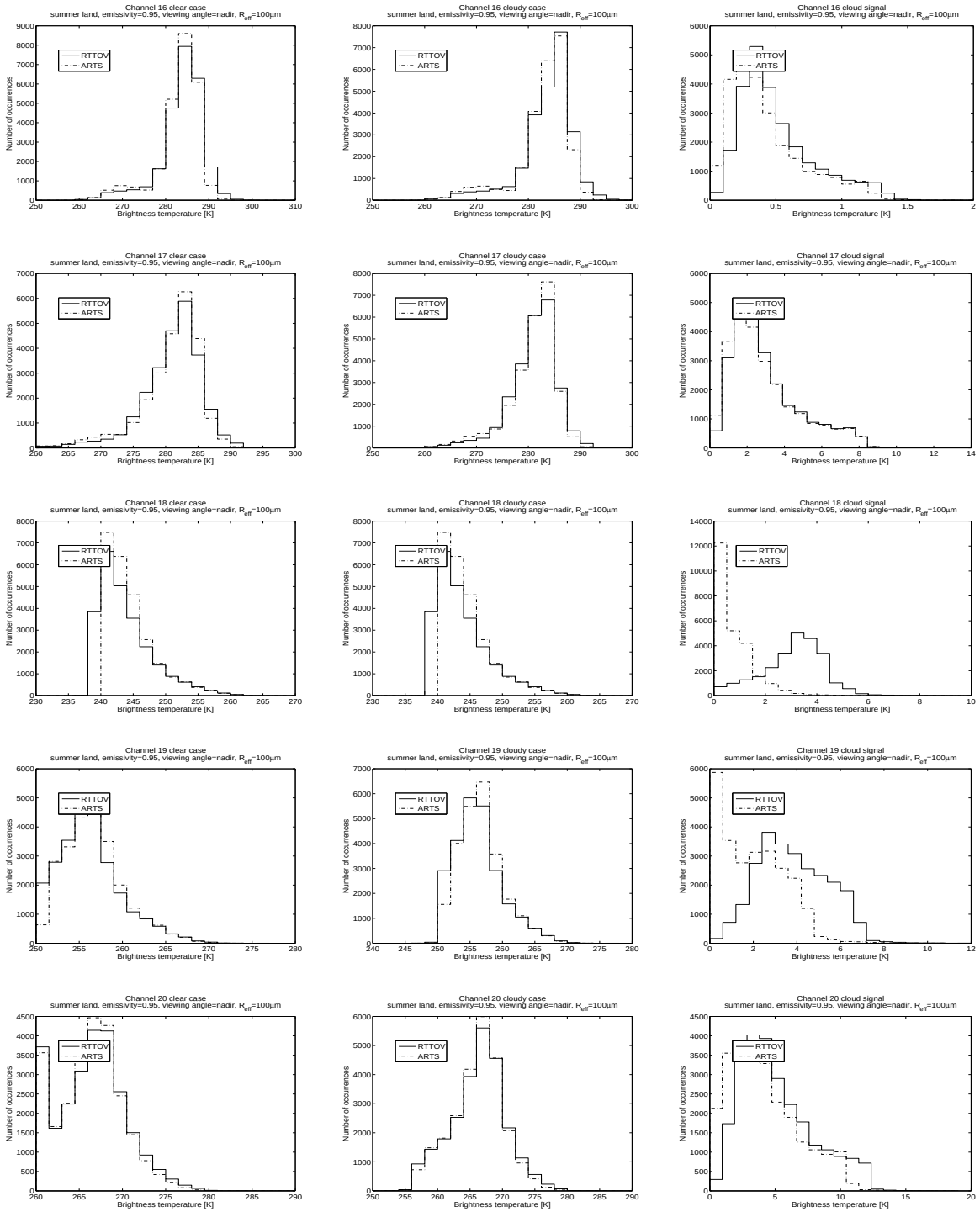

Figure 59: Histograms of BT simulated for the land summer data set by RTTOVSCATT (for both clear sky simulations and cloudy simulations), (plain line), and of BT simulated by ARTS (dashed line) for a particular set of parameters (emissivity=0.95, viewing angle=nadir, and effective radius of the ice particles= 100μm). Each line correspond to one AMSU-B channel from top to bottom channel 16 (89 GHz), 17 (150 GHz), 18 (183.31$\pm$1 GHz), 19 (183.31$\pm$3 GHz), and 20 (183.31$\pm$7 GHz). The left column correspond to clear sky simulations, the middle column corresponds to cloudy simulations and the right column corresponds to the cloud signal (clear sky BT minus cloudy BT).

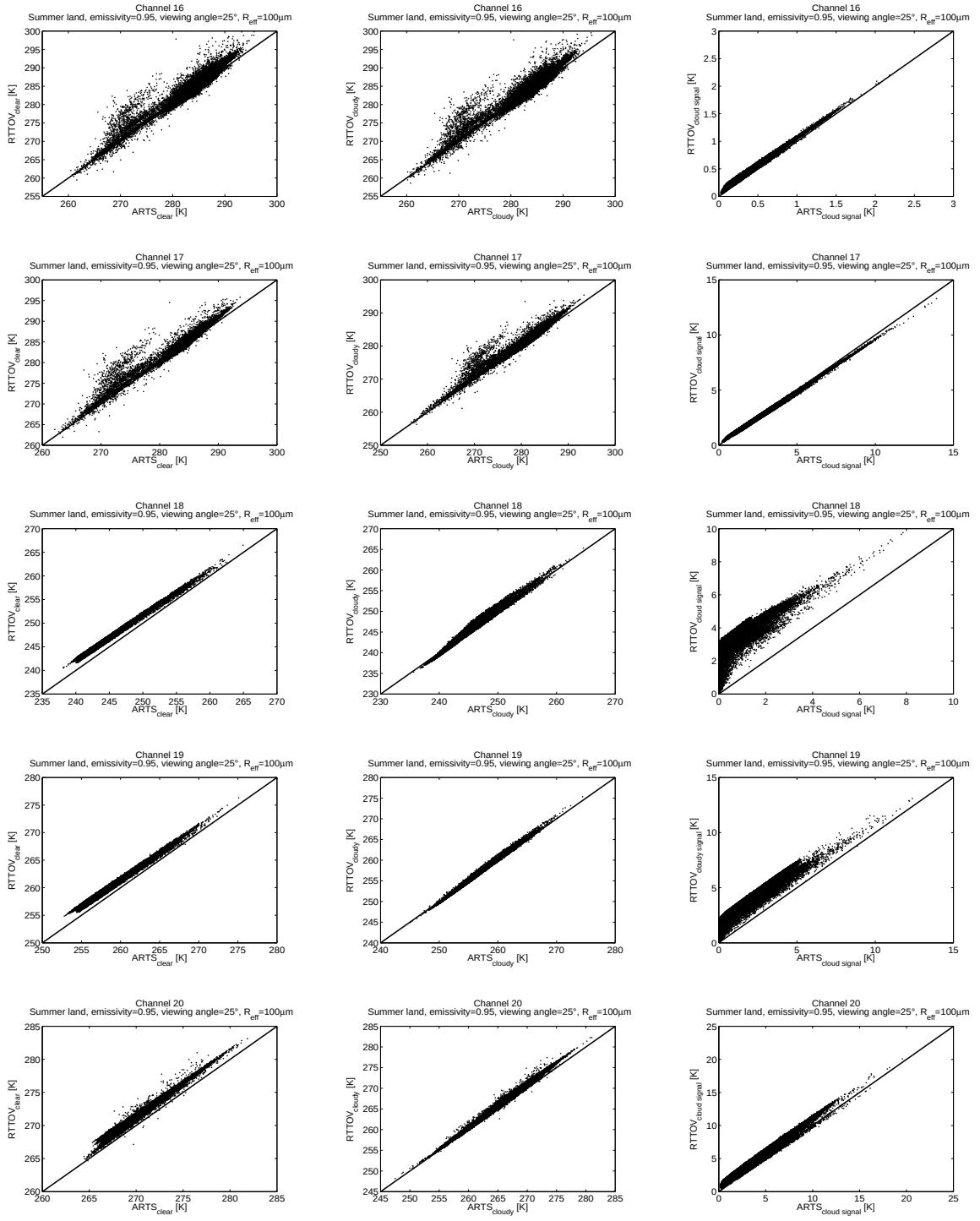

Figure 60: BT simulated for the land summer data set by RTTOVSCATT (for both clear sky simulations and cloudy simulations) against BT simulated by ARTS for a particular set of parameters (emissivity=0.95, viewing angle=25°, and effective radius of the ice particles= 100μm). Each line correspond to one AMSU-B channel from top to bottom channel 16 (89 GHz), 17 (150 GHz), 18 (183.31±1 GHz), 19 (183.31±3 GHz), and 20 (183.31±7 GHz). The left column correspond to clear sky simulations, the middle column corresponds to cloudy simulations and the right column corresponds to the cloud signal (clear sky BT minus cloudy BT).

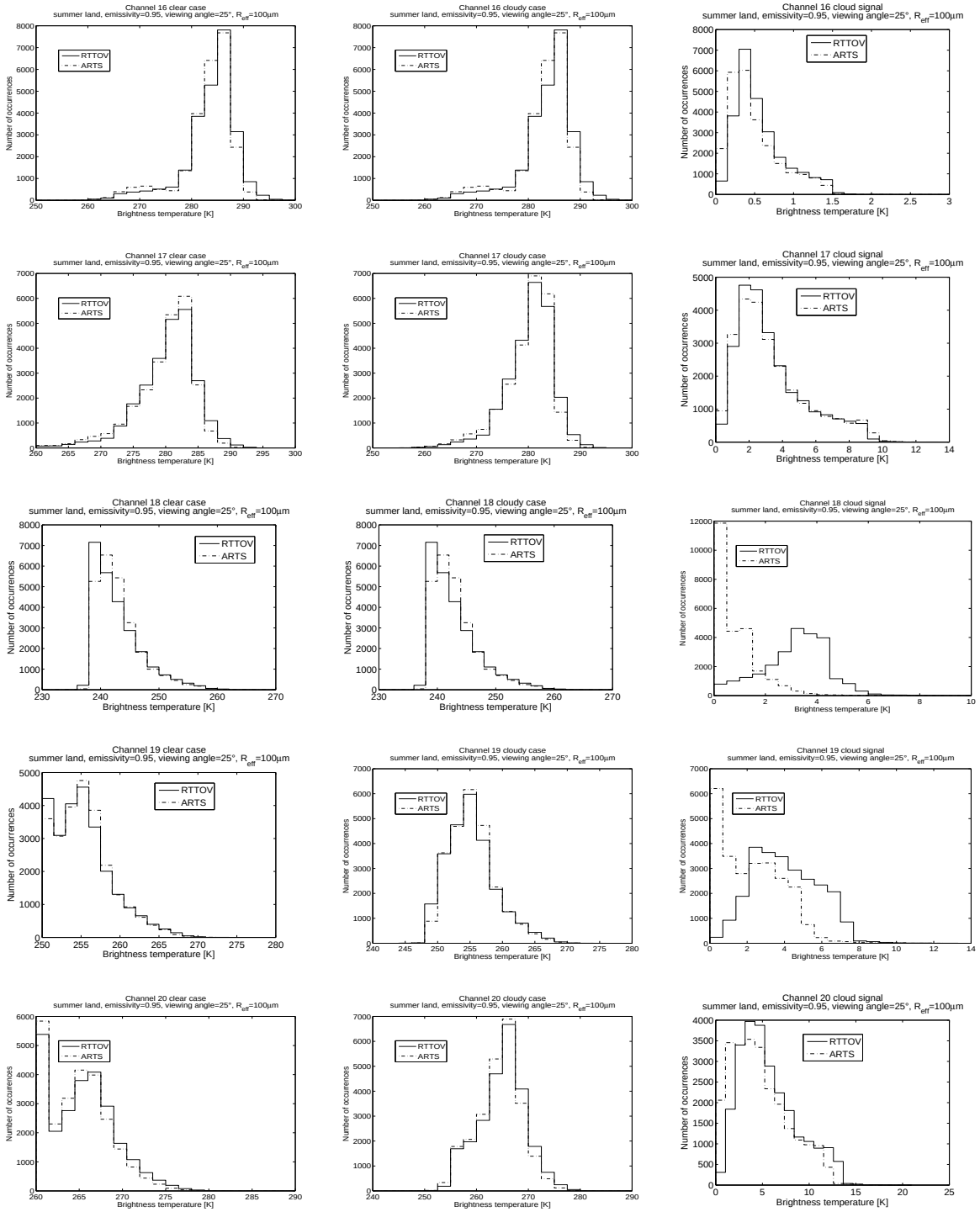

Figure 61: Histograms of BT simulated for the land summer data set by RTTOVSCATT (for both clear sky simulations and cloudy simulations), (plain line), and of BT simulated by ARTS (dashed line) for a particular set of parameters (emissivity=0.95, viewing angle=25°, and effective radius of the ice particles= 100μm). Each line correspond to one AMSU-B channel from top to bottom channel 16 (89 GHz), 17 (150 GHz), 18 (183.31±1 GHz), 19 (183.31±3 GHz), and 20 (183.31±7 GHz). The left column correspond to clear sky simulations, the middle column corresponds to cloudy simulations and the right column corresponds to the cloud signal (clear sky BT minus cloudy BT).

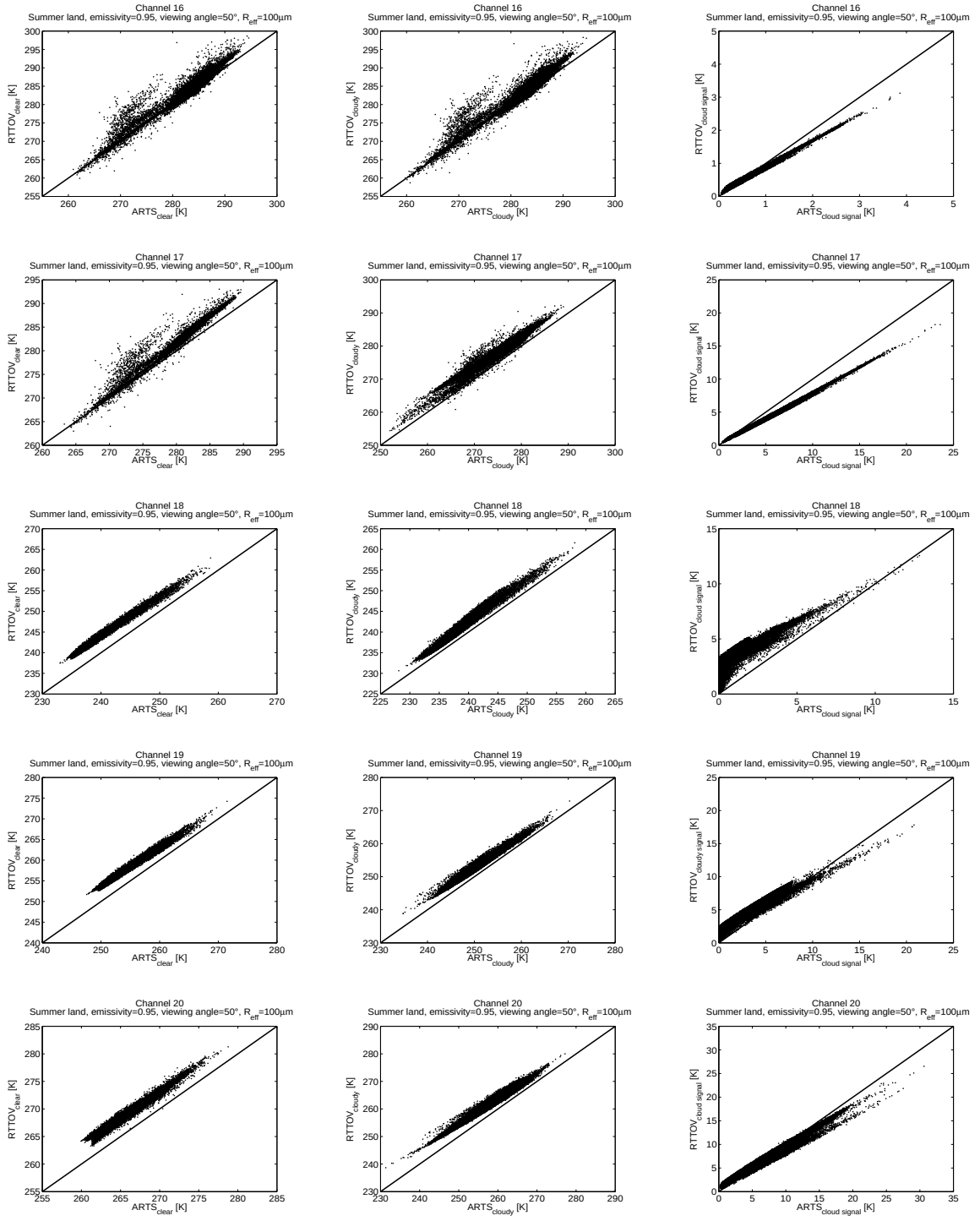

Figure 62: BT simulated for the land summer data set by RTTOVSCATT (for both clear sky simulations and cloudy simulations) against BT simulated by ARTS for a particular set of parameters (emissivity=0.95, viewing angle=50°, and effective radius of the ice particles= 100μm). Each line correspond to one AMSU-B channel from top to bottom channel 16 (89 GHz), 17 (150 GHz), 18 (183.31±1 GHz), 19 (183.31±3 GHz), and 20 (183.31±7 GHz). The left column correspond to clear sky simulations, the middle column corresponds to cloudy simulations and the right column corresponds to the cloud signal (clear sky BT minus cloudy BT).

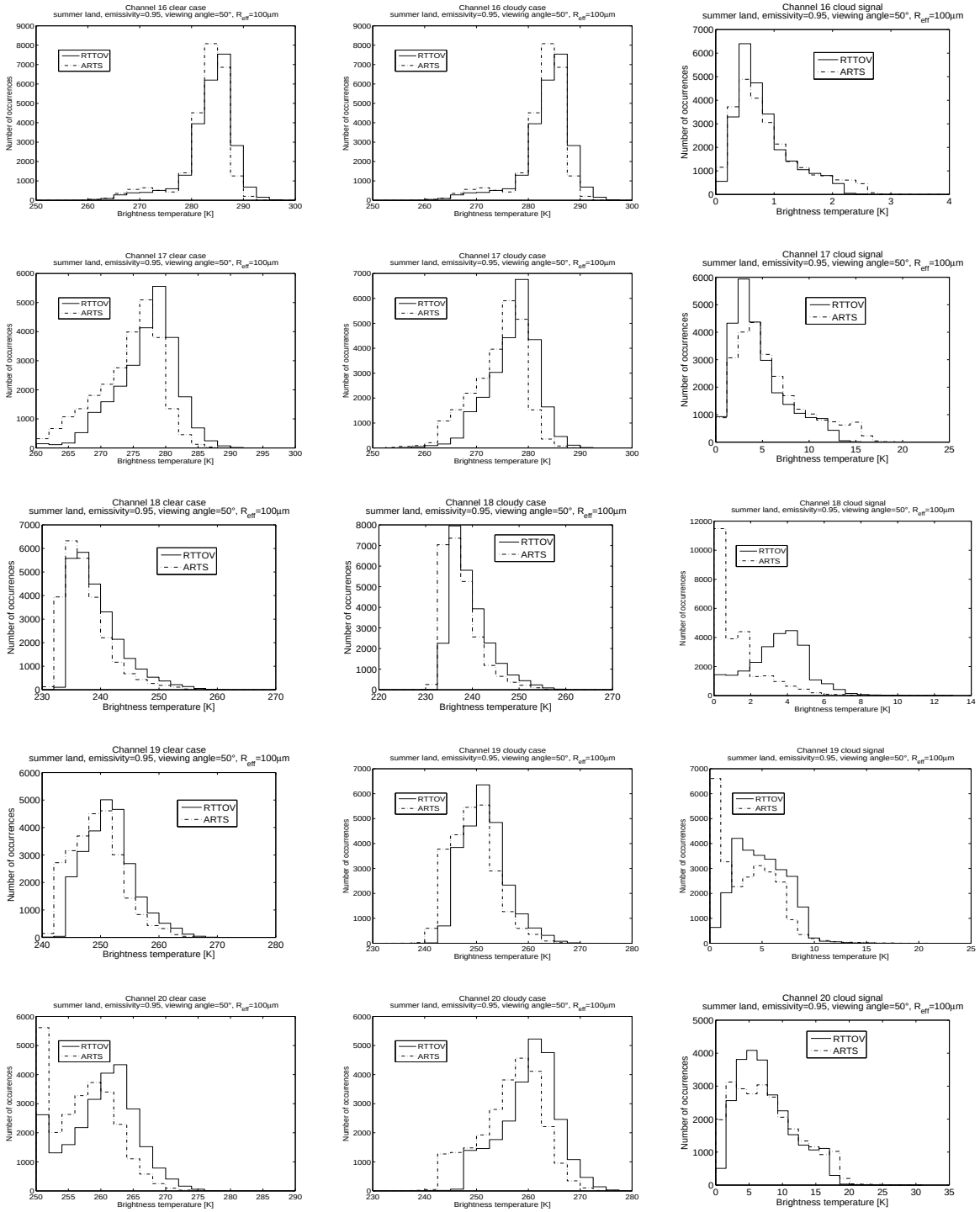

Figure 63: Histograms of BT simulated for the land summer data set by RTTOVSCATT (for both clear sky simulations and cloudy simulations), (plain line), and of BT simulated by ARTS (dashed line) for a particular set of parameters (emissivity=0.95, viewing angle=50°, and effective radius of the ice particles= 100μm). Each line correspond to one AMSU-B channel from top to bottom channel 16 (89 GHz), 17 (150 GHz), 18 (183.31±1 GHz), 19 (183.31±3 GHz), and 20 (183.31±7 GHz). The left column correspond to clear sky simulations, the middle column corresponds to cloudy simulations and the right column corresponds to the cloud signal (clear sky BT minus cloudy BT).

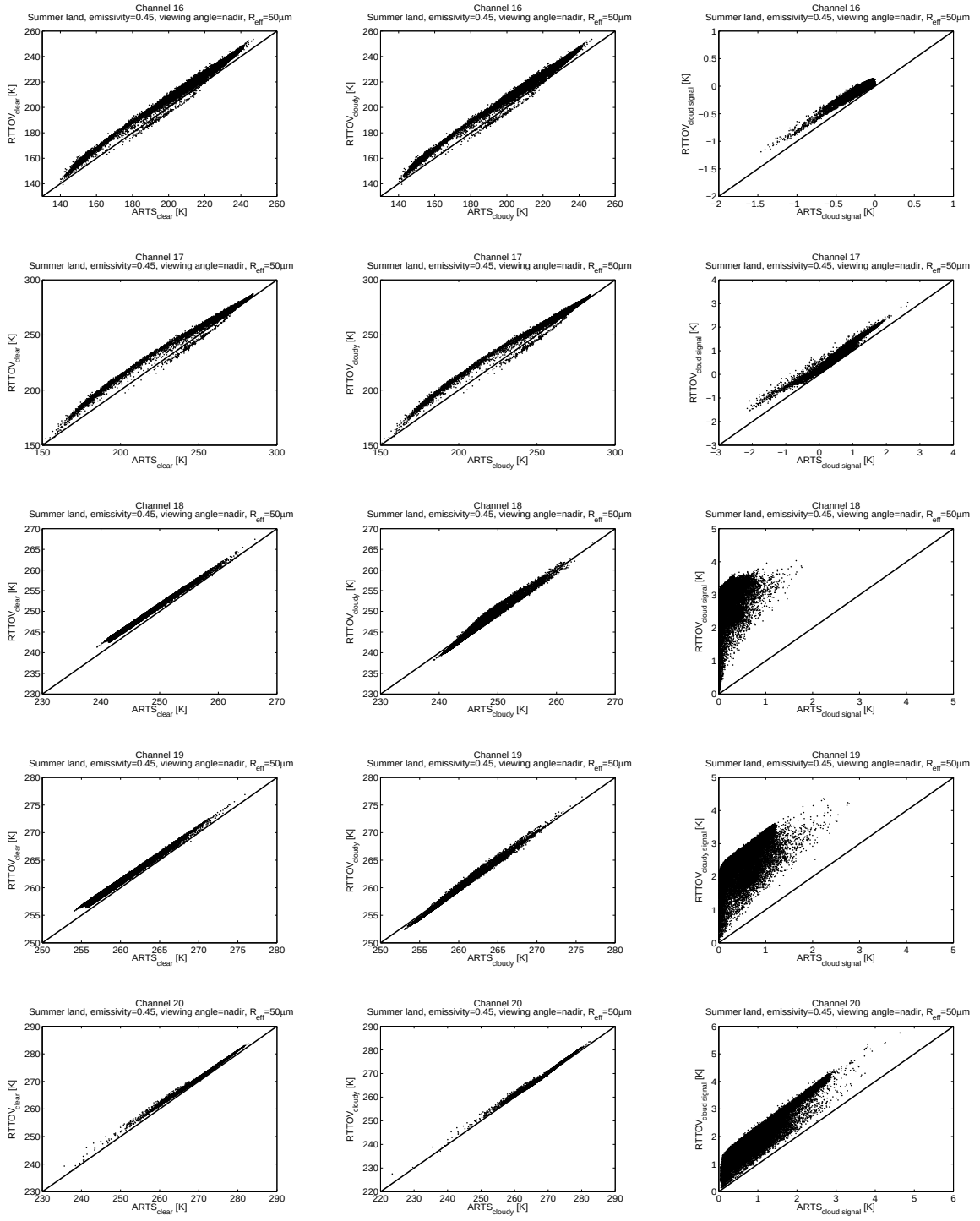

Figure 64: BT simulated for the land summer data set by RTTOVSCATT (for both clear sky simulations and cloudy simulations) against BT simulated by ARTS for a particular set of parameters (emissivity=0.45, viewing angle=nadir, and effective radius of the ice particles= 50μm). Each line correspond to one AMSU-B channel from top to bottom channel 16 (89 GHz), 17 (150 GHz), 18 (183.31±1 GHz), 19 (183.31±3 GHz), and 20 (183.31±7 GHz). The left column correspond to clear sky simulations, the middle column corresponds to cloudy simulations and the right column corresponds to the cloud signal (clear sky BT minus cloudy BT).

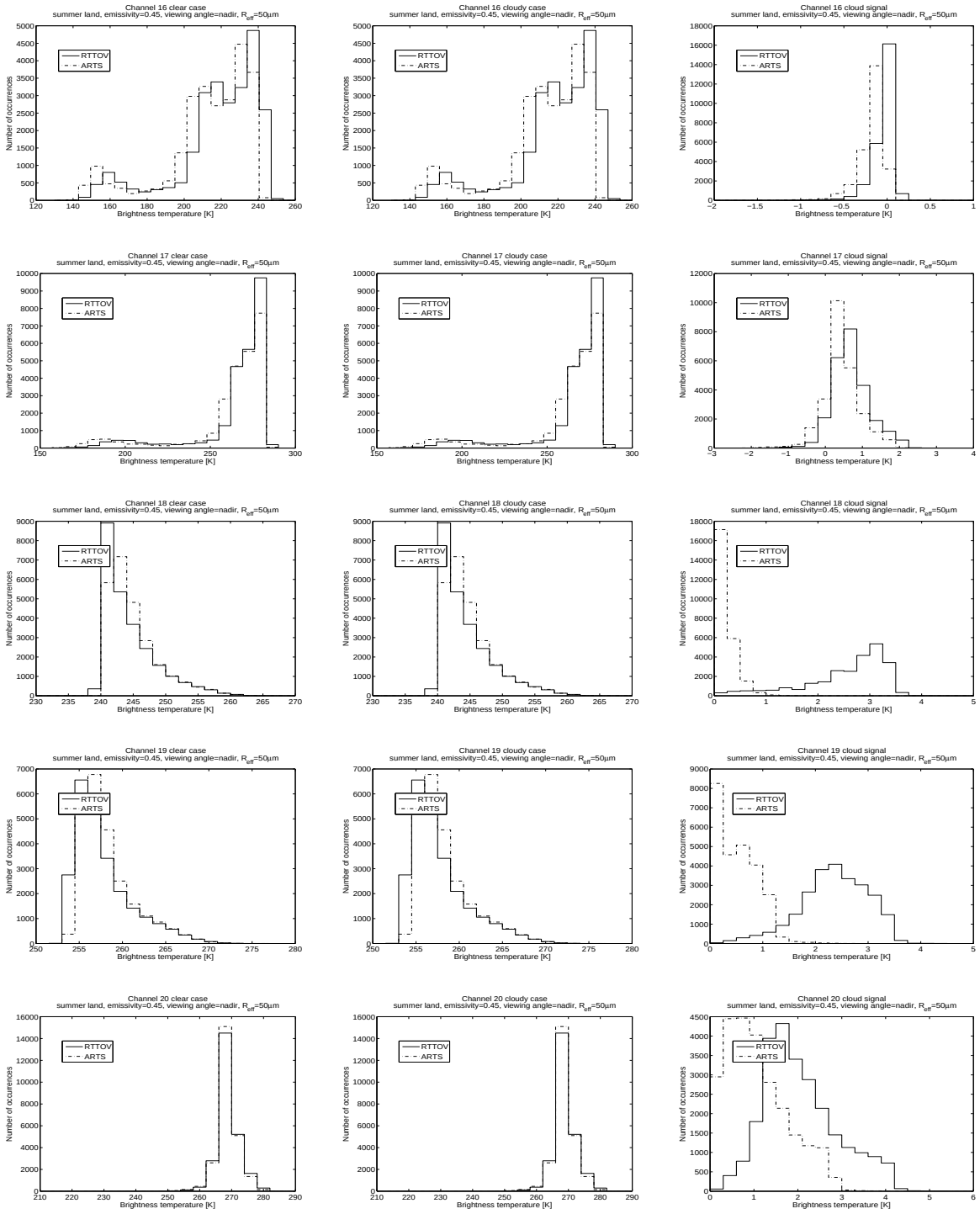

Figure 65: Histograms of BT simulated for the land summer data set by RTTOVSCATT (for both clear sky simulations and cloudy simulations), (plain line), and of BT simulated by ARTS (dashed line) for a particular set of parameters (emissivity=0.45, viewing angle=nadir, and effective radius of the ice particles= 50μm). Each line correspond to one AMSU-B channel from top to bottom channel 16 (89 GHz), 17 (150 GHz), 18 (183.31$\pm$1 GHz), 19 (183.31$\pm$3 GHz), and 20 (183.31$\pm$7 GHz). The left column correspond to clear sky simulations, the middle column corresponds to cloudy simulations and the right column corresponds to the cloud signal (clear sky BT minus cloudy BT).

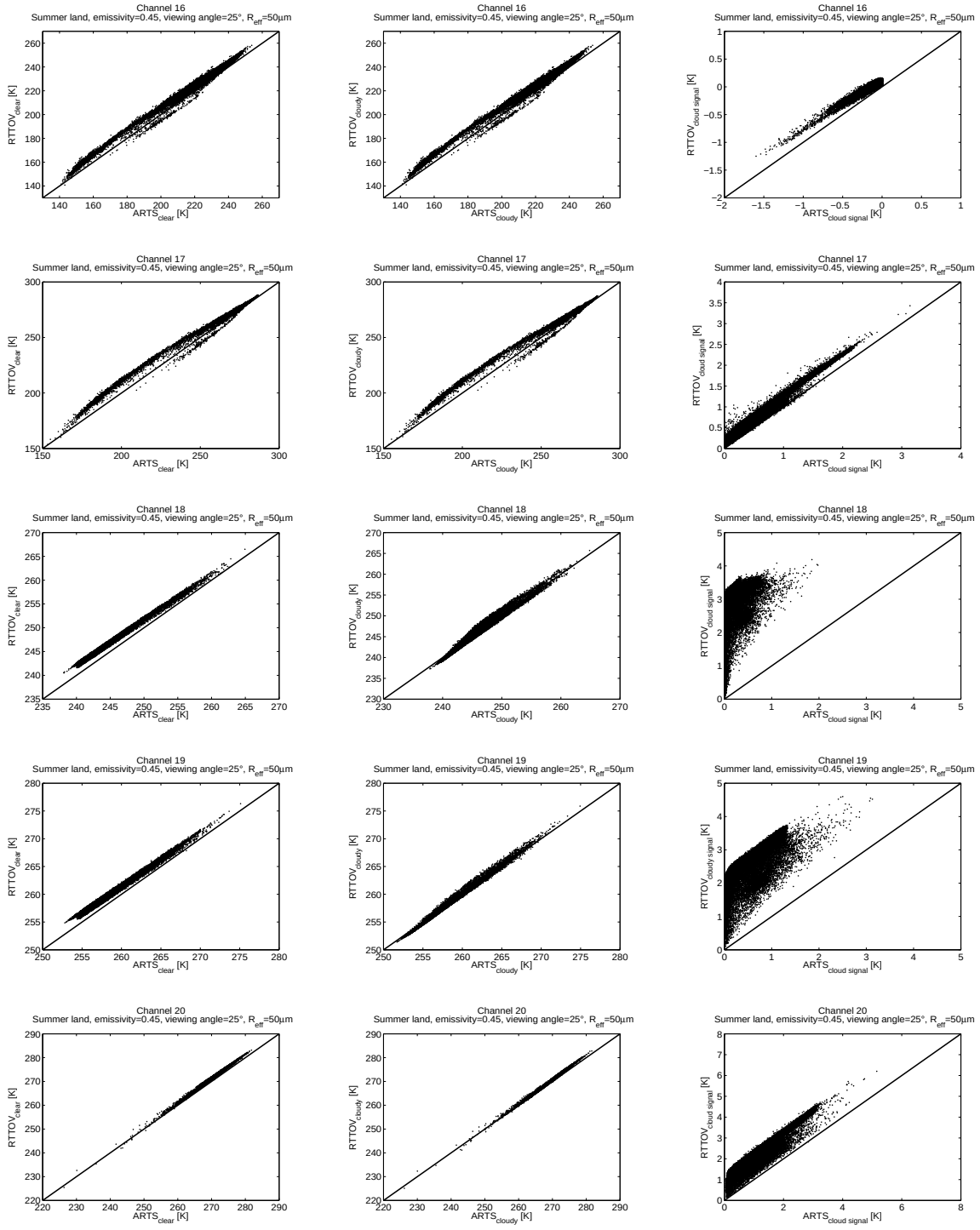

Figure 66: BT simulated for the land summer data set by RTTOVSCATT (for both clear sky simulations and cloudy simulations) against BT simulated by ARTS for a particular set of parameters (emissivity=0.45, viewing angle=25°, and effective radius of the ice particles= 50μm). Each line correspond to one AMSU-B channel from top to bottom channel 16 (89 GHz), 17 (150 GHz), 18 (183.31±1 GHz), 19 (183.31±3 GHz), and 20 (183.31±7 GHz). The left column correspond to clear sky simulations, the middle column corresponds to cloudy simulations and the right column corresponds to the cloud signal (clear sky BT minus cloudy BT).

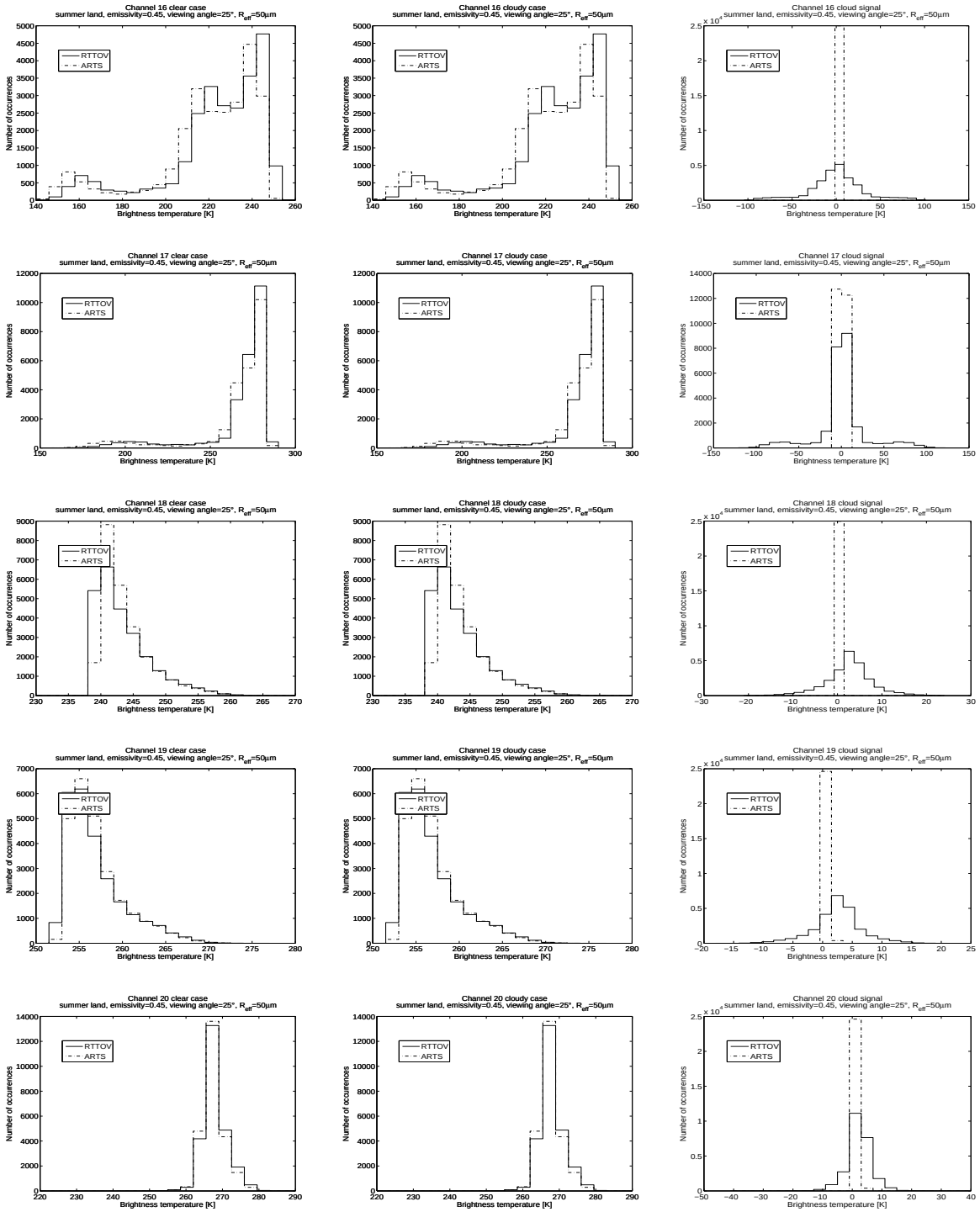

Figure 67: Histograms of BT simulated for the land summer data set by RTTOVSCATT (for both clear sky simulations and cloudy simulations), (plain line), and of BT simulated by ARTS (dashed line) for a particular set of parameters (emissivity=0.45, viewing angle=25°, and effective radius of the ice particles= 50μm). Each line correspond to one AMSU-B channel from top to bottom channel 16 (89 GHz), 17 (150 GHz), 18 (183.31±1 GHz), 19 (183.31±3 GHz), and 20 (183.31±7 GHz). The left column correspond to clear sky simulations, the middle column corresponds to cloudy simulations and the right column corresponds to the cloud signal (clear sky BT minus cloudy BT).

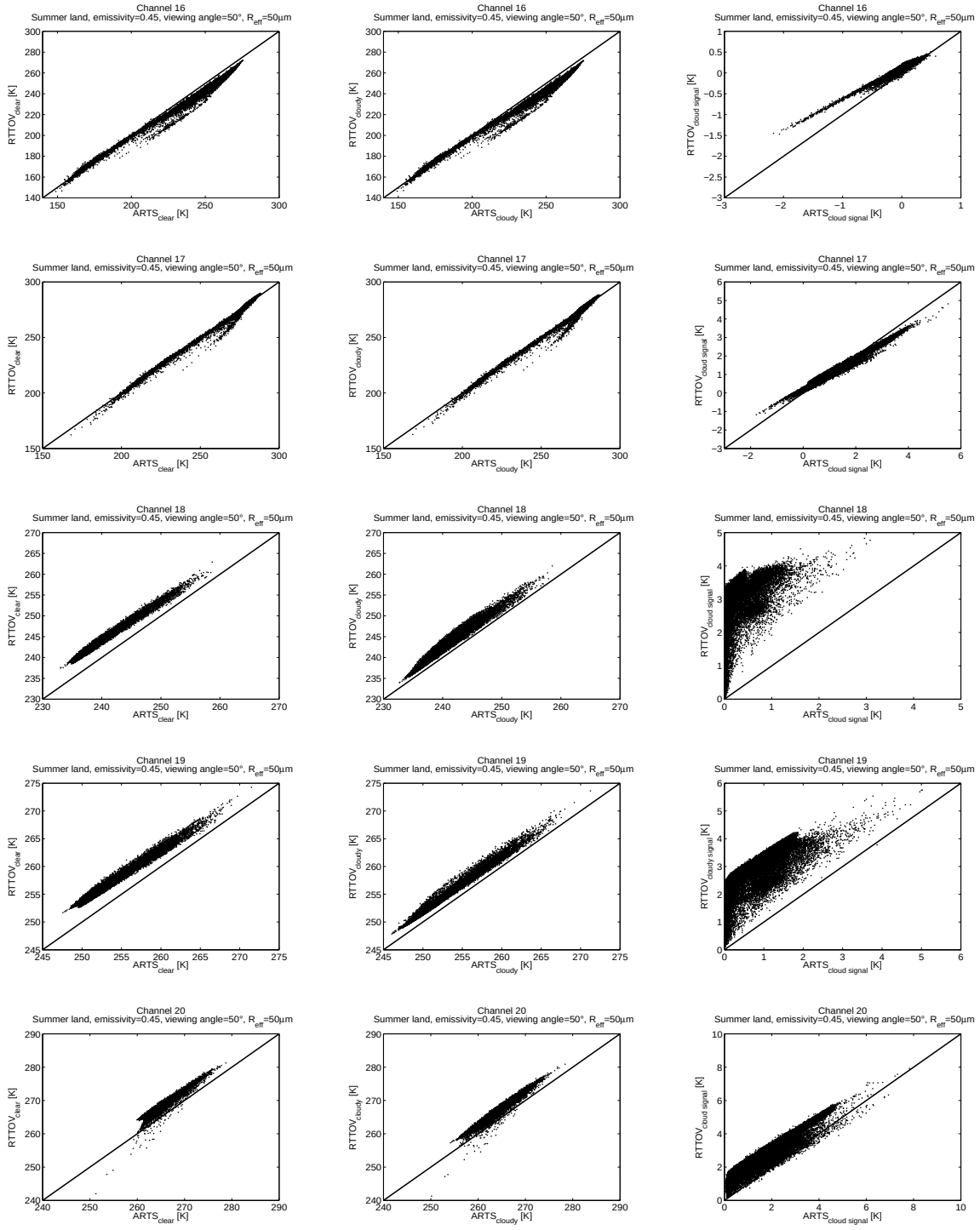

Figure 68: BT simulated for the land summer data set by RTTOVSCATT (for both clear sky simulations and cloudy simulations) against BT simulated by ARTS for a particular set of parameters (emissivity=0.45, viewing angle=50°, and effective radius of the ice particles= 50μm). Each line correspond to one AMSU-B channel from top to bottom channel 16 (89 GHz), 17 (150 GHz), 18 (183.31±1 GHz), 19 (183.31±3 GHz), and 20 (183.31±7 GHz). The left column correspond to clear sky simulations, the middle column corresponds to cloudy simulations and the right column corresponds to the cloud signal (clear sky BT minus cloudy BT).

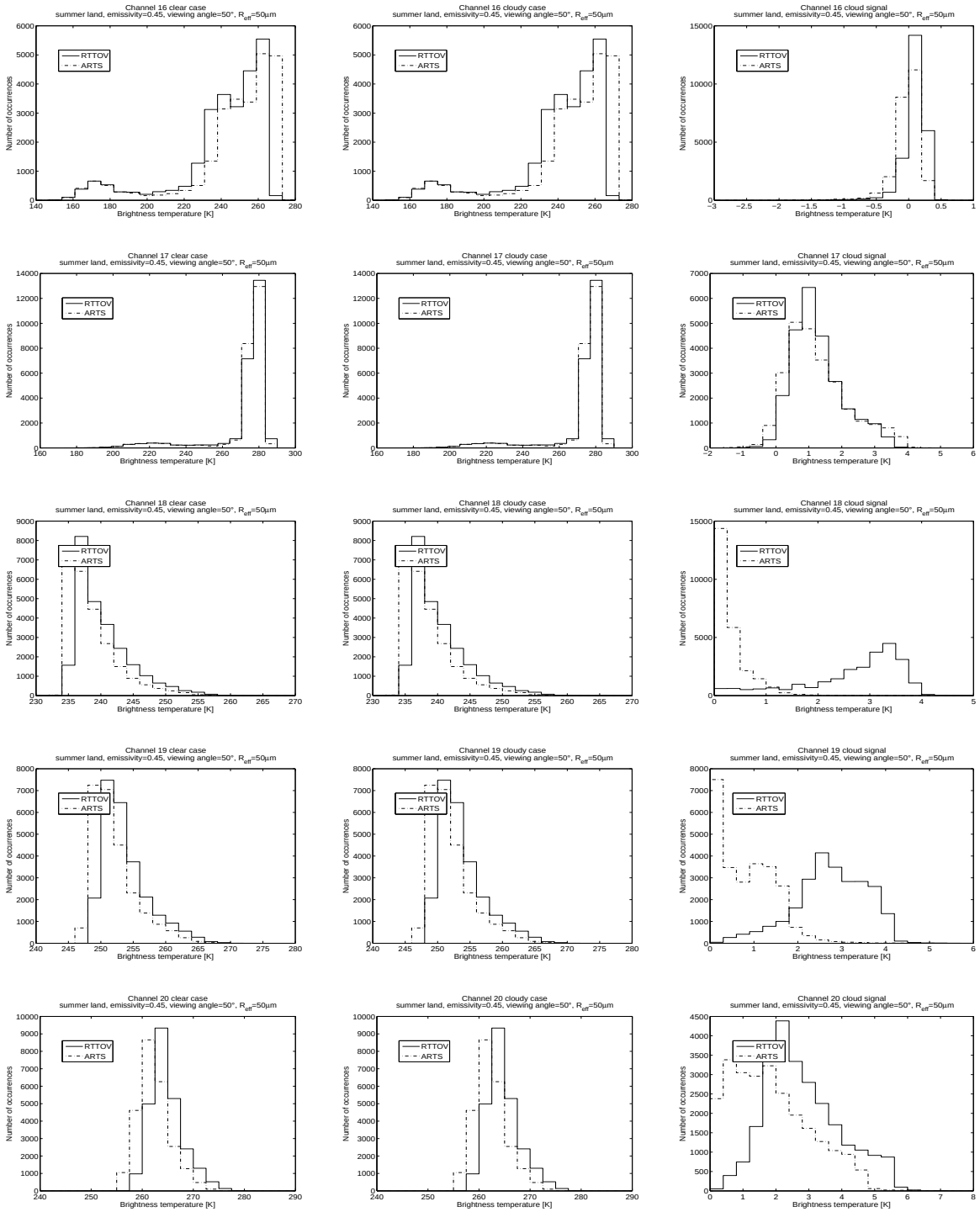

Figure 69: Histograms of BT simulated for the land summer data set by RTTOVSCATT (for both clear sky simulations and cloudy simulations), (plain line), and of BT simulated by ARTS (dashed line) for a particular set of parameters (emissivity=0.45, viewing angle=50°, and effective radius of the ice particles= 50μm). Each line correspond to one AMSU-B channel from top to bottom channel 16 (89 GHz), 17 (150 GHz), 18 (183.31±1 GHz), 19 (183.31±3 GHz), and 20 (183.31±7 GHz). The left column correspond to clear sky simulations, the middle column corresponds to cloudy simulations and the right column corresponds to the cloud signal (clear sky BT minus cloudy BT).

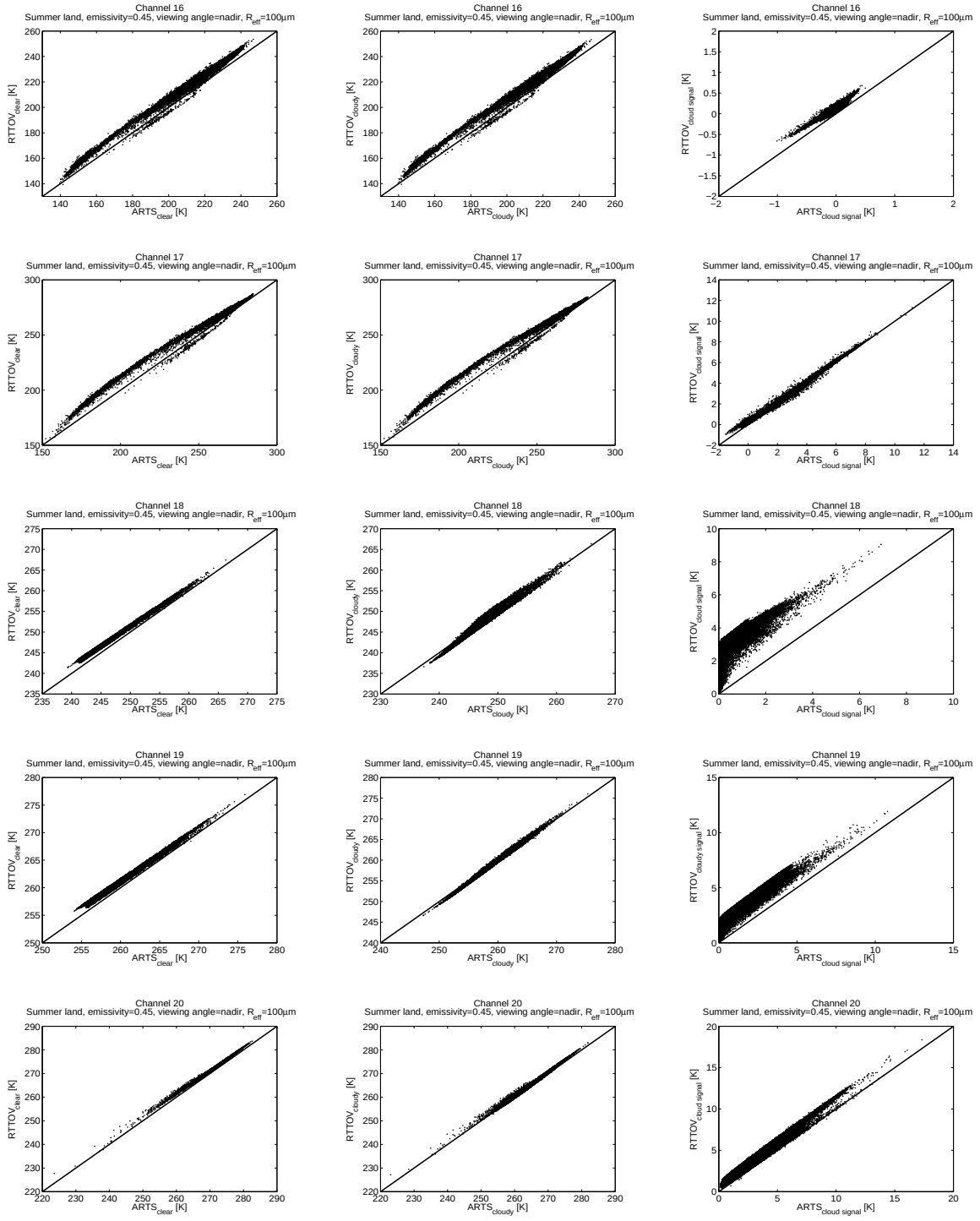

Figure 70: BT simulated for the land summer data set by RTTOVSCATT (for both clear sky simulations and cloudy simulations) against BT simulated by ARTS for a particular set of parameters (emissivity=0.45, viewing angle=nadir, and effective radius of the ice particles= 100μm). Each line correspond to one AMSU-B channel from top to bottom channel 16 (89 GHz), 17 (150 GHz), 18 (183.31±1 GHz), 19 (183.31±3 GHz), and 20 (183.31±7 GHz). The left column correspond to clear sky simulations, the middle column corresponds to cloudy simulations and the right column corresponds to the cloud signal (clear sky BT minus cloudy BT).

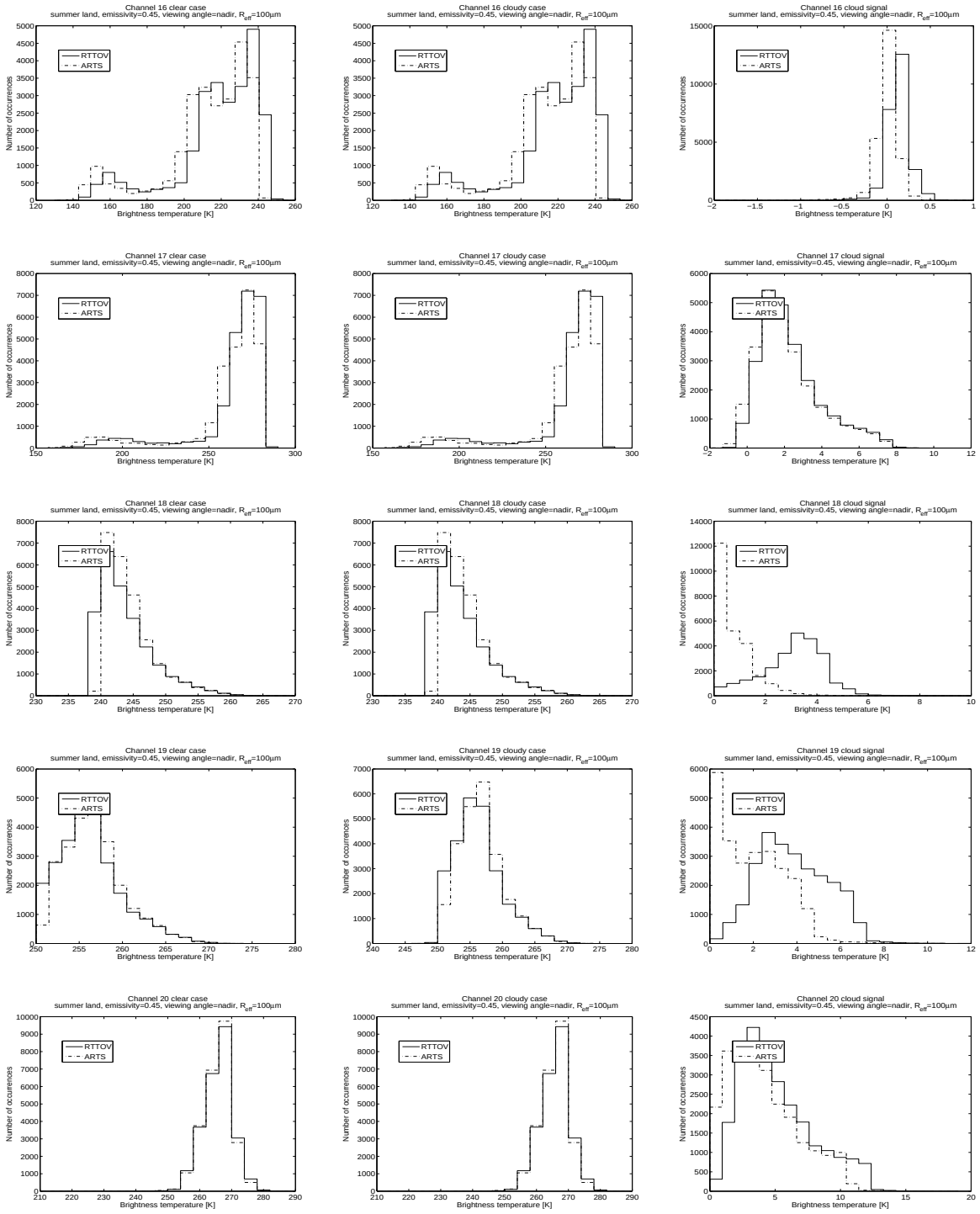

Figure 71: Histograms of BT simulated for the land summer data set by RTTOVSCATT (for both clear sky simulations and cloudy simulations), (plain line), and of BT simulated by ARTS (dashed line) for a particular set of parameters (emissivity=0.45, viewing angle=nadir, and effective radius of the ice particles= 100μm). Each line correspond to one AMSU-B channel from top to bottom channel 16 (89 GHz), 17 (150 GHz), 18 (183.31$\pm$1 GHz), 19 (183.31$\pm$3 GHz), and 20 (183.31$\pm$7 GHz). The left column correspond to clear sky simulations, the middle column corresponds to cloudy simulations and the right column corresponds to the cloud signal (clear sky BT minus cloudy BT).

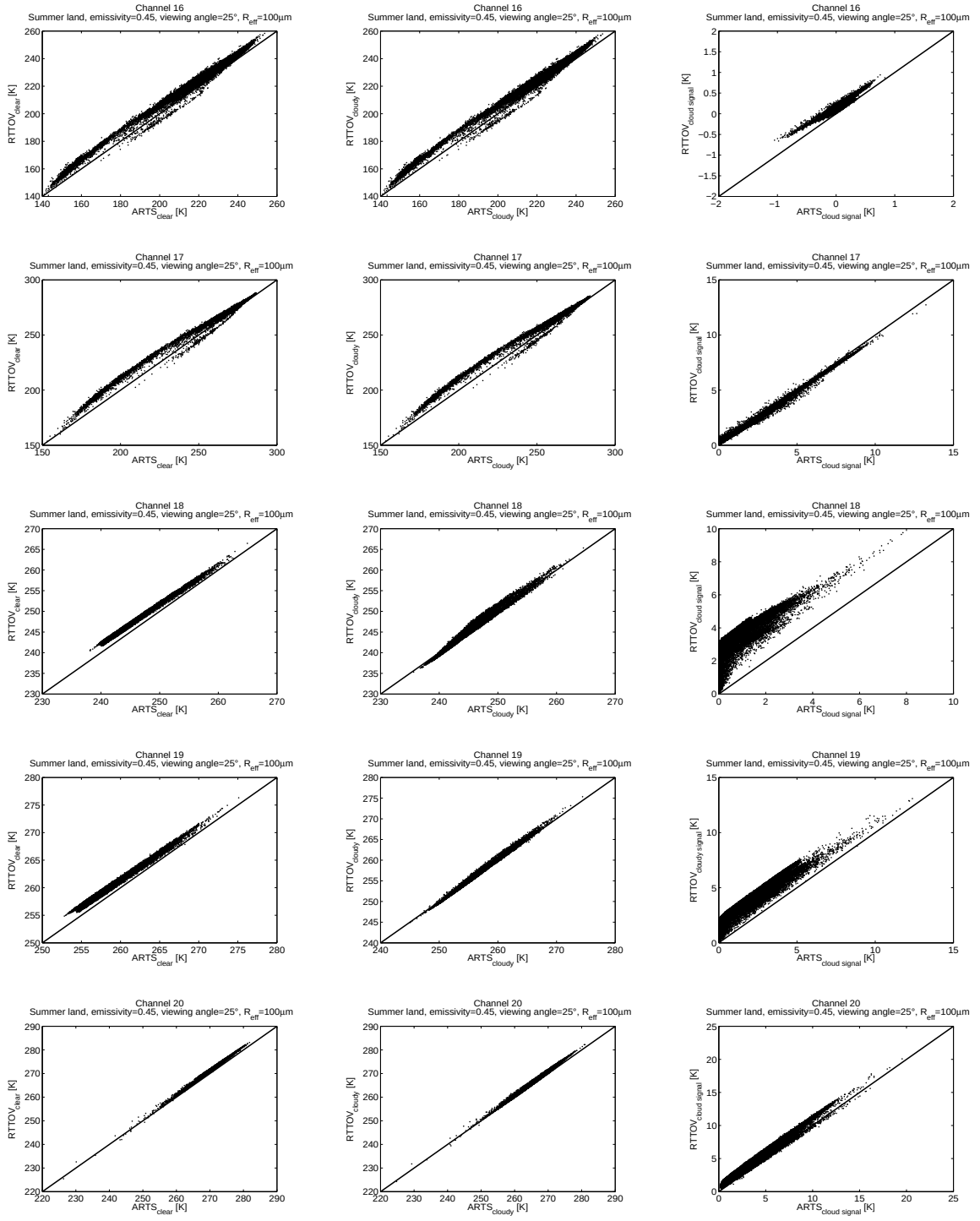

Figure 72: BT simulated for the land summer data set by RTTOVSCATT (for both clear sky simulations and cloudy simulations) against BT simulated by ARTS for a particular set of parameters (emissivity=0.45, viewing angle=25°, and effective radius of the ice particles= 100μm). Each line correspond to one AMSU-B channel from top to bottom channel 16 (89 GHz), 17 (150 GHz), 18 (183.31±1 GHz), 19 (183.31±3 GHz), and 20 (183.31±7 GHz). The left column correspond to clear sky simulations, the middle column corresponds to cloudy simulations and the right column corresponds to the cloud signal (clear sky BT minus cloudy BT).

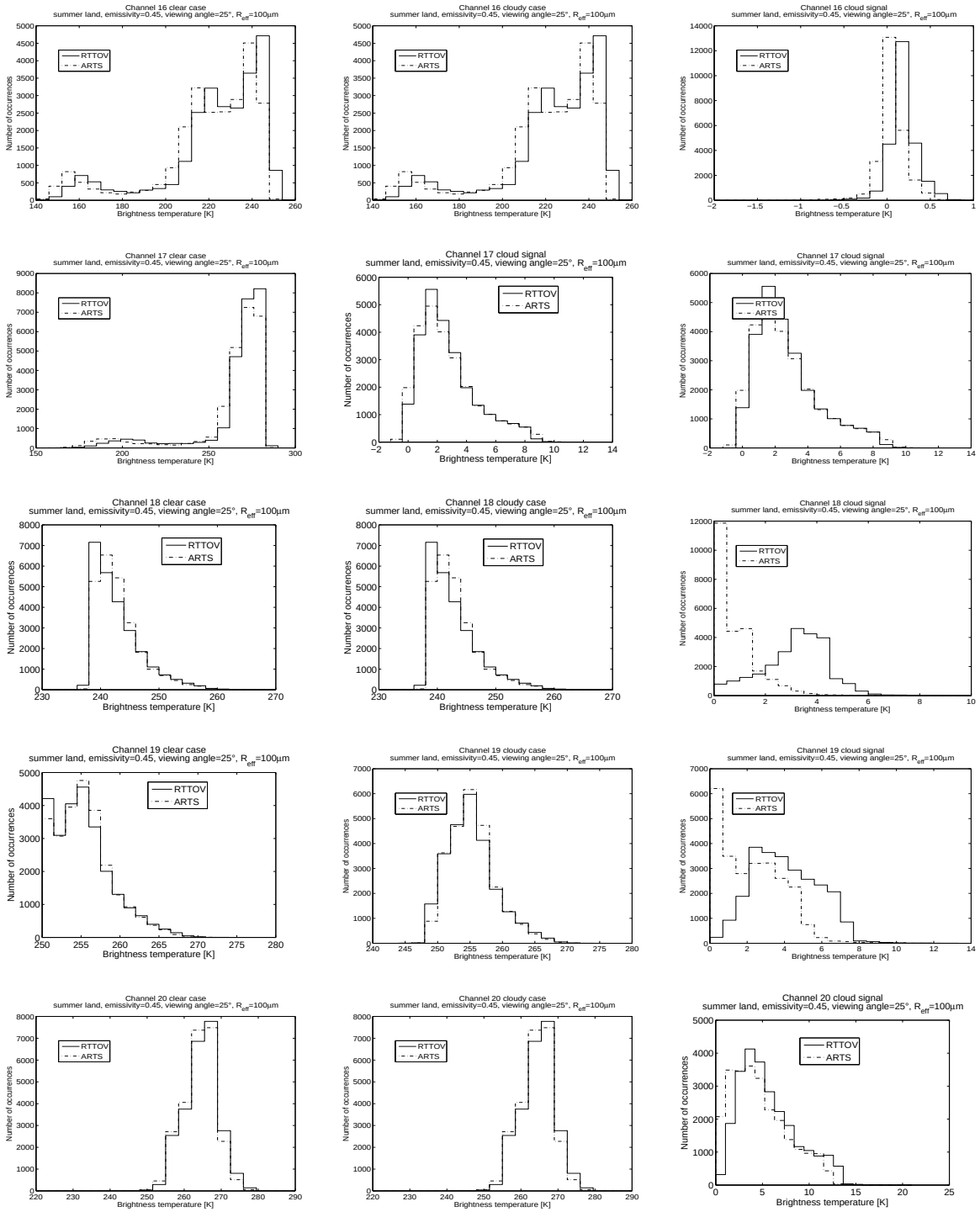

Figure 73: Histograms of BT simulated for the land summer data set by RTTOVSCATT (for both clear sky simulations and cloudy simulations), (plain line), and of BT simulated by ARTS (dashed line) for a particular set of parameters (emissivity=0.45, viewing angle=25°, and effective radius of the ice particles= 100μm). Each line correspond to one AMSU-B channel from top to bottom channel 16 (89 GHz), 17 (150 GHz), 18 (183.31±1 GHz), 19 (183.31±3 GHz), and 20 (183.31±7 GHz). The left column correspond to clear sky simulations, the middle column corresponds to cloudy simulations and the right column corresponds to the cloud signal (clear sky BT minus cloudy BT).

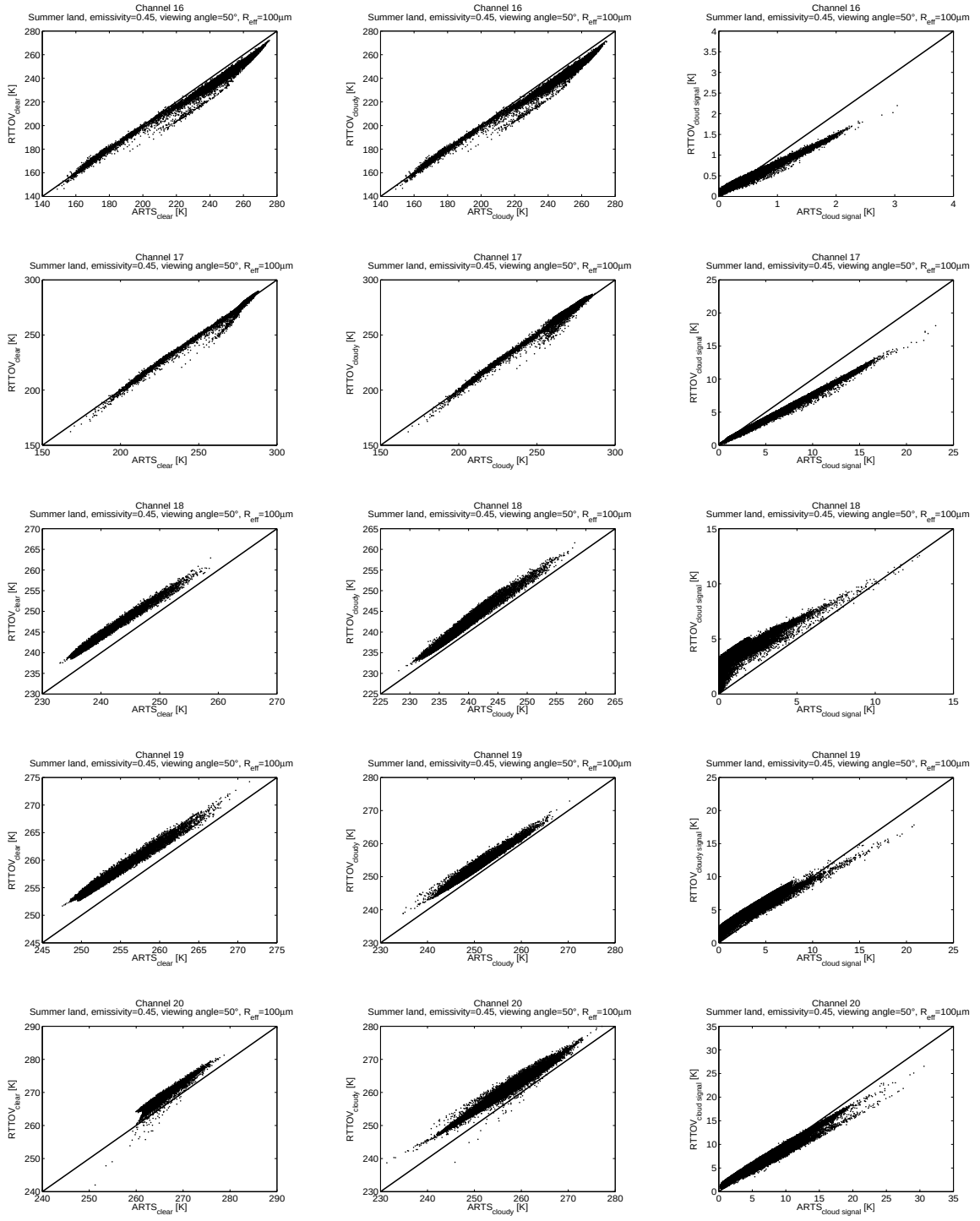

Figure 74: BT simulated for the land summer data set by RTTOVSCATT (for both clear sky simulations and cloudy simulations) against BT simulated by ARTS for a particular set of parameters (emissivity=0.45, viewing angle=50°, and effective radius of the ice particles= 100μm). Each line correspond to one AMSU-B channel from top to bottom channel 16 (89 GHz), 17 (150 GHz), 18 (183.31±1 GHz), 19 (183.31±3 GHz), and 20 (183.31±7 GHz). The left column correspond to clear sky simulations, the middle column corresponds to cloudy simulations and the right column corresponds to the cloud signal (clear sky BT minus cloudy BT).

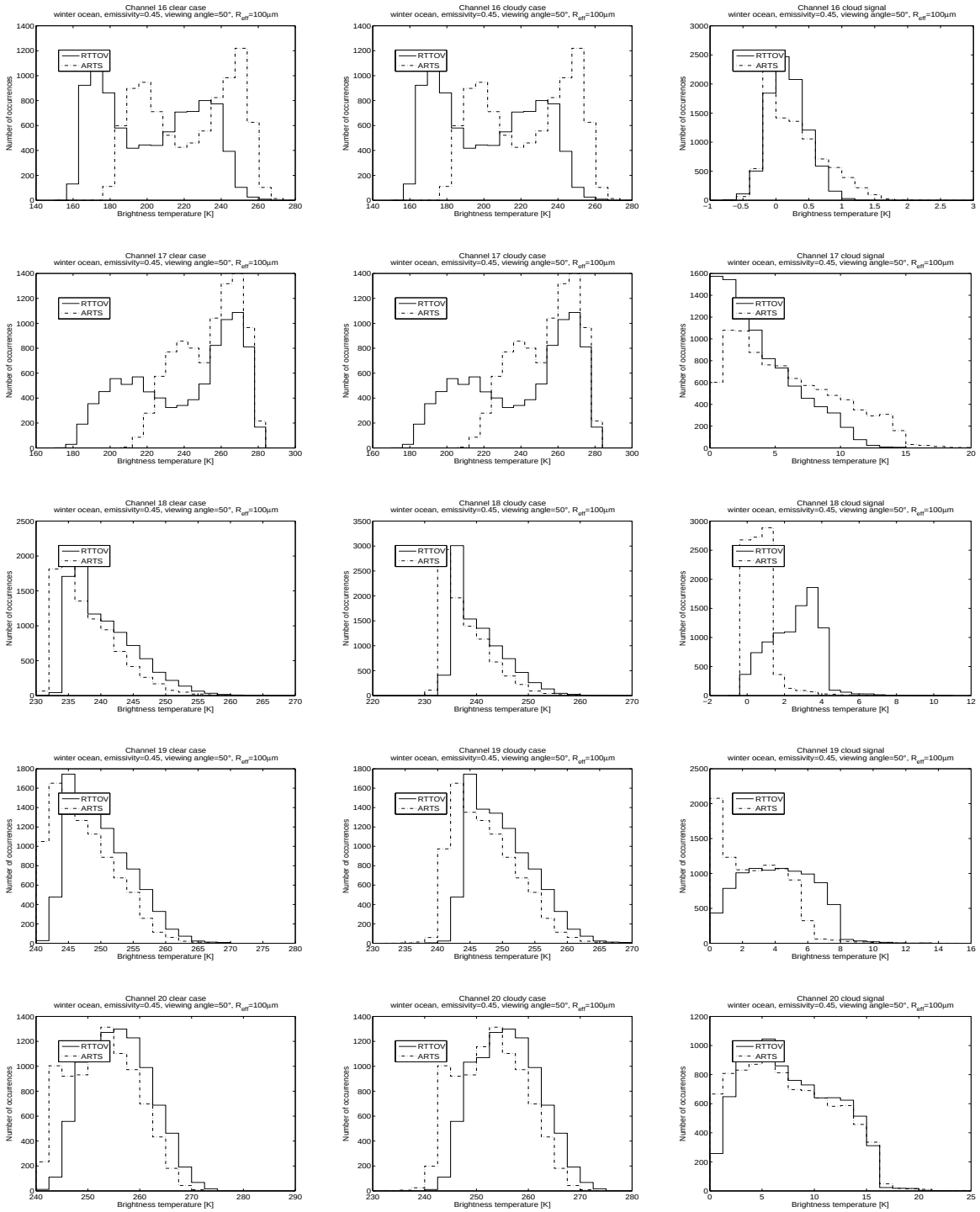

Figure 75: Histograms of BT simulated for the land summer data set by RTTOVSCATT (for both clear sky simulations and cloudy simulations), (plain line), and of BT simulated by ARTS (dashed line) for a particular set of parameters (emissivity=0.45, viewing angle=50°, and effective radius of the ice particles= 100μm). Each line correspond to one AMSU-B channel from top to bottom channel 16 (89 GHz), 17 (150 GHz), 18 (183.31±1 GHz), 19 (183.31±3 GHz), and 20 (183.31±7 GHz). The left column correspond to clear sky simulations, the middle column corresponds to cloudy simulations and the right column corresponds to the cloud signal (clear sky BT minus cloudy BT).

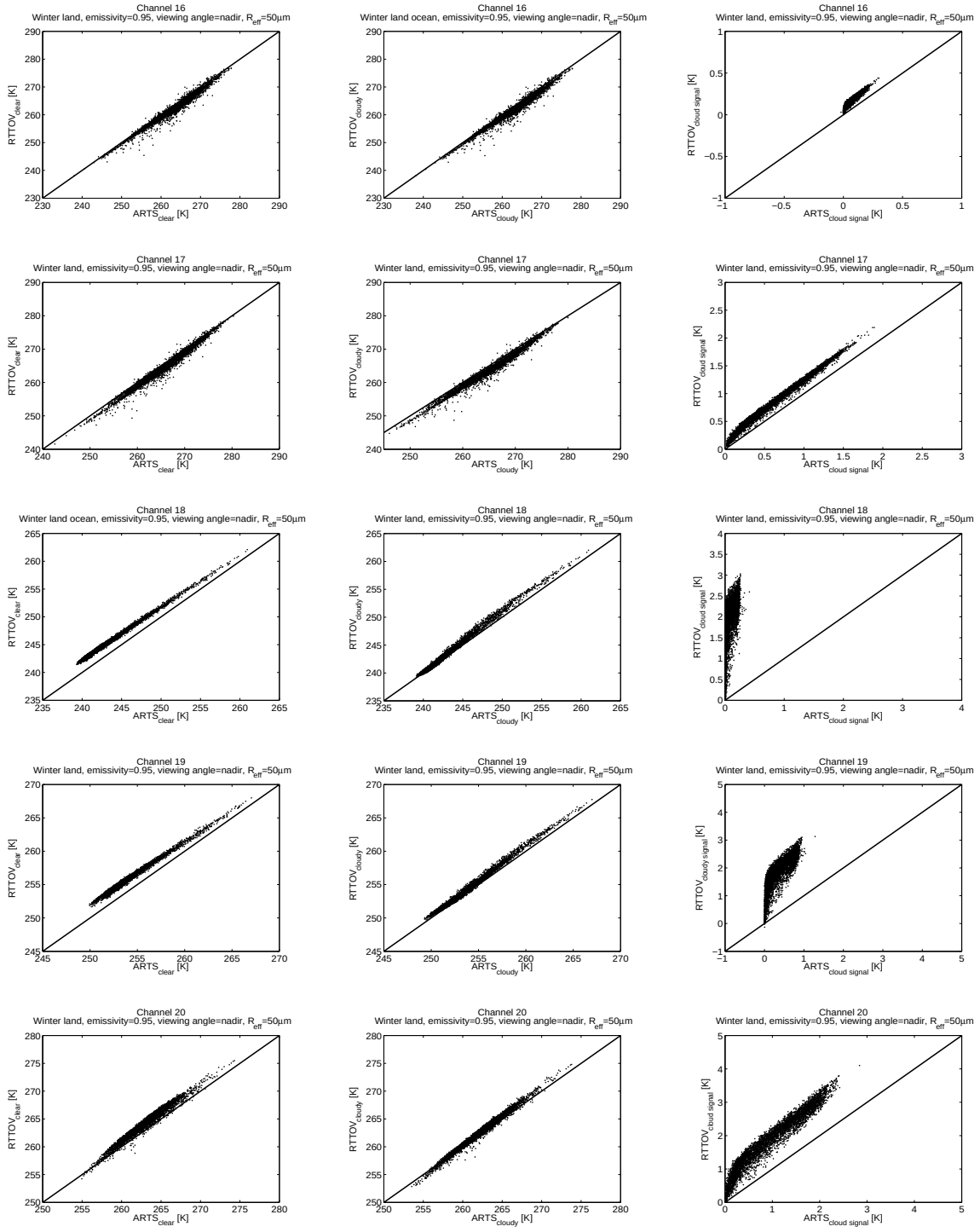

Figure 76: BT simulated for the land winter data set by RTTOVSCATT (for both clear sky simulations and cloudy simulations) against BT simulated by ARTS for a particular set of parameters (emissivity=0.95, viewing angle=nadir, and effective radius of the ice particles= 50μm). Each line correspond to one AMSU-B channel from top to bottom channel 16 (89 GHz), 17 (150 GHz), 18 (183.31±1 GHz), 19 (183.31±3 GHz), and 20 (183.31±7 GHz). The left column correspond to clear sky simulations, the middle column corresponds to cloudy simulations and the right column corresponds to the cloud signal (clear sky BT minus cloudy BT).

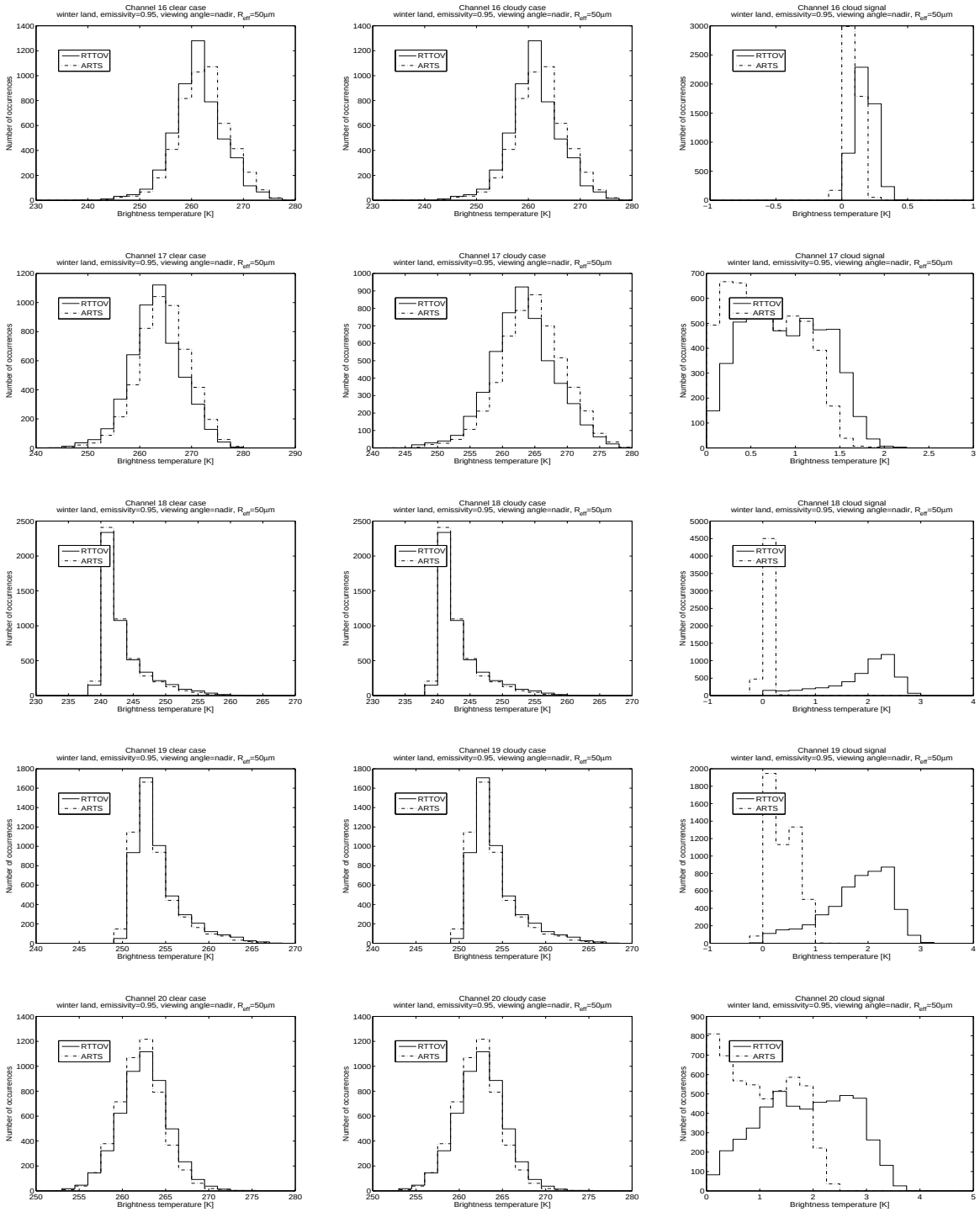

Figure 77: Histograms of BT simulated for the land winter data set by RTTOVSCATT (for both clear sky simulations and cloudy simulations), (plain line), and of BT simulated by ARTS (dashed line) for a particular set of parameters (emissivity=0.95, viewing angle=nadir, and effective radius of the ice particles= 50μm). Each line correspond to one AMSU-B channel from top to bottom channel 16 (89 GHz), 17 (150 GHz), 18 (183.31$\pm$1 GHz), 19 (183.31$\pm$3 GHz), and 20 (183.31$\pm$7 GHz). The left column correspond to clear sky simulations, the middle column corresponds to cloudy simulations and the right column corresponds to the cloud signal (clear sky BT minus cloudy BT).

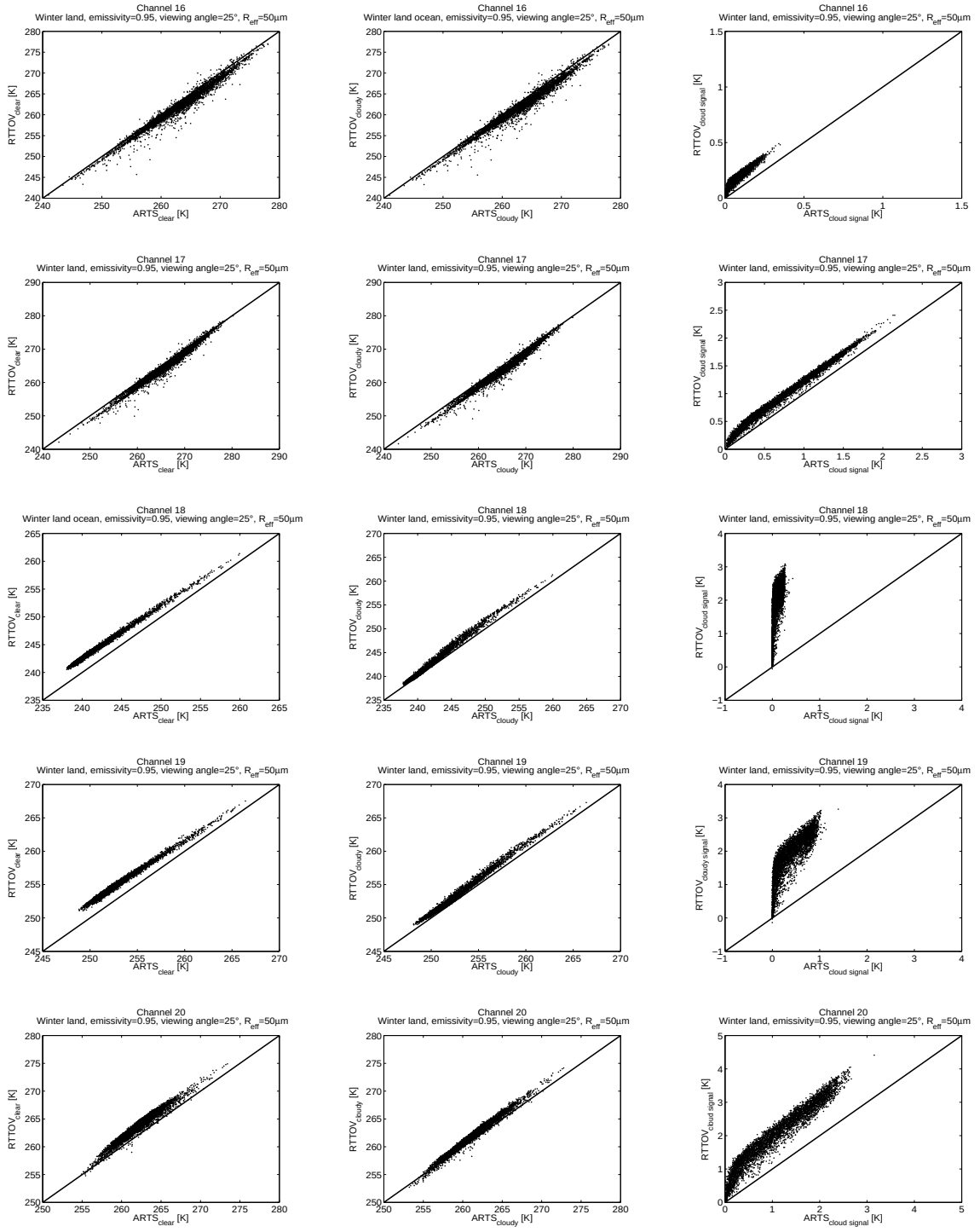

Figure 78: BT simulated for the land winter data set by RTTOVSCATT (for both clear sky simulations and cloudy simulations) against BT simulated by ARTS for a particular set of parameters (emissivity=0.95, viewing angle=25°, and effective radius of the ice particles= 50μm). Each line correspond to one AMSU-B channel from top to bottom channel 16 (89 GHz), 17 (150 GHz), 18 (183.31±1 GHz), 19 (183.31±3 GHz), and 20 (183.31±7 GHz). The left column correspond to clear sky simulations, the middle column corresponds to cloudy simulations and the right column corresponds to the cloud signal (clear sky BT minus cloudy BT).

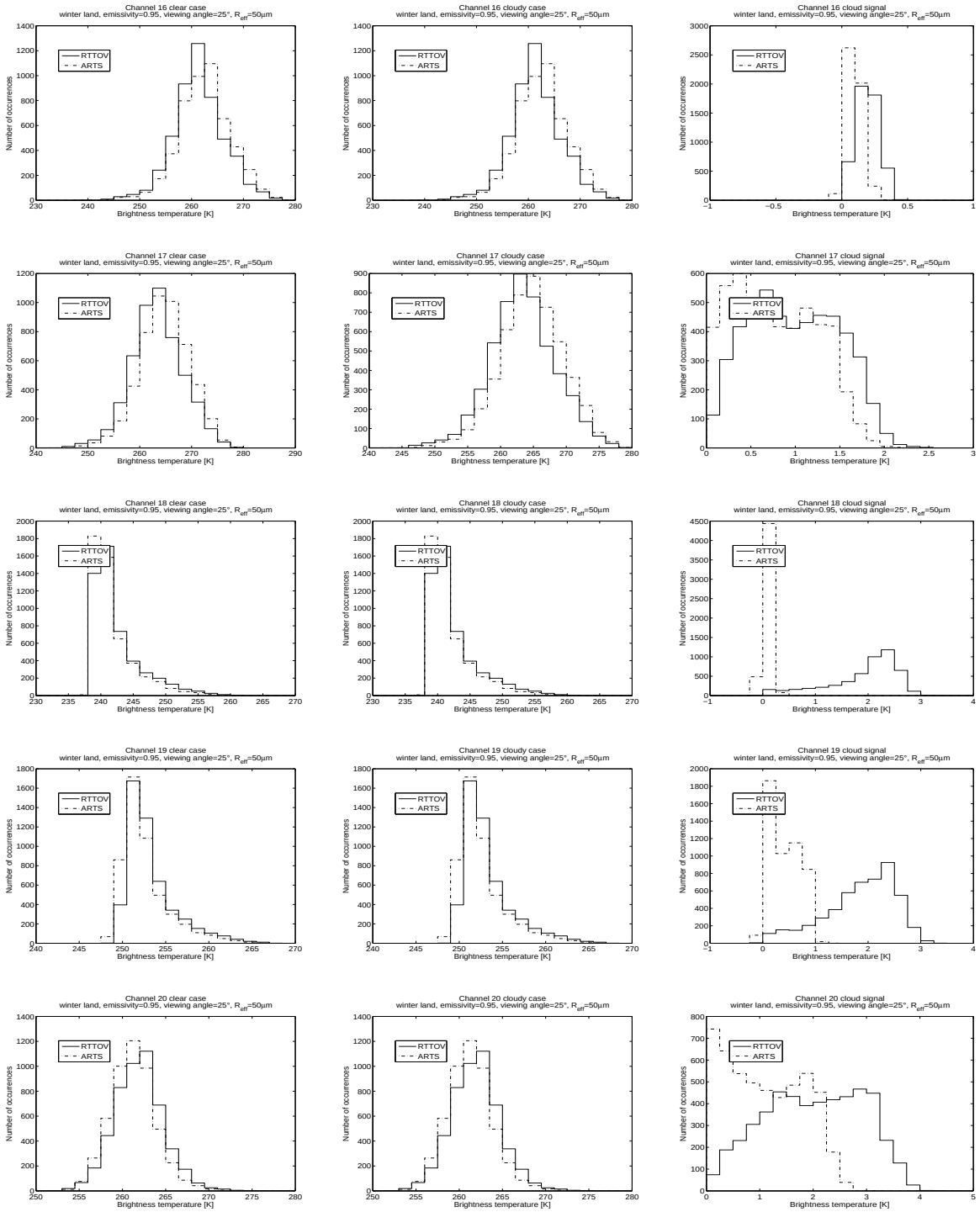

Figure 79: Histograms of BT simulated for the land winter data set by RTTOVSCATT (for both clear sky simulations and cloudy simulations), (plain line), and of BT simulated by ARTS (dashed line) for a particular set of parameters (emissivity=0.95, viewing angle=25°, and effective radius of the ice particles= 50μm). Each line correspond to one AMSU-B channel from top to bottom channel 16 (89 GHz), 17 (150 GHz), 18 (183.31±1 GHz), 19 (183.31±3 GHz), and 20 (183.31±7 GHz). The left column correspond to clear sky simulations, the middle column corresponds to cloudy simulations and the right column corresponds to the cloud signal (clear sky BT minus cloudy BT).

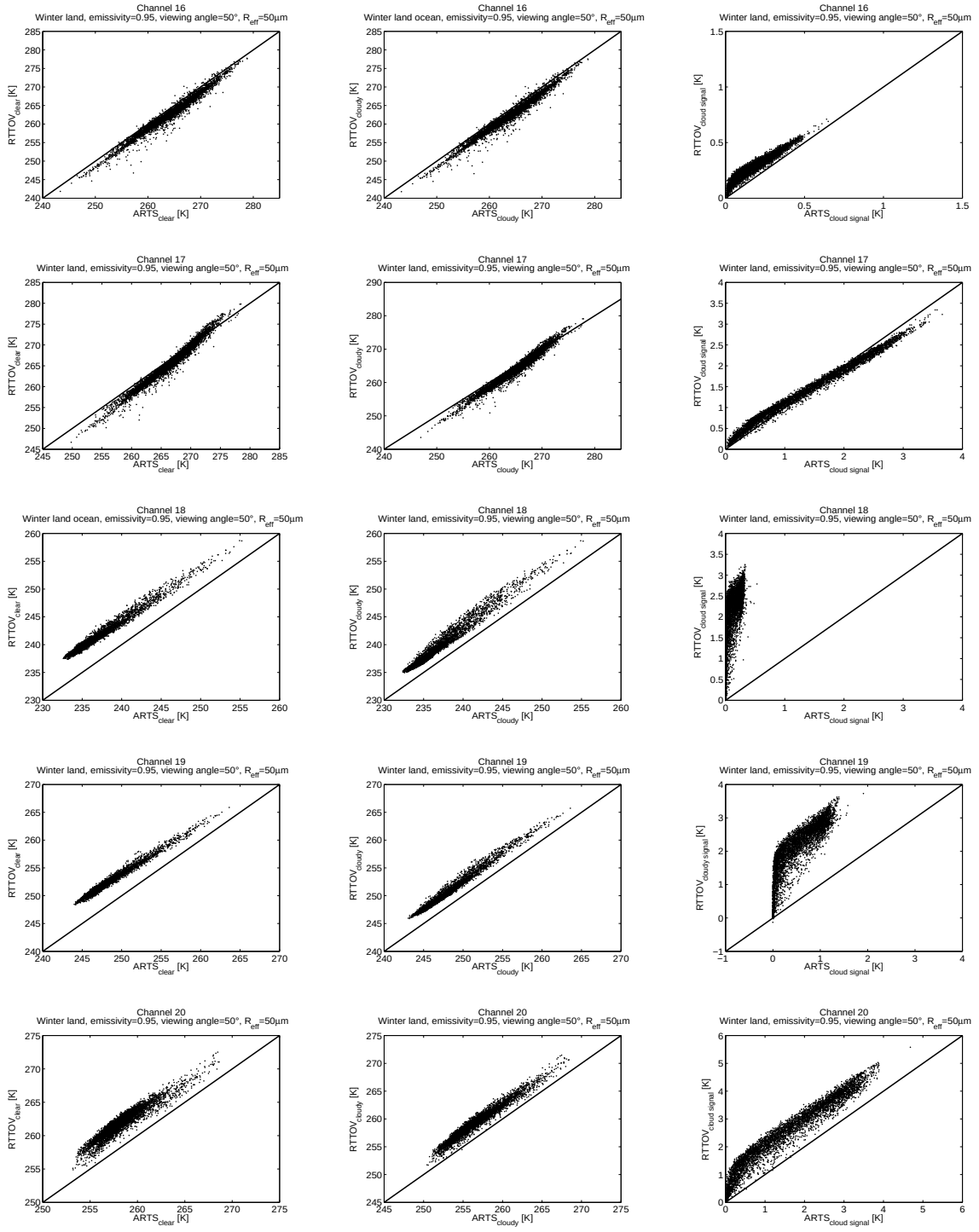

Figure 80: BT simulated for the land winter data set by RTTOVSCATT (for both clear sky simulations and cloudy simulations) against BT simulated by ARTS for a particular set of parameters (emissivity=0.95, viewing angle=50°, and effective radius of the ice particles= 50μm). Each line correspond to one AMSU-B channel from top to bottom channel 16 (89 GHz), 17 (150 GHz), 18 (183.31±1 GHz), 19 (183.31±3 GHz), and 20 (183.31±7 GHz). The left column correspond to clear sky simulations, the middle column corresponds to cloudy simulations and the right column corresponds to the cloud signal (clear sky BT minus cloudy BT).

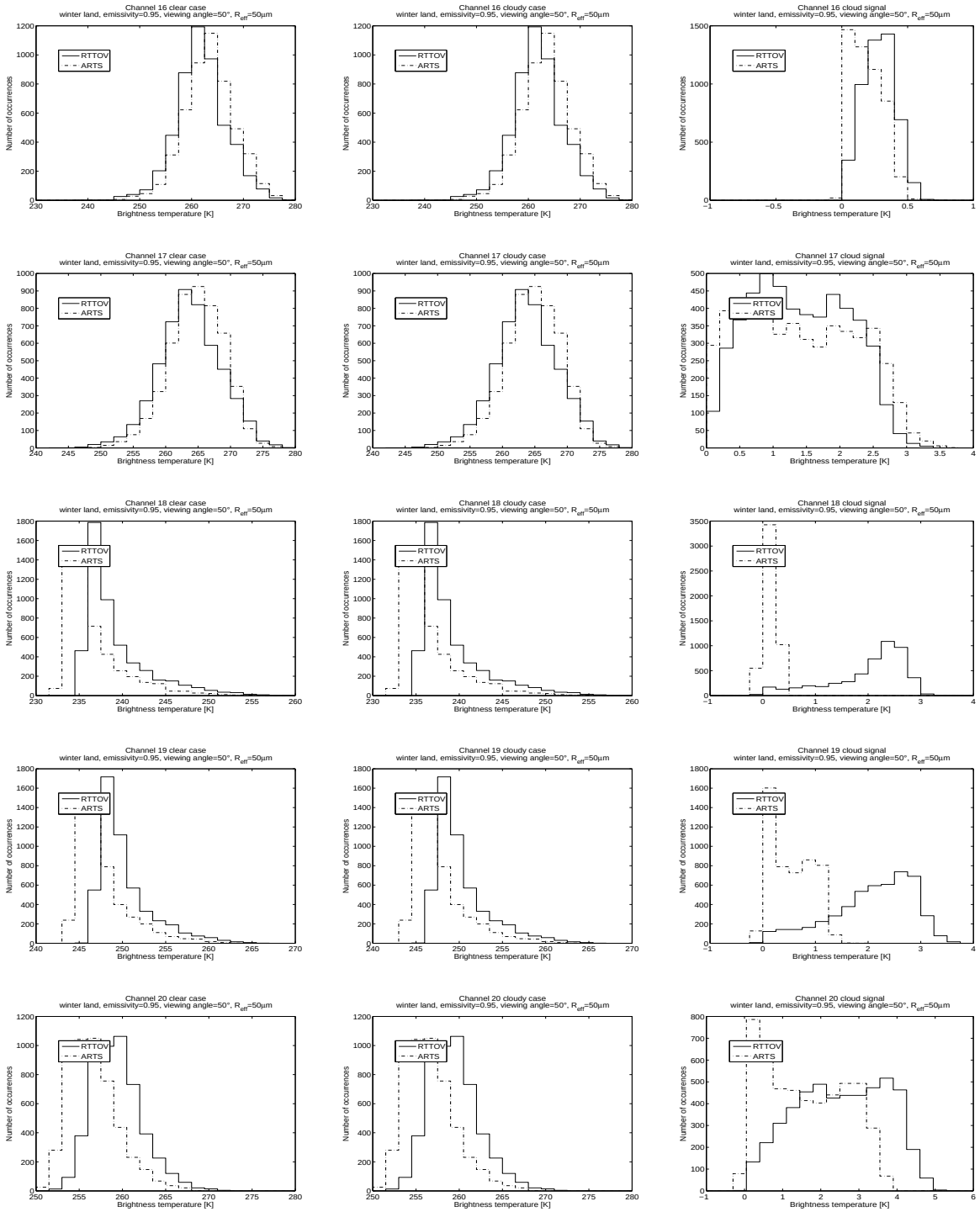

Figure 81: Histograms of BT simulated for the land winter data set by RTTOVSCATT (for both clear sky simulations and cloudy simulations), (plain line), and of BT simulated by ARTS (dashed line) for a particular set of parameters (emissivity=0.95, viewing angle=50°, and effective radius of the ice particles= 50μm). Each line correspond to one AMSU-B channel from top to bottom channel 16 (89 GHz), 17 (150 GHz), 18 (183.31±1 GHz), 19 (183.31±3 GHz), and 20 (183.31±7 GHz). The left column correspond to clear sky simulations, the middle column corresponds to cloudy simulations and the right column corresponds to the cloud signal (clear sky BT minus cloudy BT).

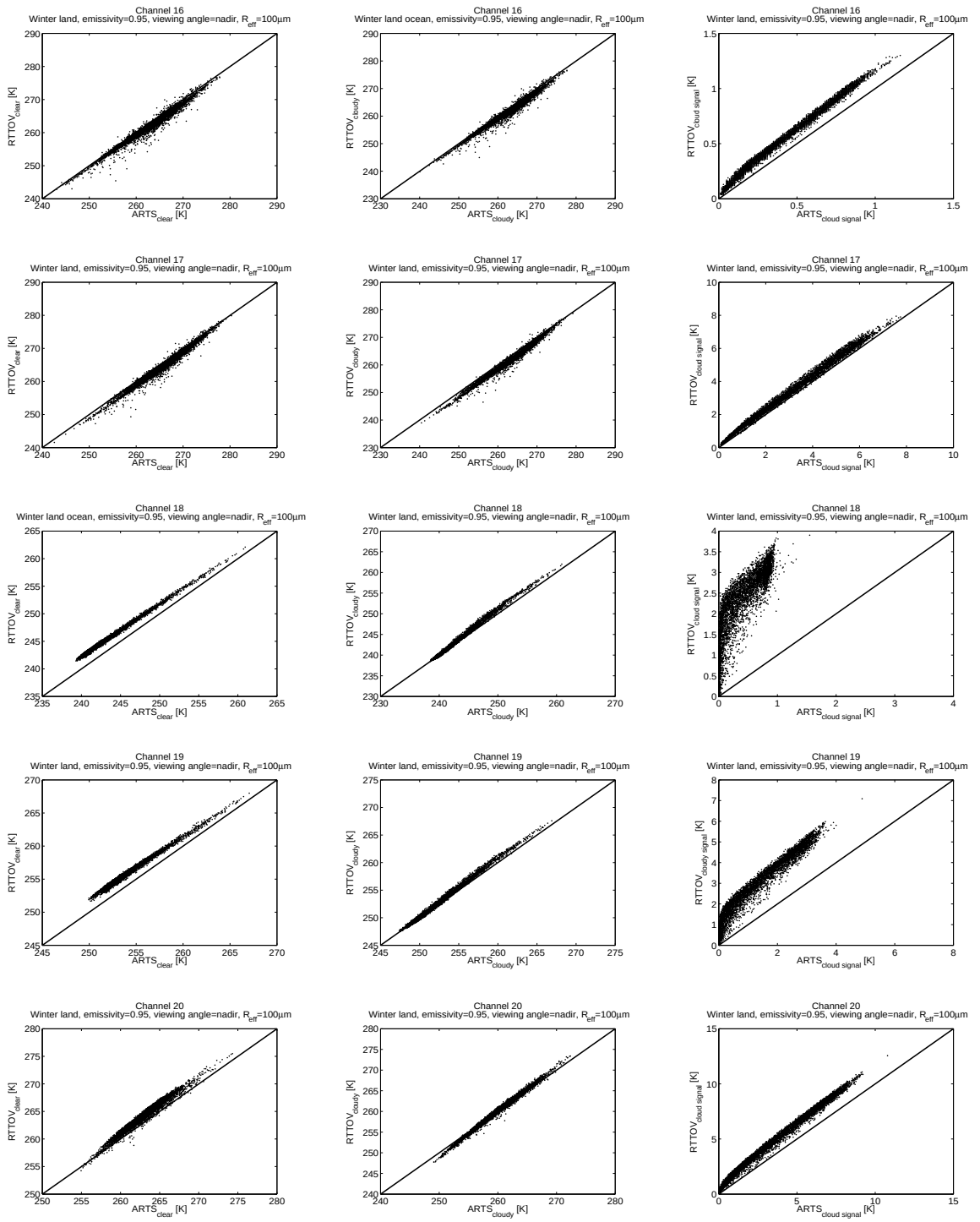

Figure 82: BT simulated for the land winter data set by RTTOVSCATT (for both clear sky simulations and cloudy simulations) against BT simulated by ARTS for a particular set of parameters (emissivity=0.95, viewing angle=nadir, and effective radius of the ice particles= 100μm). Each line correspond to one AMSU-B channel from top to bottom channel 16 (89 GHz), 17 (150 GHz), 18 (183.31±1 GHz), 19 (183.31±3 GHz), and 20 (183.31±7 GHz). The left column correspond to clear sky simulations, the middle column corresponds to cloudy simulations and the right column corresponds to the cloud signal (clear sky BT minus cloudy BT).

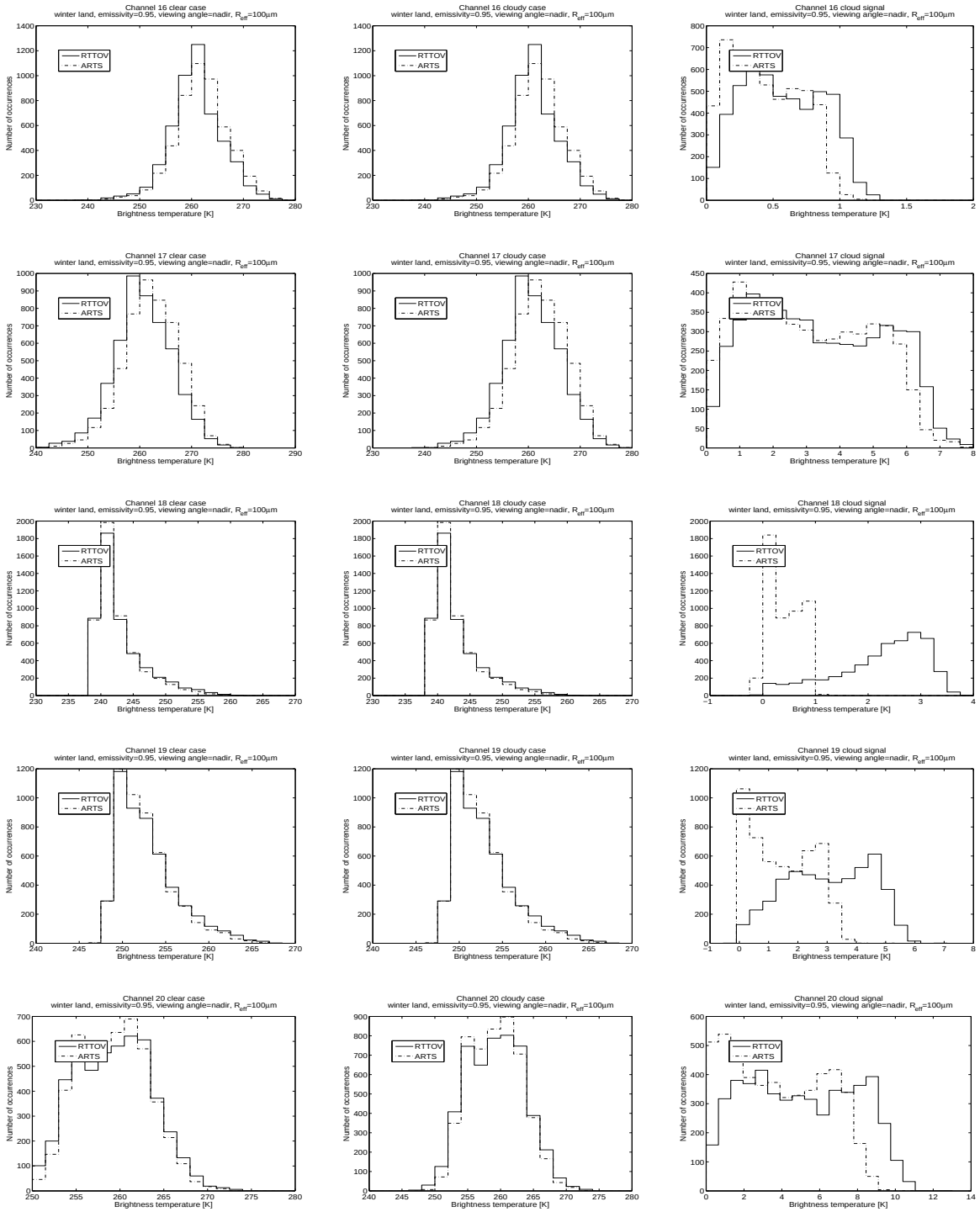

Figure 83: Histograms of BT simulated for the land winter data set by RTTOVSCATT (for both clear sky simulations and cloudy simulations), (plain line), and of BT simulated by ARTS (dashed line) for a particular set of parameters (emissivity=0.95, viewing angle=nadir, and effective radius of the ice particles= 100μm). Each line correspond to one AMSU-B channel from top to bottom channel 16 (89 GHz), 17 (150 GHz), 18 (183.31$\pm$1 GHz), 19 (183.31$\pm$3 GHz), and 20 (183.31$\pm$7 GHz). The left column correspond to clear sky simulations, the middle column corresponds to cloudy simulations and the right column corresponds to the cloud signal (clear sky BT minus cloudy BT).

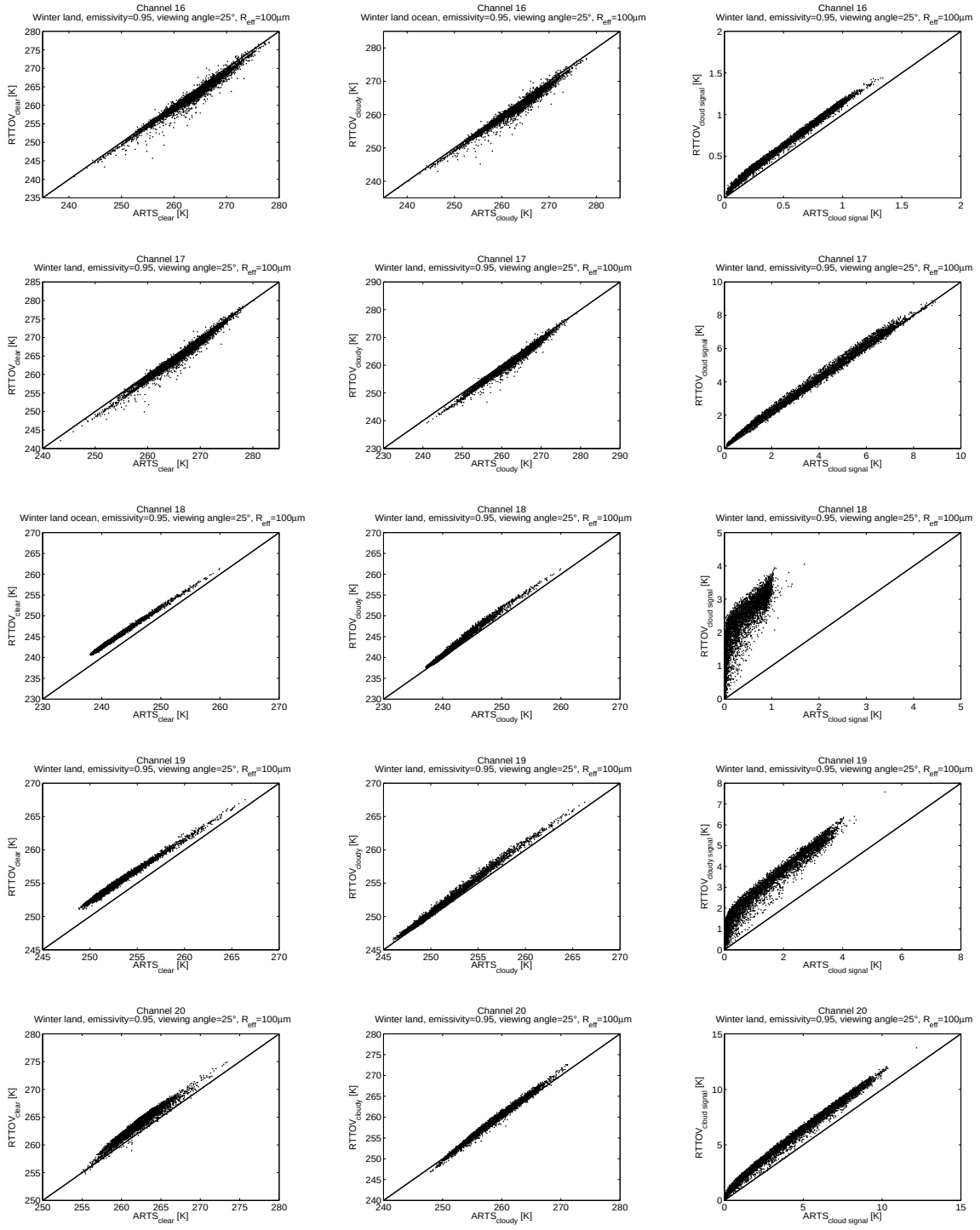

Figure 84: BT simulated for the land winter data set by RTTOVSCATT (for both clear sky simulations and cloudy simulations) against BT simulated by ARTS for a particular set of parameters (emissivity=0.95, viewing angle=25°, and effective radius of the ice particles= 100μm). Each line correspond to one AMSU-B channel from top to bottom channel 16 (89 GHz), 17 (150 GHz), 18 (183.31±1 GHz), 19 (183.31±3 GHz), and 20 (183.31±7 GHz). The left column correspond to clear sky simulations, the middle column corresponds to cloudy simulations and the right column corresponds to the cloud signal (clear sky BT minus cloudy BT).

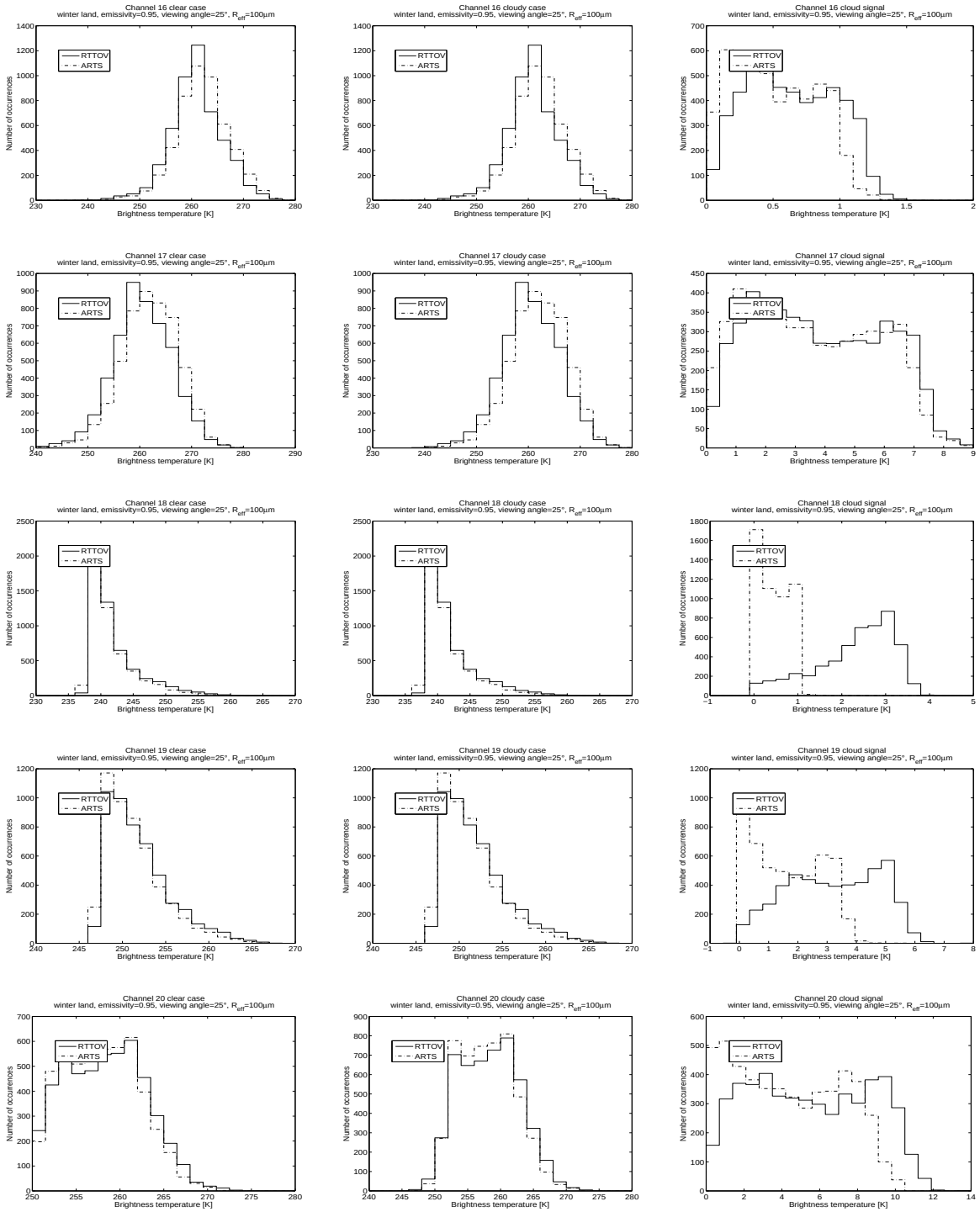

Figure 85: Histograms of BT simulated for the land winter data set by RTTOVSCATT (for both clear sky simulations and cloudy simulations), (plain line), and of BT simulated by ARTS (dashed line) for a particular set of parameters (emissivity=0.95, viewing angle=25°, and effective radius of the ice particles= 100μm). Each line correspond to one AMSU-B channel from top to bottom channel 16 (89 GHz), 17 (150 GHz), 18 (183.31±1 GHz), 19 (183.31±3 GHz), and 20 (183.31±7 GHz). The left column correspond to clear sky simulations, the middle column corresponds to cloudy simulations and the right column corresponds to the cloud signal (clear sky BT minus cloudy BT).

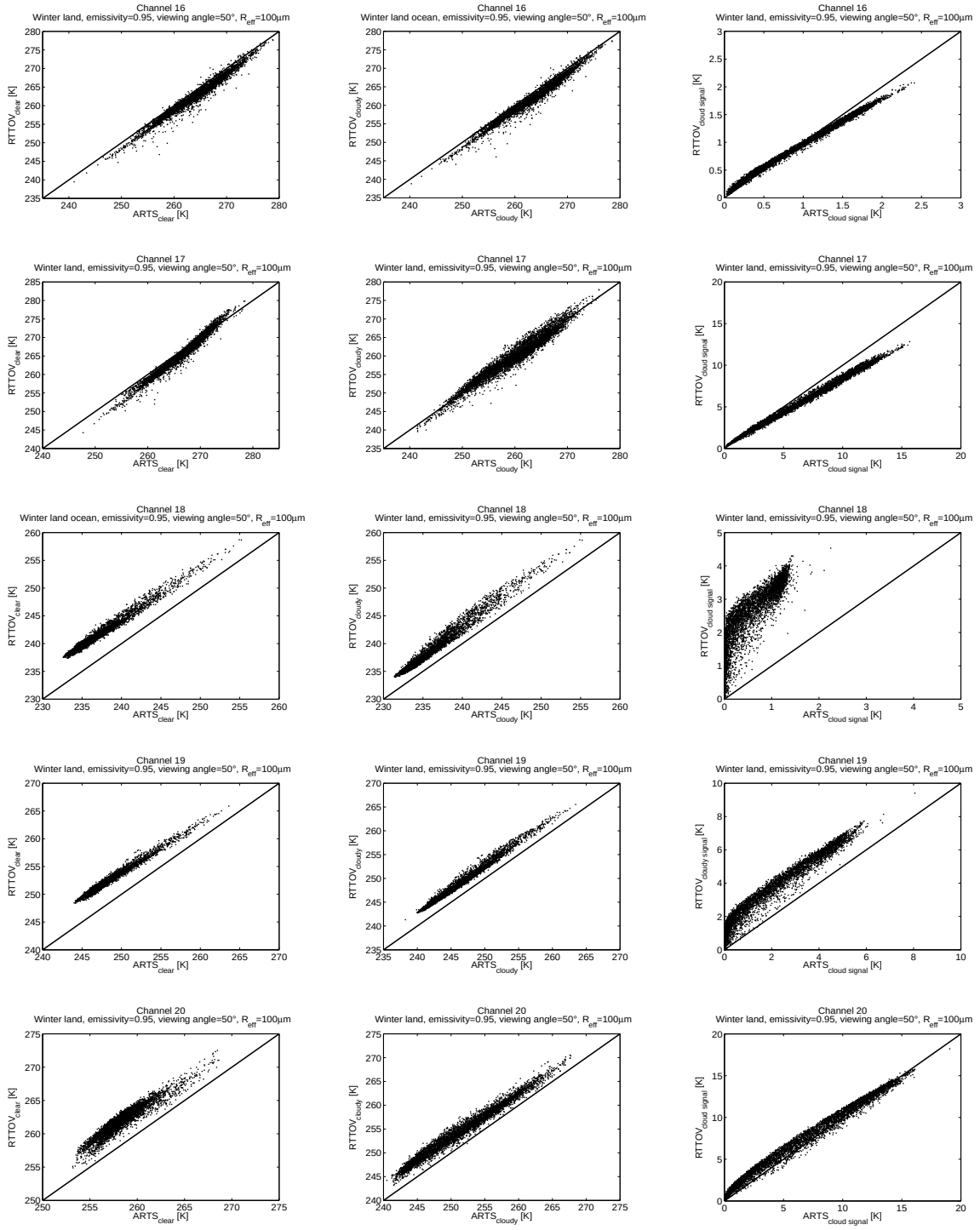

Figure 86: BT simulated for the land winter data set by RTTOVSCATT (for both clear sky simulations and cloudy simulations) against BT simulated by ARTS for a particular set of parameters (emissivity=0.95, viewing angle=50°, and effective radius of the ice particles= 100μm). Each line correspond to one AMSU-B channel from top to bottom channel 16 (89 GHz), 17 (150 GHz), 18 (183.31±1 GHz), 19 (183.31±3 GHz), and 20 (183.31±7 GHz). The left column correspond to clear sky simulations, the middle column corresponds to cloudy simulations and the right column corresponds to the cloud signal (clear sky BT minus cloudy BT).

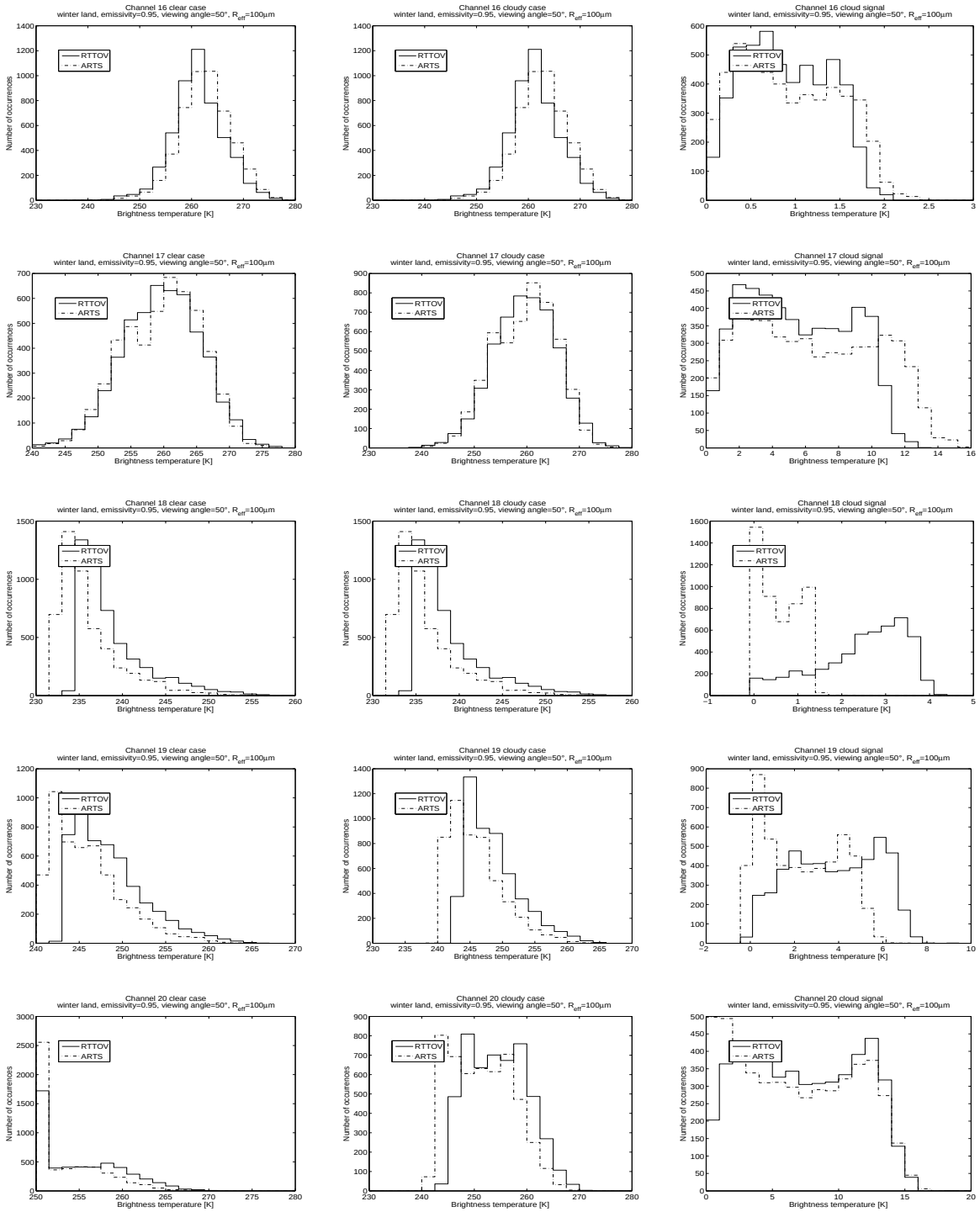

Figure 87: Histograms of BT simulated for the land winter data set by RTTOVSCATT (for both clear sky simulations and cloudy simulations), (plain line), and of BT simulated by ARTS (dashed line) for a particular set of parameters (emissivity=0.95, viewing angle=50°, and effective radius of the ice particles= 100μm). Each line correspond to one AMSU-B channel from top to bottom channel 16 (89 GHz), 17 (150 GHz), 18 (183.31±1 GHz), 19 (183.31±3 GHz), and 20 (183.31±7 GHz). The left column correspond to clear sky simulations, the middle column corresponds to cloudy simulations and the right column corresponds to the cloud signal (clear sky BT minus cloudy BT).

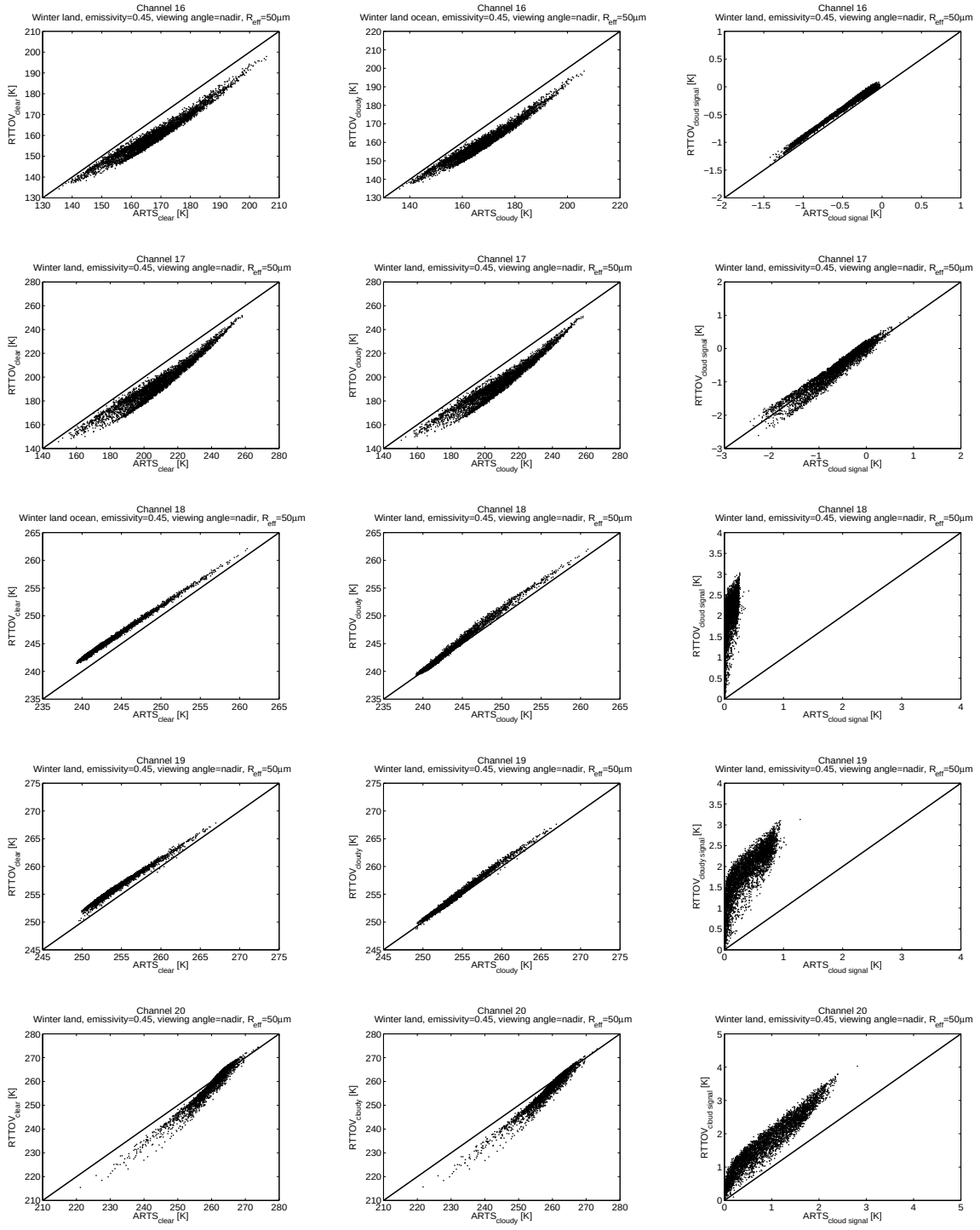

Figure 88: BT simulated for the land winter data set by RTTOVSCATT (for both clear sky simulations and cloudy simulations) against BT simulated by ARTS for a particular set of parameters (emissivity=0.45, viewing angle=nadir, and effective radius of the ice particles= 50μm). Each line correspond to one AMSU-B channel from top to bottom channel 16 (89 GHz), 17 (150 GHz), 18 (183.31±1 GHz), 19 (183.31±3 GHz), and 20 (183.31±7 GHz). The left column correspond to clear sky simulations, the middle column corresponds to cloudy simulations and the right column corresponds to the cloud signal (clear sky BT minus cloudy BT).

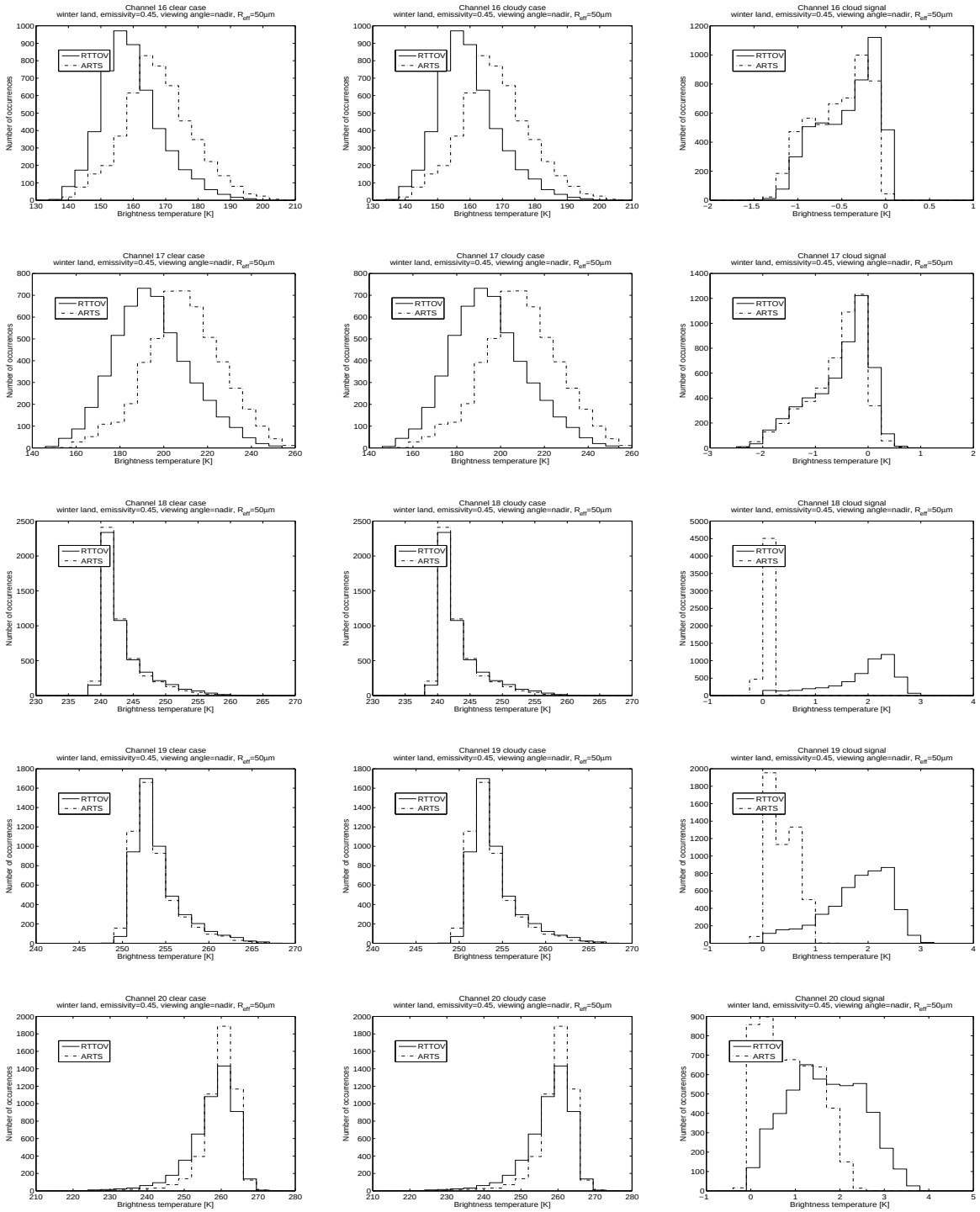

Figure 89: Histograms of BT simulated for the land winter data set by RTTOVSCATT (for both clear sky simulations and cloudy simulations), (plain line), and of BT simulated by ARTS (dashed line) for a particular set of parameters (emissivity=0.45, viewing angle=nadir, and effective radius of the ice particles= 50μm). Each line correspond to one AMSU-B channel from top to bottom channel 16 (89 GHz), 17 (150 GHz), 18 (183.31$\pm$1 GHz), 19 (183.31$\pm$3 GHz), and 20 (183.31$\pm$7 GHz). The left column correspond to clear sky simulations, the middle column corresponds to cloudy simulations and the right column corresponds to the cloud signal (clear sky BT minus cloudy BT).

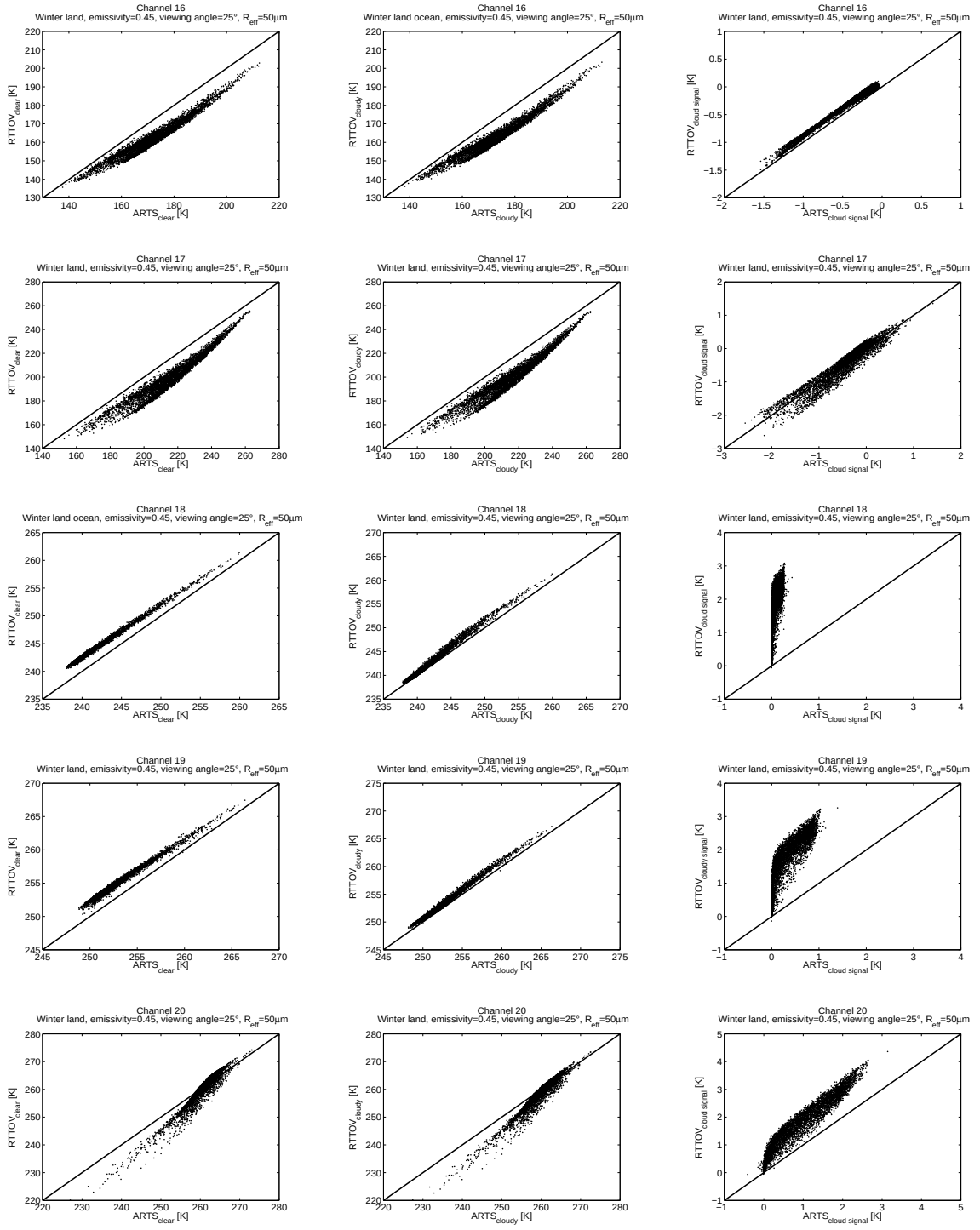

Figure 90: BT simulated for the land winter data set by RTTOVSCATT (for both clear sky simulations and cloudy simulations) against BT simulated by ARTS for a particular set of parameters (emissivity=0.45, viewing angle=25°, and effective radius of the ice particles= 50μm). Each line correspond to one AMSU-B channel from top to bottom channel 16 (89 GHz), 17 (150 GHz), 18 (183.31±1 GHz), 19 (183.31±3 GHz), and 20 (183.31±7 GHz). The left column correspond to clear sky simulations, the middle column corresponds to cloudy simulations and the right column corresponds to the cloud signal (clear sky BT minus cloudy BT).

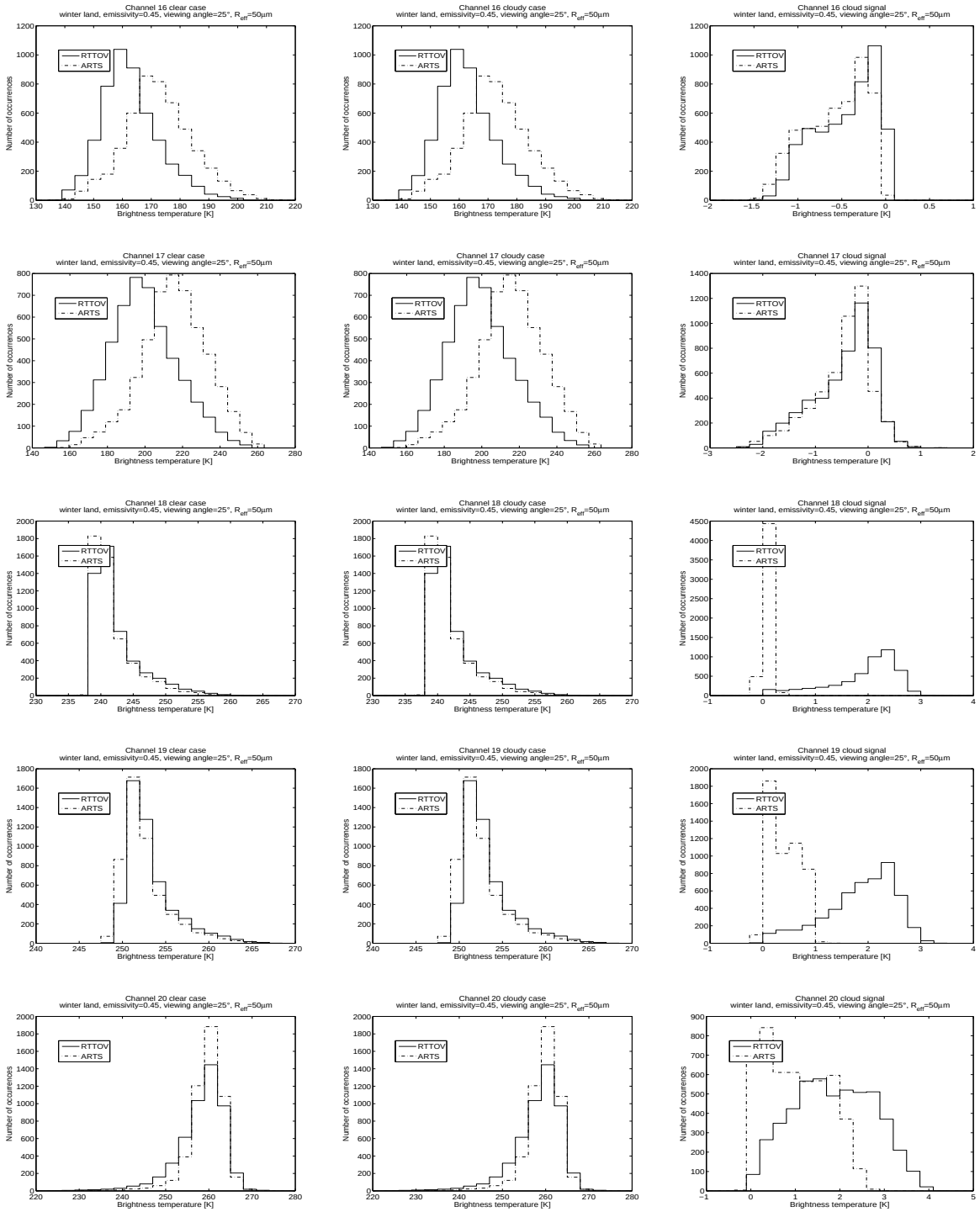

Figure 91: Histograms of BT simulated for the land winter data set by RTTOVSCATT (for both clear sky simulations and cloudy simulations), (plain line), and of BT simulated by ARTS (dashed line) for a particular set of parameters (emissivity=0.45, viewing angle=25°, and effective radius of the ice particles= 50μm). Each line correspond to one AMSU-B channel from top to bottom channel 16 (89 GHz), 17 (150 GHz), 18 (183.31±1 GHz), 19 (183.31±3 GHz), and 20 (183.31±7 GHz). The left column correspond to clear sky simulations, the middle column corresponds to cloudy simulations and the right column corresponds to the cloud signal (clear sky BT minus cloudy BT).

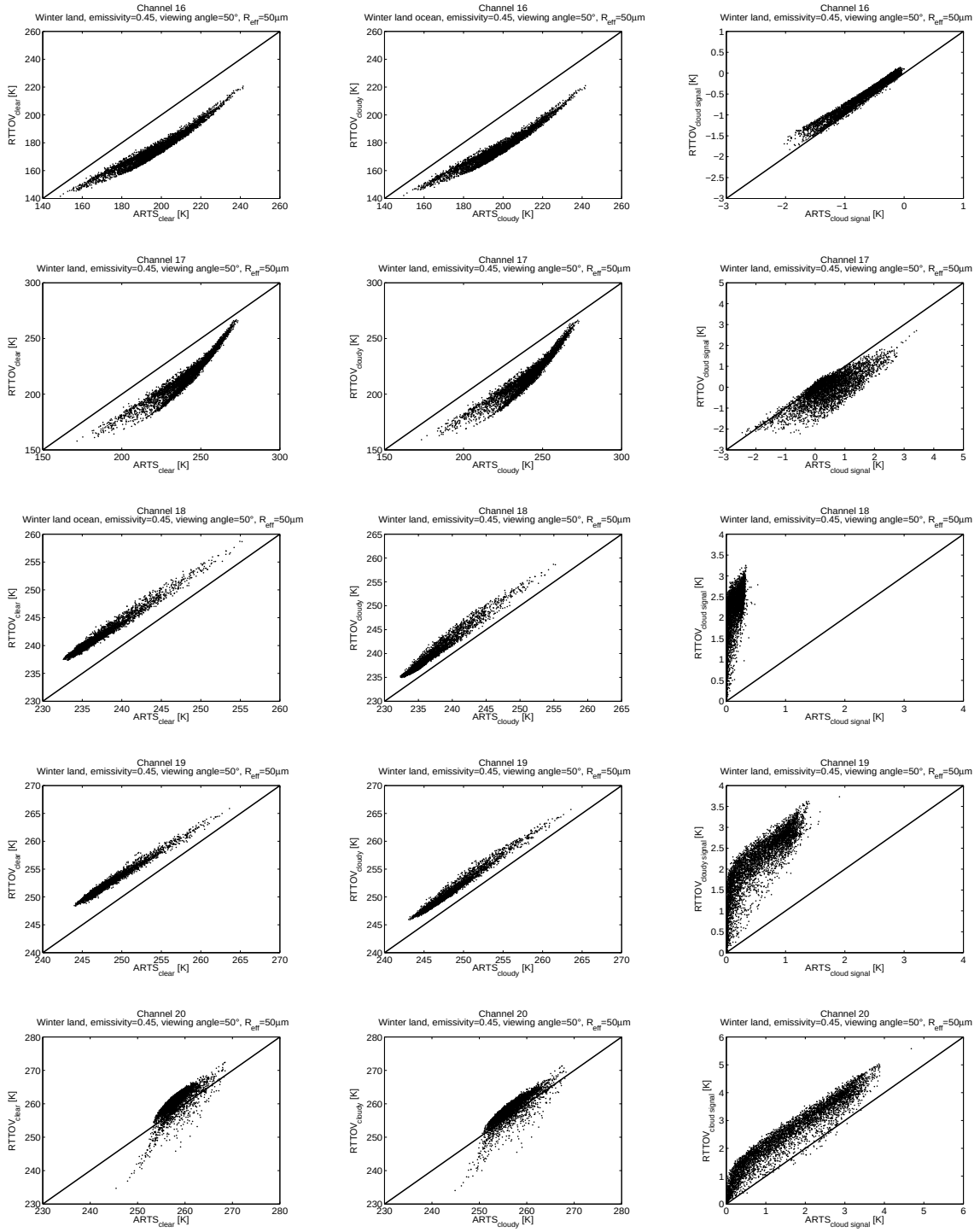

Figure 92: BT simulated for the land winter data set by RTTOVSCATT (for both clear sky simulations and cloudy simulations) against BT simulated by ARTS for a particular set of parameters (emissivity=0.45, viewing angle=50°, and effective radius of the ice particles= 50μm). Each line correspond to one AMSU-B channel from top to bottom channel 16 (89 GHz), 17 (150 GHz), 18 (183.31±1 GHz), 19 (183.31±3 GHz), and 20 (183.31±7 GHz). The left column correspond to clear sky simulations, the middle column corresponds to cloudy simulations and the right column corresponds to the cloud signal (clear sky BT minus cloudy BT).

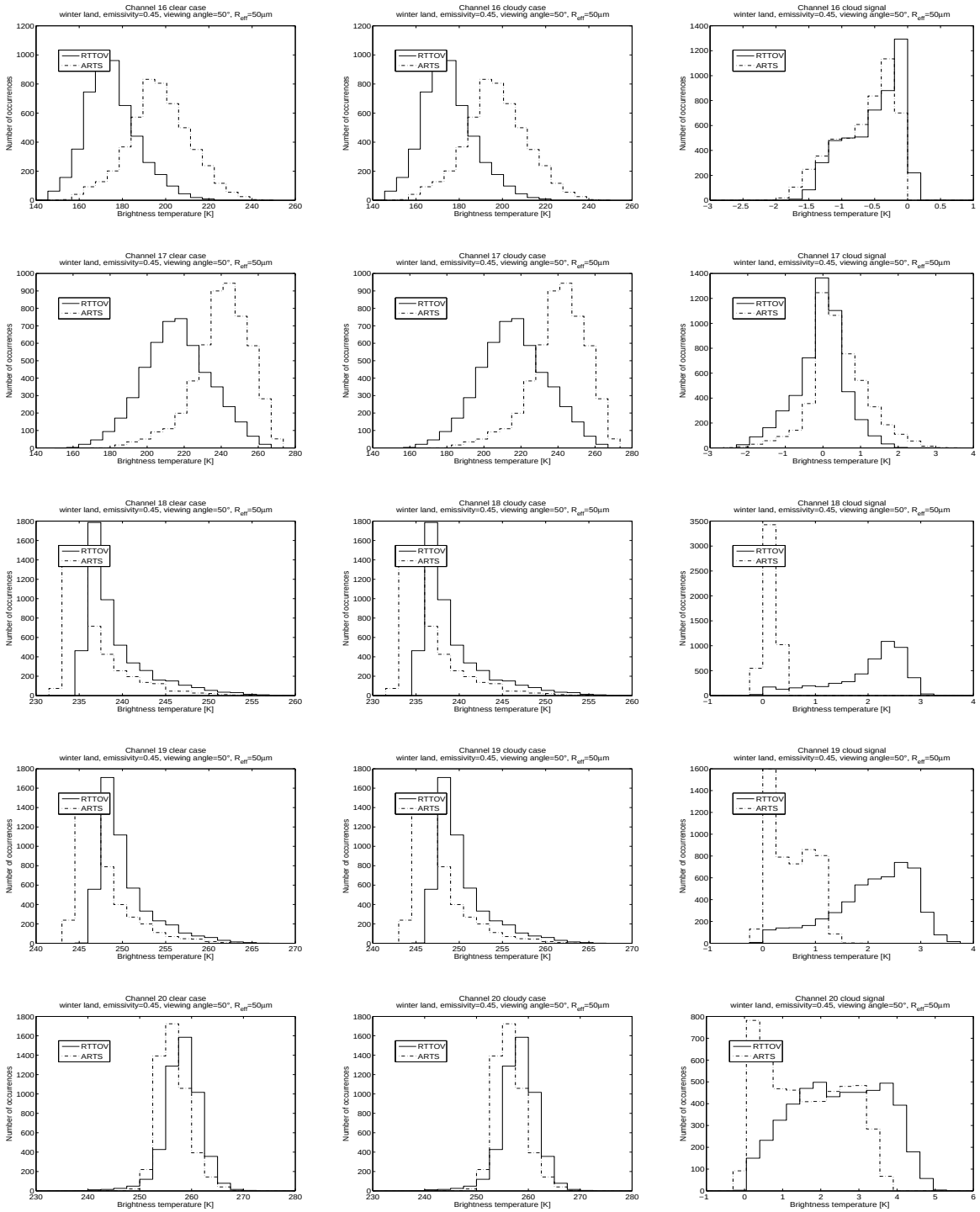

Figure 93: Histograms of BT simulated for the land winter data set by RTTOVSCATT (for both clear sky simulations and cloudy simulations), (plain line), and of BT simulated by ARTS (dashed line) for a particular set of parameters (emissivity=0.45, viewing angle=50°, and effective radius of the ice particles= 50μm). Each line correspond to one AMSU-B channel from top to bottom channel 16 (89 GHz), 17 (150 GHz), 18 (183.31±1 GHz), 19 (183.31±3 GHz), and 20 (183.31±7 GHz). The left column correspond to clear sky simulations, the middle column corresponds to cloudy simulations and the right column corresponds to the cloud signal (clear sky BT minus cloudy BT).

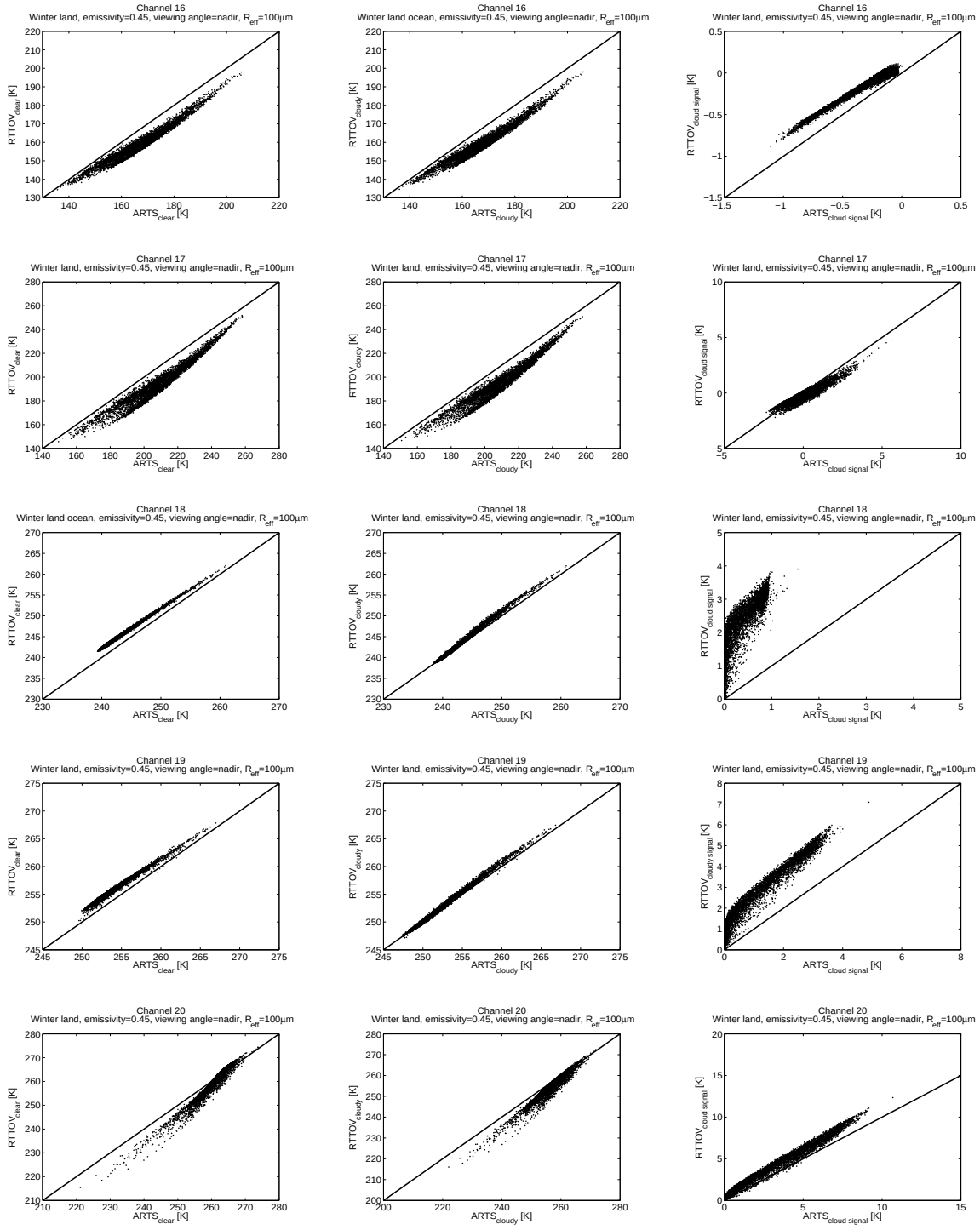

Figure 94: BT simulated for the land winter data set by RTTOVSCATT (for both clear sky simulations and cloudy simulations) against BT simulated by ARTS for a particular set of parameters (emissivity=0.45, viewing angle=nadir, and effective radius of the ice particles= 100μm). Each line correspond to one AMSU-B channel from top to bottom channel 16 (89 GHz), 17 (150 GHz), 18 (183.31±1 GHz), 19 (183.31±3 GHz), and 20 (183.31±7 GHz). The left column correspond to clear sky simulations, the middle column corresponds to cloudy simulations and the right column corresponds to the cloud signal (clear sky BT minus cloudy BT).

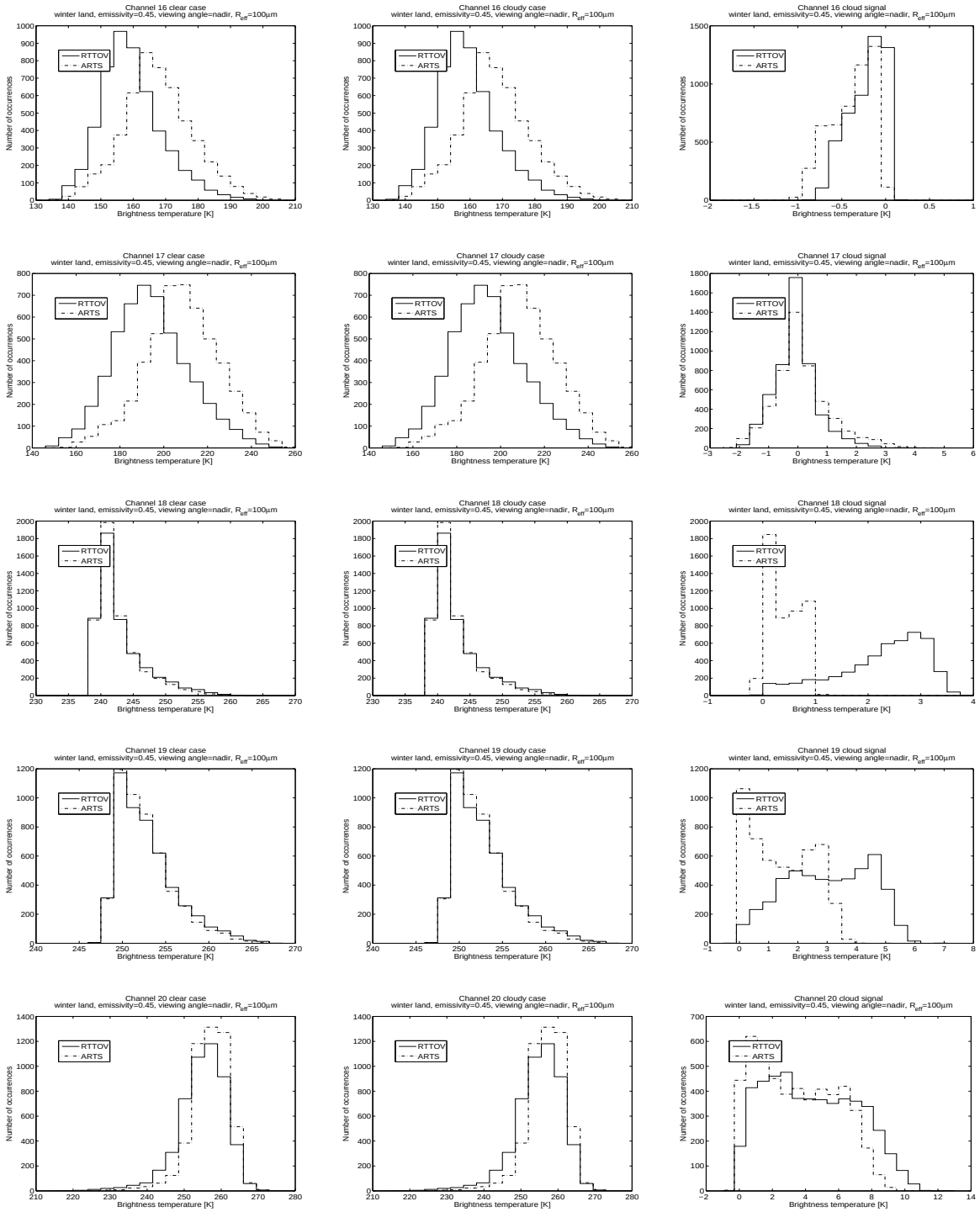

Figure 95: Histograms of BT simulated for the land winter data set by RTTOVSCATT (for both clear sky simulations and cloudy simulations), (plain line), and of BT simulated by ARTS (dashed line) for a particular set of parameters (emissivity=0.45, viewing angle=nadir, and effective radius of the ice particles= 100μm). Each line correspond to one AMSU-B channel from top to bottom channel 16 (89 GHz), 17 (150 GHz), 18 (183.31$\pm$1 GHz), 19 (183.31$\pm$3 GHz), and 20 (183.31$\pm$7 GHz). The left column correspond to clear sky simulations, the middle column corresponds to cloudy simulations and the right column corresponds to the cloud signal (clear sky BT minus cloudy BT).

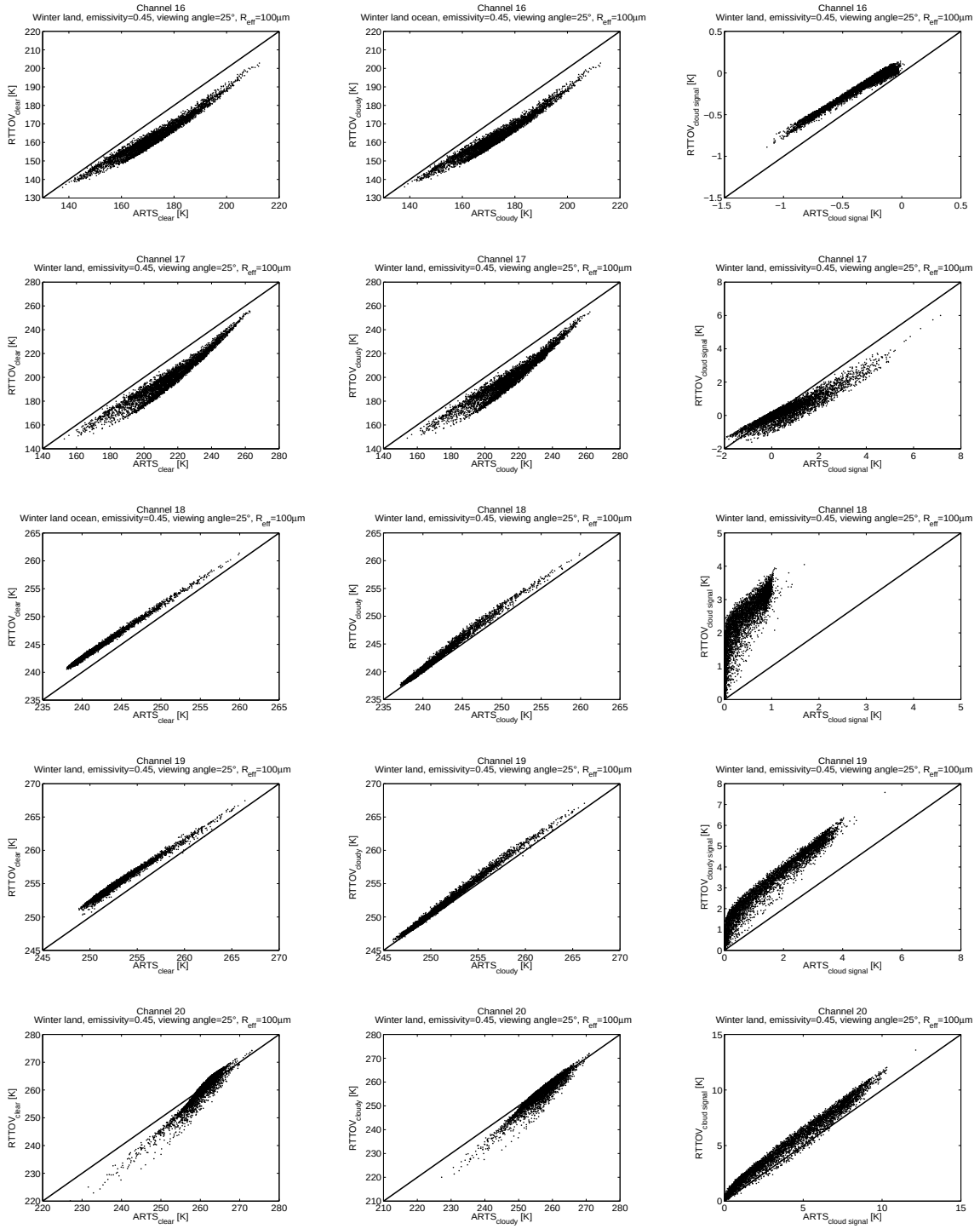

Figure 96: BT simulated for the land winter data set by RTTOVSCATT (for both clear sky simulations and cloudy simulations) against BT simulated by ARTS for a particular set of parameters (emissivity=0.45, viewing angle=25°, and effective radius of the ice particles= 100μm). Each line correspond to one AMSU-B channel from top to bottom channel 16 (89 GHz), 17 (150 GHz), 18 (183.31±1 GHz), 19 (183.31±3 GHz), and 20 (183.31±7 GHz). The left column correspond to clear sky simulations, the middle column corresponds to cloudy simulations and the right column corresponds to the cloud signal (clear sky BT minus cloudy BT).

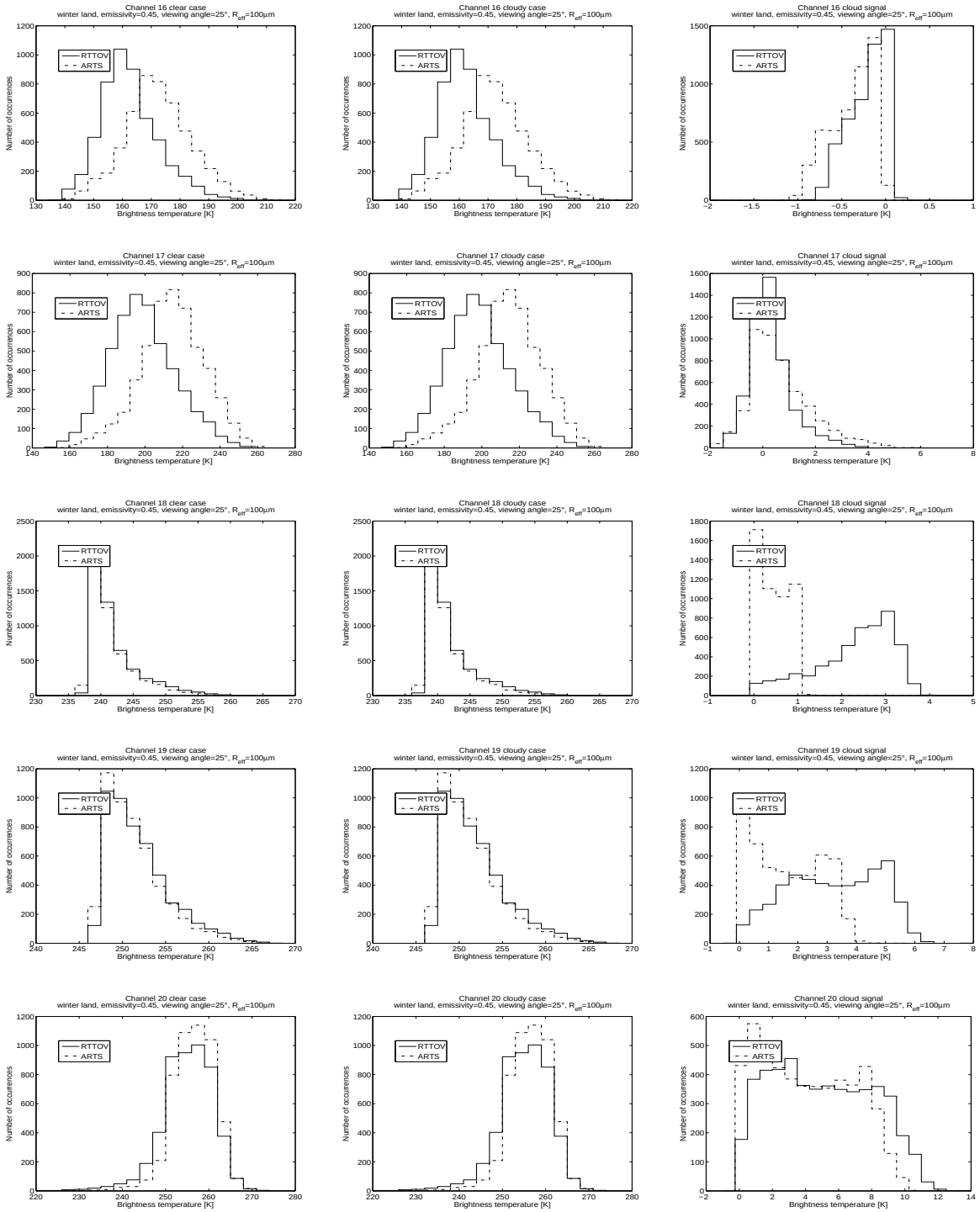

Figure 97: Histograms of BT simulated for the land winter data set by RTTOVSCATT (for both clear sky simulations and cloudy simulations), (plain line), and of BT simulated by ARTS (dashed line) for a particular set of parameters (emissivity=0.45, viewing angle=25°, and effective radius of the ice particles= 100μm). Each line correspond to one AMSU-B channel from top to bottom channel 16 (89 GHz), 17 (150 GHz), 18 (183.31±1 GHz), 19 (183.31±3 GHz), and 20 (183.31±7 GHz). The left column correspond to clear sky simulations, the middle column corresponds to cloudy simulations and the right column corresponds to the cloud signal (clear sky BT minus cloudy BT).

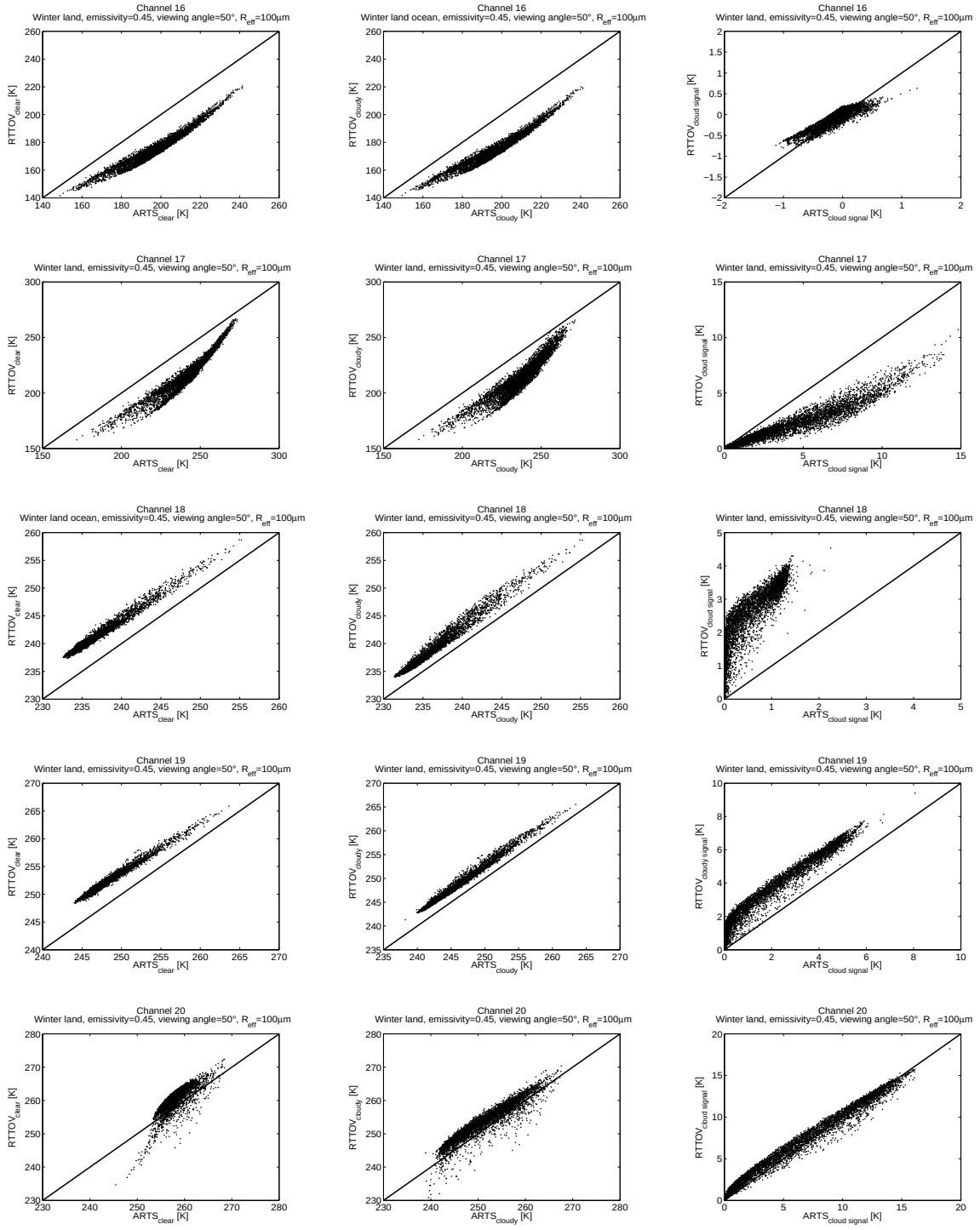

Figure 98: BT simulated for the land winter data set by RTTOVSCATT (for both clear sky simulations and cloudy simulations) against BT simulated by ARTS for a particular set of parameters (emissivity=0.45, viewing angle=50°, and effective radius of the ice particles= 100μm). Each line correspond to one AMSU-B channel from top to bottom channel 16 (89 GHz), 17 (150 GHz), 18 (183.31±1 GHz), 19 (183.31±3 GHz), and 20 (183.31±7 GHz). The left column correspond to clear sky simulations, the middle column corresponds to cloudy simulations and the right column corresponds to the cloud signal (clear sky BT minus cloudy BT).

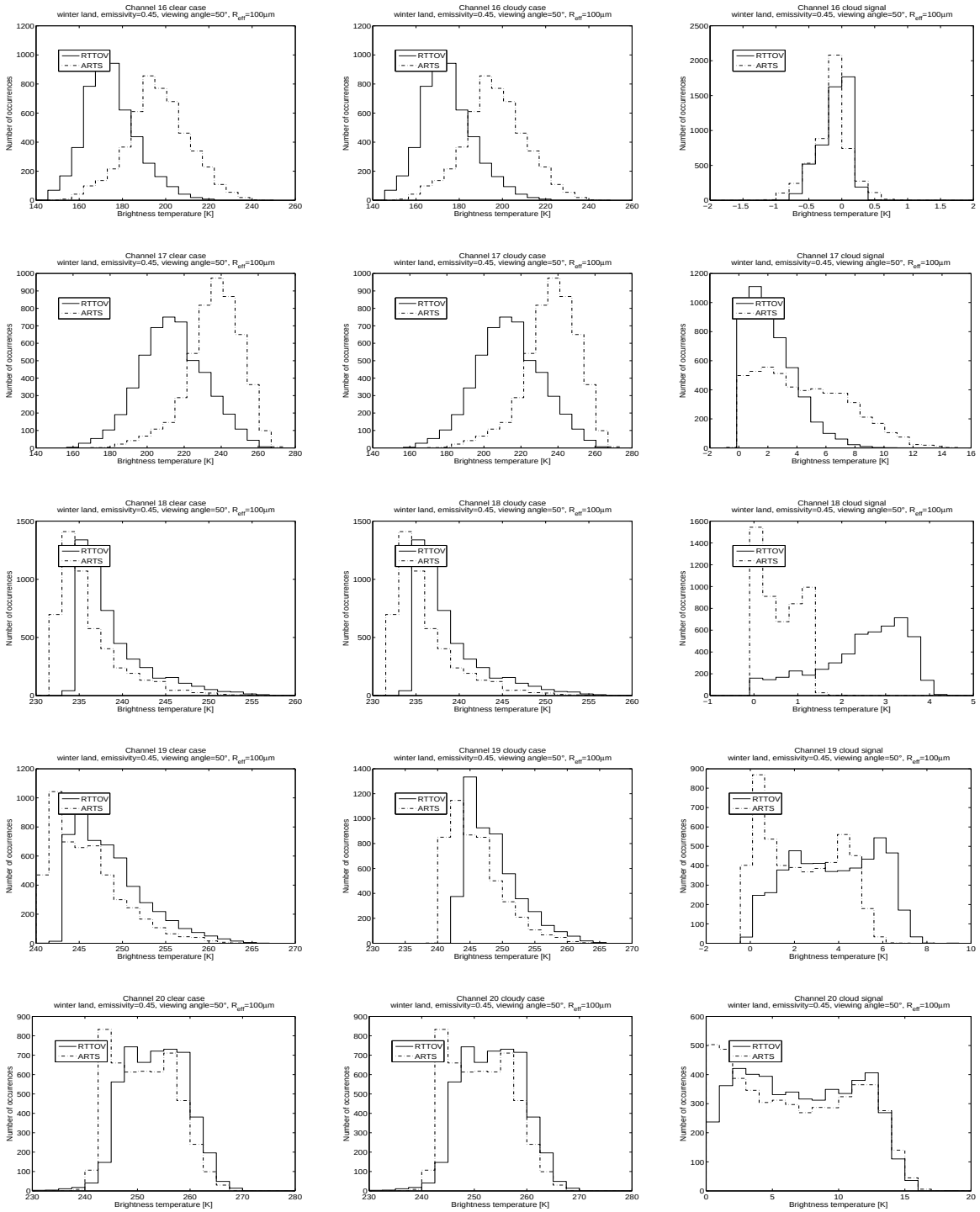

Figure 99: Histograms of BT simulated for the land winter data set by RTTOVSCATT (for both clear sky simulations and cloudy simulations), (plain line), and of BT simulated by ARTS (dashed line) for a particular set of parameters (emissivity=0.45, viewing angle=50°, and effective radius of the ice particles= 100μm). Each line correspond to one AMSU-B channel from top to bottom channel 16 (89 GHz), 17 (150 GHz), 18 (183.31±1 GHz), 19 (183.31±3 GHz), and 20 (183.31±7 GHz). The left column correspond to clear sky simulations, the middle column corresponds to cloudy simulations and the right column corresponds to the cloud signal (clear sky BT minus cloudy BT).